3224

FZK-161-1
5 JANUARY 1963

N63 21066
Code 1

INVESTIGATION OF COMBINED EFFECTS OF RADIATION AND VACUUM AND OF RADIATION AND CRYO-TEMPERATURES ON ENGINEERING MATERIALS

Annual Report

9 November 1961 through 8 November 1962

Volume I: Radiation-Vacuum Tests

4 8 1

Prepared
George C. Marshall Spa
Huntsville, Alaba

Contract No. NAS8-2450
Request No. TP65-468

NUCLEAR AEROSPACE RESEARCH FACILITY

224

CASE FILE COPY

NASA CR-50763

(FZK-161-1)
5 JANUARY 1963

OTS: $ 19.75 ph, $ 9.86 mf

GDDDDDDD

NUCLEAR AEROSPACE RESEARCH FACILITY

INVESTIGATION OF COMBINED EFFECTS OF RADIATION AND VACUUM AND OF RADIATION AND CRYO-TEMPERATURES ON ENGINEERING MATERIALS.

Annual Report

9 November 1961 through 8 November 1962

Volume I: Radiation-Vacuum Tests

E. E. KERLIN

Prepared for
George C. Marshall Space Flight Center
Huntsville, Alabama

(NASA Contract No. NAS8-2450)
Request No. TP85-468

GENERAL DYNAMICS / FORT WORTH, Tex.

This report was prepared by General Dynamics/Fort Worth under Contract No. NAS8-2450, Investigation of Combined Effects of Radiation and Vacuum and of Radiation and Cryotemperatures on Engineering Materials, for the George C. Marshall Space Flight Center of the National Aeronautics and Space Administration. The work was administered under the technical direction of the Propulsion and Vehicle Engineering Division, Engineering Materials Branch of the George C. Marshall Space Flight Center with Eugene C. McKannan acting as project manager.

ABSTRACT

21066

A series of tests was performed to measure the combined effects of nuclear radiation and vacuum on a group of non-metallic materials that are considered for use in nuclear-powered space vehicles. This group consisted of materials classified as adhesives, seals, thermal insulations, electrical insulations, potting compounds, dielectric materials, lubricants, structural laminates, and thermal-control coatings. Typical tests performed on material specimens included lap-shear strength, ultimate tensile strength, ultimate elongation, stress-strain characteristics, compressive strength, weight loss, lubricity, color changes, and spectral reflectivity.

Two vacuum systems having pumping speeds in excess of 3000 liters/sec at 10^{-6} torr were designed by General Dynamics and built by Consolidated Vacuum Corporation for use in these irradiations. Special dynamic test equipment was built for testing materials in vacuum after irradiation.

Measured properties of the materials as a function of integrated neutron flux and gamma dose are reported, and recommendations for use of the various materials in nuclear-powered spacecraft are made.

REPORT SUMMARY

Among the environmental factors associated with a nuclear-powered space vehicle are (1) the nuclear radiation from the nuclear-heat-exchanger rocket and (2) the hard vacuum of outer space. To establish the reliability of materials to be used in spacecraft, the effects of the above environmental factors must be investigated. The type of radiation leaking from the nuclear-reactor area will be of the high-energy neutron and gamma-ray type and be of sufficient magnitude to produce damaging effects in organic materials. The partial pressure associated with outer space is considered to be approximately 10^{-16} torr (1 torr = 1/760 standard atmosphere); however, the effects of outer-space pressure on the mechanical properties of organic materials can be duplicated at much higher pressures.

The effects of nuclear-reactor radiation on the physical properties of nonmetallic engineering materials in the presence of a fluid (such as air) have been investigated extensively. The resulting data show that the physical and mechanical properties of the materials are affected by the fluid present during the irradiation. In the last few years, the effects of high vacuum on the properties of engineering materials have been receiving considerable attention. Only recently, however, has testing equipment been developed which makes it possible to perform the necessary experiments. This explains why very little information has been available on the separate effects of high

Preceding page blank

vacuum and radiation on the same material. Only one report has been found on the combined effects of the two environments and this deals with only a single material.

The irradiation of materials in a high vacuum changes two conditions present in an air irradiation. The first is the absence of oxygen and ozone; the second is the separate effect of the vacuum on the free radicals produced in the material during irradiation. Each of these conditions makes it impossible to predict property changes due to vacuum irradiation on the basis of changes due to air irradiation.

The purpose of the present experimental program is to measure the effects of the combined environments of nuclear radiation and a high vacuum on some physical properties of a select group of nonmetallic engineering materials. The environments chosen approximate those which will be experienced by the component parts of a nuclear-powered spacecraft during flight. Forty-seven materials, representative of those now used in chemically powered spacecraft and most likely to be used in nuclear-powered spacecraft, were tested.

The radiation source used in this experiment was the Ground Test Reactor (GTR) located at the Nuclear Aerospace Research Facility (NARF), General Dynamics Corporation, Fort Worth, Texas. Two vacuum systems having a pumping speed of 3100 liters per second at 10^{-6} torr (with an ultimate pressure of 1.2×10^{-7} torr) were positioned near the reactor.

Determinations of the mechanical properties of materials were performed in air after irradiation in air, and in vacuum and air after irradiation in vacuum. Specially built dynamic testers determined the properties of some materials immediately after irradiation while the specimens were still in the vacuum environment. One or two materials from the following categories were tested with the dynamic testers: adhesives, laminates, seals, thermal insulations, electric insulations, potting compounds, and lubricants. Thermal-control coatings and dielectric materials were tested statically.

The single document on the combined effects of radiation and vacuum on Teflon TFE was published by du Pont. The information in this document shows that the material would maintain the same physical property value after receiving a factor-of-150 higher dose in vacuum than in air.

In view of the du Pont test and the generally held belief that a vacuum environment helps to protect the materials during irradiation by the exclusion of oxygen, it was decided to irradiate the materials to what was considered a high dose. The results of this NARF experiment show that a general statement cannot be made as to whether or not all materials are protected or all damaged by the vacuum environment during irradiation. The effects are different for the different materials tested.

The materials listed in the accompanying summary table were not affected by the indicated dose received during the vacuum irradiation. Although other materials tested suffered significant property changes, some could probably be used in nuclear-powered spacecraft applications in a much lower radiation

Summary Table of
Vacuum-Irradiated Materials Manifesting no Detectable Change
in Mechanical or Optical Properties

Material Category	Trade Name	Manufacturer	Radiation Exposure		Vacuum During Irradiation (torr)
			Gamma [ergs/gm(C)]	Neutron (n/cm^2) ($E > 2.9$ Mev)	
Adhesive	FM-1000	Bloomingdale Rubber Co.	1.7×10^{10}	2.7×10^{15}	5×10^{-7}
	Metlbond 406	Narmco Industries	1.7×10^{10}	2.7×10^{15}	5×10^{-7}
	Epon 422J	Shell Chemical Corporation	3.9×10^{10}	8.0×10^{15}	2×10^{-6}
	AF-6	Minnesota Mining & Manu.	3.9×10^{10}	8.0×10^{15}	2×10^{-6}
Thermal Insulation	Styrofoam 22	Dow Chemical Corporation	1.0×10^{10}	1.6×10^{15}	2×10^{-6}
	DS-620	American Latex Products Corp.	1.1×10^{10}	1.8×10^{15}	3×10^{-7}
Structural Laminates	Silicone DC-2106	Dow Corning Corporation	4.5×10^{10}	7.5×10^{15}	5×10^{-7}
	CTL-91-LD	Coast Manu. Company	4.5×10^{10}	7.5×10^{15}	5×10^{-7}
Electrical Insulation	Mylar-C (1 mil)	E.I. du Pont de Nemours	5.4×10^{9}	9.8×10^{13}	5×10^{-6}
	DuPont H-Film	E.I. du Pont de Nemours	8.8×10^{9}	2.5×10^{15}	3×10^{-7}
Potting Compounds	DC-R-7521	Dow Corning Corporation	9.0×10^{9}	1.4×10^{15}	2×10^{-6}
Dielectric Materials	Teslar	E.I. du Pont de Nemours	1.3×10^{9}	1.6×10^{13}	5×10^{-6}
Thermal Control Coating	Acrylic, black	Sherwin-Williams	1.7×10^{10}	1.9×10^{15}	2×10^{-6}
	Silicone, aluminum	W. P. Fuller Company	1.7×10^{10}	1.9×10^{15}	2×10^{-6}

exposure environment. It is anticipated that many of these lower radiation exposures will be determined in the coming year's work.

A series of tests to measure the combined effects of nuclear radiation and cryotemperatures was also conducted under the same NASA contract at NARF. These tests utilized three experimental assemblies designed to submerge test specimens in cryogen fluids during exposure to nuclear radiation and during subsequent tensile and compression testing. Cryogen fluids used during the experiment were liquid nitrogen (-320°F) and liquid hydrogen (-423°F). The experiment is described in Volume II of this report.

FOREWORD

Work by the Nuclear Aerospace Research Facility (NARF) at General Dynamics/Fort Worth under NASA Contract No. NAS8-2450 was conducted in two separate sections. The basic section, an experiment to measure combined effects of nuclear radiation and high vacuum on materials, was initiated 9 November 1961, and carried out under the direction of E. E. Kerlin. The work is described in this report, Volume I of GD/FW Report FZK-161. The second section, an experiment to measure the combined effects of nuclear radiation and cryotemperatures on a selected group of nonmetallic materials, was initiated on 1 July 1962 as Modification I to the original contract. The work was performed under the direction of E. T. Smith and is described in Volume II of GD/FW Report FZK-161.

The author acknowledges the services of the following people who have helped make this experiment possible: Dr. O. H. Hill for design of the vacuum portion of the vacuum system, for calibration of the vacuum pumping speed, and for performance of the gamma irradiation of Dow Corning DC 704 pumping fluid; Dr. R. P. Lightfoot, J. W. Gordon, and F. A. Haley of GD/FW and S. A. Yalof and J. Hertz of GD/Astronautics for their help in selecting the materials for testing; F. F. Fleming and W. E. Ivie for the nuclear radiation measurements; E. E. Baggett and J. R. Tucker for the detailed design of the vacuum test equipment; W. M. Brandenberg of GD/Astronautics for conducting

Preceding page blank

the optical measurements on the thermal-control coatings; and D. L. Stevenson of Consolidated Vacuum Corporation for performing the vacuum pumping speed determination of the irradiated DC 704 fluid.

Further, the author also wishes to acknowledge the following persons for writing particular sections of the report and for conducting the tests described in them: J. E. Warwick, Section 4.2; M. J. Tilly, Section 4.3; C. E. Morgan, Sections 4.4, 4.5, and 4.6; and Dr. O. H. Hill, Appendix A.

TABLE OF CONTENTS

	Page
ABSTRACT	3
REPORT SUMMARY	5
FOREWORD	11
LIST OF FIGURES	17
LIST OF TABLES	25
I. INTRODUCTION	29
II. TEST FACILITY AND EQUIPMENT	33
2.1 Radiation Effects Testing System	33
2.2 Vacuum Systems	36
2.3 Pressure Gages	43
III. RADIATION ENVIRONMENT	47
3.1 Nuclear Measurement Techniques	47
3.2 Vacuum Chamber Radiation Mapping	47
3.3 Analytical GTR Neutron Spectrum	56
IV. TEST PROCEDURES AND RESULTS	59
4.1 Vacuum Irradiation Pressure Data	61
4.2 Static Test	68
4.2.1 Experimental Equipment	68
4.2.2 Experimental Operation	69
4.2.3 Mechanical-Property-Test Results	77
4.2.3.1 Structural Adhesives	78
4.2.3.2 Seals (O-rings and tensile specimens)	79
4.2.3.3 Thermal Insulations	87
4.2.3.4 Structural Laminates	90
4.2.3.5 Electrical Insulation	94
4.2.3.6 Potting Compounds	99
4.2.3.7 Dielectric Materials	101
4.2.3.8 Elastomers	105

TABLE OF CONTENTS (cont'd)

		Page
4.3	Low-Force Dynamic Test	113
4.3.1	Experimental Low-Force Testing Equipment	113
4.3.2	Experimental Results	118
4.3.2.1	Thermal Insulations	119
4.3.2.2	Potting Compounds	124
4.3.2.3	Structural Laminates	125
4.3.2.4	Electrical Insulation	128
4.3.2.5	Seals	130
4.4	High-Force Tensile Test	134
4.4.1	Experimental Equipment	134
4.4.2	Experimental Results	144
4.5	Bearing Lubricant Test	170
4.5.1	Experimental Equipment	170
4.5.2	Experimental Results	178
4.5.2.1	Preliminary Measurements	180
4.5.2.2	Control Measurements	181
4.5.2.3	Measurements During Irradiation	183
4.5.2.4	Postirradiation Measurements	203
4.5.2.5	Discussion of Measurements	206
4.5.3	Specific Modifications	211
4.6	Weight-Loss Test	213
4.6.1	Experimental Equipment	213
4.6.2	Apparatus Calibration	215
4.6.3	Experimental Procedure	218
4.7	Optical Properties of Thermal-Control Coatings	224
4.7.1	Experimental Operation	224
4.7.2	Experimental Results	227
V.	CONCLUSIONS AND RECOMMENDATIONS	231
5.1	General Discussion	231
5.2	Experimental Test Equipment	233

TABLE OF CONTENTS (cont'd)

	Page
5.3 Experimental Test Results	235
5.3.1 Static Tests	236
5.3.1.1 Mechanical Property Tests	236
5.3.1.2 Optical Property Test	247
5.3.2 Dynamic Tests	249
5.3.2.1 Mechanical Property Tests	249
5.3.2.2 Bearing Lubricant Test	252
5.4 Experiment Evaluation	253

APPENDICES

APPENDIX A - EFFECTS OF GAMMA RADIATION ON THE PUMPING-SPEED CHARACTERISTICS OF DC-704 DIFFUSION-PUMP OIL	257
APPENDIX B - EFFECTS OF REDUCED PRESSURE ON MATERIALS AT VARIOUS TEMPERATURES	269
APPENDIX C - DESCRIPTION OF MATERIALS IRRADIATED IN A VACUUM	281
APPENDIX D - TEMPERATURES OF MATERIALS DURING VACUUM IRRADIATIONS	301
APPENDIX E - MONOCHROMATIC REFLECTIVITY AND ABSORPTIVITY CURVES FOR THERMAL-CONTROL COATING SAMPLES	321
REFERENCES	335
DISTRIBUTION	337

LIST OF FIGURES

Figure		Page
2.1	Reactor Pool	34
2.2	Radiation Effects Testing System	35
2.3	Pre- and Postirradiation Vacuum System	37
2.4	Vacuum-Irradiation System	38
2.5	Vacuum-Irradiation System in East Irradiation Position	39
3.1	Aluminum Framework for Reactor-Radiation Mapping and Static-Sample Irradiation in Vacuum System	48
3.2	Location of Neutron Detectors and Gamma Dosimeters on Radiation Mapping Rack	49
3.3	Average Flux on Rack 1 in Vacuum Chamber	50
3.4	Average Flux on Rack 2 in Vacuum Chamber	51
3.5	Average Flux on Rack 3 in Vacuum Chamber	52
3.6	Average Gamma Dose Rate on Racks in Vacuum Chamber	54
3.7	Average Neutron-Energy Spectrum Inside Vacuum Chamber	55
3.8	Analytical GTR Neutron Spectrum	57
4.1	Vacuum-Chamber Pressure During Static Tests	62
4.2	Vacuum-Chamber Pressure During Dynamic Tests	64
4.3	Vacuum-Chamber Pressure During Rerun of High-Force Dynamic Test	65
4.4	Sample Rack for Static Vacuum Irradiation	72
4.5	Location of Samples and Dosimeters for Static Irradiation: West Vacuum System; Run 1	74
4.6	Location of Samples and Dosimeters for Static Irradiation: East Vacuum System; Run 1	75
4.7	Location of Samples and Dosimeters for Static Irradiation: West Vacuum System; Run 2	76

Preceding page blank

LIST OF FIGURES (cont'd)

Figure		Page
4.8	Stress-Strain Diagram of Structural Laminate: Silicone DC-2106	92
4.9	Stress-Strain Diagram of Structural Laminate: CTL-91-LD	93
4.10	Location of Samples and Dosimeters for Low-Force Dynamic Test	115
4.11	Low-Force Dynamic Tester	117
4.12	Compression-Deflection Diagram of Thermal Insulation: Stafoam AA-402	123
4.13	Compression-Deflection Diagram of Potting Compound: RTV-60	127
4.14	High-Force Tensile Tester Equipment	136
4.15	View of Specimen Racks of High-Force Tensile Tester	137
4.16	View of High-Force Tensile Tester Before Lowering into the Vacuum-Irradiation System	138
4.17	Comparison of Strain Measured with an Irradiated Strain Gage and Strain Measured with an Unirradiated Gage	142
4.18	Comparison of Strain Measured with an Irradiated Strain Gage and Strain Measured with Unirradiated Strain Gage: Amplifier Channels Interchanged	143
4.19	Location of Samples and Dosimeters for High-Force Dynamic Test: Run 1	148
4.20	Location of Samples and Dosimeters for High-Force Dynamic Test: Run 2	149
4.21	Stress-Strain Curve of Epon 828/A Control Specimen 1	152
4.22	Stress-Strain Curve of Epon 828/A Control Specimen 2	153
4.23	Stress-Strain Curve of Conolon: Control Specimen 1	154

LIST OF FIGURES (cont'd)

Figure		Page
4.24	Stress-Strain Curve of Epon 828/A Irradiated in High-Force Tensile Test: Static Irradiation; Specimen 1	155
4.25	Stress-Strain Curve of Epon 828/A Irradiated in High-Force Tensile Test: Static Irradiation; Specimen 2	156
4.26	Stress-Strain Curve of Epon 828/A Irradiated in High-Force Tensile Test: Static Irradiation; Specimen 3	157
4.27	Stress-Strain Curve of Epon 828/A Irradiation in High-Force Tensile Test: Static Irradiation; Specimen 4	158
4.28	Stress-Strain Curve of Conolon Irradiated in High-Force Tensile Test: Static Irradiation; Specimen 1	159
4.29	Stress-Strain Curve of Conolon Irradiated in High-Force Tensile Test: Static Irradiation; Specimen 2	160
4.30	Stress-Strain Curve of Conolon Irradiated in High-Force Tensile Test: Static Irradiation; Specimen 3	161
4.31	Stress-Strain Curve of Conolon Irradiated in High-Force Tensile Test: Static Irradiation; Specimen 4	162
4.32	Stress-Strain Curve of Epon 828/A Irradiated in High-Force Tensile Test: Run 1; Specimen 1	163
4.33	Stress-Strain Curve of Epon 828/A Irradiated in High Force Tensile Test: Run 1; Specimen 2	164
4.34	Stress-Strain Curve of Conolon Irradiated in High-Force Tensile Test: Run 1; Specimen 1	165
4.35	Stress-Strain Curve of Conolon Irradiated in High-Force Tensile Test: Run 1; Specimen 2	166
4.36	Stress-Strain Curve of FM-1000 Irradiated in High-Force Tensile Test: Run 1	167

LIST OF FIGURES (cont'd)

Figure		Page
4.37	Stress-Strain Curve of Metlbond 302 Irradiated in High-Force Tensile Test: Run 1	168
4.38	Correlation of LVDT Crosshead Travel with Strain-Gage Strain	169
4.39	View of Bearing-Lubricant-Test Motors	171
4.40	Bearing-Lubricant-Test Rack	174
4.41	Circuit Diagram of Pulse Amplifier	176
4.42	Circuit Diagram of Motor Power Supply	177
4.43	Motor Coast-Down Time as a Function of Radiation Exposure and Test Time: Molykote X-15	184
4.44	Motor Coast-Down Time as a Function of Radiation Exposure and Test Time: Electrofilm 66-C	185
4.45	Motor Coast-Down Time as a Function of Radiation Exposure and Test Time: Shell ETR-H	186
4.46	Motor Coast-Down Time as a Function of Radiation Exposure and Test Time: GE F-50	187
4.47	Bearing Temperature During Test: Molykote X-15	188
4.48	Bearing Temperature During Test: Electrofilm 66-C	189
4.49	Bearing Temperature During Test: Shell ETR-H	190
4.50	Bearing Temperature During Test: GE F-50	191
4.51	Vacuum-Chamber Pressure During Bearing-Lubricant Test	192
4.52	Motor Coast-Down Time as a Function of Radiation Exposure and Running Time of Motor: Molykote X-15	193
4.53	Motor Coast-Down Time as a Function of Radiation Exposure and Running Time of Motor: Electrofilm 66-C	194
4.54	Motor Coast-Down Time as a Function of Radiation Exposure and Running Time of Motor: Shell ETR-H	195
4.55	Motor Coast-Down Time as a Function of Radiation Exposure and Running Time of Motor: GE F-50	196

LIST OF FIGURES (cont'd)

Figure		Page
4.56	No-Load Speed of Motors During Test: Molykote X-15	197
4.57	No-Load Speed of Motors During Test: Electrofilm 66-C	198
4.58	No-Load Speed of Motors During Test: Shell ETR-H	199
4.59	No-Load Speed of Motors During Test: GE F-50	200
4.60	No-Load Speed as a Function of Time for Motor Speed to Become Zero	204
4.61	Motor-Bearing Temperature as a Function of Time for Motor Speed to Become Zero	205
4.62	Weight-Loss Equipment	214
4.63	Sample Calibration Curve for Weight-Loss Apparatus	217
4.64	Weight Loss of Benzoic Acid in Vacuum	219
A-1	Views of Sample Holder with Dosimetry Packets: Co^{60} Irradiation; T $\simeq$ 30°C	263
A-2	Effects of Co^{60} Irradiation on the Air Pumping Speed of DC-704 in the CVC PMC-720 Pump	266
D-1	Specimen Temperatures During Static Test: Mobiloy AH-81, CTL-91-LD, and DC-2106	303
D-2	Specimen Temperatures During Static Test: Teflon (40 mil), Marlex 6002, and Teflon 100	304
D-3	Specimen Temperatures During Static Test: Viton A, Styrofoam 22, and Natural Rubber	305
D-4	Specimen Temperatures During Static Test: Epon 422J and AF-6	306
D-5	Specimen Temperatures During Static Test: FM-1000 and Thermal Coating	307

LIST OF FIGURES (cont'd)

Figure		Page
D-6	Specimen Temperatures During Static Test: RTV-60, DC-R-7521, and Epon 828/Z	308
D-7	Specimen Temperatures During Static Test: Teflon (40 mil), Neoprene (RA-24160), and Teslar	309
D-8	Specimen Temperatures During Static Test: Buna N (RA-30760) and Refrasil Batting (B-100)	310
D-9	Specimen Temperatures During Static Test: Teslar, Mylar C, and Mylar A	311
D-10	Specimen Temperatures During Low-Force Dynamic Test: Urethane DS-620	312
D-11	Specimen Temperatures During Low-Force Dynamic Test: Urethane DS-620 and Viton B	313
D-12	Specimen Temperatures During Low-Force Dynamic Test: Stafoam AA-402	314
D-13	Specimen Temperatures During Low-Force Dynamic Test: RTV-60	315
D-14	Specimen Temperatures During Low-Force Dynamic Test: Epon 828/A and DuPont H-Film	316
D-15	Specimen Temperatures During High-Force Dynamic Test: Conolon 506	317
D-16	Specimen Temperatures During High-Force Dynamic Test: FM-1000	318
D-17	Specimen Temperatures During High-Force Dynamic Test: Epon 828/A	319
D-18	Vacuum-Chamber Temperatures During High-Force Dynamic Test	320
E-1	Monochromatic Reflectivity and Absorptivity: Acrylic Black; Preshipment Control Samples	323
E-2	Monochromatic Reflectivity and Absorptivity: Acrylic Black; Test Control Samples and Vacuum-Irradiated Samples	324

LIST OF FIGURES (cont'd)

Figure		Page
E-3	Monochromatic Reflectivity and Absorptivity: Epoxy White; Preshipment Control Samples	325
E-4	Monochromatic Reflectivity and Absorptivity: Epoxy White; Vacuum-Irradiated Samples	326
E-5	Monochromatic Reflectivity and Absorptivity: Epoxy White; Test Control Samples	327
E-6	Monochromatic Reflectivity and Absorptivity: Silicone White; Preshipment Control Samples	328
E-7	Monochromatic Reflectivity and Absorptivity: Silicone White; Vacuum-Irradiated Samples	329
E-8	Monochromatic Reflectivity and Absorptivity: Silicone White; Test Control Samples	330
E-9	Monochromatic Reflectivity and Absorptivity: Silicone Aluminum; Preshipment Control Samples	331
E-10	Monochromatic Reflectivity and Absorptivity: Silicone Aluminum; Vacuum-Irradiated Samples	332
E-11	Monochromatic Reflectivity and Absorptivity: Silicone Aluminum; Test Control Samples	333

LIST OF TABLES

Table		Page
3.1	Neutron Flux Ratios in East Vacuum Chamber	53
4.1	Test Plan for Static Test Materials	70
4.2	Test Environment and Results of Static Test: Structural Adhesives	80
4.3	Test Environment and Results of Static Test: Seals	84
4.4	Test Environment and Results of Static Test: Thermal Insulation	88
4.5	Test Environment and Results of Static Test: Structural Laminates	91
4.6	Test Environment and Results of Static Test: Electrical Insulation	96
4.7	Test Environment and Results of Static Test: Potting Compounds	100
4.8	Test Environment and Results of Static Test: Dielectric Materials	102
4.9	Test Environment and Results of Static Test: Elastomers	106
4.10	Test Plan for Low-Force Dynamic-Test Materials	114
4.11	Test Environment and Results for Low-Force Dynamic Test Materials: Thermal Insulation	120
4.12	Test Environment and Results for Low-Force Dynamic Test Materials: Potting Compound	126
4.13	Test Environment and Results for Low-Force Dynamic Test Materials: Structural Laminates	126
4.14	Test Environment and Results for Low-Force Dynamic Test Materials: Electrical Insulation	129
4.15	Test Environment and Results for Low-Force Dynamic Test Materials: Seals	132

Preceding page blank

LIST OF TABLES (cont'd)

Table		Page
4.16	Test Plan for High-Force Dynamic Test Materials	135
4.17	Test Environment and Results for High-Force Dynamic Test Materials: Structural Adhesives	150
4.18	Test Environment and Results for High-Force Dynamic Test Materials: Structural Laminates	151
4.19	Experimental Precision of Bearing-Lubricant-Test Instruments and Accuracy of Measurements	179
4.20	No-Load Speed of Motors at 80°F Bearing Temperature	181
4.21	Bearing Lubricant Control Data	182
4.22	Reactor Schedule for Bearing Lubricant Test	202
4.23	Field Current During Bearing Lubricant Test	210
4.24	Failure Time of Lubricants	211
4.25	Control Data for Weight-Loss Test	220
4.26	Thermal Control Coatings Tested in the Vacuum-Irradiation	225
4.27	Equipment Used in Optical-Property Determination of Thermal-Control Coatings	228
4.28	Optical Properties of Thermal-Control-Coatings Test Samples	229
5.1	Summary of Property Changes in Materials Irradiated in Vacuum and Air and Tested in Air	237
5.2	Summary of Optical Changes for Thermal-Control Coatings Irradiated in Vacuum and Tested in Air	248
5.3	Summary of Property Changes for Materials Irradiated and Tested in Vacuum	250
5.4	Summary of Lubricant Changes of Small Servomotor Bearings During the Vacuum Irradiation Test (Pressure = 2×10^{-6} torr)	254

LIST OF TABLES (cont'd)

Table		Page
A-1	Dosimetry Data for DC 704 Irradiation	264
B-1	Effect of Reduced Pressure on Selected Materials at Various Temperatures	272
B-2	Effect of Vacuum and Elevated Temperatures on Metlbond 406-1	273
B-3	Effect of Vacuum and Elevated Temperatures on Epon VIII Adhesive Bond	274
B-4	Effect of Vacuum and Elevated Temperatures on FM-1000 Adhesive Film	275
B-5	Effect of Vacuum and Elevated Temperatures on Epon 422J	276
B-6	Effect of Vacuum and Elevated Temperatures on FM-47 Adhesive Bond	277
B-7	Effect of Vacuum and Elevated Temperatures on Metlbond 302A	278
B-8	Effect of Vacuum and Elevated Temperatures on AF-6 Adhesive	279
B-9	Effect of Vacuum and Elevated Temperatures on Metlbond 408	280
C-1	Materials Used in Structural-Adhesive Tests	283
C-2	Materials Used in Lubricant Tests	288
C-3	Materials Used in Seal Tests	290
C-4	Materials Used in Thermal-Insulation Tests	291
C-5	Materials Used in Structural-Laminate Tests	292
C-6	Materials Used in Electrical Insulation Tests	294
C-7	Materials Used in Potting Compound Tests	295
C-8	Materials Used in Dielectric-Material Tests	296
C-9	Materials Used in Thermal-Control-Coatings Tests	297
C-10	Materials Used in Elastomer Tests	298

I. INTRODUCTION

The success of nuclear-powered spacecraft will depend, among other things, on the selection (or development) of materials that have predictable and useful properties in an environment that combines the extreme cold and vacuum of space with radiation from a nuclear reactor. Until recently, techniques and equipment had not been developed which permitted the testing of materials in a combination environment of high vacuum and radiation or cryotemperature and radiation, let alone a combination of the three. Thus, although tests have been performed on materials in either a radiation environment, a high vacuum, or at cryotemperatures, little is known about the probable synergistic nature of their combined effects on spacecraft materials.

The purpose of the present experimental program is to measure the effects of combined environments on some physical properties of a group of nonmetallic materials selected as representative of those most likely to be used in a nuclear-powered spacecraft. The first year's work on this program is reported in two volumes: Volume I, reported here, covers the combination environment of nuclear radiation and high vacuum; Volume II (Ref. 1) covers the combination environment of nuclear radiation and cryotemperatures (liquid nitrogen and liquid hydrogen).

For the vacuum-radiation experiment, 47 materials from the following classifications were selected: adhesives, seals, thermal

Preceding page blank

insulations, structural laminates, electrical insulations, potting compounds, dielectric materials, lubricants, and thermal-control coatings. After irradiation in a vacuum, the physical properties of these materials were tested either in an Instron Tensile Tester under standard laboratory conditions or in specially built dynamic testers while still in the vacuum environment. The dynamic testers include high- and low-force testers for measuring the various moduli and physical properties of the material specimens, a dynamic lubricant tester, and a weight-loss testing device for continuous monitoring of material weight changes.

The dynamic-testing equipment was designed to satisfy the ASTM standard procedures whenever these were applicable. It should be pointed out that dynamic testing, as described in this report, inherently involves the development of radiation-resistant sensors, transducers, and equipment that can be monitored remotely. ASTM testing methods, which may be satisfied explicitly in ordinary laboratory situations, must often be modified during investigations of this type in order to maintain the required environmental conditions.

This vacuum-radiation experiment utilized specially built high-vacuum ($\sim 10^{-6}$ torr) test chambers having an available test space 20 inches in diameter by 30 inches in depth. Each vacuum system has a pumping speed in excess of 3100 liters/sec at 10^{-6} torr, with an ultimate pressure of 1.2×10^{-7} torr.

The radiation source used in this experiment was the Ground Test Reactor (GTR) located at the Nuclear Aerospace Research Facility (NARF), General Dynamics/Fort Worth. The GTR provided a radiation rate on the samples in the vacuum of approximately 7.5×10^8 ergs/gm(C)-hr of gamma radiation and 3.6×10^{10} n/cm^2-sec ($E > 2.9$ Mev) of neutron radiation.

II. TEST FACILITY AND EQUIPMENT

In this section, the reactor facility, the vacuum systems, and the two types of pressure gages are discussed. Other equipment required for the individual tests is described in the particular subsection of Section IV where the procedures and results are given.

2.1 Radiation Effects Testing System

The radiation source used in the Radiation Effects Testing System is the Ground Test Reactor (GTR), a heterogeneous, highly enriched, thermal reactor utilizing water as neutron moderator and reflector, as radiation shielding, and as coolant (Ref.2). Maximum power generation is three megawatts.

The irradiation pool, shown in Figure 2.1, is divided into two sections: a south section, which forms the reactor pool and is filled with water, and a north section, which is the irradiation cell and is kept dry. The reactor closet in the center of the pool divider extends into the irradiation cell to provide three sides for irradiation. In Figure 2.1, the reactor is in the fully retracted position on the horizontal positioning mechanism. This mechanism enables the reactor to be positioned at any distance from 2 to 90 inches from the north face of the closet.

The reactor closet is partially covered by $\frac{1}{4}$-inch boral. The boral extends 36 inches east and west along the pool divider from the closet, and up and down 36 inches from the horizontal centerline of the reactor. The centerline is 57 inches above the cell floor.

Preceding page blank

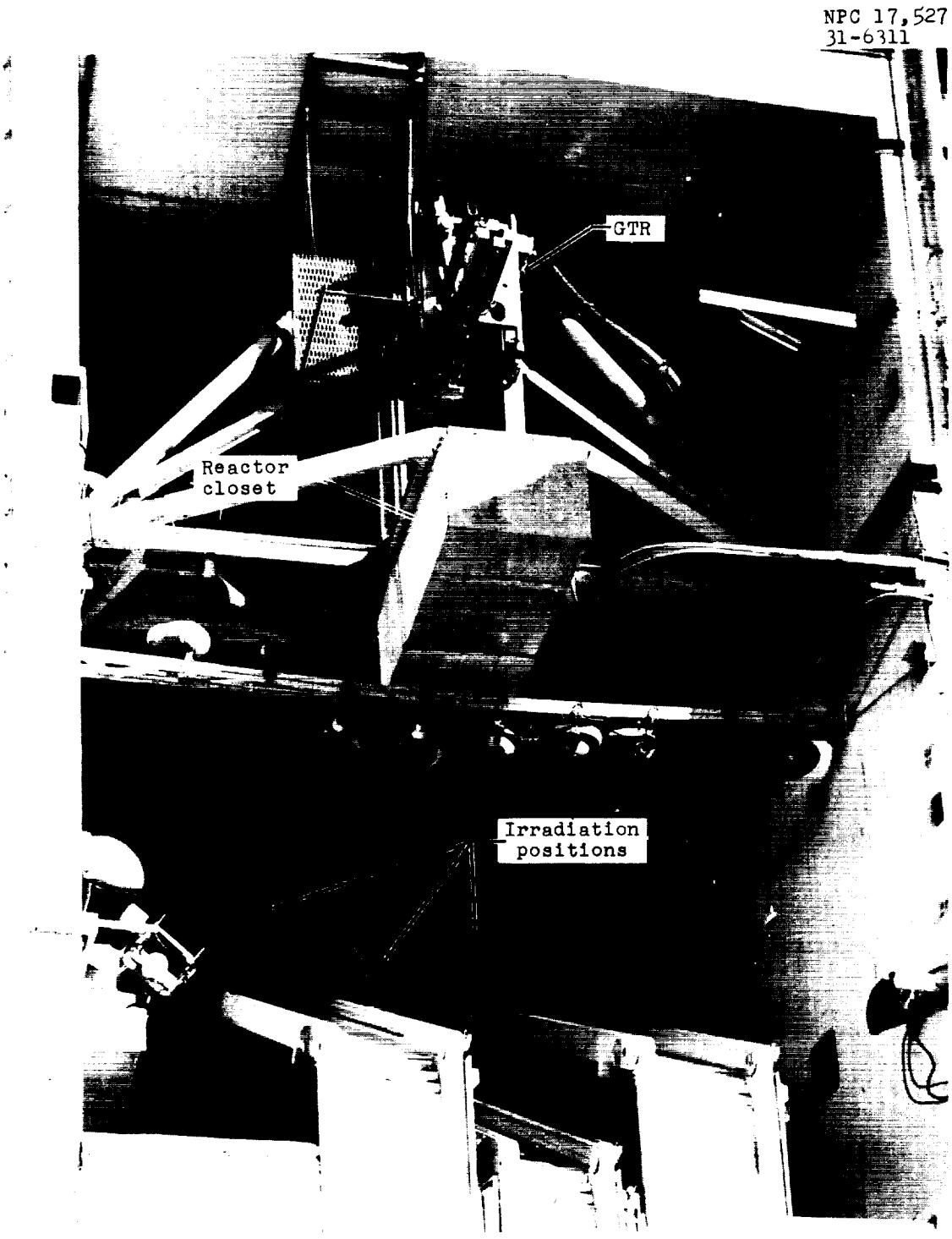

Figure 2.1 Reactor Pool

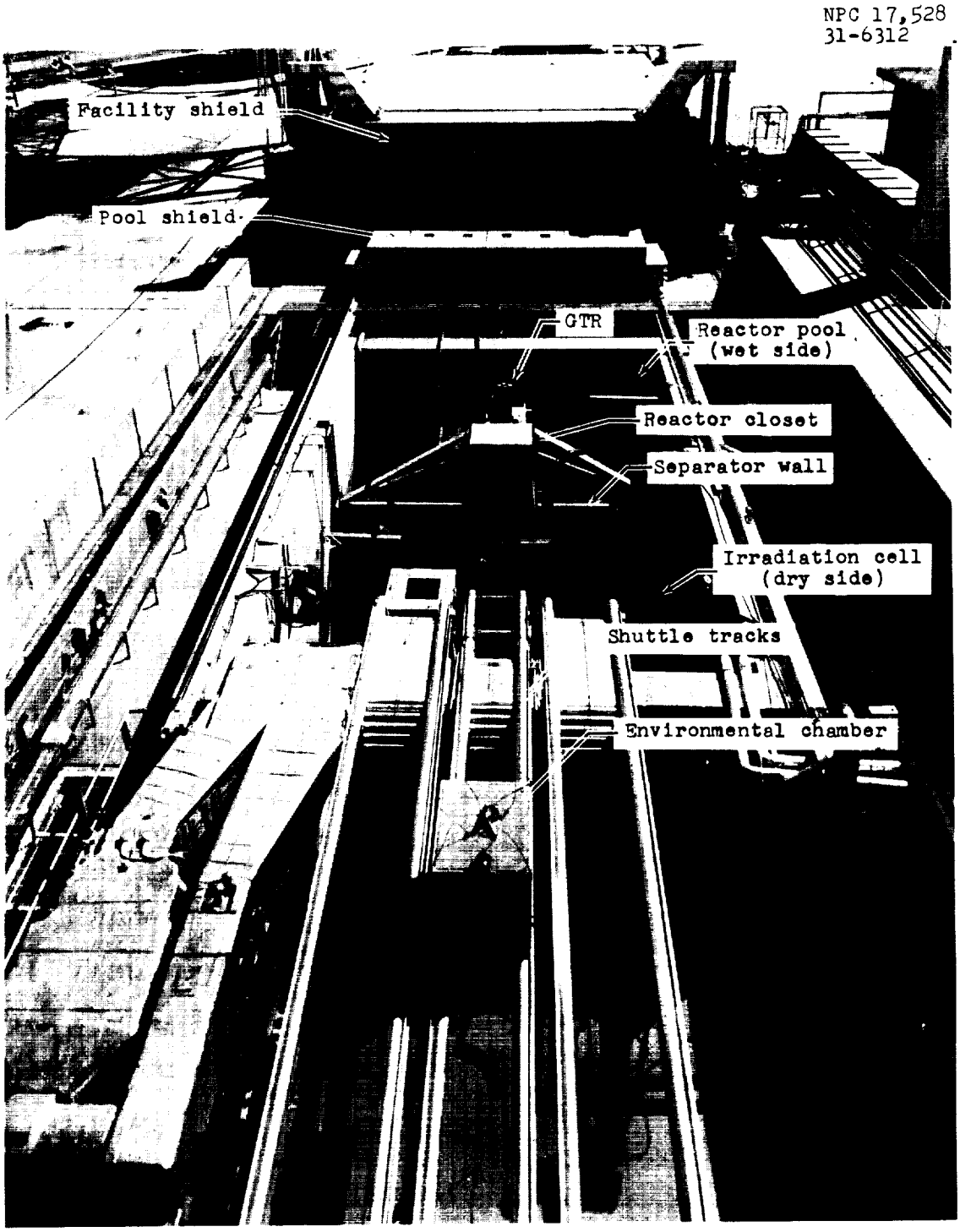

NOT REPRODUCIBLE

Figure 2.2 Radiation Effects Testing System

Adjacent to the north wall of the irradiation cell is the handling area. Equipment permanently installed in this area includes a gas-monitoring system, a Davis explosion meter, and environmental equipment for the Radiation Effects Testing System. The auxiliary equipment necessary for the vacuum experiments was also located in the handling area. Figure 2.2 is a view (looking south) of the Radiation Effects Testing System showing the concrete pool shields, the irradiation pool, the shuttle-system tracks, and the handling area (right foreground under tracks).

The vacuum-irradiation experiments did not make use of the shuttle system. Each vacuum system - consisting of the steel chamber, pumps, motors, and essential structural members - weighed well over two tons, thus exceeding the maximum weight limit of the shuttle dollies. The vacuum chambers were lowered into position in the irradiation cell by means of the overhead mobile crane.

2.2 Vacuum Systems

Three high-vacuum systems are available at NARF for materials testing. A pre- and postirradiation vacuum system located in the Irradiated Materials Laboratory (IML) is used for preirradiation outgassing, leak-checking of dynamic systems, and pre- and postirradiation testing of materials and systems (Fig. 2.3). The other two vacuum systems were designed to fit next to the east and west faces of the GTR (Fig. 2.4). Figure 2.5 shows one of the vacuum systems in the east irradiation position.

NPC 17,474
31-6521

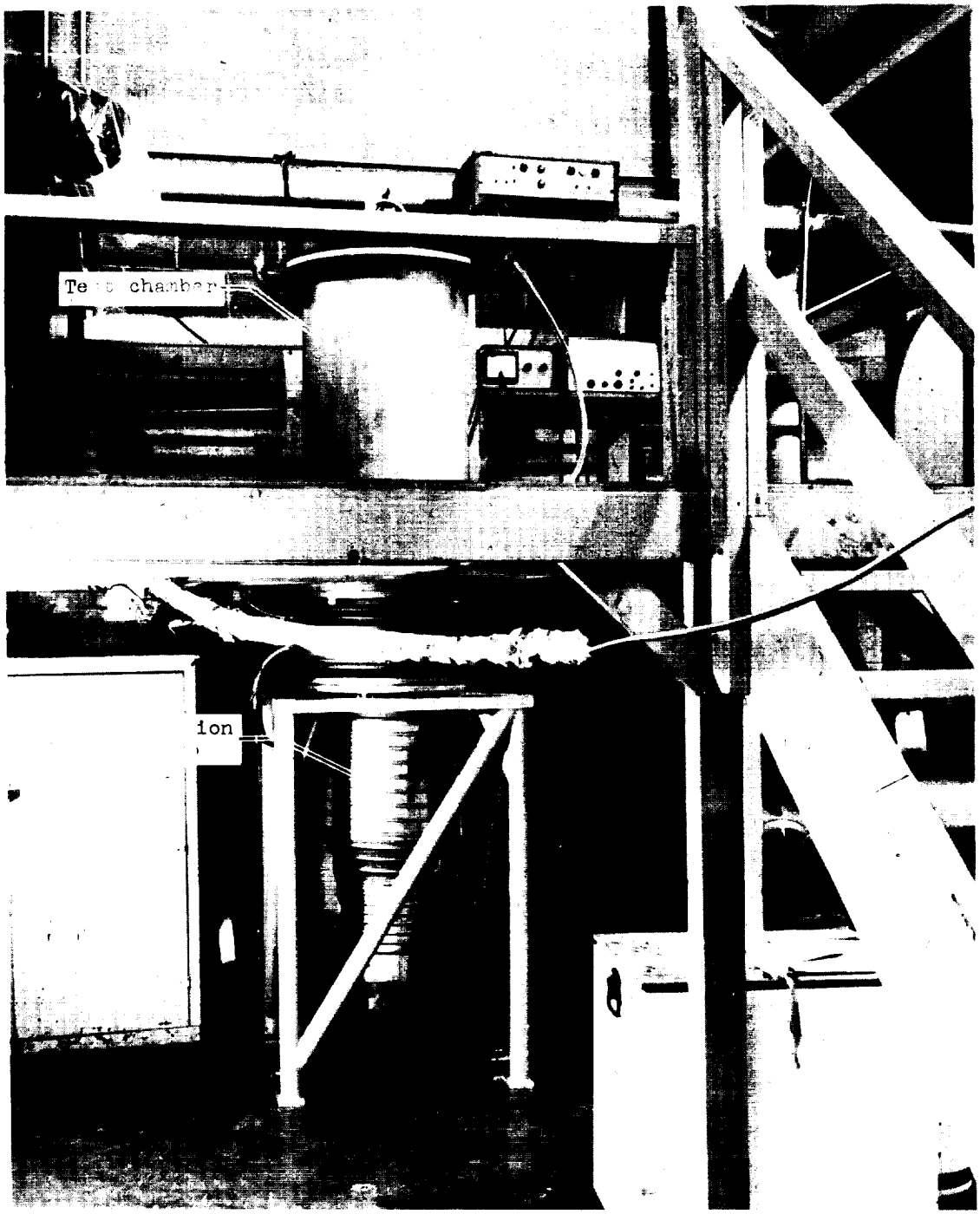

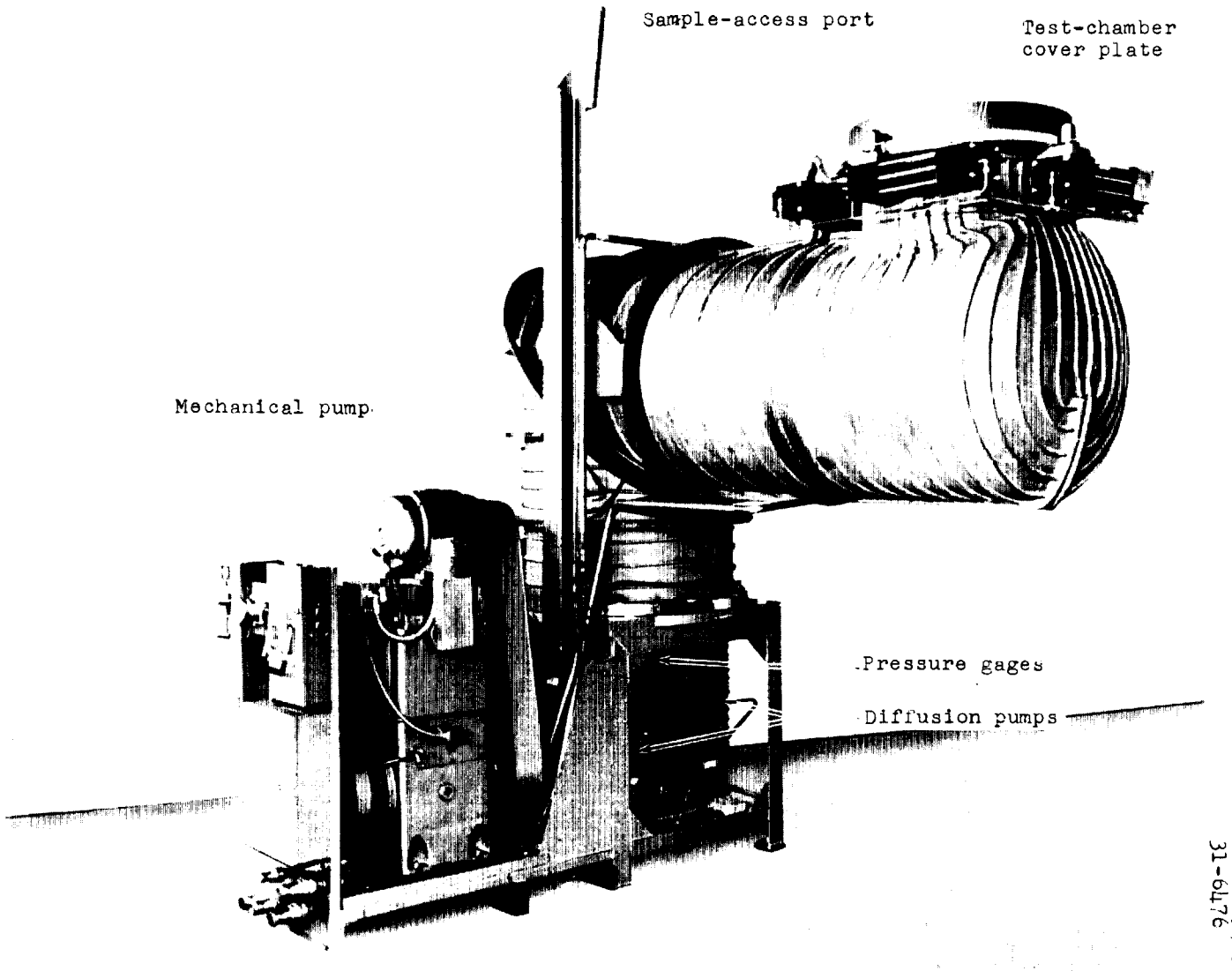

Figure 2.4 Vacuum-Irradiation System

NPC 17,473
31-6480

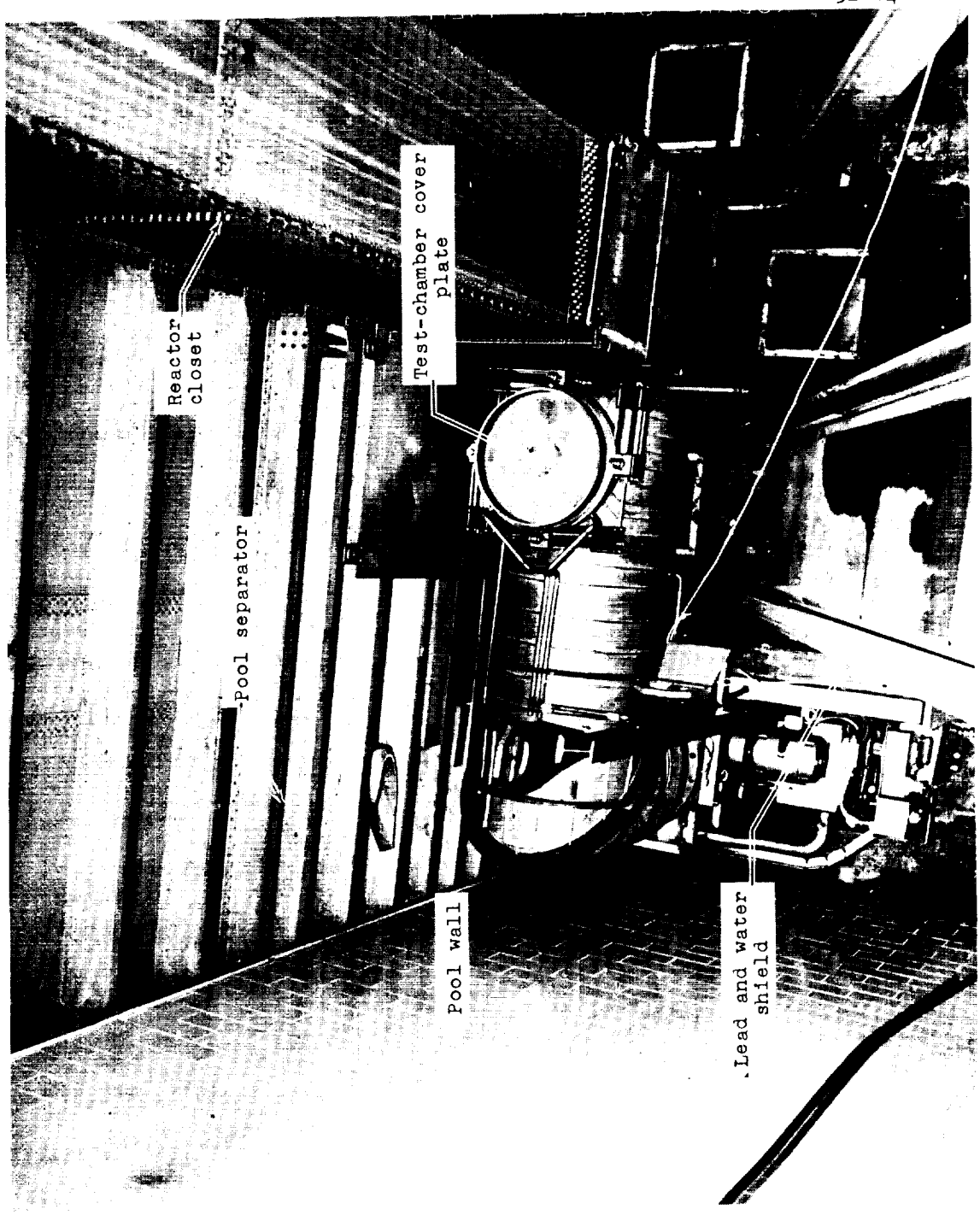

Figure 2.5 Vacuum-Irradiation System in East Irradiation Position

The vacuum system in the IML has a 16-in. diffusion pump, Type 0130, made by National Research Corporation. The test chamber is mounted above a liquid-nitrogen baffle on the diffusion pump. This vacuum system is capable of maintaining reduced pressures as low as 6×10^{-7} torr.

The two vacuum-irradiation chambers were built to the General Dynamics design by Consolidated Vacuum Corporation (CVC), Palo Alto, California. During testing, lead and water shields protect the mechanical forepump, diffusion pumps, and system accessories from the intense reactor radiation (Fig. 2.5). The usable test volume, which is 20 inches in diameter and 30 inches deep, is located near the centerline of the reactor. The two vacuum systems are similar in design: each contains a Model 212-H Stokes mechanical forepump and two 10-in. diffusion pumps, CVC Model PMC 4100. Pump-down time of the vacuum-irradiation chamber to a reduced pressure of 1×10^{-6} torr is approximately three hours, depending on materials, moisture, and condensable gasses in the system at startup. Mounting plates were installed on the floor of the dry side of the GTR irradiation pool to facilitate positioning of the chambers next to the east and west faces of the reactor closet.

The diffusion pumps use silicone DC-704 pumping fluid, which has a vapor pressure of approximately 1.2×10^{-7} torr. The silicone was selected because of the low outgassing rates during irradiation. An experiment to determine the change in vacuum-pump operational characteristics while using irradiated oil is described in Appendix A.

In order to maximize the pumping speed available from the CVC Model PMC 4100 diffusion pumps, no internal cooling baffles were incorporated into the duct design. One external set of cooling coils mounted on the duct above the pump throats is designed to provide a condensation wall for the oil should one be required in future test programs. The CVC pumps are fitted with "radiation caps", designed to provide a considerable reduction in back-streaming of the oil vapor.

The use of the 30-inch-diameter ducts was based upon a desire to maximize the effective conductance between the sample position and the pump throats and to provide the largest possible sample port compatible with the geometrical limitations imposed by the reactor facility. The question of defining the effective pumping speed at the sample position may be arbitrarily resolved by treating the entire duct between the sample and the pumps as a conductance element instead of a portion of the chamber itself. Since the nominal centerline distance between the sample and pumps is approximately 94 inches, an extremely conservative conductance value of approximately 15,000 liters/second may be deduced for the assembly (Ref. 3). Using a conservative value of 5000 liters/second at 10^{-6} torr pressure for the pumping speed of the pair of CVC Model 4100 pumps (which have a plateau speed of approximately 3800 liters/second, each), one may deduce a net pumping speed at the sample position of approximately 3700 liters/second, which more than satisfies the design requirements.

During preliminary evaluations the systems have demonstrated pumping speeds of at least 3100 liters/second at the sample position. In these experiments, however, the pressures monitored at the sample position with a tubulated CVC VG-1A vacuum-gauge tube did not track the nude, Hughes Type 6578 tubes employed at the position of the pump throats. Present plans for further evaluation and calibration of the pumping systems include comparison calibrations employing the nude-type Hughes tubes at both the sample and pump-throat positions so that pressure distributions more realistically characteristic of the systems can be obtained. The small increases in pressure ($2\text{-}4 \times 10^{-7}$ torr) observed at the pump throats during sample irradiation suggests that the gas-handling capabilities of the systems have been adequate for the sample volumes employed to date.

The material samples and the test fixtures to be irradiated were inserted into the test chamber through the top access port and secured by a remotely operated, air-driven latching mechanism. To offset gamma heating and to provide lower chamber-wall temperatures during the test, cooling water was passed through coils that surround the test chamber. In the second quarterly progress report (Ref. 4), the heat-transfer effects between the specimens and the chamber wall are discussed and a method of determining the chamber-wall temperature required to maintain a predetermined specimen temperature is described.

A preliminary experiment to establish pumping speeds required of the vacuum systems to accommodate the radiation outgassing of the organic materials is also discussed in the second quarterly progress report. The pumping speeds of the two vacuum-irradiation chambers were measured and found to be approximately 3100 liters/sec at 1×10^{-6} torr; therefore, the radiation-induced gasses evolved from the test materials determined the size and quantity of materials that were included in each test.

2.3 Pressure Gages

The specification of pressure in the vacuum assemblies is subject to a number of qualifications. No commercial pressure-gaging equipment capable of remote readout is available for evaluating absolute pressures in the range of 10^{-5} to 10^{-7} torr. Knudsen gages, and modifications thereof, have been used under laboratory conditions with absolute pressure sensitivities extending to 5×10^{-9} torr, but these units are extremely sensitive to vibration, and remote pressure readout is not practical in the pressure ranges of interest (Ref. 3). Commercial hot-filament- as well as cold-cathode-type ionization-gage pressure measurements depend sensibly upon the composition of the monitored vapors, and calibrations are usually provided with respect to dry air.

In the present vacuum assemblies, the radiation-induced decomposition products liberated by sample materials extend over a wide range of molecular weights and are a function of the

material composition. If the vapor composition could be established, it is theoretically possible to evaluate the absolute pressure in the system by appropriately weighting the positive-ion contribution from each of the vapor species based upon the sensitivity of the gages for each of these types of molecules. This is not practical in engineering studies of this type, and, therefore, the pressure measurements recorded by commercial ionization gages are not absolute measurements in any sense of the word, but merely a statement of the relative number of positive ions formed in a given gauging system normalized with respect to electron emission. The term "nominal pressure" will be used to qualify the compromise inherent in such pressure measurements.

Two separate gage systems were used with the vacuum-radiation chambers - the primary system, utilizing a nude Bayard-Alpert-type tube sensing element, and the secondary system, using a cold cathode Philips tube. Both vacuum-gage tubes were mounted at the interface where the vertical section of the 30-in.-diam duct was bolted to the diffusion pumps. This position was chosen because it is well shielded from the direct radiation generated by the nuclear reactor, and therefore the sensors are subjected to a minimum of additional positive-ion formation from this source of radiation, which would correspond to a positive error in the indicated pressure.

The nude Bayard-Alpert-type ionization gage, Type 6578, is made by the Vacuum Tube Division of Hughes Aircraft. This gage utilizes the vacuum chamber for its enclosure, eliminating the tubulation and self-pumping problems which are inherent with enclosed gages. The electronic equipment used for excitation and readout was the Hughes IGC-101 Ionization Gage Controller. The gages, with their associated electronic equipment, were calibrated by the GD/FW Standards Laboratory. The ionization gages were within 10% of the calibration standard.

The cold cathode ionization gage is the CVC Philips Gage PHG-09. This unit has an extended scale in the high range (500 microns) that is useful during pump-down and leak-check. Discrepancies in the PHG-09 pressure readings and modifications for the chart recorder required that the gages and electronic equipment be returned to the vendor for rework. The gages were returned from the vendor only in time to be used on the last irradiation.

The Hughes ionization gage, when used in the pre- and post-irradiation vacuum system in the IML, functioned very satisfactorily; there was no trouble with the electronic equipment or tube filaments. However, when used in the irradiation chambers, the filaments burned out much quicker or changed in effective electron emission. This presented a major problem in only one irradiation. Since each gage tube contains three filaments, a new one was connected when one became inoperative.

III. RADIATION ENVIRONMENT

3.1 Nuclear Measurement Techniques

The total gamma dose inside the vacuum chamber was measured with nitrous-oxide dosimeters, while the magnitude and energy spectrum of the neutrons were measured by the foil-activation method (Ref. 5).

Nuclear-radiation mapping of the vacuum chamber was accomplished on 8 August 1962. An aluminum test cage, which was later used for the static irradiations, was mounted with neutron foil detectors and nitrous-oxide gamma dosimeters, as shown in Figure 3.1, and placed in the vacuum chamber. The mapping experiment was performed at a reactor power level of one megawatt for a period of one hour.

To measure the neutron flux and the energy spectrum in the vacuum chamber, manganese foils (bare and cadmium-covered) were used for thermal neutrons; indium foils for neutrons with $E > 0.85$ Mev; sulfur pellets for $E > 2.9$ Mev; magnesium foils for $E > 7.5$ Mev; and aluminum foils for $E > 8.1$ Mev. The positions of neutron detectors and gamma dosimeters on each of the three racks used in mapping the vacuum chamber are shown in Figure 3.2.

3.2 Vacuum Chamber Radiation Mapping

Figures 3.3, 3.4, and 3.5 show the average neutron flux (n/cm^2-sec-Mw) along the longitudinal centerline of each rack as a function of distance below the top plate of the chamber.

Preceding page blank

NPC 17,476
31-6522

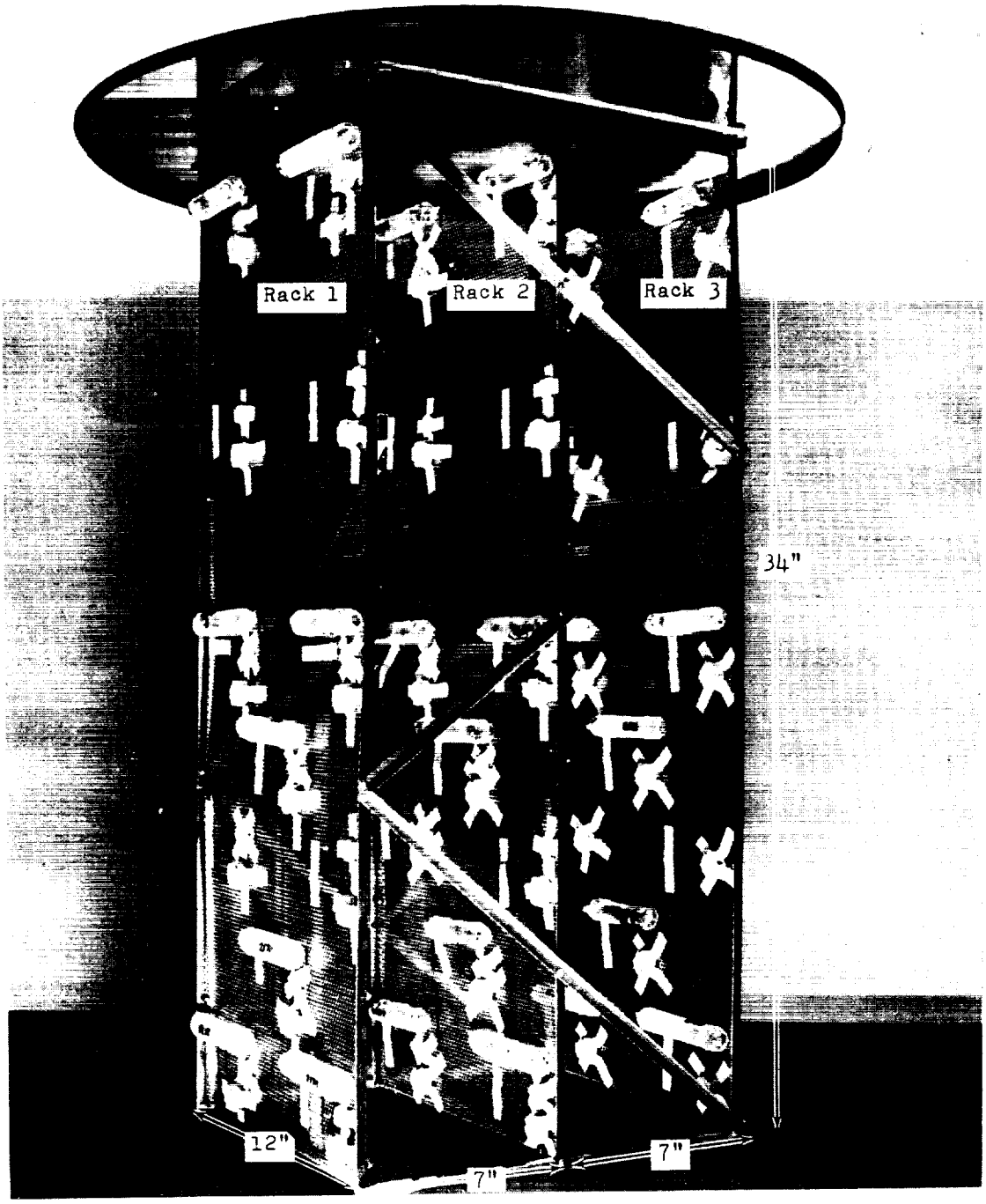

Figure 3.1 Aluminum Framework for Reactor-Radiation Mapping and Static-Sample Irradiation in Vacuum System

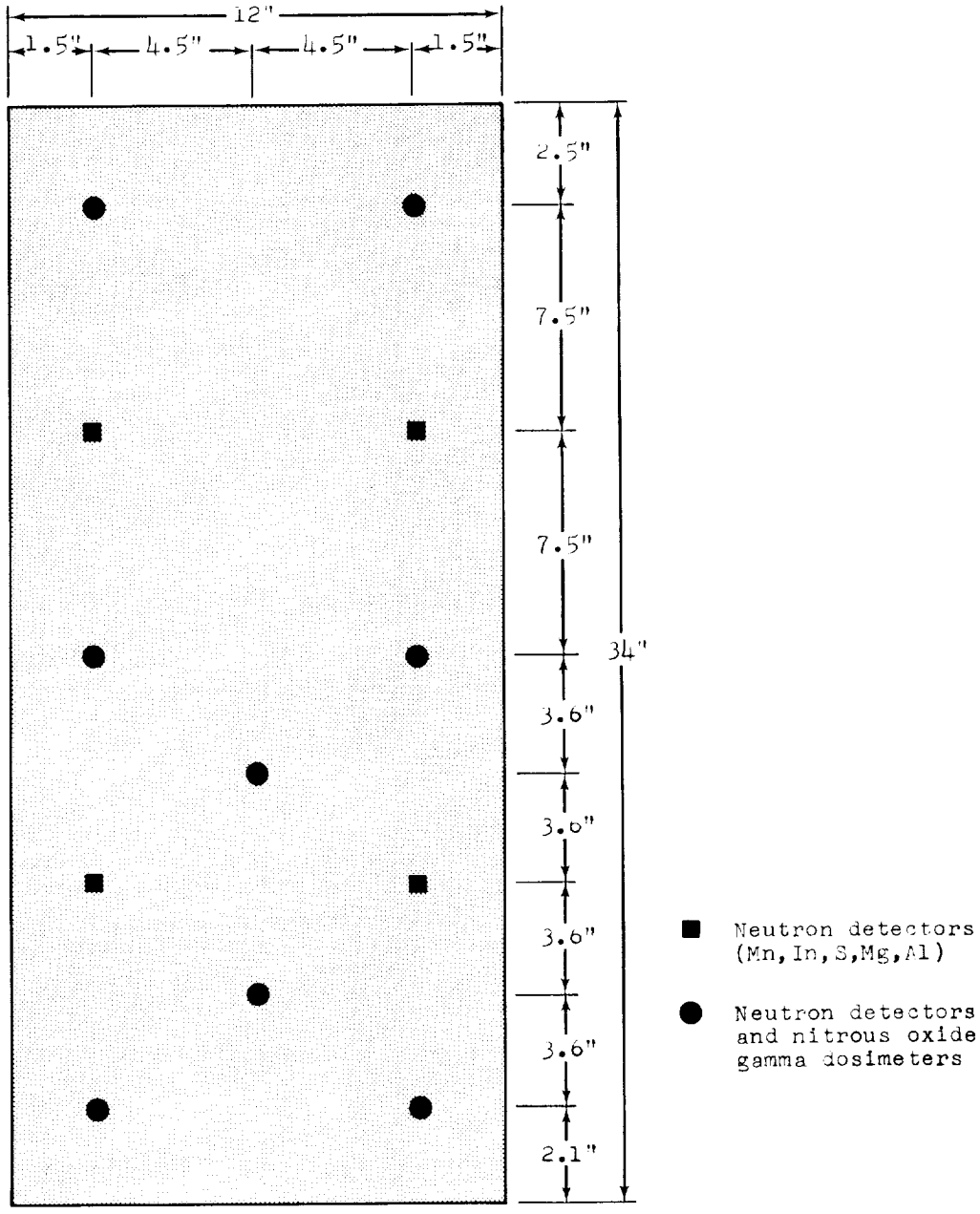

Figure 3.2 Location of Neutron Detectors and Gamma Dosimeters on Radiation Mapping Rack

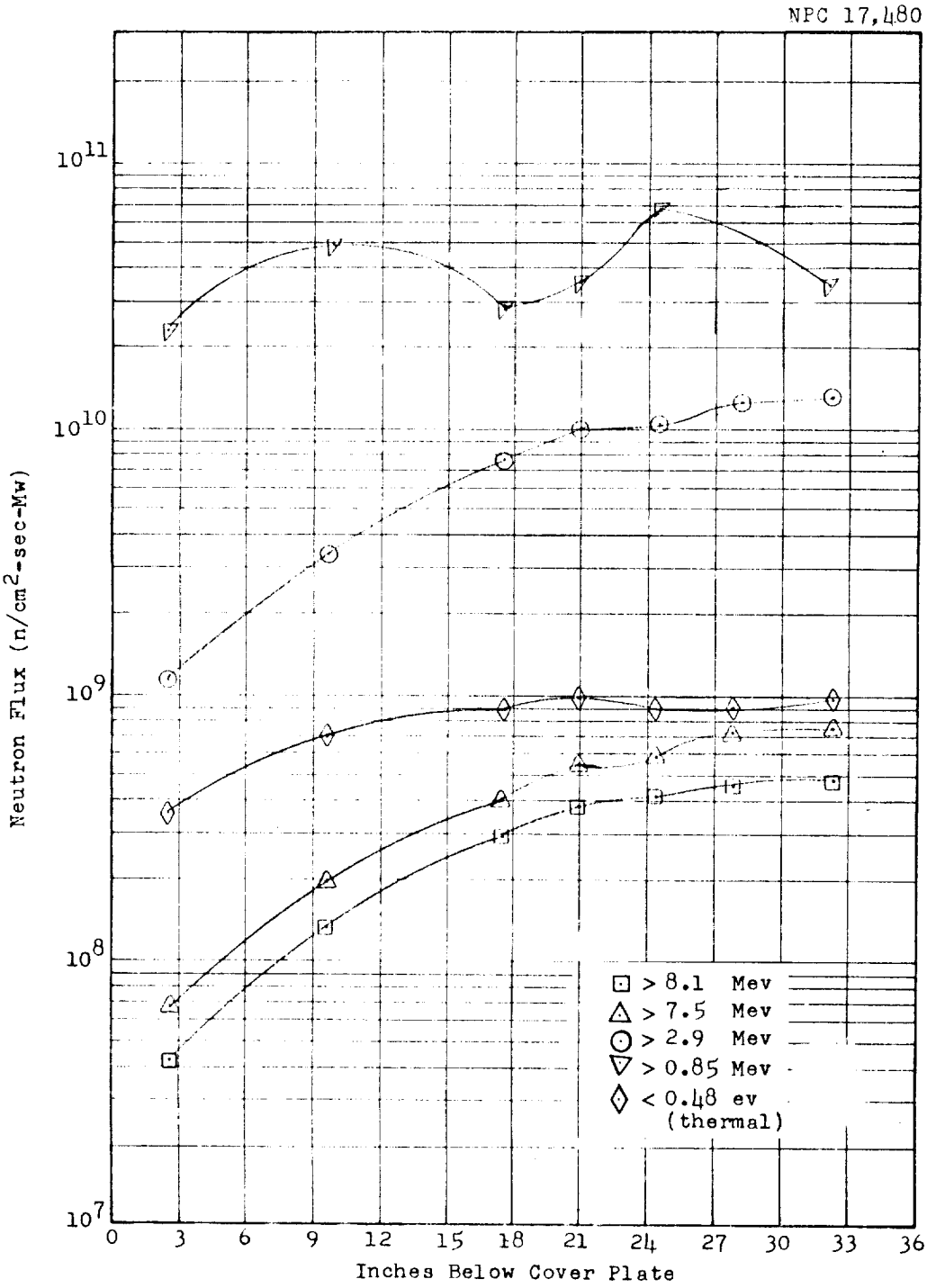

Figure 3.3 Average Neutron Flux on Rack 1 in Vacuum Chamber

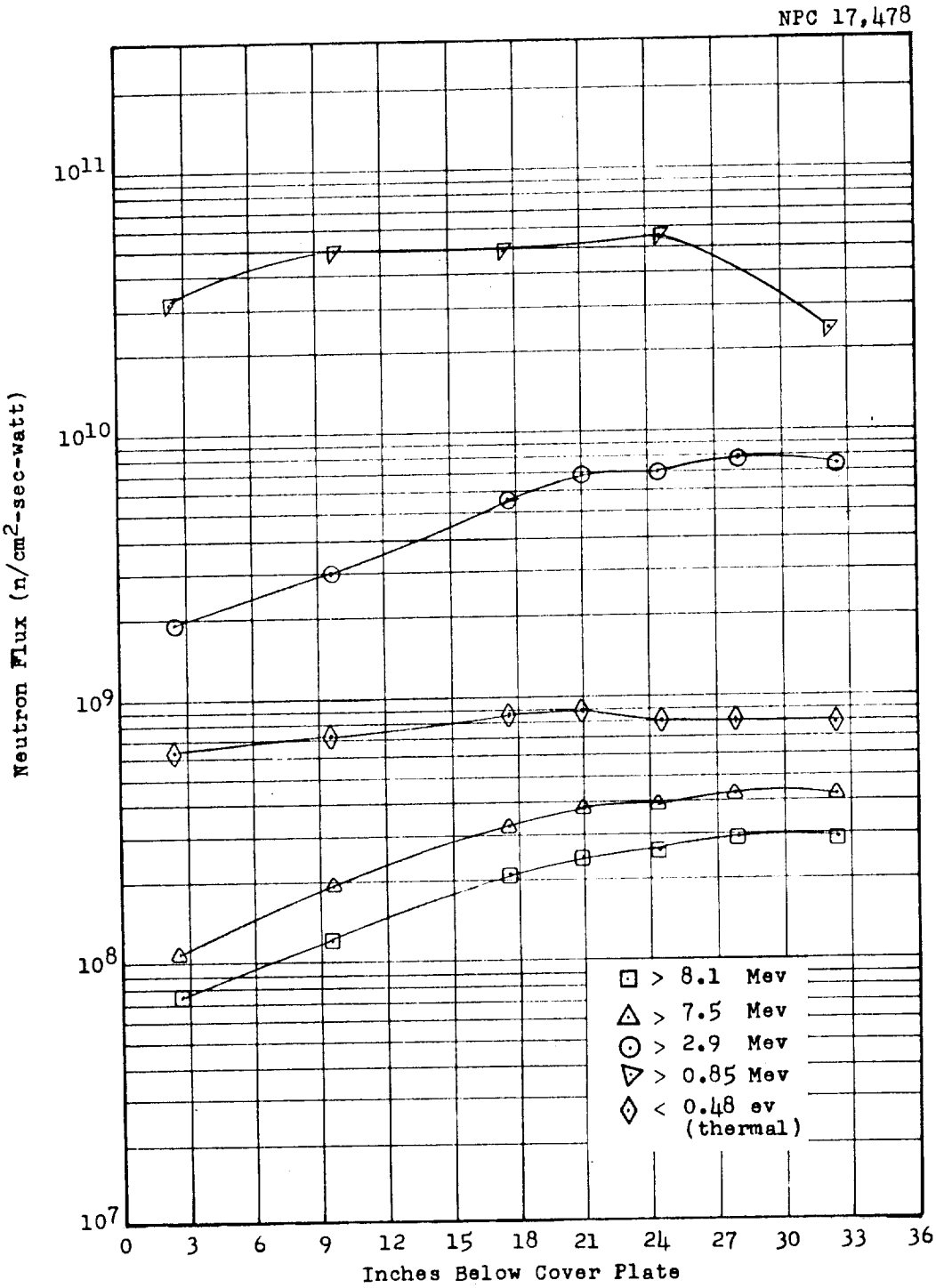

Figure 3.4 Average Neutron Flux on Rack 2 in Vacuum Chamber

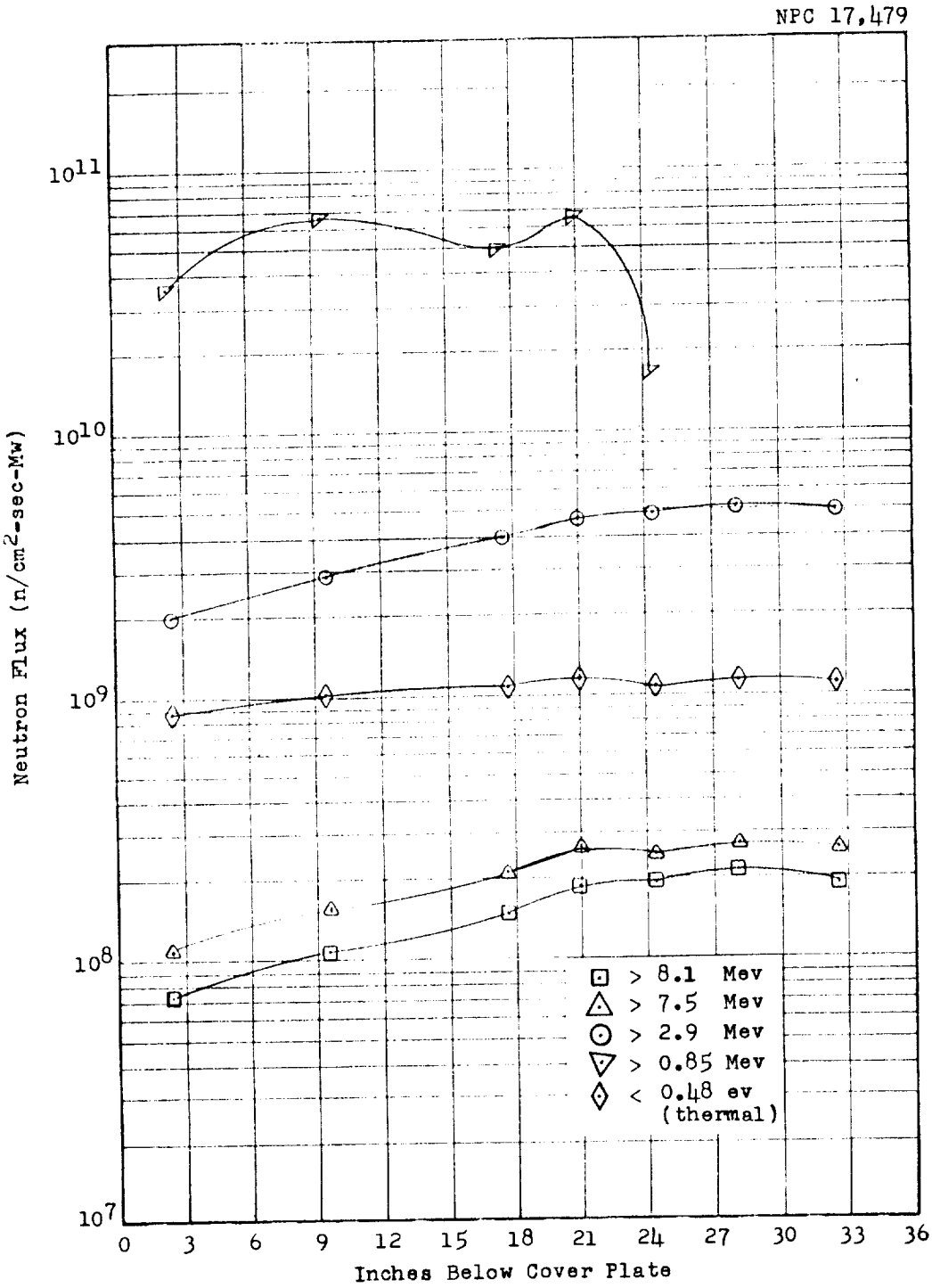

Figure 3.5 Average Neutron Flux on Rack 3 in Vacuum Chamber

Figure 3.6 shows the corresponding average gamma dose rate [ergs/gm(C)-hr-Mw] for each rack. Figure 3.7 shows the neutron spectrum inside the vacuum chamber as determined from the foil measurements. This spectrum is given for the energy interval 100 ev $\leq$ E $\leq$ 10 Mev and agrees closely with that of the analytical GTR spectrum which is discussed in Section 3.3.

The flux ratios shown in Table 3.1 are based on values obtained by averaging the neutron flux measured at the five detector positions between 17 and 25 inches below the top of the racks (see Fig. 3.2). All of these values, except those for the indium flux (E > 0.85 Mev), agree favorably with previous measurements of a similar nature (Ref. 6). No ready explanation is available for the erratic nature of the indium values, with the exception of possible errors in count-rate data reduction.

Table 3.1

Neutron Flux Ratios in East Vacuum Chamber

Rack No.	$\frac{\phi(E>2.9\ \text{Mev})}{\phi(E<0.48\ \text{ev})}$	$\frac{\phi(E>2.9\ \text{Mev})}{\phi(E>0.85\ \text{Mev})}$	$\frac{\phi(E>2.9\ \text{Mev})}{\phi(E>7.5\ \text{Mev})}$	$\frac{\phi(E>2.9\ \text{Mev})}{\phi(E>8.1\ \text{Mev})}$
1	13	0.23	18.5	27.5
2	9.3	0.12	17.8	26.2
3	4.3	0.30	19.0	27.0

The decay of irradiated indium is characterized by three activity levels, which, in order of half-lives, are 54 minutes for In^{116}, 4.5 hours for In^{115m}, and 43 days for In^{114}. The reaction

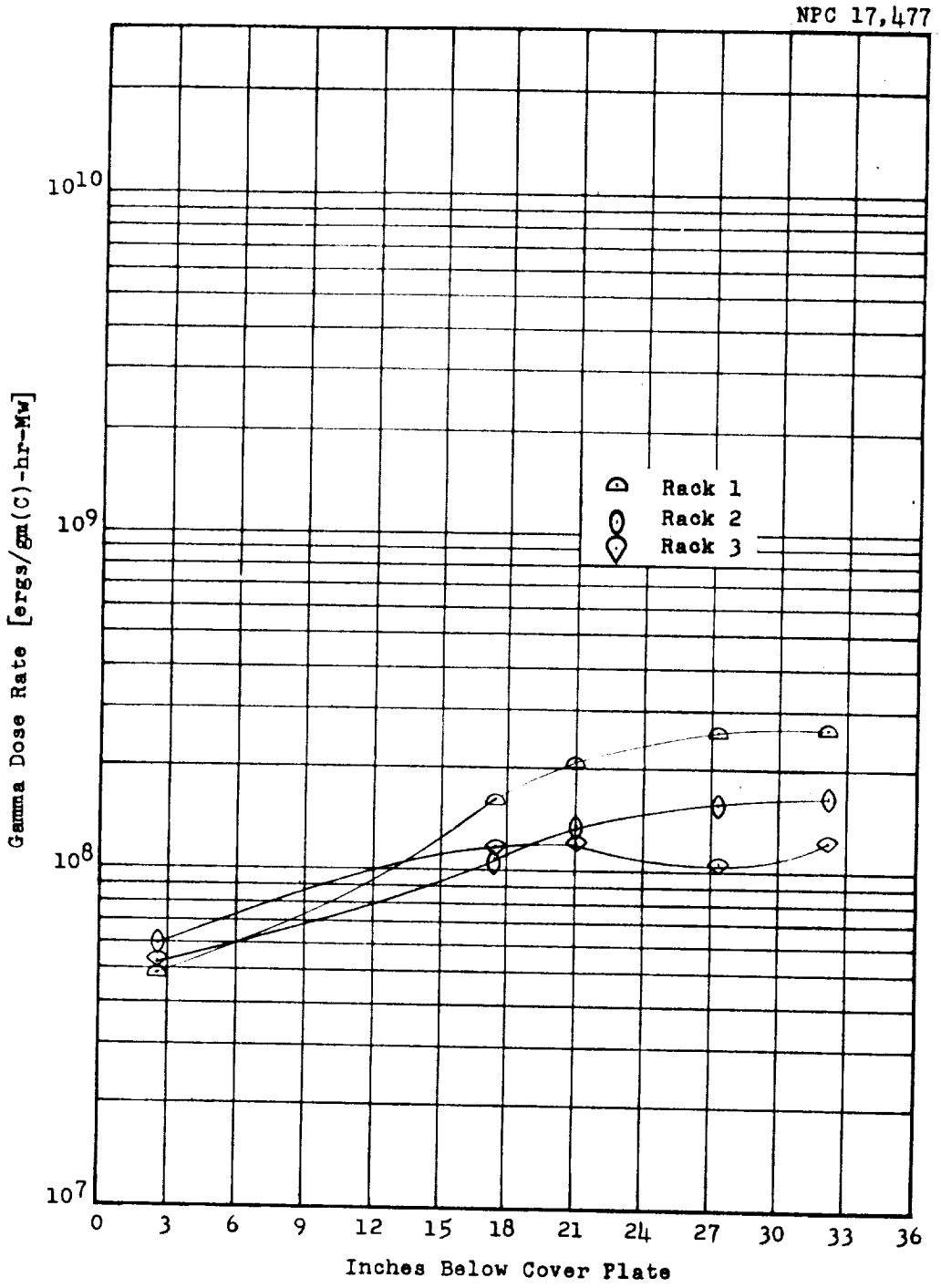

Figure 3.6 Average Gamma Dose Rate on Racks in Vacuum Chamber

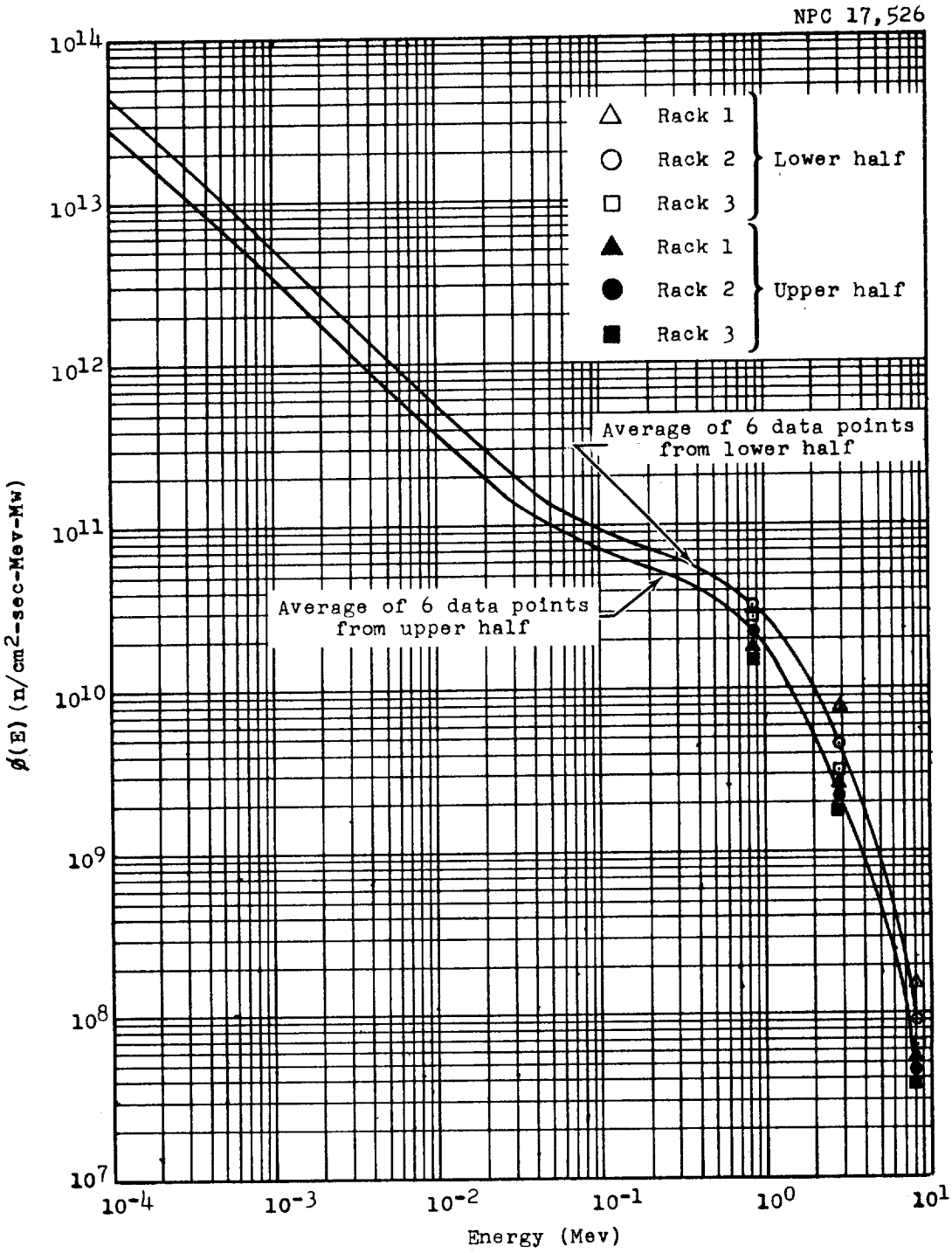

Figure 3.7 Average Neutron-Energy Spectrum Inside Vacuum Chamber

$In^{115}(n,n')In^{115m}$ is the reaction of interest here, having an effective threshold energy for the GTR spectrum of 0.85 Mev. The activity resulting from this reaction is much the weakest of the three, and frequently the separation of this activity is hindered by the two stronger activities. Work on the resolution of this problem is in progress and an early solution is anticipated.

Spatial distribution of the gamma flux (Fig. 3.6) is entirely acceptable and agrees well with previously measured data (Ref. 7). The neutron-flux and gamma-dose measurements are in good agreement with predictions. The 95% confidence interval for neutron data on one foil is $\pm$4%. From past experiments, the 95% confidence interval for an individual nitrous-oxide dosimeter has been determined to be $\pm$8%.

3.3 Analytical GTR Neutron Spectrum

The spectrum (Ref. 8) of the GTR in a water moderator has been measured to be Maxwellian at thermal energies ($E < 0.48$ ev), approximately E^{-1} from about 0.5 ev to 0.1 Mev, and essentially a fission spectrum for higher energies. In Figure 3.8, this spectral shape has been mathematically altered to account for the attenuation of the neutron flux by the boral surrounding the reactor in the dry-pool configuration. The resulting analytical spectrum has been shown to represent the actual spectrum fairly accurately.

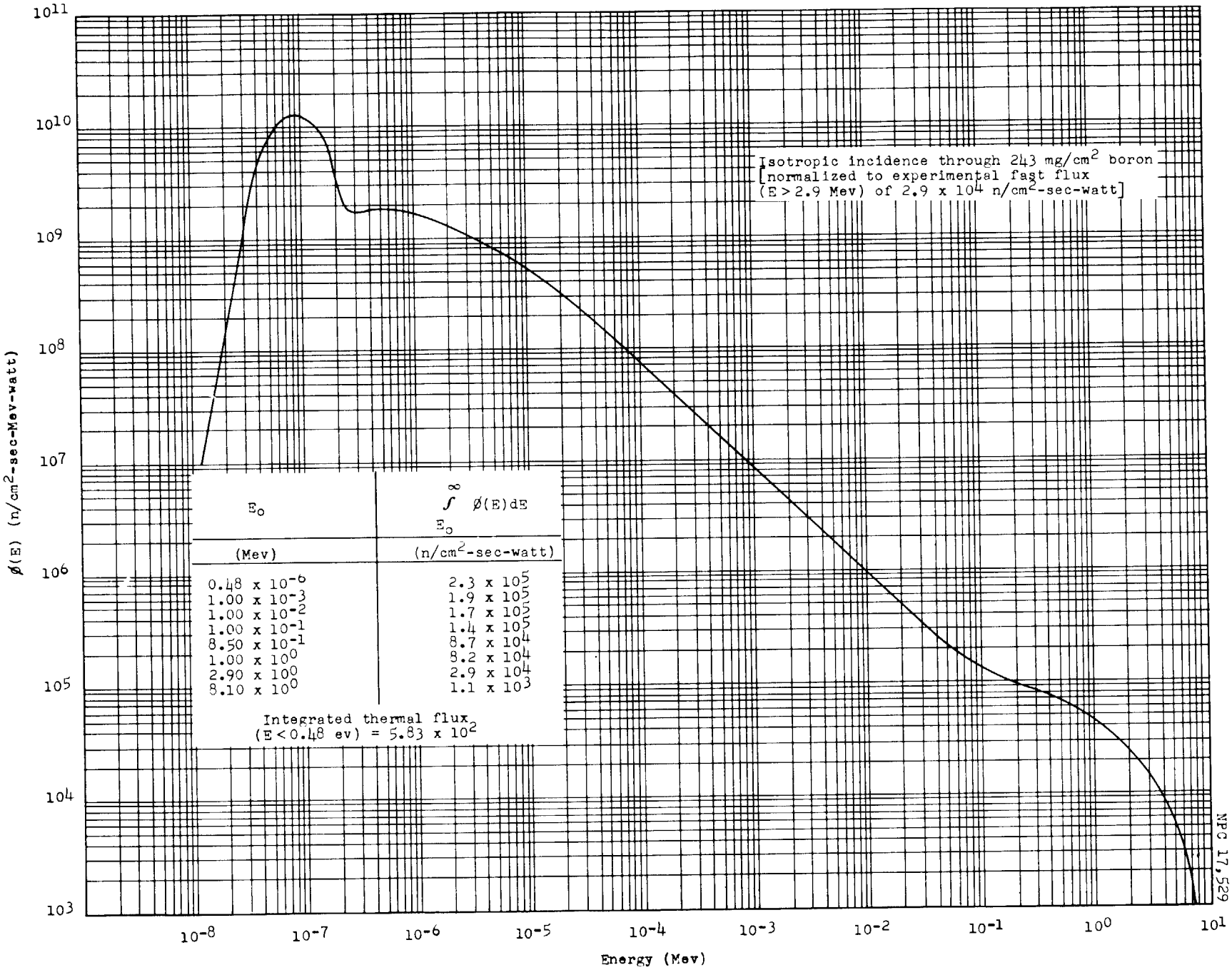

E_o (Mev)	$\int_{E_o}^{\infty} \phi(E)dE$ (n/cm²-sec-watt)
0.48 x 10⁻⁶	2.3 x 10⁵
1.00 x 10⁻³	1.9 x 10⁵
1.00 x 10⁻²	1.7 x 10⁵
1.00 x 10⁻¹	1.4 x 10⁵
8.50 x 10⁻¹	8.7 x 10⁴
1.00 x 10⁰	8.2 x 10⁴
2.90 x 10⁰	2.9 x 10⁴
8.10 x 10⁰	1.1 x 10³

Integrated thermal flux
(E < 0.48 ev) = 5.83 x 10²

Figure 3.8 Analytical GTR Neutron Spectrum

Flux measurements have been made in the thermal-, epithermal-, and fast-energy ranges by use of a variety of thermal, resonance, and threshold detectors. Measurements made in the dry side with the boral in place, in the energy range above 2.9 Mev, agree well with those made in the wet-pool side. The measured thermal flux is in general agreement with that obtained by integration of the analytical curve shown in Figure 3.8. Measurement of the epithermal flux by use of resonance detectors is very difficult and values differing by as much as a factor of 2 are obtained by the various detectors.

An experiment (Ref. 9) performed for Sandia Corporation mapped the irradiation volumes with plutonium, neptunium, and uranium foils, and sulfur pellets of the type used by GD/FW. The foil counting and data reduction were done by Sandia. The results as reported by Sandia show that Sandia and GD/FW agree within a few percent on sulfur measurements ($E > 2.9$ Mev) and that fission-foil data agree favorably with the analytical spectrum at all locations.

The neutron spectrum above 0.5 Mev has also been determined at one location by means of Ilford neutron plates (type E-1). Integrals of this spectrum agree closely with integrals of the analytical spectrum.

In June 1960, a comprehensive foil calibration experiment encompassing both GD/FW and Aerojet-General Nucleonics (AGN) foils was conducted (Ref. 8). The results of the two independent counting and data-reduction programs agree within a few percent.

IV. TEST PROCEDURES AND RESULTS

Seven vacuum irradiations were performed during this phase of the experiment, with the exposure ranging in value (depending on the radiation resistance of the materials) from 1.3×10^9 ergs/gm(C) and 1.57×10^{14} n/cm^2 (E > 2.9 Mev) to 4.8×10^{10} ergs/gm(C) and 7.7×10^{15} n/cm^2 (E > 2.9 Mev). The narrow range of doses obtainable during one vacuum irradiation resulted in some compromises on the desired radiation exposure of a few materials.

The late delivery of the vacuum systems from the vendor prevented the determination of most of the vacuum control values. Tests to determine the effects of high vacuum on materials at various temperatures have been performed by the George C. Marshall Space Flight Center. The results of these tests, which were used during the materials selection, are given in Appendix B.

The results of the mechanical tests performed on static irradiated samples and on dynamic irradiated samples are presented in Section 4.2 and in Sections 4.3 through 4.6, respectively. Each section dealing with dynamic irradiated samples is titled by the type of test equipment used. In Section 4.7 are the results of the optical tests performed on the static irradiated thermal-control coatings. A table is presented at the start of each section listing the materials tested. A complete list of the test materials, their manufacturers, and special cure information is given in Appendix C for each of the material categories.

Graphs of sample temperatures taken during the vacuum irradiation are presented in Appendix D. A description of the standard and special test techniques used in this experiment are given in the applicable sections.

4.1 Vacuum-Irradiation Pressure Data

The first vacuum-irradiation test was conducted on static material samples in August 1962 (Sec. 4.2). The pressures maintained in the test chambers during this test are plotted as a function of time in Figure 4.1. Since the Philips gage was being recalibrated, only the Hughes gage was used to monitor the pressure.

Shortly after reactor startup, a diffusion pump in the east system was automatically shut off by a thermoswitch incorporated as a safety feature to prevent overheating of the diffusion pumps. This caused the rise in pressure shown in Figure 4.1. Changing to a new cooling system allowed the diffusion pump to restart. The pressure rise in the west system after approximately 45 hours of radiation was due to loss of air pressure to the latching mechanism. This occurred when the engine-driven air compressor was turned off for servicing.

A second static test was conducted in the west chamber later in August 1962 to take advantage of an open reactor position. The vacuum systems were too radioactive to permit changing of the Hughes gage tubes. Although the one remaining filament functioned satisfactorily at the start of the test, the grid current decreased shortly after from the standard 5 μa to 1.2 μa, even with maximum filament voltage. The grid current stayed at this level throughout the irradiation.

The vacuum-system pressure had been decreasing at about the same rate as in the first test when the grid current began to change. From the rate of pressure decrease and the amount of time that elapsed

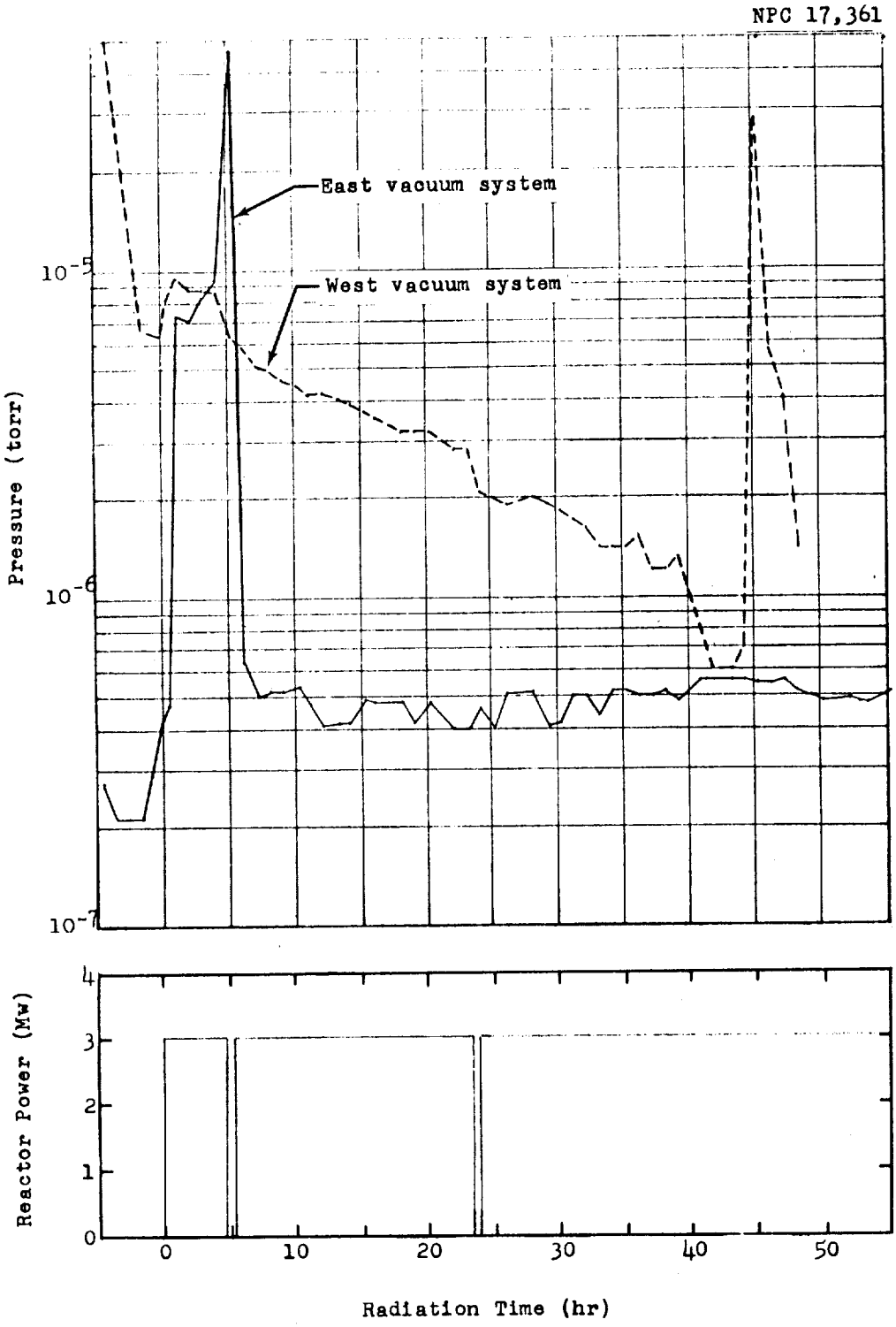

Figure 4.1 Vacuum-Chamber Pressure During Static Tests

from the beginning of pump-down to the pressure-gage failure, it was estimated that an ultimate vacuum of at least 5×10^{-6} torr was reached. Since the recorded pressure-gage readings are in error, they are not included in the report.

The first dynamic tests in the vacuum chambers were conducted in September 1962. The Low-Force Dynamic Tester was in the east vacuum system and the High-Force Dynamic Tester was in the west system. The chamber pressures maintained during these tests are shown in Figure 4.2.

Shortly after reactor startup, the automatic-control system turned off the diffusion-pump heaters in the west chamber because of low cooling-water pressure. This action resulted in an increase in the vacuum-chamber pressure, which did not decrease when the diffusion pumps were returned to operation. It appeared that a leak had developed in the chamber and that removal of the vacuum system from the reactor pool would be necessary in order to find and repair the leak. This was not possible at the time because of the reactor schedule, so the test was continued.

Since Hughes nude ionization gages will not operate at pressures above 10^{-4} torr, the pressure in the west vacuum chamber was monitored with the thermocouple gage in the forepump line. It was later determined that approximately 300 microns was maintained in this chamber during the remainder of the test.

The east chamber maintained a high vacuum throughout the radiation period.

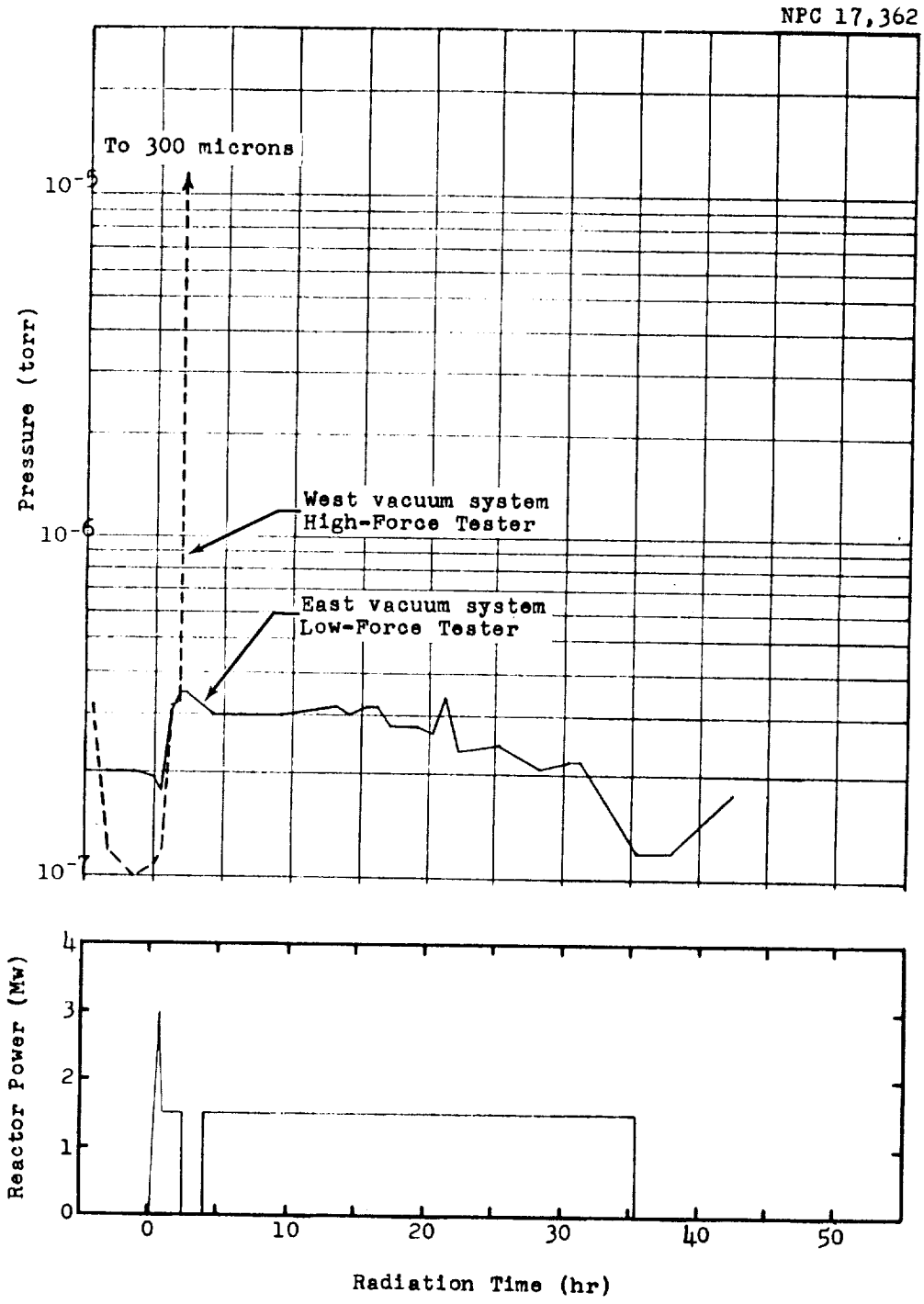

Figure 4.2 Vacuum-Chamber Pressure During Dynamic Tests

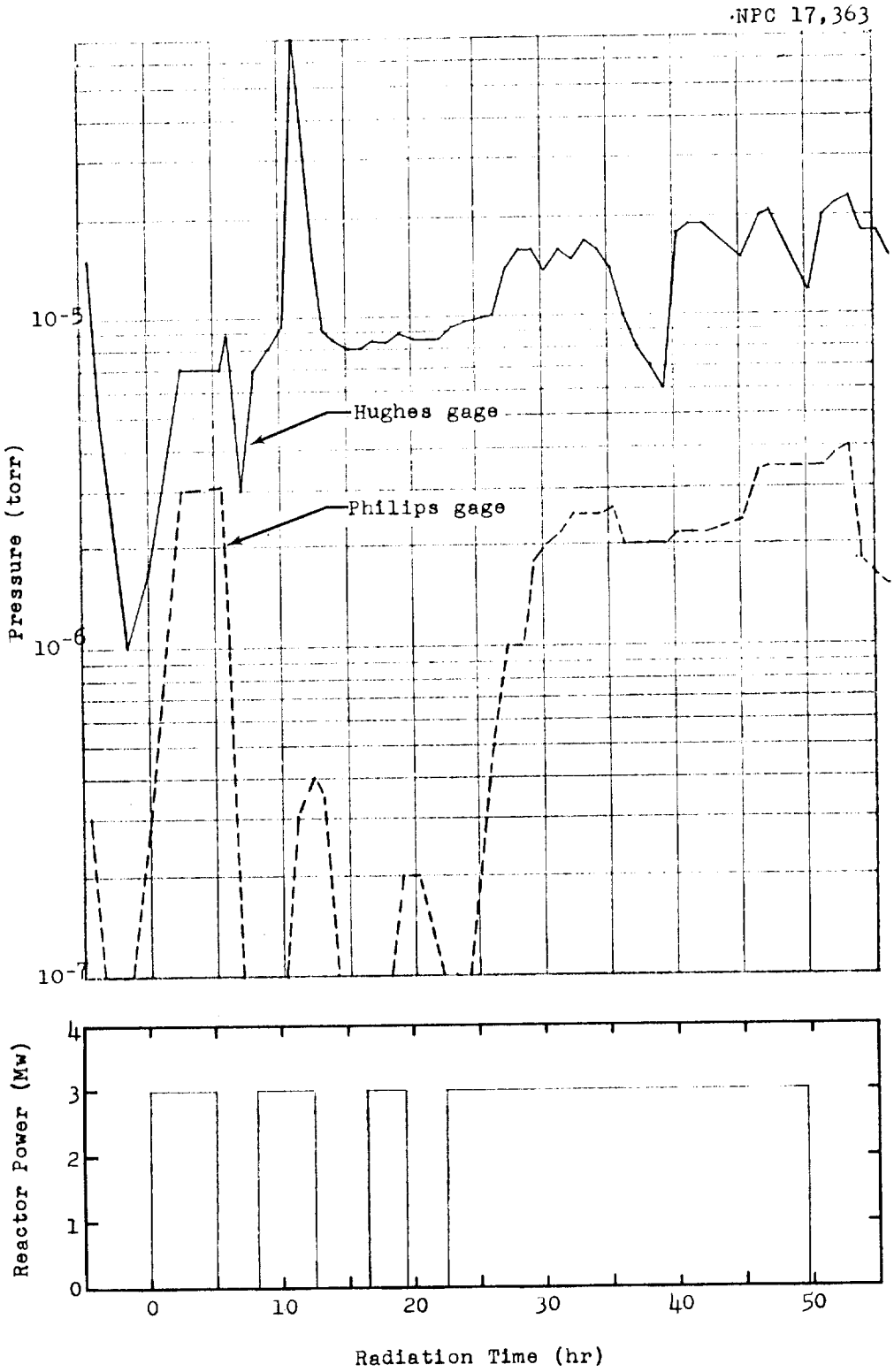

Figure 4.3 Vacuum-Chamber Pressure During Rerun of High-Force Dynamic Test

The High-Force Dynamic Tester was rerun later in the west system. The recalibrated Philips gage had been installed and both the Hughes and the Philips gages were monitored during the radiation period. The discrepancies in the pressure readings of the two gages, as shown in Figure 4.3, might be due to the internal pumping characteristics of the Philips gage.

A determination of the effect of reactor radiation on vacuum gages was made during the first static irradiations. The Hughes 1GC-101 Gage Controller with the 6578 nude Bayard-Alpert-type tube was used. Pressure readings taken in the standard way with the emission current turned on produced a pressure reading of 4.8×10^{-7} torr in the east chamber and 3.2×10^{-6} torr in the west chamber. With the emission current turned off and the electronic equipment standardized, a "vacuum reading" of 2.8×10^{-7} torr for the east chamber and 2.7×10^{-7} torr for the west chamber was observed. While still operating, the reactor was withdrawn from the closet at its maximum speed of 90 in./min, essentially eliminating the radiation field at the vacuum systems in about 10 seconds. With the reactor removed, the gage readings immediately fell to approximately 5×10^{-7} torr and stabilized at 3×10^{-9} torr after some 10 minutes.

From these gage observations, it was concluded that the "background" readings of $\sim 2.7 \times 10^{-7}$ torr were not due to additional radiation-induced positive-ion formation in the gaging elements,

since these would have responded to the pressure differences of approximately a factor of 10 in the two systems. A radiation-induced deterioration of the insulation resistance of the gage cables that run some 125 feet to the control room is a more likely source of the gage observations, since a large segment of the cable path lies outside the radiation shield in a reduced but, nevertheless, high dose-rate field. A shunting impedance as low as $\sim 2\text{x}10^{10}$ ohms would provide the observed ion-current reading ($\sim 10^{-8}$ amp) with the 180-volt differential that is employed between the grid and the collector. This problem has been eliminated, however, by relocating the gage cables, and the gage systems have provided satisfactory service within the inherent limitations discussed earlier.

During the time the reactor was out of the closet, pressure readings taken with the emission current turned on gave values of $2.2\text{x}10^{-6}$ torr approximately 8 minutes after reactor removal. The pressure reading of $4.8\text{x}10^{-7}$ torr in the east system decreased to $1.8\text{x}10^{-7}$ torr with reactor removed but emission on. This value, recorded 4 minutes after reactor removal, was maintained during the time of this test. When the emission current was turned off a reading of $2.8\text{x}10^{-9}$ torr was observed.

4.2 Static Test

A static test is one in which the specimens, after being subjected to the combined environments of vacuum and nuclear radiation, are tested under standard laboratory conditions. In the present static test, the specimens consisted of a wide variety of organic compounds in various test configurations. These compounds are classified according to their application in Table 4.1. The manufacturer and a complete description of each material are given in Appendix C.

4.2.1 Experimental Equipment

The equipment employed during the experiment included racks for mounting the specimens, an Instron tester, vacuum and transport specimen chambers, and a balance.

To facilitate the mounting of static specimens, an aluminum framework was designed that could be attached to the vacuum-chamber cover plate. This framework and the plate are shown in Figure 4.4. The specimens were wired to a grid of expanded metal, which in turn was wired to the framework.

The postirradiation testing of the tensile and compression properties of the specimens was conducted with a 10,000-lb Model TT Instron tester. This machine has five tensile load cells and two compressive cells to cover the 10,000-lb range. Each cell has six load ranges. The accuracy of the load-range detection system is independent of the range in use, and is better than $\pm$ 0.5% of that range.

The pre- and postirradiation vacuum chamber constructed in the IML is described in Section 2.2. This chamber was used for preirradiation out-gassing of the specimens and to leak-check the thermocouple Kovar seals.

A detailed description of the vacuum-irradiation chambers may be found in Section 2.2.

Transport chambers were used to prevent exposure of the test specimens to inclement weather during transport between the setup area in the IML and the reactor test area. These chambers are shown in Figure 13, page 84 of Reference 10.

The balance used for determination of weight change was a 200-gm Satorius Selecta automatic balance.

4.2.2 Experimental Operation

The static specimens were subjected to the combined effects of vacuum and radiation during two static runs and during the high- and low-force dynamic runs. The static specimens included in the dynamic runs were of the same material as the dynamic specimens. Therefore, for reasons of comparison and continuity, these static specimens are discussed in Sections 4.3 and 4.4.

After the specimens were fabricated from the various materials, they were measured and cleaned with either reagent grade acetone or isopropyl alcohol. The specimens were then placed in a dessicator for storage until preirradiation weighing and mounting on the specimen test racks. The approximate

Table 4.1

Test Plan for Static Test Materials

Material Application	Run No.	Test Chamber	Test Specimens		
			Type	Trade Name	Number Tested
Structural Adhesives	1	East	Lap shear	FM-1000	5
				Epon VIII	5
				Metlbond 406	5
		West	Lap shear	Epon 422J	5
				FM-47	5
				AF-6	4
				Metlbond-408	5
Seals	1	West	O-ring	Natural Rubber	3
				Buna N (66-581)	3
			Tensile	Buna N (66-581)	3
Thermal Insulation	1	East	Compression	Eccofoam Q	3
		West	Compression	Styrofoam 22	3
	2	West	Compression	Refasil Batting B-100	6
Structural Laminates	1	East	Tensile	CTL-91-LD	3
				Silicone DC-2106	3
				Mobiloy AH-81	3
Electrical Insulation	1	West	Tensile	Kel-F-81	3
				Mylar (10 mil)	3
				Silicone DC 7-170	3
	2	West	Film	Mylar A (3 mil)	8
				Mylar C (1 mil)	8
Potting Compounds	1	West	Compression	Epon 828/Z	3
				Silicone DC R-7521	3

Table 4.1 (cont'd)

Material Application	Run No.	Test Chamber	Test Specimens		
			Type	Trade Name	Number Tested
Dielectric Materials	1	East	Film	Teflon (40 mil) Teflon (10 mil) Marlex 6002 (14 mil) Teflon 100 (40 mil)	3 (no data) 3 (no data) 3 3
	2	West	Film	Teflon (40 mil) Teflon (10 mil) Teslar	4 4 8
Elastomers	1	East	Tensile	Viton A	4
		West	Tensile	Buna N (66-581)	3
	2	West	Tensile	Buna N (RA 30760) Neoprene (RA 24160)	8 8
Thermal-Control Coatings	1	West	See Section 4.7 for a complete description of these specimens	See Section 4.7	See Section 4.7

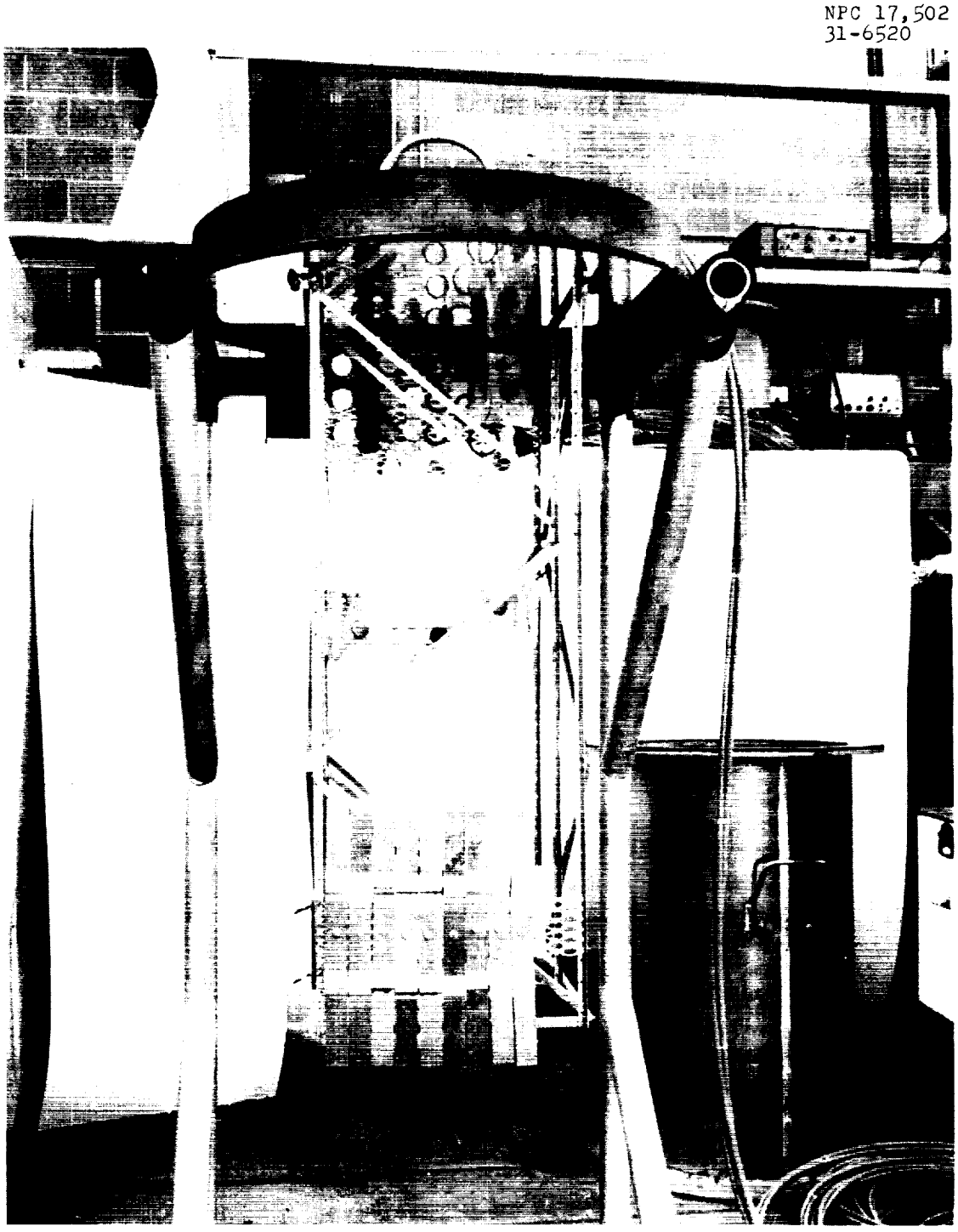

Figure 4.4 Sample Rack for Static Vacuum Irradiation

sample locations on the test racks are given in Figures 4.5, 4.6, and 4.7. After the specimens had been mounted on the test racks, thermocouples made from 3-mil copper-constantan wire were embedded in a representative temperature specimen. Where the geometry of the specimens would not allow embedding of the thermocouples (such as thin-film specimens), the thermocouples were attached with a small piece of fiber-glass tape.

Dosimetry packets containing both neutron and gamma detectors were mounted on the racks and the racks installed in the preirradiation vacuum chamber for leak checking of the irradiation-chamber cover and specimen de-gassing ($\sim$ 15 hours). Following this procedure, the racks were removed, installed in transport chambers, and transferred to the reactor test area for installation in the vacuum-irradiation chambers.

The vacuum-irradiation chambers were pumped down, checked for leaks, and set in the test position. When a sufficient vacuum was obtained, the irradiation run was started. The temperature of the specimens and the vacuum-chamber pressure were monitored throughout the irradiation period. Because of the high-radiation field following the irradiation period, approximately one day was required before the samples could be removed from the vacuum-irradiation chambers. The specimens were then transported to the IML in the transport chambers where they were weighed and stored in a dessicator until postirradiation testing was performed. Postirradiation testing started one week after the completion of the irradiation and continued until all specimens were tested.

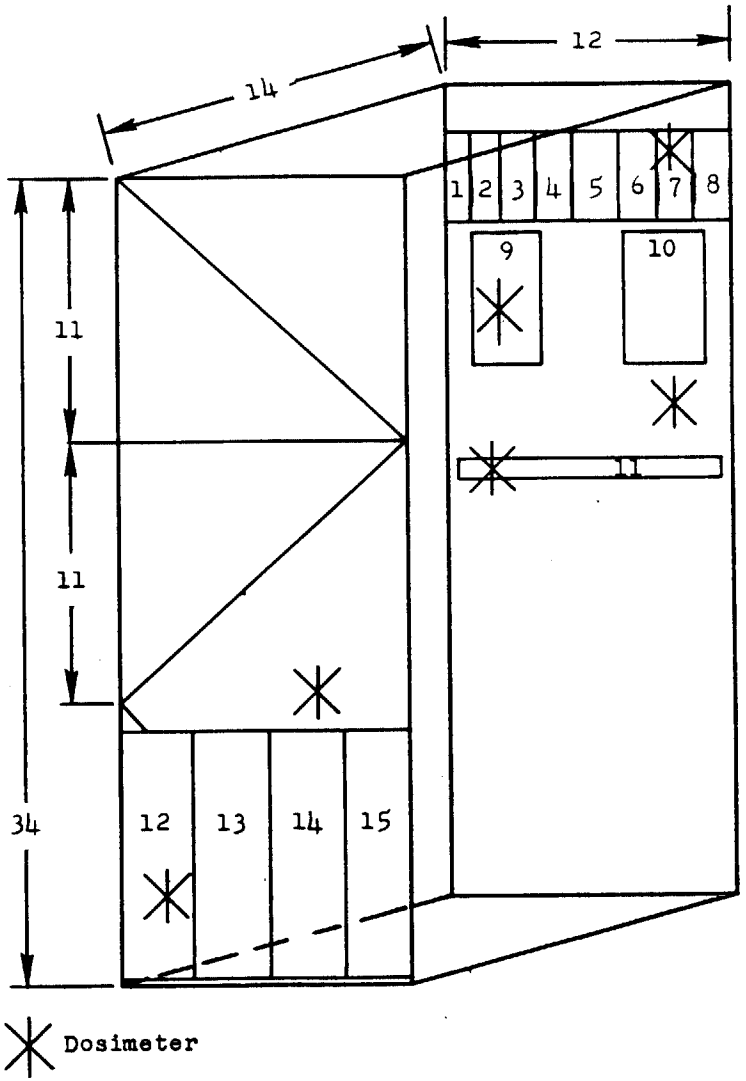

Material Samples

1. Styrofoam 22
2. Epon 828
3. RTV 501
4. Silicone DC-R7521
5. Natural Rubber O-ring
6. Silicone 7-170
7. Buna N O-ring
8. Buna N (tensile)
9. Mylar
10. Kel-F-81
11. Thermal Coatings
12. FM-47
13. Epon 422J
14. AF-6
15. Metlbond 403

All dimensions in inches

Figure 4.5 Location of Samples and Dosimeters for Static Irradiation: West Vacuum System; Run 1

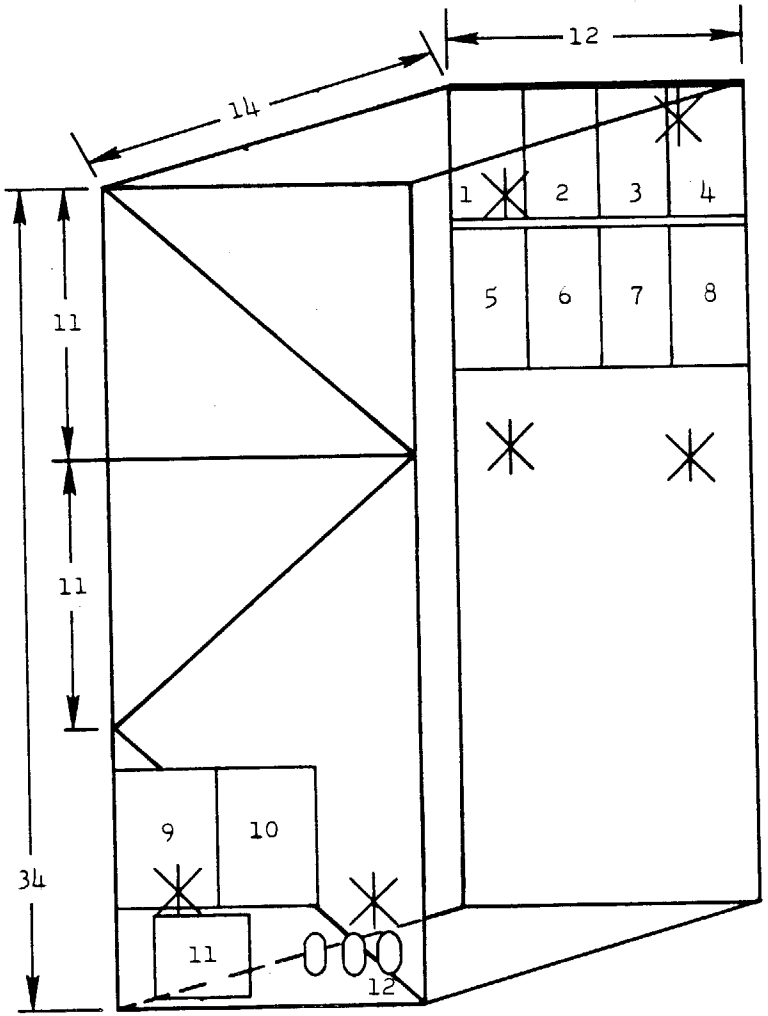

Material Samples

1. Teflon (40 mil)
2. Teflon (10 mil)
3. Marlex
4. Teflon 100
5. Epoxy VIII
6. Metlbond 406
7. FM 1000
8. Viton A
9. CTL-91-LD
10. DC-2106
11. Mobiloy AH-81
12. Eccofoam

All dimensions in inches

Figure 4.6 Location of Samples and Dosimeters for Static Irradiation: East Vacuum System; Run 1

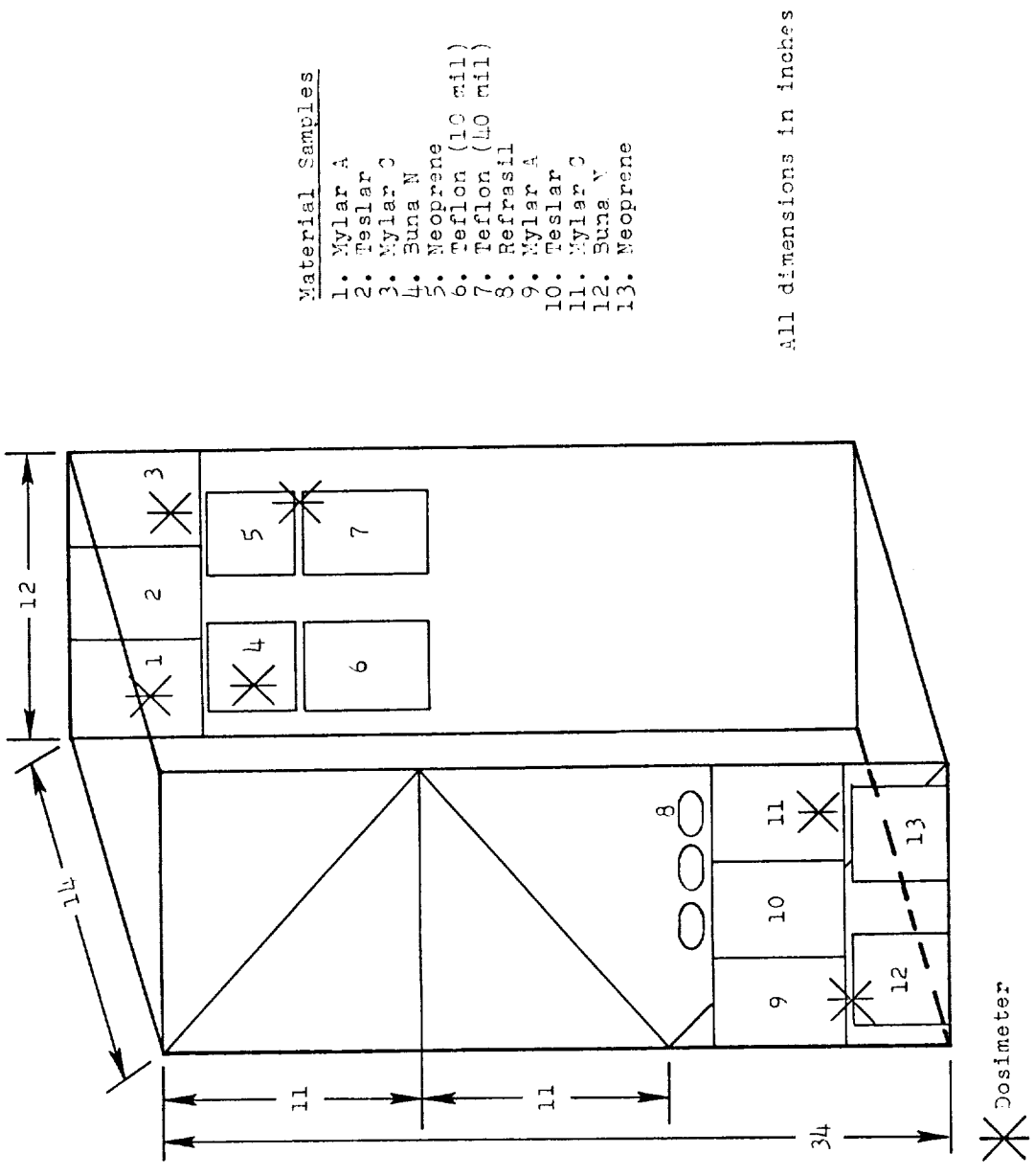

Figure 4.7 Location of Samples and Dosimeters for Static Irradiation: West Vacuum System; Run 2

Two static runs were conducted. During the first, the east and west vacuum chambers were used. The average gamma dose received for the 55-hr irradiation at 3 Mw in the west chamber was 3.83×10^{10} ergs/gm(C) on the front rack and 1.43×10^{10} ergs/gm(C) on the rear rack. In the east chamber, for the same irradiation period, the gamma doses were 4.63×10^{10} and 1.30×10^{10} ergs/gm(C) for the front and rear racks, respectively. (The front racks had two dosimeters, the rear racks had four as shown in Figures 4.5 and 4.6) During the second static irradiation of 16 hours duration at 1.25 Mw power level, the west chamber was used. The total gamma dose in the chamber during this run averaged 6.2×10^{9} and 1.55×10^{9} ergs/gm(C) for the front and rear racks, respectively. The dosimeter locations are shown in Figure 4.7. The neutron fluxes and gamma doses given in Tables 4.2 through 4.9 are those from the detectors closest to the material specimens.

Plots of specimen temperature vs radiation time are located in Appendix D. Plots of vacuum-chamber pressure vs radiation time are given in Section 4.1, Figure 4.1.

4.2.3 Mechanical-Property-Test Results

Data obtained from the mechanical-property tests of the vacuum-irradiated and control samples are presented in Tables 4.2 through 4.9. The control specimens were tested in the "as-received" condition to establish the quality of the batch.

Photographs of the test samples, showing the change in color between the vacuum-irradiated samples and the control samples, were made. Copies of these photographs are on file with NASA at Huntsville. Because of the difficulty involved in reproducing true color in photographs, these pictures are not included in this report.

The color changes that occurred in these specimens are noted in the results for each material. These are color changes visible to the eye and are not the result of colorimetric analysis.

The following paragraphs describe the test procedures and discuss the results of the mechanical-property tests.

4.2.3.1 Structural Adhesives

The structural adhesives were fabricated and tested as lap-shear specimens in accordance with ASTM D-1002-53T. The specimens were tested in the Instron tester, with the force-at-failure recording in Table 4.2 as pounds per square inch of shear area.

The data show that radiation produced no detectable change in the lap-shear strength of the FM-1000, Metlbond 406, Epon 422-J, and AF-6 specimens. In some materials, however, the lap-shear strength was altered: Metlbond 408 decreased 78% in lap-shear strength, Epon VIII decreased by about 12%, and FM-47 decreased by approximately 42%. As indicated in Reference 4, FM-47 only lost 36% of its lap-shear strength after a

dose of 8.6×10^{10} ergs/gm(C) at 180°F. This was twice the dose received during the present test, yet the material experienced less change in tensile strength.

Metlbond 406 was also tested in the cryotemperature portion of this experiment. Full details of these tests are given in Reference 1. For comparison purposes, the data on the samples that were irradiated in air are given in Table 4.2. The test samples for these two experimental programs were fabricated in two batches, which resulted in a difference in ultimate tensile shear strength of the control samples. In view of this, only the general trends will be indicated here. For a dose of 1.1×10^{10} ergs/gm(C) the air-irradiation samples showed a small increase in the average ultimate shear strength, while the vacuum-irradiation samples showed a small decrease. For the higher dose in air of 4.9×10^{10} ergs/gm(C), the samples showed a decrease of 85% in ultimate shear strength.

4.2.3.2 Seals (O-rings and tensile specimens)

O-rings out of two materials, Parker Compound 66-581 (Buna N) and a natural-rubber compound provided by NASA, were included in the static tests. Both materials were tested for tensile properties in accordance with ASTM D-1414-56T. Buna N tensile specimens were also tested in accordance with ASTM D-412-51T. A weight-loss determination was conducted on all specimens. Results are presented in Table 4.3.

Table 4.2

Test Environment and Results of Static Test: Structural Adhesives

Material	Radiation Exposure				Ultimate Shear Strength (psi)	Temperature		Pressure	
	Gamma [ergs/gm(C)]	Neutron (n/cm^2)				Avg (^oF)	Fig. No.	Avg (torr)	Fig. No.
		Thermal	E>2.9 Mev	E>8.1 Mev					
FM-1000 (epoxy-nylon)	0	0 (control specimens)	0	0	6302 6117 6004 5946 5955 6065/153[a]	77	-	760	-
	1.67(10)	5.14(14) (vacuum irradiation)	2.7(15)	1.0(14)	6455 6004 6321 5642 6185 6121/350	112[b]	D-5	5(-7)	4.1
Epon VIII (epoxy)	0	0 (control specimens)	0	0	2114 2399 2297 2189 2669 2495 2361/219	77	-	760	-
	1.67(10)	5.14(14) (vacuum irradiation)	2.7(15)	1.0(14)	1954 2083 2207 2087 2028 2072/109	112[b]	-	5(-7)	4.1

[a]Average value/standard deviation on an individual basis

[b]Estimated value based on similar temperatures of FM-1000

Table 4.2 (cont'd)

Material	Radiation Exposure				Ultimate Shear Strength (psi)	Temperature		Pressure	
	Gamma [ergs/gm(C)]	Neutron (n/cm^2)				Avg (°F)	Fig. No.	Avg (torr)	Fig. No.
		Thermal	E>2.9 Mev	E>8.1 Mev					
Metlbond 406 (epoxy polyamide) Batch No. 1	0	0 (control specimens)	0	0	4715 4177 5601 4736 4951 4760 4823/562	77	-	760	-
	1.67(10)	5.14(14) (vacuum irradiation)	2.7(15)	1.0(14)	4255 3836 5020 5321 4126 4512/638	112[a]	-	5(-7)	4.1
Metlbond 406 (epoxy polyamide) Batch No. 2 (Ref. 1)	0	0 (control specimens)	0	0	5000 5800 5950 5350 5724 5560	77	-	-	-
	1.1(10)	0 (air irradiation)	2.5(15)	0	5500 6080 5520 6160 5950 5940	77	-	760	-
	4.9(10)	0 (air irradiation)	1.6(16)	0	1000 500 690 800 770 752	77	-	760	-

[a] Estimated value based on similar temperatures of FM-1000

Table 4.2 (cont'd)

Material	Radiation Exposure				Ultimate Shear Strength (psi)	Temperature		Pressure	
	Gamma [ergs/gm(C)]	Neutron (n/cm^2)				Avg (°F)	Fig. No.	Avg (torr)	Fig. No.
		Thermal	E>2.9 Mev	E>8.1 Mev					
Epon 422J (epoxy phenolic)	0	0 (control specimens)	0	0	2495 2409 2288 2470 2312 2200 2362/116		-	760	-
	3.9(10)	4.8(14) (vacuum irradiation)	8.0(15)	2.8(14)	2257 2415 2475 2672 2441 2452/178	190	D-4	2(-6)	4.1
FM-47 (vinyl phenolic)	0	0 (control specimens)	0	0	3996 4143 3992 4333 4434 4180/190	77	-	760	-
	3.9(10)	4.8(14) (vacuum irradiation)	8.0(15)	2.8(14)	2709 2235 2351 2263 2519 2415/204	190[a]	D-4	2(-6)	4.1

[a] Estimated value based on similar temperature of Epon 422J

Table 4.2 (cont'd)

Material	Radiation Exposure				Ultimate Shear Strength (psi)	Temperature		Pressure	
	Gamma [ergs/gm(C)]	Neutron (n/cm^2)				Avg (^oF)	Fig. No.	Avg (torr)	Fig. No.
		Thermal	E>2.9 Mev	E>8.1 Mev					
Scotchweld AF-6 (nitrile phenolic)	0	0 (control specimens)	0	0	3094 2573 2358 2648 2134 2662 2578/379	77	-	760	-
	3.9(10)	4.8(14) (vacuum irradiation)	8.0(15)	2.8(14)	2252 2634 2327 2427 2410/186	200	D-4	2(-6)	4.1
Metlbond 408 (epoxy nylon)	0	0 (control specimens)	0	0	4346 4462 3846 4208 3553 4083/391	77	-	760	-
	3.9(10)	4.8(14) (vacuum irradiation)	8.0(15)	2.8(14)	1007 835 845 838 953 896/73.9	200[a]	D-4	2(-6)	4.1

[a] Estimated value based on similar temperature of Scotchweld AF-6

Table 4.3

Test Environment and Results of Static Test: Seals

Material	Radiation Exposure				Sample Weight		Tensile Strength (psi)				Ultimate Elongation %	Temperature		Pressure	
	Gamma [ergs/gm(C)]	Neutrons (n/cm^2)			Original (gm)	Change (gm)	@ 25% Elongation	@ 50% Elongation	@ 100% Elongation	Ultimate		Avg (°F)	Fig. No.	Avg (torr)	Fig. No.
		Thermal	E>2.9 Mev	E>8.1 Mev											
Parker Compound 66-581 (Buna-N) O-rings	0	0 (control specimens)	0	0	-	-	-	-	280 270 280 283 278/6.31	1349 1322 1355 1300 1331/26.7	487 480 493 512 493/15.5	77	-	760	-
	8.06(9)	2.8(14) (vacuum irradiation)	1.2(15)	4.5(13)	1.5945 1.5988 1.6067	-0.0206 -0.0203 -0.0200	500 356 407 421/85.0	1155 1000 1150 1102/91.6	- - - 	1818 1965 1690 1824/162	76 87 70 78/10.0	112[a]	-	2(-6)	4.1
	3.2(9)	- (air irradiation)	4.7(14)	-	-	-	-	-	636/1.7/3	1530/3.8/3[b]	246/1.8/3	-	-	-	-
	1.1(10)	- (air irradiation)	1.8(15)	-	-	-	-	-	1951/12/3	2077/9.1/4	104/13/4	-	-	-	-
Parker Compound 66-581 (Buna-N) Tensile Specimens	0	0 (control specimens)	0	0	-	-	183 199 174 150 176.5/23.8	238 285 267 250 260/22.8	320 430 449 350 387.2/62.7	1440 1331 1423 1350 1386/52.9	412 408 425 415 415/8.2	77	-	760	-
	8.06(9)	2.8(14) (vacuum irradiation)	1.2(15)	4.5(13)	4.5873 4.9099 4.5546	-0.0646 -0.0613 -0.0590	820 860 782 821/46.1	- - - 	- - - 	1588 1740 1855 1728/158	55 62 70 62/8.9	112[a]	-	2(-6)	4.1

[a]Estimated value based on similar temperatures of natural rubber

[b]Average value/standard deviation on an individual basis/number of specimens

Table 4.3 (cont'd)

Test Environment and Results of Static Test: Seals

Material	Radiation Exposure				Sample Weight		Tensile Strength (psi)				Ultimate Elongation %	Temperature		Pressure	
	Gamma [ergs/gm(C)]	Neutrons (n/cm^2)			Original (gm)	Change (gm)	@ 25% Elongation	@ 50% Elongation	@ 100% Elongation	Ultimate		Avg (°F)	Fig. No.	Avg (torr)	Fig. No.
		Thermal	E>2.9 Mev	E>3.1 Mev											
Natural Rubber Compound RA33860 (O-ring)	0	0 (control specimens) September 1962	0	0	-	-	117 108 94 101 108 108 106/9.1	192 180 166 176 180 173 178/10.3	330 313 296 316 309 302 311/13.4	1880 2030 2070 2270 2150 2065 2105 2081/144	416 456 474 477 460 468 480 462/23.7	77	-	760	-
		(control specimens) February 1963					115 106 106 117 124 114/7.7	184 184 181 192 206 189/10.7	330 326 326 330 337 330/4.7	2206 1986 2180 2241 1745 2072/213	441 423 456 468 395 437/31.4	77	-	-	-
		(vacuum controls) February 1963			1.0029 0.9934 0.9950 0.9909 0.9935	-0.0101 -0.0097 -0.0099 -0.0087 -0.0105	121 121 128 121 131 124/4.3	195 192 206 199 213 201/9.0	340 340 348 348 358 347/7.7	1950 2177 1997 1986 1915 2005/113	407 444 426 425 407 422/15.9	77	-	1(-6)	-
	9.03(9)	2.9(14)	1.4(15)	5.1(13) (vacuum irradiation)	0.9971 0.9980 0.9932	-0.0001 +0.0007 +0.0006	277 284 270 277/8.3	497 515 515 509/10.6	980 1010 1050 1013/41.3	1100 1073 1073 1082/43.1	120 114 109 114/6.5	112	D-3	3(-6)	4.1

Parker Compound 66-581. Because the number of O-rings made from Buna N was limited, values for the control specimens were taken from previous data generated at NARF (Ref.11). These data include the tensile strength at 100% elongation, the ultimate tensile strength, and the ultimate elongation. Comparison of these values with those from the vacuum-irradiation specimens shows that the ultimate tensile strength of the irradiated O-rings increased by 37% over that of the control O-rings and that the ultimate elongation decreased by 85%. The average weight loss was 1.27%.

Data are also given on the effects of irradiating Buna N O-rings in air (Ref. 10). These data show that the ultimate elongation of specimens decreased more when irradiated in a vacuum with a dose of 8.06×10^9 ergs/gm(C). Thus, the exclusion of oxygen does not enhance the tensile properties enough to offset the damaging effect of the vacuum.

When Parker Compound 66-581 was tested in the form of tensile specimens, the ultimate tensile strength increased by approximately 25% and the ultimate elongation decreased by 85%. The average weight loss was 1.32%.

Natural-Rubber Compound. Table 4.3 shows that, compared to the September 1962 control specimens, the ultimate tensile strength of this material decreased 48% and the ultimate elongation decreased approximately 75% after a vacuum irradiation of 9×10^9 ergs/gm(C). Although there was a minute gain in the weight of the specimens, it is not considered significant and is attributed to moisture absorption prior to the postirradiation weighing.

A second set of control specimens in the "as received" condition were tested in the Instron with the vacuum control specimens. These data, presented in Table 4.3 (February 1963), show no significant changes in the material properties due to shelf aging. Also shown are the vacuum control results, which show no change in physical properties.

4.2.3.3 Thermal Insulations

Three thermal insulation materials were tested during the two static runs: Refrasil Batting B-100, Styrofoam 22, and Eccofoam Q.

Refrasil Batting B-100. The Refrasil was tested in the form of compression stacks 0.5 inch high by 1 inch square. As shown in Table 4.4, the compressive strength of Refrasil decreased 24% at 80% deflection and 31% at 40% deflection because of the vacuum-irradiation exposure.

Styrofoam 22. Styrofoam discs measuring 0.5 inch high by 1.129 inches in diameter were tested for compressive properties in accordance with ASTM D-1565-58T. The compressive strength at 25% deflection is given in Table 4.4. There was no significant change due to the vacuum-irradiation exposure. An average weight loss of 0.66% occurred for the three specimens tested.

A second set of specimens in the "as received" condition were tested in the Instron with the vacuum control specimens. These data, presented in Table 4.4 (February 1963), show no significant changes in the material properties. The vacuum

Table 4.4

Test Environment and Results of Static Test: Thermal Insulation

Material	Radiation Exposure				Sample Weight		Compressive Strength (psi)				Temperature		Pressure	
	Gamma [ergs/gm(C)]	Neutrons (n/cm^2)			Original (gm)	Change (gm)	@ 20% Deflection	@ 40% Deflection	@ 60% Deflection	@ 80% Deflection	Avg (°F)	Fig. No.	Avg (torr)	Fig. No.
		Thermal	E>2.9 Mev	E>8.1 Mev										
Refrasil Batting B-100 (silicone oxide)	0	0	0	0	-	-	1.2 0.7 0.8 0.85 0.8 0.87/0.21	5.2 4.7 4.9 5.3 5.5 5.1/0.34	24.3 22.3 22.5 24.4 24.8 23.7/1.1	138 129 133 136 134 134/3.9[a]	77	-	760	-
		(control specimens)												
	5.4(9)	9.2(12)	9.8(13)	3.7(12)	-	-	0.65 0.65 0.9 0.9 0.7 0.7 0.75/0.099	3.5 3.3 3.5 3.6 3.3 3.5 3.5/0.12	17.3 15.2 15.0 15.8 14.4 15.0 15.7/1.14	118 98.5 99 98.6 97 99.5 101.8/8.3	80	D-8	5(-6)	-
		(vacuum irradiation)												
Styrofoam (styrene)	0	0	0	0	-	-	@ 25% Deflection 28.5 30.5 32.4 30.5/2.3				77	-	760	-
		(control specimens) August 1962												
		(control specimens) February 1963					30.6 30.5 28.5 31.5 30.3/1.46				77		760	- -
		(vacuum controls) February 1963			0.2278 0.2344 0.2370 0.2279	-0.0043 -0.0047 -0.0048 -0.0046	25.8 27.7 29.7 26.8 27.5/1.9				77	-	1(-6)	-
	1.0(10)	3.1(14)	1.6(15)	5.8(13)	0.2431 0.2317 0.2359	-0.0016 -0.0016 -0.0015	31.5 29.4 - 30.5/1.9				112	D-3	2(-6)	4.1
		(vacuum irradiation) August 1962												
	5.0(9)	-	1.2(15)	-	-	-	14.5				-	-	760	-
		(air irradiation) Ref. 1												
	1.0(10)	-	2.6(15)	-	-	-	10.5				-	-	760	-
		(air irradiation) Ref. 1												

[a]Average value/standard deviation on an individual basis

controls were in vacuum for the same period of time as the irradiated samples. The resulting tests show a small decrease in weight loss and compression strength.

The resulting data from air irradiations of samples performed during the cryogenic portion (Ref. 1) of these experiments are included in Table 4.4. The samples were fabricated from the same batch of materials and tested in a similar manner. The results from the tests after vacuum irradiation of 1.0×10^{10} ergs/gm(C) show no change in compressive strength, but, for the air irradiation of 5.0×10^{9} ergs/gm(C), the compressive strength decreased 52% and, for the higher dose of 1.0×10^{10} ergs/gm(C), the compressive strength decreased 66%. This shows that the material was benefited by the exclusion of oxygen.

Eccofoam Q. The Eccofoam was tested in accordance with ASTM D-695-54. This material was to be fabricated into cylindrical specimens 0.5 inch in diameter by 1 inch tall; however, the hard, porous structure of this material made this configuration impractical, since attempts to fabricate the specimens in a lathe failed to produce specimens of consistent size. For this reason, the specimens were fabricated into 1-inch cubes.

The postirradiation test chosen for this material proved to be inadequate. The hard, porous nature of this material made comparison of compressive properties impossible. When a compressive force was applied to the specimens, the cell

structure began to break down and a very erratic trace of sharp peaks and valleys was recorded on the Instron. In comparing the control-specimen traces with the irradiated-specimen traces, no pattern of difference was detectable.

The test data required by ASTM D-695-54 was not included, since it would be misleading and meaningless.

4.2.3.4 Structural Laminates

Silicone DC-2106, phenolic CTL-91-LD, and phenolic Mobiloy AH-81 were irradiated in the east vacuum chamber during Run 1. Silicone DC-2106 and CTL-91-LD were fabricated into Type I tensile specimens and tested in accordance with ASTM D-638-58T. An extensometer was used on the specimens during postirradiation testing so that stress-strain curves could be obtained.

Mobiloy AH-81 was fabricated into straight specimens measuring 0.018 by 1.0 by 6.0 inches. This was done because the material was received as a single sheet and therefore could not be fabricated into Type I tensile specimens. The specimens were bench-marked and the ultimate elongation measured manually.

Silicone DC-2106. As shown in Table 4.5 and Figure 4.8, there was no significant change in the tensile strength and elongation of this material when subjected to the radiation exposure and vacuum pressure shown. The average weight loss was 0.188%.

Table 4.5

Test Environment and Results of Static Test: Structural Laminates

Material	Radiation Exposure				Sample Weight		Ultimate Tensile Strength (psi)	Ultimate Elongation (%)	Temperature		Pressure	
	Gamma [ergs/gm(C)]	Neutrons (n/cm^2)			Original (gm)	Change (gm)			Avg (^oF)	Fig. No.	Avg (torr)	Fig. No.
		Thermal	E >2.9 Mev	E >8.1 Mev								
DC-2106 (silicone)	0	0 (control specimens)	0	0	-	-	22072 26231 23603 23750 23914/815	1.26 1.58 1.42/0.28[a]	77	-	760	-
	4.48(10)	6.0(14) (vacuum irradiation)	7.5(15)	3.2(14)	17.9872 18.1944 18.1373	-0.0319 -0.0398 -0.0306	23876 19904 20047 21276/2346	1.36 1.31 1.29 1.32/0.04	104	D-1	5(-7)	4.1
CTL-91-LD (phenolic)	0	0 (control specimens)	0	0	-	-	24023 27735 26905 26016 26170/1803	1.06 1.15 1.11/0.08	77	-	760	-
	4.48(10)	6.0(14) (vacuum irradiation)	7.5(15)	3.2(14)	18.9568 18.5061 18.4980	-0.1101 -0.1219 -0.1054	32081 29762 27603 29815/2645	1.31 1.15 1.23/0.14	110	D-1	5(-7)	4.1
Mobiloy AH-81 (phenolic)	0	0 (control specimens)	0	0	-	-	25278 25444 25556 23556 26333 23056 25833 25008/1212	3 3 2 1 2 2.2/0.86	77	-	760	-
	1.67(10)	5.14(14) (vacuum irradiation)	2.7(15)	1.0(14)	-	-	22556 19889 20833 21093/1575	-	112	D-1	5(-7)	4.1

[a]Average value/standard deviation on an individual basis

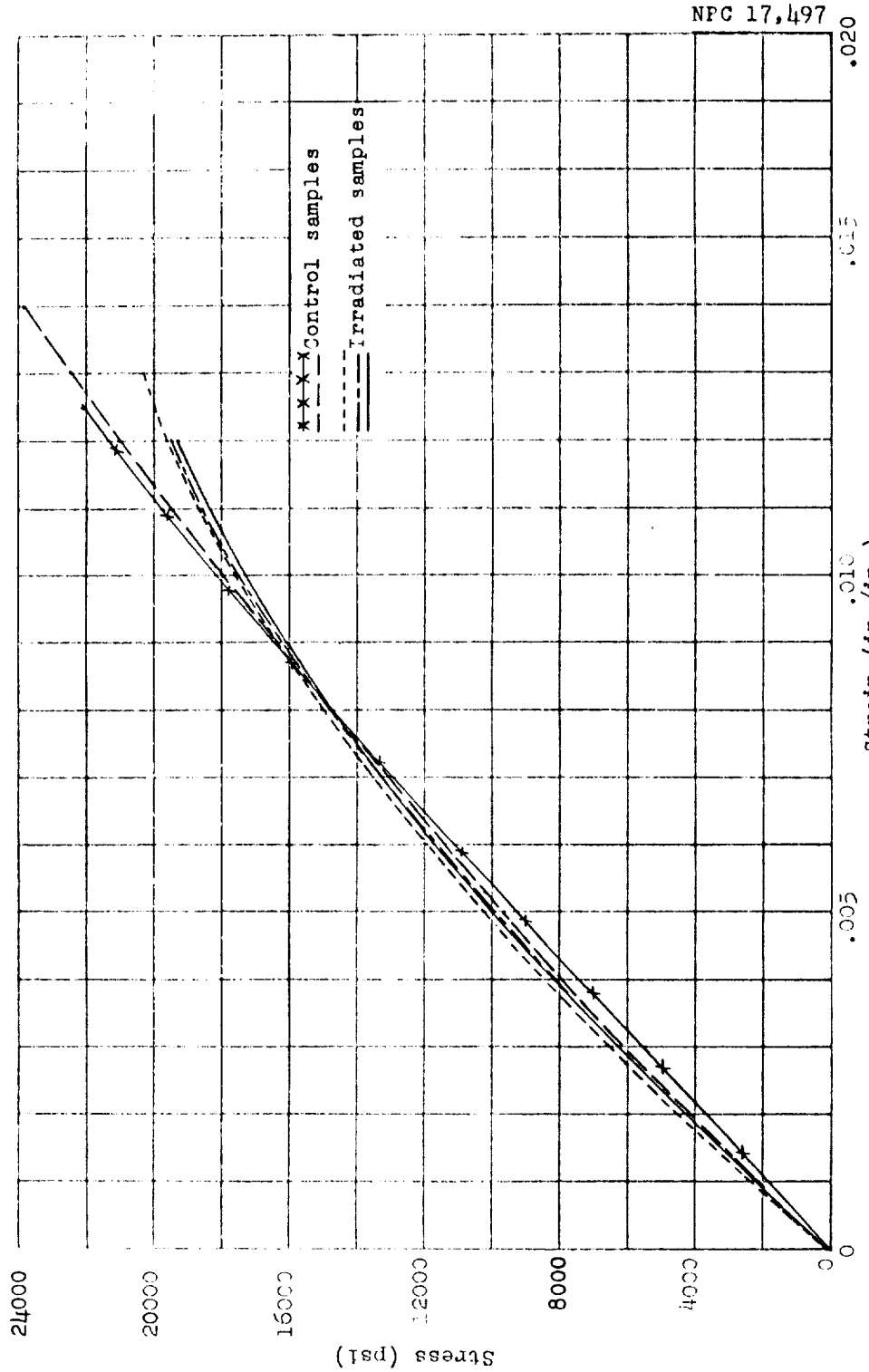

Figure 4.8 Stress-Strain Diagram of Structural Laminate: Silicone DC-2106

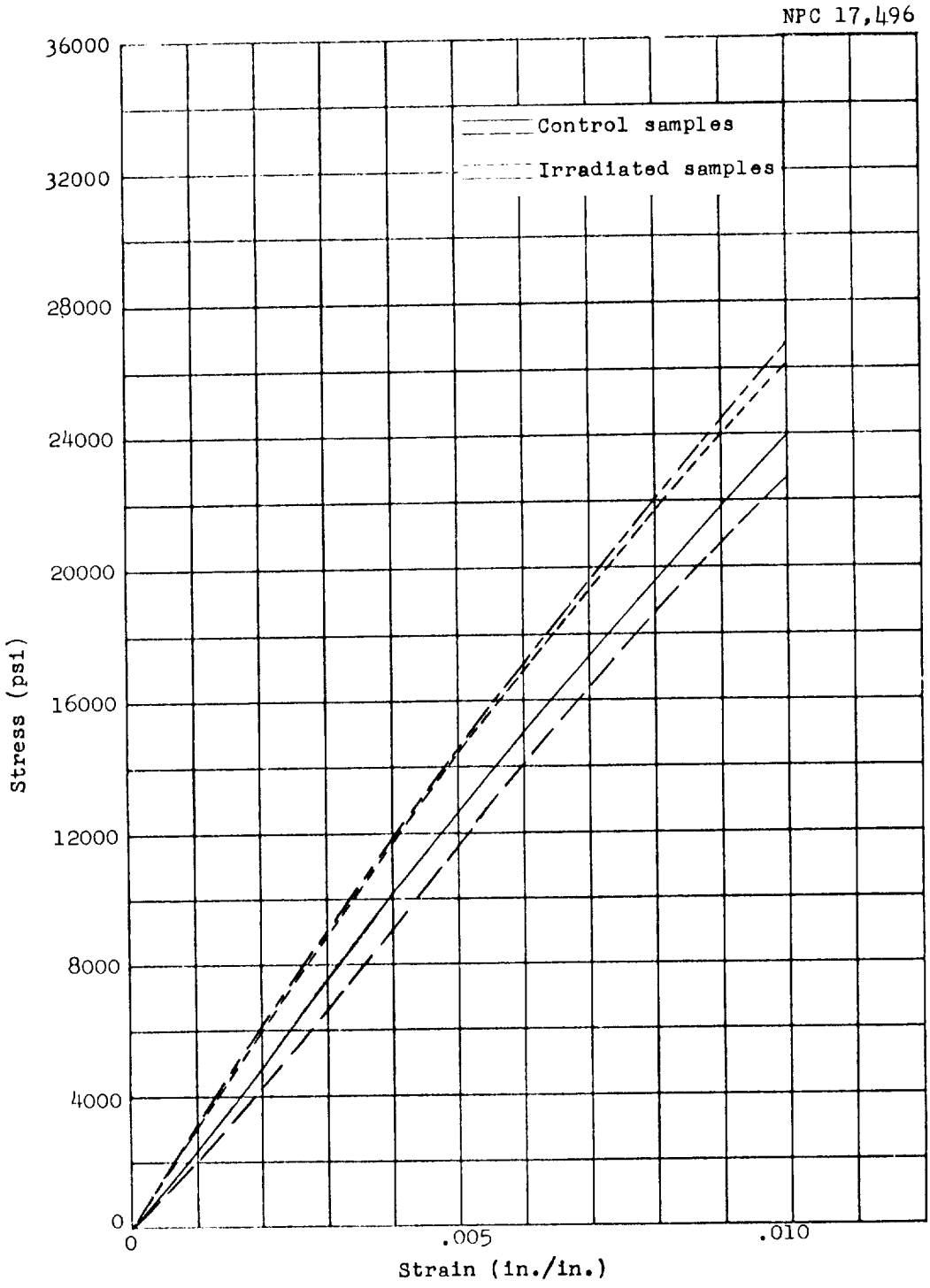

Figure 4.9 Stress-Strain Diagram of Structural Laminate: CTL-91-LD

CTL-91-LD. Figure 4.9 shows stress-strain curves that compare the data of two control with two irradiated specimens. Although there appears to be a significant difference in the curves, the data in Table 4.5, which includes additional specimens, show no significant changes in the tensile and elongation properties of the material. The average weight loss of the three vacuum-irradiated specimens was 0.60%.

Mobiloy AH-81. Table 4.5 shows that there was an approximate decrease of 16% in the tensile strength of this material. The elongation properties also decreased, but the magnitude of the changes could not be measured by the bench-mark method.

4.2.3.5 Electrical Insulation

Kel-F-81, Mylar, Mylar A, Mylar C, and Silicone DC 7-170 were tested for changes in tensile properties due to the irradiation-vacuum exposure. Kel-F-81 was fabricated into tensile specimens and tested in accordance with ASTM D-638-57T. Mylar, Mylar A, and Mylar C were tested as straight film specimens 1 inch wide by 6 inches long in accordance with ASTM D-882-56T. Silicone DC 7-170 was fabricated into specimens and tested in accordance with ASTM D-412-51T. The specimens were cut with Standard Die C.

Kel-F-81. As indicated in Table 4.6, severe damage resulted at the irradiation exposure and vacuum pressure obtained during Run 1. The brittleness of the vacuum-irradiation specimens precluded postirradiation testing on two of the specimens.

One was broken during removal from the vacuum chamber and one was broken as it was being installed in the Instron. During irradiation, this material suffered a weight loss of 0.29%, and changed to a pink color. This material exhibited a higher change in mechanical properties than was expected from the literature survey.

Mylar (10 mil). This material exhibited a severe decrease in ultimate elongation but no significant change in ultimate tensile strength. The weight loss is not considered significant. The material changed in color during the vacuum-irradiation from a light to a dark straw color.

Mylar A (3 mil). This material was subjected to two radiation doses, as shown in Table 4.6. Although no significant difference in the tensile properties of the specimens exists between the two doses, the tensile-strength values for the irradiated specimens were approximately 150% higher than those for the control specimens. The elongation values of the irradiated specimens were approximately 51% higher than the control values. There was no significant change in either the weight or the color of this material during the irradiation.

Mylar A polyester, manufactured by DuPont, was also investigated by Harrington and Giberson (Ref. 12). At 1×10^{10} ergs/gm(C) in air, they report that the material retained a substantial amount of physical toughness and flexibility, showing a 30%

Table 4.6

Test Environment and Results of Static Test: Electrical Insulation

Material	Radiation Exposure				Sample Weight		Tensile Strength (psi)				Ultimate Elongation (%)	Temperature		Pressure	
	Gamma [ergs/gm(C)]	Neutrons (n/cm^2)			Original (gm)	Change (gm)	@ 25% Elongation	@ 50% Elongation	@ 100% Elongation	Ultimate		Avg (°F)	Fig. No.	Avg (torr)	Fig. No.
		Thermal	E>2.9 Mev	E>8.1 Mev											
Kel-F-81 (fluoro-carbon)	0	0	0 (control specimens)	0	-	-	3890	3670	4260	5240	153	77	-	760	-
	1.47(10)	3.4(14)	2.1(15) (vacuum irradiation)	7.8(13)	20.9974 21.2226 20.9352	-0.0415 -0.0806 Broken				40	<1	115[a]	-	2(-6)	4.1
	5.5(9)	-	1.08(15) (air irradiation) Ref. 1	-	-	-				1568/3	0.58				-
	8(9)	-	2.2(15) (air irradiation) Ref. 1							Specimen crumbled					-
Mylar (10 mil) (polyester)	0	0	0 (control specimens)	0	-	-	13000 13500 13400 13300/264	13300 13500 13600 13467/224	15500 15100 15500 15367/290	16000 16000 17000 18300 16825/1090	103 120 130 140 123/15.7[b]	77	-	760	-
	2.42(10)	3.7(14)	2.2(15) (vacuum irradiation)	8.4(13)	1.2589 1.2578 1.2690	-0.0002 0.0000 -0.0009	-	-	-	17700 14000 15850/3280	<2 <2	118[a]	-	2(-6)	4.1
Mylar A (3 mil) (polyester)	0	0	0 (control specimens)	0	-	-	18330 18180 17300 17800 17902/500	20650 20850 19833 20267 20400/494	broke in jaws	23650 24350 22167 22133 23076/107	85 70 75 77/8.9	77	-	760	-
	1.3(9)	5.8(12)	1.6(13) (vacuum irradiation)	6.1(11)	1.2455 1.2643 1.2533 1.2477	+0.0003 +0.0007 0.0000 +0.0004	-	-	-	51600 56700 66000 64400 59675/6994	80 105 135 135 114/26.7	82	D-9	5(-6)	-

[a] Estimated value based on temperature of natural rubber

[b] Average value/standard deviation on an individual basis

Table 4.6 (cont'd)

Material	Radiation Exposure				Sample Weight		Tensile Strength (psi)				Ultimate Elongation (%)	Temperature		Pressure	
	Gamma [ergs/gm(C)]	Neutrons (n/cm²)			Original (gm)	Change (gm)	@ 25% Elongation	@ 50% Elongation	@ 100% Elongation	Ultimate		Avg (°F)	Fig. No.	Avg (torr)	Fig. No.
		Thermal	E>2.9 Mev	E>8.1 Mev											
Mylar A (cont'd)	7.0(9)	8.1(12)	8.3(13)	3.1(12) (vacuum irradiation)	1.2389 1.2632 1.2308 1.2668	+0.0007 +0.0005 +0.0008 +0.0002	-	-	-	60000 62667 56300 52600 57892/4889	130 145 110 85 118/29.1	82	D-9	5(-6)	-
Mylar C (1 mil) (polyester)	0	0	0	0 (control specimens) for vacuum test	-	-	17500	20300	broke in jaws	24500 20700 22600/3369	70 55 63/22.2	77	-	760	-
Batch 1	1.3(9)	6.4(12)	1.5(13)	5.8(11) (vacuum irradiation)	0.1218 0.1201 0.1194 0.0012	+0.0009 0.0000 +0.0003 +0.0017	-	-	-	22800 16400 15000 21300 18875/3788	85 15 75	80	D-9	5(-6)	-
	5.4(9)	9.2(12)	9.8(13)	3.7(12) (vacuum irradiation)	0.1191 0.1189 0.1125 0.1191	+0.0001 0.0000 +0.0001 +0.0001	-	-	-	17300 18800 12500 20300 17225/3788	40 50 80 57/23.6	80	D-9	5(-6)	-
Mylar C (1 mil) (polyester) Batch 2	0	0	0	0 (control specimens) for air test	-	-				17400 17700 17600	47.2 52.5 49.7	77	-	760	-
	4.9(9)	-	1.3(15)	- (air irradiation) Ref. 1	-	-	-	-	-	38000 38000 38000 38000	64 64 64 64	-	-	760	-
	8.0(9)	-	2.2(15)	- (air irradiation) Ref. 1	-	-	-	-	-	16500 15500 18500 16800	38.6 22.4 58.5 42	-	-	760	-
DC 7-170 (silicone)	0	0	0	0 (control specimens)	-	-	240 214 212 201 176 244 215/26.8	548 488 481 446 385 396 457/64.3	-	788 703 642 748 743 716 723/57.6	70 71 62 97 95 79/15.0	77	-	760	-
	9.03(9)	2.9(14)	1.4(15)	5.1(13) (vacuum irradiation)	3.8692 3.6586 3.7556	-0.0099 -0.0088 -0.0040	-	-	-	1690 1890 1715 1765/118	10 16 13 13/3.5	112[a]	-	2(-6)	4.1

[a] Estimated value based on temperature of natural rubber

decrease in ultimate elongation. Thus, the irradiation in vacuum produced a significant increase in both of the mechanical properties, while the air irradiation produced a decrease in these properties. This material showed the most significant improvement in physical properties after the vacuum irradiation of any material tested.

Mylar C (1 mil). This material exhibited no significant change in tensile strength, elongation, weight, or color when subjected to the two radiation doses shown in Table 4.6.

During postirradiation testing of this material, it was noticed that a few minute pin holes developed in the specimens. These holes would appear at approximately 30% elongation and are attributed to improper curing during manufacture. It is believed that these faults may have affected the tensile properties of the material in some way and that further testing should be performed before any conclusions are drawn as to the effects of radiation and vacuum on this material.

A different batch of Mylar C was tested in the cryotemperature irradiation program reported in Reference 1. The data from an air irradiation at ambient temperature ($77^{\circ}F$) is reported here for use in comparison (Table 4.6). The ultimate tensile strengths for the air-irradiation tests show an increase of 117% for the 4.9×10^9-erg /gm(C) dose and a decrease of 4.5% after the 8.0×10^9-erg/gm(C) dose. Because of the pin holes in the vacuum-irradiated test samples and the difference in control strength of the batches, no effort will be made to compare the results of the two batches.

Silicone DC 7-170. There was a significant change in the tensile properties of this material. As shown in Table 4.6, the ultimate tensile strength increased 144% and the elongation decreased 83.5%. The average weight loss for the three irradiated specimens was 0.201%. This material changed in color from a light cream to a dark brown during the vacuum irradiation.

Newell (Ref. 13) reports the changes in DC 7-170 mechanical properties after an air irradiation of 1×10^{10} ergs/gm(C) and associated neutrons. These data show a decrease of only 45% in elongation and an increase of 38% in tensile strength. This means that the mechanical properties were more severely affected by the vacuum-irradiation environment than by the air-irradiation environment.

4.2.3.6 Potting Compounds

The potting compounds, Epon 828/Z and DC R-7521, were fabricated into test specimens and tested for compressive properties in accordance with ASTM D-695-54.

Epon 828/Z. The ultimate compressive strength of this material increased approximately 6% when subjected to the radiation dose and vacuum-chamber pressure shown in Table 4.7. This change is not considered significant. There was no significant change in the weight of this material, and its color changed from amber to a very dark brown.

Table 4.7

Test Environment and Results of Static Test: Potting Compounds

Material	Radiation Exposure				Sample Weight		Ultimate Compressive Strength (psi)	Temperature		Pressure	
	Gamma [ergs/gm(C)]	Neutrons (n/cm^2)			Original (gm)	Change (gm)		Avg (^oF)	Fig. No.	Avg (torr)	Fig. No.
		Thermal	E>2.9 Mev	E>8.1 Mev							
DC R-7521 (silicone)	0	0	0	0	-	-	23424 22940 23182/429	77	-	760	-
		(control specimens)									
	9.03(9)	2.9(14)	1.4(15)	5.1(13)	8.5021 7.6400 7.7806	+0.0011 +0.0010 +0.0009	24103 20791 17539 20811/3877	117	D-6	2(-6)	4.1
		(vacuum irradiation)									
Epon 828/z (epoxy)	0	0	0	0	-	-	19811 19621 19716/168	77	-	760	-
		(control specimens)									
	1.0(10)	3.1(14)	1.6(15)	5.8(13)	9.8382 9.8654 9.8658	-0.0102 -0.0086 -0.0097	20833 20892 20849 20858/35	116	D-6	2(-6)	4.1
		(vacuum irradiation)									

Silicone DC R-7521. As shown in Table 4.7, there was no significant change in the compressive strength, since the average change was less than the statistical variation within the sample batch. The weight change for this material was not significant, and its color changed from a straw color to a dark brown.

4.2.3.7 Dielectric Materials

All of the dielectric materials were tested in the form of straight specimens 1 inch wide by 6 inches long. The post-irradiation testing was conducted in accordance with ASTM D-882-56T.

During Run 1, samples of Teflon TFE were irradiated in the east vacuum chamber to a dose of 1.07×10^{10} ergs/gm(C). This exposure damaged the material so severely that no tensile-strength data could be obtained. During Run 2, Teflon TFE samples were irradiated in the west vacuum chamber to a dose of approximately 1.8×10^{9} ergs/gm(C). These data are reported in Table 4.8.

Teflon TFE (40-mil). This material was severely damaged by a vacuum-irradiation exposure of 1.9×10^{9} ergs/gm(C), as is evidenced by the data in Table 4.8. A decrease of 44.5% in ultimate tensile strength and a decrease of 96% in ultimate elongation occurred. There was no significant change in the weight of this material. The color changed from white to a very light pink during irradiation.

Table 4.8

Test Environment and Results of Static Test: Dielectric Materials

Material	Radiation Exposure				Sample Weight		Tensile Strength (psi)				Ultimate Elongation (%)	Temperature		Pressure	
	Gamma [ergs/gm(C)]	Neutrons (n/cm^2)			Original (gm)	Change (gm)	@ 25% Elongation	@ 50% Elongation	@ 100% Elongation	Ultimate		Avg (°F)	Fig. No.	Avg (torr)	Fig. No.
		Thermal	E>2.9 Mev	E>8.1 Mev											
Teflon TFE (40 mil)	0	0 (control specimens)	0	0	-	-	1614 1619 1560 1598/34.8	1683 1690 1660 1678/17.7	1767 1762 1764/4.4	2881 2595 2738/254	290 315 302/22.1[a]	77	-	760	-
	1.9(9)	6.7(12) (vacuum irradiation)	2.9(13)	8.0(11)	8.7099 8.7756 8.8495 9.0502	-0.0003 +0.0012 0.0000 -0.0001	-	-	-	1564 1512 1481 1519/49.0	15 5 15 11.7/5.9	80	D-7	5(-6)	-
Teflon TFE (10 mil)	0	0 (control specimens) August 1962	0	0	-	-	1630 1690 1670 1670 1665/29.1	1750 1840 1800 1800 1798/43.7	1970 2050 1930 1990 1985/58.3	2280 2130 2120 2280 2202/77.7	155 118 139 148 140/18.0	77	-	760	-
	0	0 (control specimens) February 1963	0	0	-	-	1620 1580 1780 1660/118	1800 1800 1950 1850/88.6	- 2110 2180 2145/62.1	2240 2210 2300 2250/53.2	160 125 130 138/20.7	-	-	-	-
	0	0 (vacuum controls) February 1963	0	0	2.1280 2.0628 2.0423 2.1156 2.1127	+0.0002 +0.0002 +0.0008 +0.0011 +0.0004	- 1660 1711 1680 1660 1663/53.4	- 1820 1875 1870 1850 1854/26.7	- 2070 2130 2070 2080 2088/29.1	- 2180 2260 2280 2220 2235/48.6	- 130 132 137 120 130/8.3	77	-	1(-6)	-
	1.7(9)	6.5(12) (vacuum irradiation)	1.9(13)	7.3(11)	2.1373 2.1778 2.1397 2.0991	+0.0023 0.0000 -0.0002 +0.0032	-	-	-	1300 1250 1275/44.3	2 3 2.5/0.89	80[b]	D-7	5(-6)	-
Teflon 100 (40 mil)	0	0 (control specimens)	0	0	-	-	1690 1725 1725 1713/20.7	1750 1770 1770 1763/11.8	1775 1800 1805 1793/17.7	2108 1910 2165 2061/151	283 235 268 262/28.4	77	-	760	-

[a] Average value/standard deviation on an individual basis

[b] Estimated value based on temperature of Teflon (40 mil)

Table 4.8 (cont'd)

Material	Radiation Exposure				Sample Weight		Tensile Strength (psi)				Ultimate Elongation (%)	Temperature		Pressure	
	Gamma [ergs/gm(C)]	Neutrons (n/cm^2)			Original (gm)	Change (gm)	@ 25% Elongation	@ 50% Elongation	@ 100% Elongation	Ultimate		Avg (°F)	Fig. No.	Avg (torr)	Fig. No.
		Thermal	E >2.9 Mev	E >8.1 Mev											
Teflon 100 (cont'd)	8.6(9)	3.7(14) (vacuum irradiation)	1.3(15)	4.6(13)	8.2465 8.1375 8.1265	-0.0250 -0.0187 -0.0197	-	-	-	1307 1141 1224/73.6	2 1 1.5/0.89	110	D-2	5(-7)	4.1
Marlex 6002 (poly-ethylene)	0	0 (control specimens)	0	0	-	-	-	-	-	4143 3857 3929 4214 3571 3929 3941/254	(>800)[c] (>800)[c] (>800)[c] (>800)[c] 1060 950 1005/97.5	77	-	760	-
	1.1(10)	3.6(14) (vacuum irradiation)	1.3(15)	5.5(13)	1.2836 1.2862 1.2548	-0.0006 -0.0004 -0.0007	-	-	-	5429 5500 5286 5405/126	50 75 40 55/20.7	114	D-2	5(-7)	4.1
Teslar	0	0 (control specimens)	0	0	-	-	6050 6100 6250 6215 5950 6113/129	6100 6100 6500 6375 6090 6233/176	6700 6800 7500 7000/472	9100 7500 7200 6765 7641/1134	170 100 90 78 110/44.7	77	-	760	-
	1.3(9)	6.1(12) (vacuum irradiation)	1.55(13)	5.95(11)	0.3060 0.3060 0.2967 0.3095 0.3058	+0.0005 +0.0005 +0.0009 +0.0005 +0.0004	-	-	-	7650 8150 8100 7800 7925/243	90 105 105 105 101/7.3	100	D-9	5(-6)	-
	6.2(9)	8.6 (vacuum irradiation)	9.1(13)	3.4(12)	0.2914 0.2872 0.2810 0.3050	+0.0001 -0.0002 +0.0001 -0.0005	-	-	-[d]	7900 6800 9000 7500 7800/1068	90 70 100 75 84/14.5	100	D-9	5(-6)	-

[c]The elongation was greater than 800% but was not the ultimate, since the original gage length selected for this specimen was too large and resulted in an insufficient amount of total crosshead travel required to break the specimen. This did not affect the maximum strength, however, since this value is obtained when the specimen yields.

[d]Specimen broke in jaws

Teflon TFE (10 mil). When subjected to a dose of 1.7×10^9 ergs/gm(C) and the vacuum-chamber pressure shown in Table 4.8, these specimens of Teflon also exhibited extreme decreases in ultimate tensile strength and ultimate elongation. The tensile strength decreased 42% while the ultimate elongation decreased 98%. This material was very brittle, and two specimens were broken while attempting to insert them into the jaws of the Instron tester. The weight loss was negligible and there was no apparent color change.

A second set of "as received" control values, determined when the effects of vacuum exposure were measured, are presented in Table 4.8. The vacuum controls were in vacuum for the same period of time as the irradiated samples. The resulting data show that there was no change in the mechanical properties of Teflon TFE from the vacuum exposure.

Teflon 100 (40-mil). The data in Table 4.8 show that the ultimate tensile strength of Teflon 100 decreased 40.5% and the ultimate elongation decreased approximately 99% after a dose of 8.6×10^9 ergs/gm(C). The color changed from a milky color to a light pink. The average weight loss of the three specimens was 0.26%.

Marlex 6002. As shown in Table 4.8, the tensile strength of this material increased 37% and the ultimate elongation decreased 94.5% after a radiation dose of 1.1×10^{10} ergs/gm(C). The weight loss of this material was not significant, and the color changed from white to a straw color.

Harrington and Giberson (Ref. 12) report that Marlex rapidly deteriorates at low exposures in air and is extremely brittle and crumbly after a dose of 5×10^9 ergs/gm(C). Exclusion of air helped considerably, as the material was not brittle after being irradiated in a vacuum to 1×10^{10} ergs/gm(C). It lost most of its elongation under these conditions, but retained a substantial amount of its tensile strength. This shows that the material benefited by the exclusion of oxygen.

Teslar. This material was subjected to two radiation exposure levels at the vacuum-chamber pressure shown in Table 4.8. There was no significant change in either the tensile strength or the ultimate elongation, since the average change was less than the statistical variations within the sample batch. There was no significant change in either the weight or the color of this material.

4.2.3.8 Elastomers

All of the materials tested in this category were fabricated into specimens and tested in accordance with ASTM D-412-51T. The specimens were cut with Standard Die C.

Included in Table 4.9, along with the vacuum-irradiation results, are data for these materials when irradiated in air. These data were generated at NARF during a previous irradiation test. Only the average tensile values at the given gamma-radiation doses are listed. The complete data may be found in Reference 10.

Table 4.9

Test Environment and Results of Static Test: Elastomers

Material	Radiation Exposure				Sample Weight		Tensile Strength (psi)				Ultimate Elongation (%)	Temperature		Pressure	
	Gamma [ergs/gm(C)]	Neutrons (n/cm^2)			Original (gm)	Change (gm)	@ 25% Elongation	@ 50% Elongation	@ 100% Elongation	Ultimate		Avg (^oF)	Fig. No.	Avg (torr)	Fig. No.
		Thermal	E>2.9 Mev	E>8.1 Mev											
Buna N (RA30760)	0	0	0	0	-	-	99 103 101 101	137 141 134 140	170 185 168 173	2511 2679 2598 2732	690 680 670 700	77	-	760	-
		(control specimens) August 1962					101/1.9	138/3.4	174/10.0	2630/108	685/14.6[a]				
	1.7(9)	6.5(12)	1.9(13)	7.3(11)	3.8288 3.8104 3.8988 3.9816	+0.0020 +0.0020 +0.0012 +0.0012	-[b] 14 14 13	-[b] 21 20 20	-[b] - 30 29	-[b] 197 207 203	-[b] 440 460 450	80	D-8	5(-6)	-
		(vacuum irradiation) August 1962					13.7/0.6	20.3/0.6	29.5/0.9	203/5.9	450/11.8				
	7.0(9)	8.1(12)	8.3(13)	3.1(12)	3.8052 3.9753 3.8066 3.8906	-0.0006 +0.0004 +0.0014 +0.0006	25 - 22 22	46 - 38 39	87 - 81 71	212 195 210 180	180 - 220 200	80	D-8	5(-6)	-
		(vacuum irradiation) August 1962					23/1.8	41/4.7	80/9.4	199/15.5	200/23.6				
	0	0	0	0	-	-	138 122 140 112	193 161 168 156	- 239 224 210	- 2583 2447 2034	- 672 660 620	-	-	-	-
		(control specimens) February 1963					128/13.6	170/17.8	224/17.1	2355	647				
	0	0	0	0	3.8931 3.8703 3.8334 3.8295 3.8063	+0.0020 -0.0025 -0.0025 -0.0028 -0.0026	- 133 112 141 129	177 167 157 180 169	221 222 214 230 219	2553 2400 2646 2730 2011	650 635 650 670 575	-	-	-	-
		(vacuum controls) February 1963					129/14.1	170/9.9	221/6.9	2468/309	636/40.8				
	0	0	0	0	-	-	109/11/4	160/6.4/5	211/8.6/5	2459/496/5	643/51/5[a]	-	-	-	-
		(control specimens) May 1962													
	1.87(9)	(air irradiation) May 1962			-	-	159/30/5	220/23/5	348/12/5	2174/630/5	391/67/5	-	-	-	-
	2.06(10)	(air irradiation) May 1962			-	-	1177/129/4	1999/92/4	3495/233/4	3512/206/5	100/4.9/4	-	-	-	-
Neoprene (RA24160)	0	0	0	0	-	-	135 141 131 150	233 222 222 227	415 384 354	3306 3182 3005 2878 3300	445 450 420 390 425	77	-	760	-
		(control specimens) (for vacuum test)					139/9.2	226/5.3	384/36.0	3134/227	426/25.8				

[a] Average value/standard deviation on an individual basis/number of samples

[b] No tensile values were obtained for this specimen

Table 4. 9 (cont'd)

Material	Radiation Exposure				Sample Weight		Tensile Strength (psi)				Ultimate Elongation (%)	Temperature		Pressure	
	Gamma [ergs/gm(C)]	Neutrons (n/cm^2) Thermal	$E>2.9$ Mev	$E>8.1$ Mev	Original (gm)	Change (gm)	@ 25% Elongation	@ 50% Elongation	@ 100% Elongation	Ultimate		Avg (°F)	Fig. No.	Avg (torr)	Fig. No.
Neoprene (RA24160)	1.9(9)	6.7(12)	2.9(13)	8.0(11)	4.9747	-	19	28	-	237	260	80	D-7	5(-6)	-
		(vacuum irradiation) August 1962			5.2147	+ 0.0093	21	32	64	158	190				
					5.0148	+ 0.0100	18	33	63	197	220				
					5.1056	+ 0.0100	18	36	68	172	200				
							19/1.5	32/3.9	65/3.0	191/38.4	218/34.0				
	5.4(9)	9.2(12)	9.8(13)	3.7(12)	5.0792	+ 0.0400	31	75	-	115	115	80	D-7	5(-6)	-
		(vacuum irradiation) August 1962			5.0785	+ 0.0385	30	76	-	130	80				
					4.9626	+ 0.0361	29	66	-	147	115				
					4.8844	+ 0.0276	35	72	-	142	80				
							31/2.9	72/4.9	-	134/15.5	98/17.0				
	0	0	0	0	-	-	153/12.9/5	220/8.6/5	392/18.9/4	3297/244/5	454/29.6/5	-	-	-	-
		(control specimens) May 1962													
	1.87(9)	(air irradiation) May 1962			-	-	186/24.9/5	316/26.2/5	628/46.4/5	2769/224/5	265/21.5/5	-	-	-	-
	2.06(10)	(air irradiation) May 1962			-	-	-	-	-	203/40/5	35/6.4/5	-	-	-	-
Viton A (RA29360)	0	0	0	0	-	-	116	174	550	1300	-	77	-	760	-
		(control specimens) August 1962			-	-	114	205	455	1307	170				
							121	209	440	1305	175				
							130	215	466	1249	163				
							119	209	452	1390	168				
							117	212	469	1508	183				
							119/6.3	204/16.2	472/43.4	1343/102	172/8.6/5				
	0	0	0	0			-	-	-	1621	190	77	-	-	-
		(control specimens) February 1963, Group A					111	194	417	1850	200				
							116	188	419	1647	190				
							106	188	441	2212	220				
							117	199	439	2029	195				
							113/5.3	192/5.3	429/11.6	1872/254	199/12.9				
	0	0	0	0			-	-	452	1774	186	77	-	-	-
		(control specimens) February 1963, Group B					-	203	424	1638	185				
							-	201	431	2155	187				
							-	203	452	2034	200				
							-	202/1.2	440/13.6	1900/251	190/7.2				

Table 4.9 (cont'd)

Material	Radiation Exposure				Sample Weight		Tensile Strength (psi)				Ultimate Elongation (%)	Temperature		Pressure	
	Gamma [ergs/gm(C)]	Neutrons (n/cm^2)			Original (gm)	Change (gm)	@ 25% Elongation	@ 50% Elongation	@ 100% Elongation	Ultimate		Avg (°F)	Fig. No.	Avg (torr)	Fig. No.
		Thermal	E >2.9 Mev	E >8.1 Mev											
Viton A (cont'd)	0	0	0	0	-	-	-	-	416	1272	165	77	-	-	-
		(control specimens) February 1963, Group C					-	207	517	1121	150				
							-	211	427	1023	145				
							-	234	444	1257	160				
							-	119	427	1146	150				
								212/17	446/43.4	1164/107	154/8.6				
	0	0	0	0	6.6364	-0.0013	132	205	415	1731	177	77	-	1(-6)	-
		(vacuum controls) February 1963			6.3081	-0.0023	119	196	446	2179	210				
					6.9514	-0.0019	157	236	466	1927	180				
					6.8042	-0.0017	136	216	426	1648	180				
					6.8525	-0.0012	119	205	438	2148	200				
							133/16.3	212/17.2	438/13.3	1927/228	189/14.1				
	1.58(10)	4.6(14)	2.4(15)	9.0(13)	6.7632	-0.0807				1650	25	110	D-3	5(-7)	4.1
		(vacuum irradiation) August 1962			6.4987	-0.0748				1420	22				
					6.5979	-0.0758				2280	36				
					6.5264	-0.0724				1970	40				
										1830/418	31/6.8				
	0	0	0	0	-	-	117/8.6/5	196/3.4/5	445/10.7/4	1895/271/5	209/20.2/5	-	-	-	-
		(control specimens) May 1962													
	1.87(9)	(air irradiation) May 1962			-	-	167/16.8/5	342/32.2/5	1170/138/5	1491/182/5	113/16.5/4	-	-	-	-
	2.06(10)	(air irradiation) May 1962			-	-				2629/200/5	36/4.9/4	-	-	-	-

Buna N (RA 30760). Buna N specimens were subjected to two levels of radiation. In comparing the control-specimen values with the values of the vacuum-irradiated specimens subjected to the 1.7×10^9-erg/gm(C) gamma dose, it is found that the ultimate tensile strength decreased 91.5% and the ultimate elongation decreased 34.3%. Comparing the specimens subjected to a gamma dose of 7.0×10^9 ergs/gm(C) with the controls reveals a decrease of approximately 92% for the ultimate tensile strength and a decrease of 71% for the ultimate elongations.

Comparison of the control specimens for the air irradiation with those which were subjected to a gamma dose in air of 1.87×10^9 ergs/gm(C) shows that the ultimate tensile strength of the exposed specimens decreased 12% and the ultimate elongation decreased 39%. The specimens subjected to a gamma dose of 2.06×10^{10} ergs/gm(C) showed an increase of 43% in tensile strength and a decrease of 85% in elongation.

From the data in Table 4.9, a significant change in the ultimate tensile strength is evident between those specimens irradiated in vacuum to a dose of 1.7×10^9 ergs/gm(C) and those irradiated in air to a dose of 1.87×10^9 ergs/gm(C). The average value for the vacuum-irradiation specimens was 203 psi, whereas that for the air-irradiation specimens was 2174 psi - a factor of 10 difference. The effect of a higher dose of 7×10^9 ergs/gm(C) on specimens in a vacuum was not significantly different from that

at the lower dose. However, an increase in the dose to 2.06×10^{10} ergs/gm(C) on specimens in air caused the tensile strength to increase 43% (or to 3512 psi).

The changes in ultimate elongation produced by the vacuum-irradiation were less than those produced by the air-irradiation. At the lower exposure of $\sim 1.8 \times 10^{9}$ ergs/gm(C), the percent ultimate elongation of the vacuum-irradiation specimens was higher than the value for the air-irradiation specimens (450% and 391%, respectively).

A third set of specimens in the "as received" condition was tested in the Instron with the vacuum control specimens. These data (February 1963), presented in Table 4.9, show a small shelf-aging effect for the year. The vacuum controls, in the vacuum for the same period of time as the irradiated samples, show no significant change in mechanical properties.

The air irradiation of this material produced a harder and more brittle material, while the vacuum irradiation produced a weak, tacky, ductile material. It should be stated at this point, however, that this cannot be made a general conclusion for all vacuum-versus-air-irradiation tests of elastomeric materials (see Viton elastomers in this section).

Neoprene (RA 24160). Neoprene was also subjected to two levels of radiation while in a vacuum. The ultimate tensile strength of the specimens subjected to a gamma dose of 1.9×10^{9} ergs/gm(C) decreased 94% from the control values, while the

ultimate elongation decreased approximately 49%. The ultimate tensile strength of the specimens subjected to the 5.4×10^9-erg/gm(C) gamma dose decreased approximately 96%, the ultimate elongation 77%.

The ultimate tensile strength of the specimens irradiated in air to a gamma dose of 1.87×10^9 ergs/gm(C) decreased 16% from the control values and the ultimate elongation decreased 42%. For the specimens subjected to a gamma dose of 2.06×10^{10} ergs/gm(C) the ultimate tensile strength decreased 94% and the ultimate elongation decreased 92%.

Viton A (RA 26360). Five sets of specimens cut from sheet material in the "as received" condition were tested over a 10-month period in the Instron. The data in Table 4.9 show a wide variation in mechanical properties for these five sets of control specimens. This is due to sheet-to-sheet variation in the sample materials. In view of this large variation within the batch, only general trends and large changes will be indicated. An average of the highest three groups will be used in discussion as the average control (ultimate tensile strength, 1890 psi; ultimate elongation, 199%). The samples exposed to a vacuum of 1×10^{-6} torr for the same period of time that the irradiated samples were in vacuum showed no significant change in properties.

As shown in Table 4.9, this material was subjected to only one radiation level during the vacuum-irradiation exposure. The ultimate tensile strength showed no significant change and

the ultimate elongation decreased 82% from the control values. The Viton A elastomers retained the same tensile strength, conversely to the Buna N compound, while the elongation properties of Viton A were more severly affected by the vacuum irradiation than those of the Buna N.

Table 4.9 includes the air-irradiation data generated in May 1962 and used for a first evaluation of the material. The tensile strength and ultimate elongation of the air-irradiated specimens subjected to the radiation exposure of 1.87×10^{9} ergs/gm(C) decreased approximately 21% and 43%, respectively. For the radiation exposure of 2.06×10^{10} ergs/gm(C) the tensile strength increased 39% and the ultimate elongation decreased 83%.

4.3 Low-Force Dynamic Test

The low-force testing apparatus was designed for applying a maximum force of 200 pounds on material specimens in either tension, compression, or bending while in an environment of high vacuum and nuclear radiation. The 16 test positions of the low-force apparatus consisted of eight tensile-test positions, six compression-test positions, and two bending-test positions. The eight tensile positions contained three specimens of DuPont H-film electrical-insulation material, three specimens of Viton B O-ring seals, and two speciments of Buna N O-ring seals. The six compression positions contained two compression buttons of RTV-60 potting compound, two of Urethane DS-620, and two of Stafoam AA-402; the Urethane DS-620 and Stafoam AA-402 are thermal insulations. Each of the six button specimens measured 1.129 inches diameter by 0.5 inch high. The two bending positions contained Epon 828/A structural laminate flexure specimens. The materials tested are listed in Table 4.10. The sample and dosimetry locations are shown in Figure 4.10.

Two to four static samples of the above materials were attached to a 16.75-inch-diameter circular plate located in the same area as the dynamic test specimens for similar doses. These samples were tested at the IML in an Instron tester along with the control samples.

4.3.1 Experimental Low-Force Testing Equipment

The principle of operation of this test apparatus was discussed in detail in the second quarterly progress report (Ref. 4). The low-force testing apparatus used during the vacuum-irradiation test

Table 4.10

Test Plan for Low-Force Dynamic-Test Materials

Material Application	Test Specimens			
	Type	Trade Name	Number Tested	
			Dynamically	Statically
Thermal Insulation	Compression	Urethane DS620, Stafoam AA-402	2 2	2 2
Potting Compound	Compression	RVT-60	2	2
Structural Laminate	Flexure	Epon 828/A	2	3
Electrical Insulation	Film (Tensile)	DuPont H-Film	3	4
Seals	O-ring (Tensile)	Buna N (Parker 66-581), Viton B (Precision 19007)	2 3	- 3

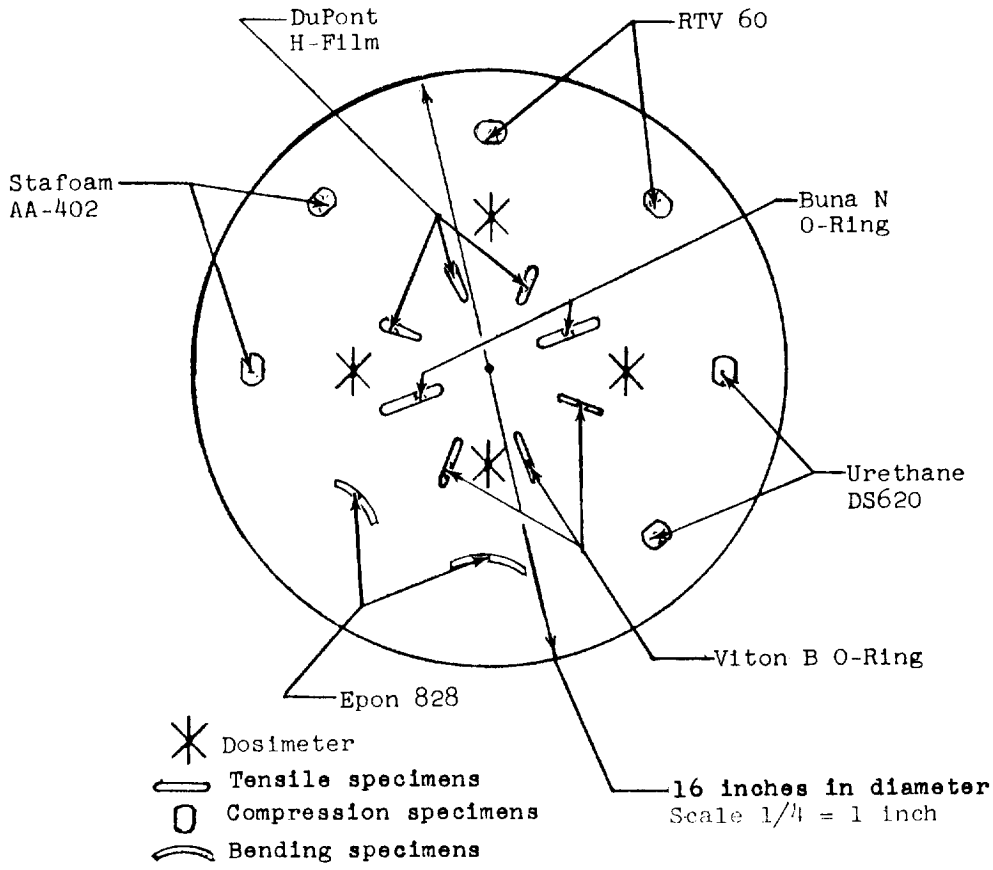

Figure 4.10 Location of Samples and Dosimeters for Low-Force Dynamic Test

is shown in Figure 4.11. The pulling cylinder (slave) was connected hydraulically through 165 feet of tubing to an identical master cylinder connected to the load cell of an Instron tester located in the reactor control room. This allowed a force to be applied to the test specimen at a constant rate (inches/inch-min). The hydraulic fluid used in this system was MIL-H-8446B.

The Instron tester measured the load applied to the master hydraulic cylinder. The drag force from the O-rings located in the hydraulic cylinders and the hydraulic-fluid friction forces of the 165 feet of 0.25-in.-diameter tubing are included in the Instron value. To obtain a value that was not biased by these forces, a transducer was used on the pulling rod of the low-force tester. The bellows seal provided a linear spring rate that was subtracted during data reduction.

The force applied to the specimen was measured by a type TDC-4A200 force transducer. The pull-rod movement was obtained by a type 600ES-L displacement transducer. These transducers, made by Schaevitz Engineering, Pennsauken, New Jersey, utilized the principle of the Linear Variable Differential Transformers (LVDT). The LVDT signals were recorded on an Offner Electronics Type-R Dynagraph recorder.

The 16-position rotary switch was fitted with 15 wire-wound, 100-ohm resistors to indicate, by accumulative resistance reading, the specimen being tested. During the first indexing operation of the vacuum-irradiation test, the position indication was lost. This

NPC 17,501
31-6547

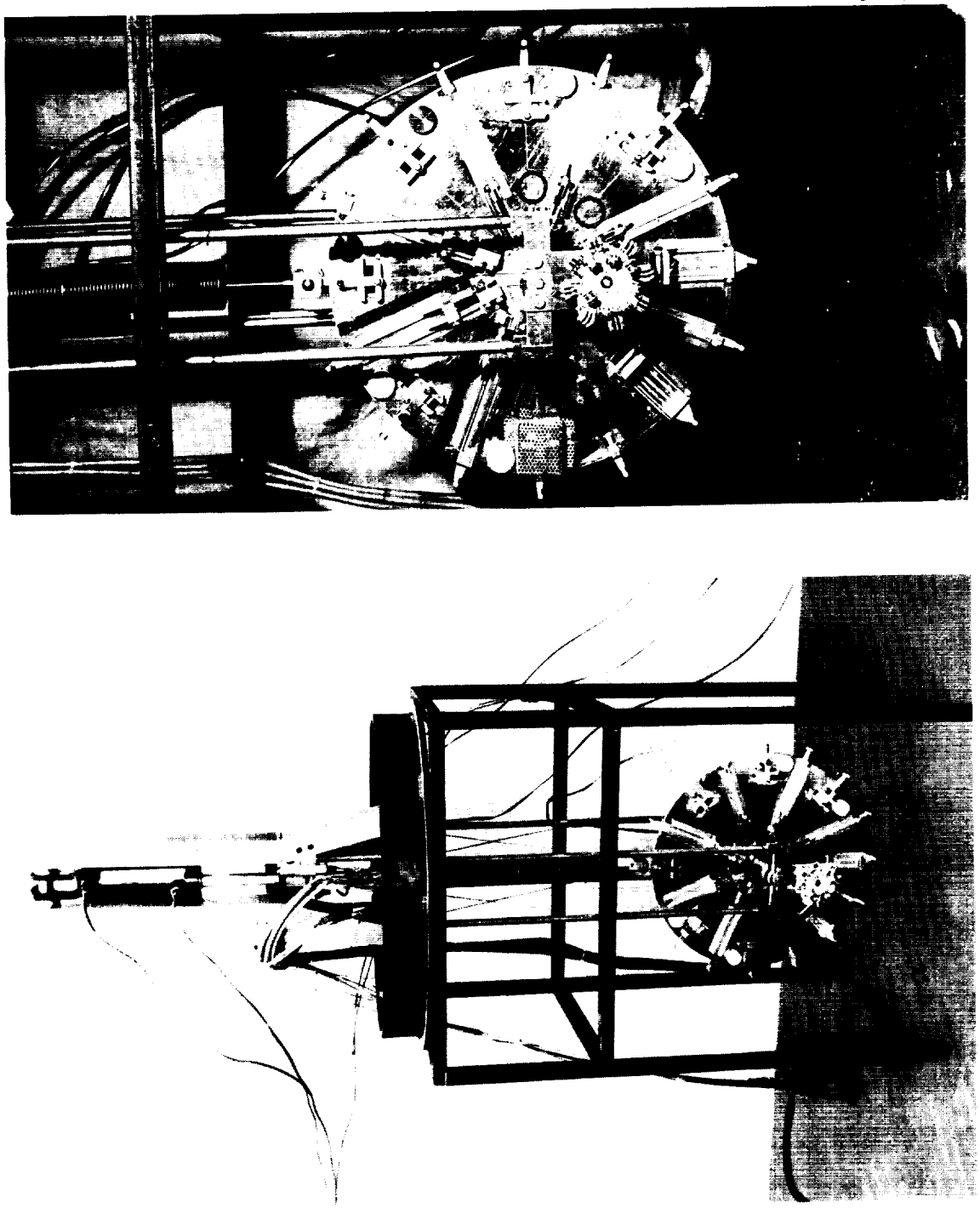

Figure 4.11 Low-Force Dynamic Tester

was later determined to be due to slippage of the mechanical linkage between the rotating shaft and the 16-position rotary switch. Because of the length of stroke and visual observation of the data on the following positions, it was assumed that normal indexing was being accomplished. This assumption was incorrect, for it was later determined that the tester was four positions off. This resulted in incomplete data from two positions and improper crosshead speed in one position determination. Travel indication was lost after the eleventh determination, which was the first H-film pulled. This loss of travel was due to the metal core of the displacement LVDT transducer being pulled out of the transformer and not re-entering, as it had done in the control tests and previous dynamic tests.

The dynamic tests were conducted in the high vacuum $7\frac{1}{2}$ hours after the termination of the irradiation. The test-sample temperature had returned to approximately $80^{o}F$ or less after $7\frac{1}{2}$ hours.

The tests in the IML of the static samples irradiated next to the dynamic samples were performed two weeks later. The samples were in a partial vacuum ($\sim$500 microns) for 48 hours, then removed to the laboratory where they were stored in a dry chamber until testing.

4.3.2 Experimental Results

The materials tested in the low-force apparatus during the vacuum-irradiation test received an approximate dose of 8.9×10^{9} ergs/gm(C). The actual dose received by each specimen was obtained by monitoring dosimetry and is given in the tables along with the test results. The specimen temperatures throughout the irradiation

period are given in Figures D-10 through D-14 in Appendix D. The pressure maintained in the test chamber during the vacuum-irradiation test is given in Figure 4.2 of Section 4.1.

4.3.2.1 Thermal Insulations

The flexible-foam thermal insulation tested during the vacuum-irradiation test was Urethane DS-620, a polyester resin urethane. This organic, nonrigid foam was tested according to ASTM D-1565-58T. The specimen was compressed 25% (0.125 inch) and the load read after 60 seconds. The results of the low-force-apparatus specimens were considered unreliable because of the inaccuracy of the apparatus in the range of extremely low loads necessary for 25% deflection. The inaccuracy occurred in distinguishing between the low specimen load ($\sim$0.5 lb), the bellows load, and the noise pickup in the range of the Offner Dynagraph.

The static samples attached to the test setup during the vacuum-radiation test were tested in the Instron. The results of these tests are given in Table 4.11. The temperatures of the specimens during the vacuum-irradiation test are given in Figures D-10 and D-11 (App. D).

The change in the average compressive strengths between the static-irradiation and control samples was less than the statistical variation within the sample batch; therefore, it is felt there is no significant change in compressive force of the urethane due to the vacuum and radiation environment of this test. The irradiated specimens did change color to a yellowish tint, remained soft and pliable, and lost approximately 4% of their original weight.

Table 4.11

Test Environment and Results for Low-Force Dynamic-Test Materials: Thermal Insulation

Material and Test Equipment	Radiation Exposure				Sample Weight		Compressive Strength (psi)		Temperature		Pressure	
	Gamma [ergs/gm(C)]	Neutrons (n/cm^2)			Original (gm)	Change (gm)	@ 25% Deflection	Ultimate	Avg (^oF)	Fig. No.	Avg (torr)	Fig. No.
		Thermal	E>2.9 Mev	E>8.1 Mev								
Urethane DS-620												
Instron Tester	0	0 (control specimens)	0	0	-	-	0.55 0.70 0.70 0.60 0.64/0.073[a]	-	77	-	760	-
Instron Tester	1.05(10)	1.3(14) (vacuum irradiation)	1.77(15)	6.7(13)	0.2732 0.2732	-0.0106 -0.0119	0.625 0.60 0.6125/0.022	-	145	D-10 D-11	3(-7)	4.2
Stafoam AA-402												
Instron Tester	0	0 (control specimens) September 1962	0	0	-	-	37.7 37.0 38.4 39.3 39.5 38.4/1.1	44.8 42.3 42.0 39.8 38.5 41.5/2.7	77	-	760	-
Instron Tester	0	0 (control specimens) February 1963	0	0	-	-	42.8 40.4 41.8 41.5 41.6/1.2	46.0 44.0 46.0 44.9 45.4/0.5	-	-	-	-
Instron Tester	0	0 (vacuum controls) February 1963	0	0	0.2776 0.2798 0.2945 0.2879 0.2798	-0.0053 -0.0057 -0.0059 -0.0055 -0.0055	39.5 38.3 37.7 38.3 38.7 37.6/0.77	43.7 43.8 42.6 43.4 43.9 43.5/0.56	-	-	1(-6)	-

[a]Average value/standard deviation on an individual basis

Table 4.11 (cont'd)

Material and Test Equipment	Radiation Exposure				Sample Weight		Compressive Strength (psi)		Temperature		Pressure	
	Gamma [ergs/gm(C)]	Neutrons (n/cm^2)			Original (gm)	Change (gm)	@ 25% Deflection	Ultimate	Avg (°F)	Fig. No.	Avg (torr)	Fig. No.
		Thermal	E>2.9 Mev	E>8.1 Mev								
Stafoam AA-402 (cont'd)												
Low-Force Tester	8.9(9)	1.54(14)	1.53(15) (vacuum irradiation) September 1962	5.8(13)	-	-	51.0 49.1 50.0/1.7	51.8 49.7 50.8/1.91	130	D-12	3(-7)	4.2
Instron Tester	8.9(9)	1.54(14)	1.53(15) (vacuum irradiation) September 1962	5.8(13)	0.3070 0.3155	-0.0060 -0.0064	33.6 33.3 33.4/0.26	38.0 37.5 37.8/0.44	104	D-12	3(-7)	4.2
Instron Tester	5.0(9)	-	1.2(15) (air irradiation) October 1962 Ref.	-	-	-	15.0	15.0	-	-	760	-
Instron Tester	8.0(9)	-	2.2(15) (air irradiation) October 1962 Ref.	-	-	-	14.0	14.0	-	-	760	-

The second thermal insulation tested was a rigid foam, Stafoam AA-402, a halocarbon-blown polyether-resin urethane foam. This organic foam insulation was tested according to ASTM D-1056-58T, which required a compressive force sufficient to produce 25% deflection. Because of the loss of the position indication, the specimens were compressed beyond the 25% deflection. Stress-strain curves of the standard control samples, the two static vacuum-irradiation samples, and the dynamic vacuum-irradiation specimens are presented in Figure 4.12. The compression at 25% deflection obtained from the stress-strain curves is included in Table 4.11. The control and static samples were compressed in the Instron tester to 50% deflection (0.25 inch) instead of 25% at a crosshead speed of 0.05 inch per minute, the same speed as used in the dynamic tester. The temperature of the Stafoam during the vacuum-irradiation test is given in Figure D-12.

The ultimate compressive-strength value reported in Table 4.11 is the maximum strength carried by the sample during the compression-deflection test. As can be seen from Figure 4.12, this value is higher than the compression strength at 25% deflection. The original compression strength at 25% deflection of 38.4 psi decreased significantly during the static-vacuum irradiation to 33.4 psi. This amounted to a 13% change. The dynamic compressive strength of 50 psi after the same dose and vacuum environment showed a significant increase. Values for dynamic-test specimens will be determined

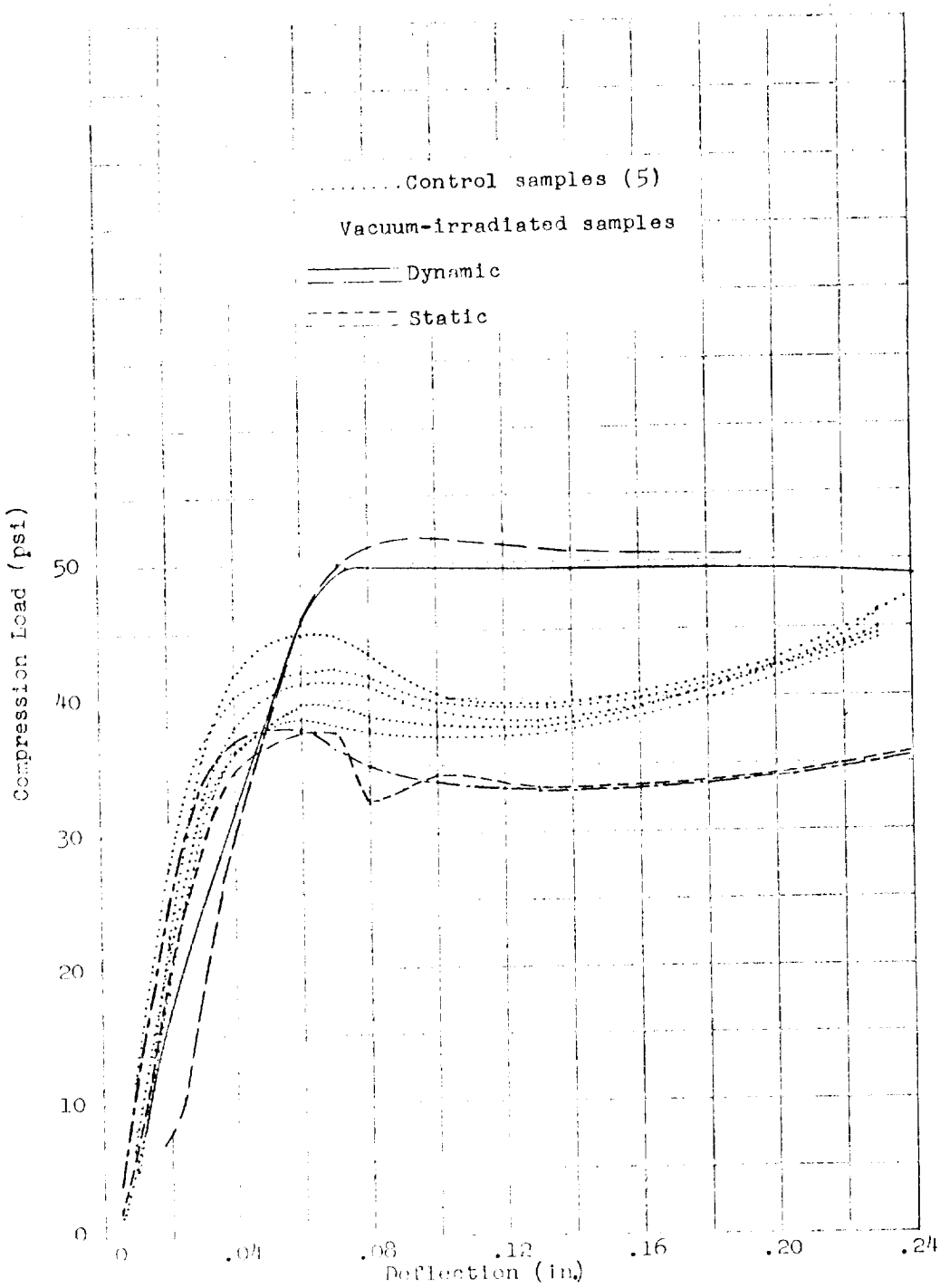

Figure 4.12 Compression-Deflection Diagram of Thermal Insulation: Stafoam AA-402

during the next quarter for comparison with these values. The texture of the material did not change, but the color turned to a light tan.

A set of "as received" controls were tested in the Instron with the vacuum control specimens. These data, presented in Table 4.11 (February 1963), show that the material increased significantly in compression strength during the five months of shelf-aging. The sample exposed to the $1x10^{-6}$-torr vacuum for the same period of time that the irradiated samples were in vacuum decreased slightly in compression strength.

The resulting data from air irradiation of samples for the cryogenic portion (Ref. 1) of these experiments is included in Table 4.11. The samples were fabricated from the same batch of material and tested in a similar manner. The results from the test after vacuum irradiation of $8.9x10^{9}$ ergs/gm(C) show a decrease in compressive strength of 13%. The results from the same dose in the air irradiation show a decrease of 63% in compression strength.

4.3.2.2 Potting Compounds

The nonrigid organic potting compound RTV-60, a silicone, was tested according to ASTM D-575-46, except that the maximum force of the Low-Force Tester (200 lb) was the limiting factor instead of the 25% (0.125 inch) deflection. The specimens were also run at 0.05-inch/minute crosshead speed and only one deflection (no conditioning deflection).

Because of the loss of position indication, only the results of one vacuum-irradiation specimen of the Low-Force Tester were usable. Stress-strain plots of tests on this specimen, the control specimens, and the static samples tested in the Instron are shown in Figure 4.13. The compressive forces required to produce a 0.02-inch deflection in the specimens are included in Table 4.12. The values were taken from the curves in Figure 4.13. The temperatures of the specimens during the vacuum-irradiation test are given in Figure D-13.

The results of the mechanical-property test on RTV-60 potting compound are presented in Table 4.12. The static and dynamic specimens showed an increase in compressive strength for a deflection of 0.02 inch after a dose of 8.6×10^9 ergs/gm(C). The one dynamic sample required a 76% increase in load to compress it 0.02 inch. The static samples tested in the Instron several weeks later required a 386% increase in load. To compress the static irradiated sample 25% required an increase in load from the average control value of 203 psi to 1549 psi, or 667%.

These samples experienced a greater change in their mechanical properties than had been expected from the preirradiation literature analysis.

4.3.2.3 Structural Laminates

The structural plastic laminates tested in flexure were composed of glass cloth (181) with a Volon A finish impregnated with Epon 828/A epoxy resin. These laminates were tested according to ASTM D-790-58T and had the required specimen dimensions of 0.125 by 1 by 4 inches,

Table 4.12

Test Environment and Results for Low-Force Dynamic-Test Materials: Potting Compounds

Material and Test Equipment	Radiation Exposure				Sample Weight		Compressive Strength (psi)		Temperature		Pressure	
	Gamma [ergs/gm(C)]	Neutrons (n/cm^2)			Original (gm)	Change (gm)	0.02 in. Deflection	@ 25% Deflection	Avg (°F)	Fig. No.	Avg (torr)	Fig. No.
		Thermal	E>2.9 Mev	E>8.1 Mev								
RTV-60 (silicone)												
Instron Tester	0	0 (control specimens)		0	-	-	22.5 21 20 19 22 20.9/1.4	218 200 210 185 198 202.2/12.5[a]	77	-	760	-
Low-Force Tester	0	0 (control specimens)		0	-	-	41	-	77	-	760	-
Low-Force Tester	8.6(9)	1.5(14) (vacuum irradiation)	1.4(15)	5.4(13)	-	-	72.5	-	170	D-13	3(-7)	4.2
Instron Tester	8.6(9)	1.5(14) (vacuum irradiation)	1.4(15)	5.4(13)	11.8049 12.2921	-0.0715 -0.0789	96 109 102/9.5	1508 1590 1549/71.8	167	D-13	3(-7)	4.2

[a]Average value/standard deviation on an individual basis

Table 4.13

Test Environment and Results for Low-Force Dynamic-Test Materials: Structural Laminates

Material and Test Equipment	Radiation Exposure				Sample Weight		Ultimate Flexural Strength (psi)	Ultimate Deflection (inches)	Temperature		Pressure	
	Gamma [ergs/gm(C)]	Neutrons (n/cm^2)			Original (gm)	Change (gm)			Avg (°F)	Fig. No.	Avg (torr)	Fig. No.
		Thermal	E>2.9 Mev	E>8.1 Mev								
Epon 828 Instron Tester	0	0 (control specimens)		0	-	-	79700 77000 78350/2394	0.163 0.161 0.162/0.0018[a]	77	-	760	-
Instron Tester	7.5(9)	1.51(14) (vacuum irradiation)	1.74(15)	6.8(13)	14.0906 14.0892 14.4764	-0.0058 -0.0062 -0.0078	71000 75500 83400 76633/7324	0.150 0.150 0.165 0.155/0.0089	169	D-14	3(-7)	4.2

[a]Average value/standard deviation based on an individual basis

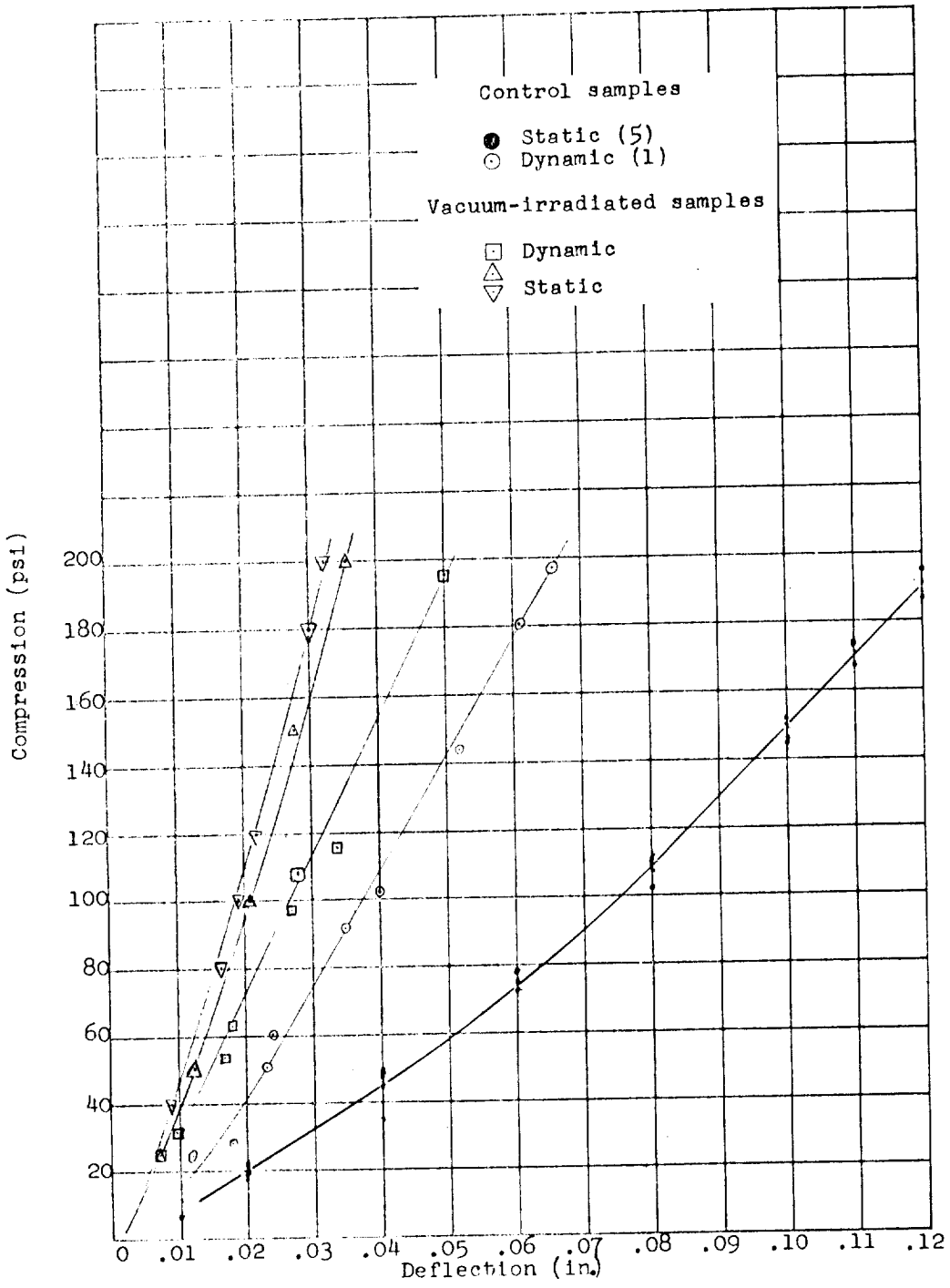

Figure 4.13 Compression-Deflection Diagram of Potting Compound: RTV-60

a span of 2 inches, and a crosshead speed of 0.05 inch per minute. The results of tests on the vacuum-irradiation specimens were inconclusive because of the loss of the position indication. During the dynamic testing, these laminate specimens were assumed to be the urethane specimens and were tested for 25% (0.125 inch) deflection. The vacuum-irradiation static samples attached to the circular plate were tested in the Instron along with the control specimens. The results of these tests are presented in Table 4.13. The temperatures of the specimens during the vacuum-irradiation test are given in Figure D-14.

A color change due to the radiation from a light green to a dark brown was noted in the epoxy laminates. No significant change in weight occurred. It is felt that the vacuum-irradiation did not affect the flexural ability of the laminates, since the difference in the average flexural strengths of the static irradiation and the control specimens was less than the statistical variation within the sample batch.

4.3.2.4 Electrical Insulation

The electrical insulation tested in the Low-Force Tester was DuPont H-film. The film was tested according to ASTM D-882-56T. Only the results of the static samples of the vacuum-irradiation test are reported in Table 4.14 because of the loss of travel indication and the fact that the films on the Low-Force Tester were pulled the maximum travel of the tester (3 inches) but did not break. Without the travel indication, a stress-strain curve could not be obtained

Table 4.14

Test Environment and Results for Low-Force Dynamic-Test Materials: Electrical Insulation

Material and Test Equipment	Radiation Exposure				Machine Crosshead Speed (in./min)	Tensile Strength (psi)				Ultimate Elongation (%)	Temperature		Pressure	
	Gamma [ergs/gm(C)]	Neutrons (n/cm^2)				@ 25% Elongation	@ 50% Elongation	@ 100% Elongation	Ultimate		Avg (°F)	Fig. No.	Avg (torr)	Fig. No.
		Thermal	E>2.9 Mev	E>8.1 Mev										
H-Film Instron Tester	0	0 (control specimens) January 1962	0	0	5	15110/200/3	15960/200/3	-	20990/470/3	151/8.9/3[a]	77	-	760	-
Instron Tester	1.58(10)	0 (air irradiation) January 1962	4.8(15)	0	5	15138/363/8	16101/376/7	-	19795/714/8	118/10.5/8	-	-	-	-
Instron Tester	4.04(10)	0 (air irradiation) January 1962	7.5(15)	0	5	15045/360/6	16186/234/6	-	17983/647/5	81.6/7.3/5	-	-	-	-
Instron Tester	0	0 (control specimens) December 1962	0	0	5	14700/340/4	15362/243/4	17772/180/4	20520/923/4	155/16.5/4	77	-	760	-
Instron Tester	0	0 (control specimens) October 1962	0	0	0.5	14220 14160 14400 14580 14650 14402/211	15000 14580 15230 15500 15500 15162/396	17200 16950 17020 17620 17192/335	17380 18230 17370 19740 17110 17966/1131	105 130 101 138 119/21.9	77	-	760	-
Instron Tester	8.75(9)	1.52(14) (vacuum irradiation) September 1962	2.47(15)	5.6(13)	0.5	14150 14580 13800 14177/461	15420 15500 14830 15250/396	[b]	16600 20600 18400 16950 18138/1943	85 149 120 94 112/28.3	132	D-14	3(-7)	4.2
Instron Tester		(control specimens) February 1963			0.5	14492 14153 14746 14407 14450/288	15254 14746 15593 15085 15195/411	17203 16780 17966 17288 17309/576	18475 16780 17966 17288 17627/823	118 100 100 100 105/8.7	-	-	-	-
Instron Tester		(vacuum controls) February 1963			0.5	14831 14915 14746 14576 14767/165	15932 15848 15509 15509 15700/205	18220 18136 17712 17881 17987/247	19831 19273 19322 18475 19216/659	127 118 130 113 122/8.3	-	-	-	

[a]Average value/standard deviation based on an individual basis/number of specimens

[b]Broke in jaws

for the dynamic test data. The temperature of a static sample during the vacuum-irradiation test is given in Figure D-14.

The data presented in Table 4.14 resulted from mechanical-property tests performed after air and vacuum static irradiation tests. The data from the air irradiation was reported in detail in the second quarterly progress report so that only the averages are given for comparison. After a dose of 4.0×10^{10} ergs/gm(C) in air, the ultimate elongation was reduced by 46% of the original value and the ultimate tensile strength decreased by 15% of the original value.

It is felt that there was no significant change in ultimate tensile strength and ultimate elongation due to the high-vacuum and radiation-dose environment. The difference in averages between the vacuum-irradiation static samples and the control samples is less than the statistical variation within the sample batch.

The variation between the average ultimate tensile strength and ultimate elongation of the controls tested in January 1962 and the controls tested after the dynamic test is due to the difference in crosshead speeds and not from shelf-aging. This statement is supported by the results of a rerun at 5 in./min crosshead speed on controls from the same roll of film in December 1962. The differences between the January and December tests were within the statistical variation of the samples.

4.3.2.5 Seals

The O-ring seals tested in the Low-Force Tester were Buna N, a Parker-Hannifen Co. compound (Parker 66-581) and Viton B, a

Precision Rubber Products Corp. compound (Precision 19007). The O-rings were tested according to ASTM D-1414-56T, with a crosshead speed of 0.5 in./min.

No results were obtained from the Buna N specimens because of binding of the hangers on the Low-Force Tester. Time did not permit a complete checkout of all of the tensile-testing positions before the radiation. The Buna N hangers functioned satisfactorily with no load, but were subject to binding under the load of the O-rings, resulting in very erratic measurements. Extra Buna N O-rings were not available at the time of the test; therefore, no vacuum-irradiation static sample results were obtained.

Viton B O-ring results from the vacuum-irradiation test are presented in Table 4.15; the temperatures of the specimens during the test are given in Figure D-11. The data in Table 4.15 show that, on the average, the O-rings tested in the dynamic tester underwent a 79% reduction in ultimate elongation and an increase of 7% in ultimate tensile strength from the original control values. The static vacuum-irradiation Viton B O-rings were tested in the IML two weeks later. These samples showed a decrease of 88% in ultimate elongation, and a decrease in ultimate tensile strength of 21%. This result indicates that the Viton B further degraded after being exposed to the atmosphere; however, these O-rings remained in the vacuum following reactor shutdown approximately 18 hours before being exposed to the atmosphere for two weeks. The variability of the two static samples tested lowers the confidence to be placed in these values.

Table 4.15

Test Environment and Results for Low-Force Dynamic-Test Materials: Seals

Material and Test Equipment	Radiation Exposure				Machine Crosshead Speed (in./min)	Tensile Strength (psi)				Ultimate Elongation (%)	Temperature		Pressure	
	Gamma [ergs/gm(C)]	Neutrons (n/cm^2)				@ 25% Elongation	@ 50% Elongation	@ 100% Elongation	Ultimate		Avg (°F)	Fig. No.	Avg (torr)	Fig No.
		Thermal	E>2.9 Mev	E>8.1 Mev										
Viton B (PRP 1900) Instron Tester	0	0 (control specimens) September 1962	0	0	0.5	330 288 330 322 318/20	495 429 495 486 476/32	925 834 890 883 883/45	1302 1305 1834 1365 1312 1334/27	109 146 159 157 152 157/4.9[a]	77	-	760	-
Low-Force Tester	9.0(9)	1.4(14) (vacuum irradiation) September 1962	1.7(15)	6.75(13)	0.5	-	-	-	1451 1398 1437 1429/27.5	34 31.5 34 33.2/1.44	167	D-11	3(-7)	4.2
Instron Tester	9.0(9)	1.4(14) (vacuum irradiation) September 1962	1.7(15)	6.75(13)	0.5	-	-	-	1180 918 1049/144	19.8 17.1 18.5/2.4	167	D-11	3(-7)	4.2
Instron Tester	0	0 (control specimens) January 1962	0	0	20.0	-	-	-	1984/4.5/3	254/9.1/3	-	-	-	-
Instron Tester	1.2(9)		2.3(14) (air irradiation) January 1962		20.0	-	-	-	2047/8.9/3	141/3.8/3	-	-	-	-
Instron Tester	0	0 (control specimens) October 1962	0	0	20.0	-	-	-	1710 1485 1650 1585 1607/96	183 151 165 165 166/13	-	-	-	-

[a]Average value/standard deviation on an individual basis/number of specimens

The mechanical properties of Viton B O-rings tested in January 1962 and reported in the second quarterly progress report are also included in Table 4.15 for comparison purposes. This table shows a noticeable difference in the average ultimate tensile strength between the controls tested in January 1962 and the controls tested after the dynamic test. This variation is due to the use of different crosshead speeds during the test and to the storage-aging of the elastomers. The O-rings tested in January 1962 were pulled at a 20-in./min crosshead speed, while the vacuum-irradiation specimens and controls were tested at a 0.05-in./min crosshead speed. The slower speed was required because of the hydraulic master-slave equipment setup. The values from control samples tested recently at 20 in./min are given in Table 4.15 to show the effects of 10 months of shelf aging on the materials. The ultimate elongation was not as significantly affected by the change in crosshead speed as was the ultimate tensile strength.

Because of the factor-of-9 difference in dose between the air-irradiation specimens of January 1962 and the recent vacuum-irradiation specimens, no attempt will be made to determine damage caused by vacuum.

4.4 High-Force Tensile Test

A special tensile tester was built to perform mechanical property tests on high-tensile-strength samples in a vacuum and irradiation environment. This tester was used to test Conolon 506 and Epon 828/A laminate materials and FM-1000 and Metlbond 302 adhesive materials (Table 4.16). Strain gages were bonded to the laminates toprovide data for stress-strain plots. These data will also be compared to the crosshead travel.

A vacuum leak that developed in the tensile tester soon after the start of the first test necessitated the irradiation of the samples at a pressure of approximately 300 microns. This test was repeated, with the samples being irradiated at a lower pressure.

4.4.1 Experimental Equipment

The mechanics of operation of the high-strength tensile tester, shown in Figures 4.14, 4.15, and 4.16, are given in Reference 4, the Second Quarterly Progress Report. This tester uses a hydraulic master-slave setup similar to the one described in Section 4.3.1 (Low-Force Dynamic Tester). Schaevitz Engineering Dynamometer Type TDC-4A5000 and Linear Transformer Type 600ES-L were used in the tester for measuring load and displacement.

All strain gages used in the high-load dynamic test were Type AB-3-S13 gages manufactured by the Baldwin-Lima-Hamilton Corporation. This type of gage has a bakelite backing and a constantan wire grid of gage length equal to 13/16 inch. All gages are from the same manufacturer's batch and have a gage factor of 2.08 $\pm$ 1% and resistance of 119.5 $\pm$ 0.5 ohms. The temperature characteristics of the gages are

Table 4.16

Test Plan for High-Force Dynamic-Test Materials

Material Application	Run No.	Test Specimens			
		Type	Trade Name	Number Tested	
				Dynamically	Statically
Structural Adhesives	1	Lap Shear	FM-1000 Metlbond 302	5 5	5 5
	2	Lap Shear	FM-1000 Metlbond 302	5 5	5 5
Structural Laminates	1	Tensile	Conolon 506 Epon 828/A	4 4	4 4
	2	Tensile	Conolon 506 Epon 828/A	4 4	

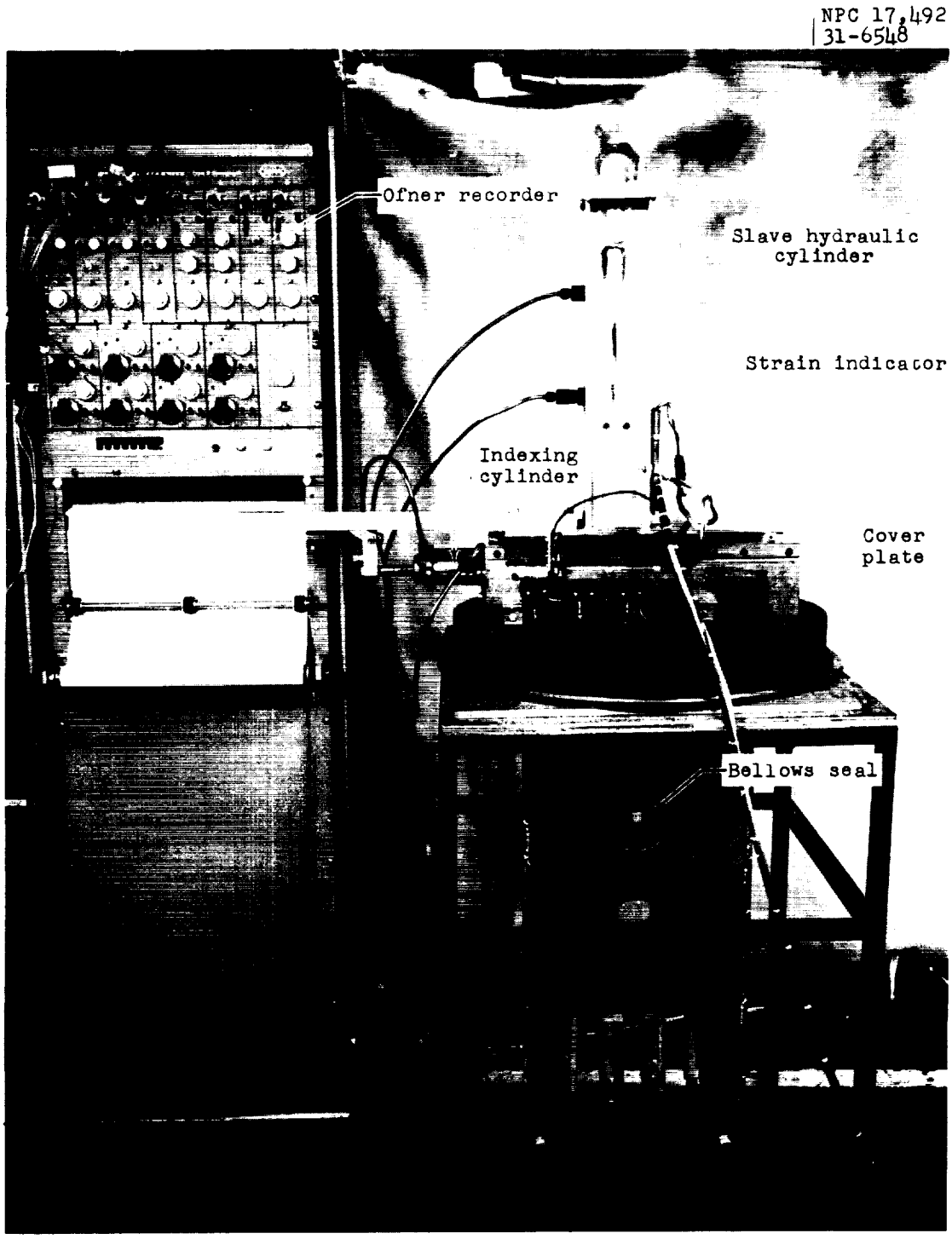

Figure 4.14 High-Force Tensile Tester Equipment

NPC 17,491
31-6543

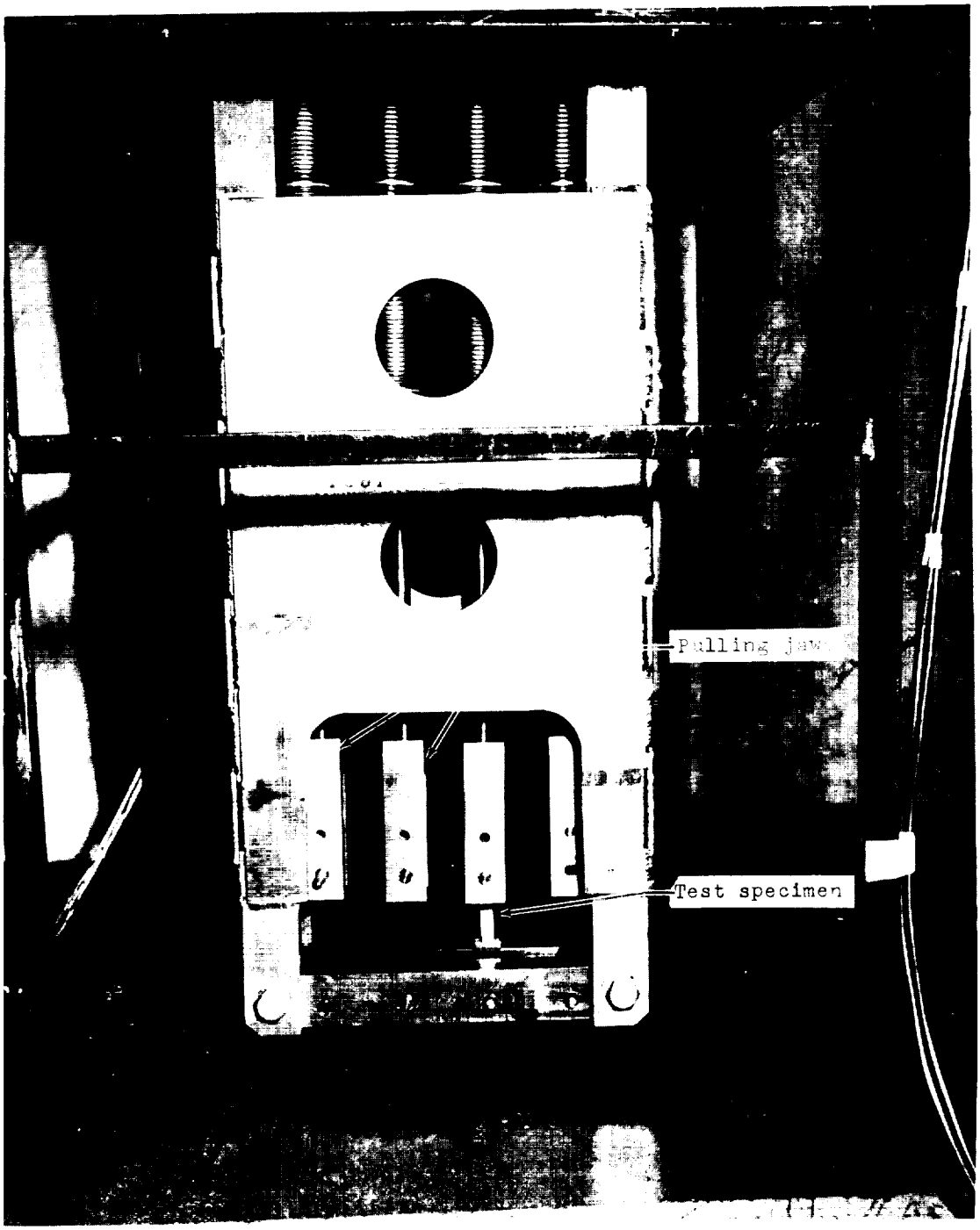

Figure 4.15 View of Specimen Racks of High-Force Tensile Tester

NPC 17,490
31-6596

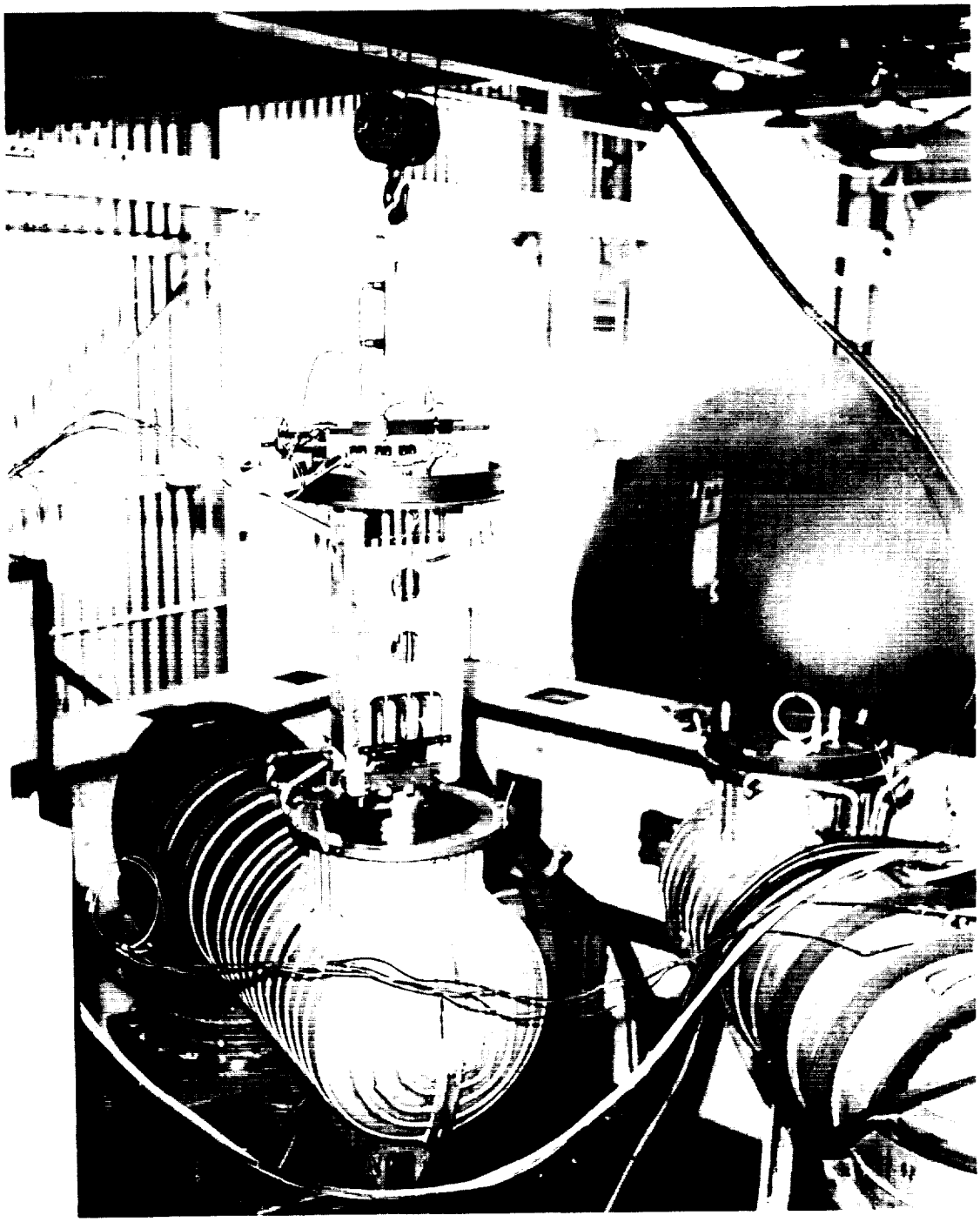

Figure 4.16 View of High-Force Tensile Tester Before Lowering into the Vacuum-Irradiation System

such that the maximum apparent strain due to temperature effects in the range of from 50°F to 240°F is 150 microinches per inch when bonded to a 2024-T4 Dural specimen.

The method of application of the strain gages to the specimens was selected to give a bond that would be reliable under the radiation environment to which the specimens would be exposed. The strain gages were bonded with an epoxy consisting of three parts by weight of Versamid 140 curing agent to one part of Epon 828 resin. The bonds were cured 18 hours overnight at 75°F and followed by two hours at 100°F to give sufficiently hard bonds for good operation of the strain gages. The wire grid of each strain gage was oriented to within less than two degrees of the specimen axis. The wire grid was also centered on the specimen gage length. These operations were facilitated by the translucent strain-gage backing, which enabled one to see the wire grid through the backing and which, in addition, facilitated removal of all air bubbles visible under the gage. The epoxy bond was kept as thin as possible to ensure that the gage was parallel to the surface of the specimen. After hardening of the bond, the thickness of the strain gage and bond on the specimen was usually 0.007 inch. The usual techniques of strain-gage application, such as careful cleaning with acetone and avoidance of contamination with moisture, were also employed. These techniques resulted in a very good bond, which withstood irradiation and did not fail even when the specimens broke.

A Type R Offner Dynagraph was used for readout of the strain-gage signals during tensile testing of the specimens. The ranges of sensitivity used during the tests were 0.2 mv/cm, 0.5 mv/cm, 1 mv/cm, 2 mv/cm, and 5 mv/cm - all of which were obtained by switching the gain of the Offner preamplifier. The highest sensitivity range enabled one to read the strain-gage signal to around 10 microinches per inch strain, depending on the overall gain characteristics of the Offner system of coupler, preamplifier, amplifier, and pen drive. The Offner recorder produced a chart having a trace of specimen strain vs time (chart speed = 1 mm/sec), which could be directly correlated with a simultaneous trace showing load vs time from the test-rig dynamometer and displayed on one of the other seven channels of the Offner Dynagraph.

Each strain gage bonded to a specimen was connected in a single-active-arm Wheatstone bridge. Two arms of the bridge were precision resistors in the Offner Dynagraph coupler and the remaining two external arms consisted of the specimen, or active, gage and a dummy strain gage of the same type and from the same lot.

Prior to irradiation and to pulling of the specimens in the high-load dynamic test apparatus, the insulation resistance and conductivity of the electrical circuit associated with the strain gages were checked to ensure that the gages would function properly. This was particularly necessary because of the use of a 165-ft signal cable from the test rig at the east face of the GTR to the Offner

recorder in the reactor control room. Normally, it is desirable for the insulation resistance to be at least 70 megohms to ground; however, because of extremely adverse weather conditions during the entire test, it was not possible to maintain such a high insulation resistance. This point is discussed in greater detail in Section 4.4.2.

Immediately before pulling the specimens, the strain gages were calibrated in the usual fashion by shunting various precision resistors across the active strain gage and measuring the recorder-pen deflection.

As it was reported in Reference 10, the effect of irradiation on phenolic-backed strain gages was expected to be minor on the basis of the results obtained with Duco gages. Tests on AB-3 bakelite gages subjected to the same radiation dose and vacuum environment as those used in the high-load dynamic test have borne out this expectation. The major discernible effect of both vacuum and reactor radiation on the AB-3 gages is a reduction of the total strain to which the gage can be subjected before the backing and wire grid break. This is illustrated in Figures 4.17 and 4.18. Each curve in these figures was obtained from an irradiated AB-3 gage bonded to the surface of an unirradiated AB-3 gage which, in turn, was bonded to a glass-cloth-laminate tensile specimen. The order of bonding of the gages to the tensile specimen was alternated to eliminate the effects of bending stresses that might be present. Two channels of the Offner Dynagraph were used - one for the irradiated strain gage, one for the

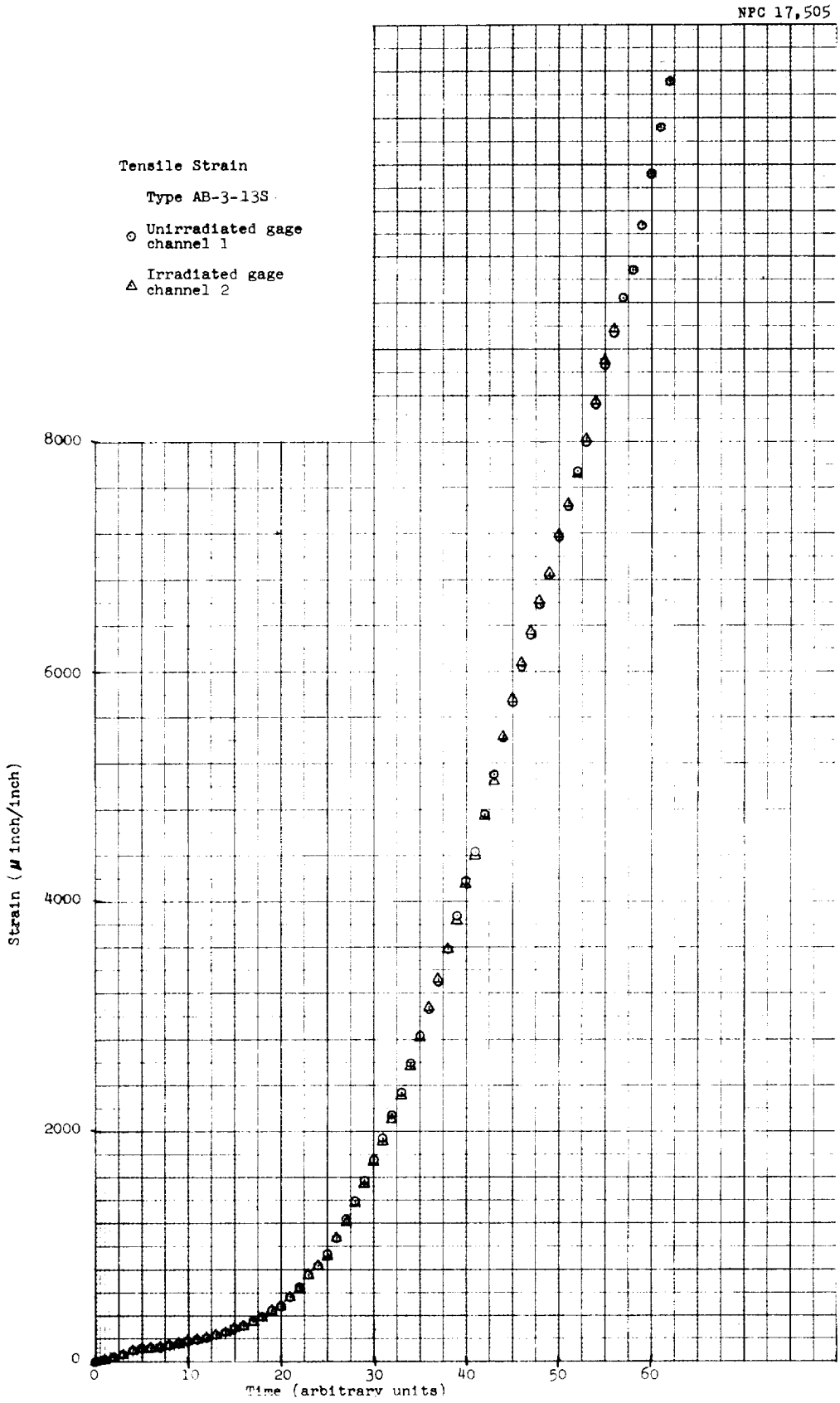

Figure 4.17 Comparison of Strain Measured with an Irradiated Strain Gage and Strain Measured with an Unirradiated Strain Gage

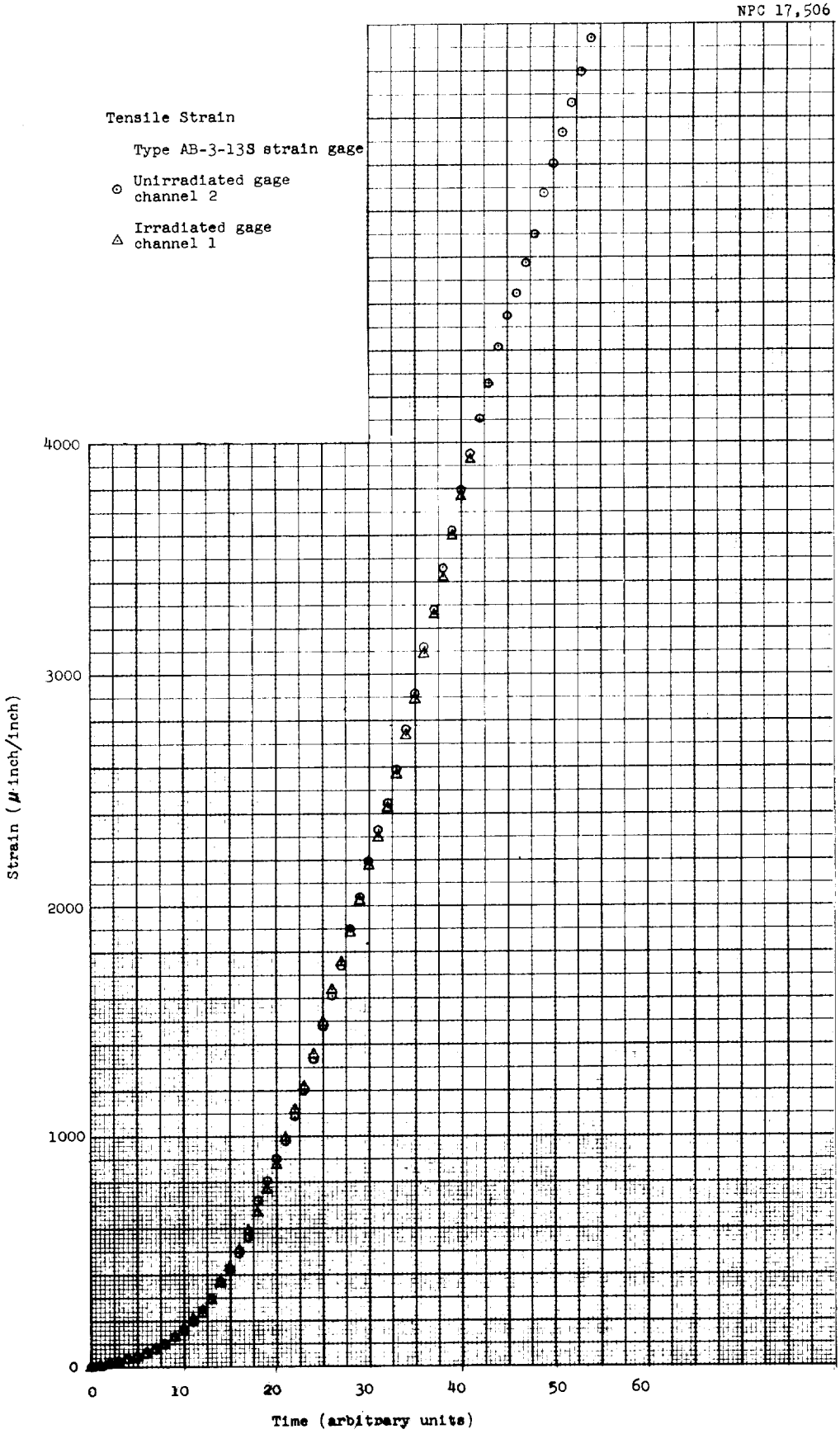

Figure 4.18 Comparison of Strain Measured with Irradiated Strain Gage and Strain Measured with Unirradiated Strain Gage: Amplifier Channels Interchanged

unirradiated gage. The Offner channels were alternated from irradiated strain gage to unirradiated strain gage, or vice versa, each time a new set of gages was tested. This allowed corrections to be applied to the data to eliminate small differences in gain and linearity between the two channels - differences which show up as a constant bias to the data, regardless of the condition of the strain gage. The largest such correction was 0.5 millivolts on the 5-mv/cm scale. After correction of the data, no significant difference could be found between the irradiated and unirradiated strain gages. All results obtained so far show no detectable effect of vacuum irradiation (identical to that used in the high-load dynamic test) on the gage factor of the AB-3 strain gages and no significant effect on the initial gage resistance and gage bond.

4.4.2 Experimental Results

The purpose of the high-force tensile test was to measure the ultimate tensile strength, ultimate elongation, and stress-strain characteristics over the range of from 0 to 3% strain of Conolon 506 and Epon 828/A bonded-glass-cloth laminates and of FM-1000 and Metlbond 302 aluminum lap-shear joints. It is felt that these objectives were attained and the test was highly successful.

Descriptions of the specimen materials, test procedures, and tensile sample preparation are given in Appendix C. Four sets of specimens of each type of material were tested: a set of controls, a set of static irradiated specimens, and two sets of dynamic

irradiated specimens (High-Force Run 1 and Run 2). The control specimens and the static irradiated specimens were pulled on the Instron. Stress was measured with the load cell on the Instron and strain was measured by strain gages in conjunction with the Offner Dynagraph. The dynamic irradiated specimens were pulled in the vacuum chamber on the high-force tensile tester immediately after irradiation. Stress was measured with a dynamometer; strain, with strain gages in conjunction with the Offner Dynagraph; and crosshead travel, with a LVDT.

During the first irradiation run, a leak developed in the vacuum chamber and the run was carried out at a pressure of 300 microns. Pressure data are given in Figures 4.2 and 4.3 of Section 4.1 for irradiation Run 1 and irradiation Run 2, respectively. As mentioned previously, slight flooding of the Reactor Handling Area, which was produced by a severe rainstorm during the last day of Run 1, resulted in drastically lowered insulation resistance of the strain-gage cables leading to the high-force test rig. The insulation resistance could not be brought back to the desired value even after the cables were dried; hence, it was necessary to pull the specimens with resistance to ground of the two external arms of the strain-gage bridge between 5000 and 5200 ohms. However, the gages were recalibrated after the cables dried, and this recalibration largely nullified the effect of the low insulation resistance. The low insulation resistance acted as a shunt across the active strain gage and thus made the apparent strain of the gage smaller than the true strain.

Had the gages not been recalibrated, the maximum error due to the low insulation resistance would be 4.7% at 10000 microinches-per-inch strain. However, calibration in the presence of the leakage resistance greatly reduced this effect of the leakage resistance. The gain and sensitivity of the strain-gage system was reduced by 5%, but this is not considered detrimental. Also, because of the reduced impedance on the input of the Offner Dynagraph, one of the strain-gage channels was noisy, but, again, this did not produce a large enough effect to obscure the reading on that channel.

The temperatures of specimens during Run 1 are given in Figures D-15 and D-16 of Appendix D, and the temperatures during Run 2 are given in Figure D-17. Temperatures of the vacuum chamber are given in Figure D-18. In both irradiation runs, specimens of each type of material were placed in the racks of the high-force tensile tester, pumped down to pressure, irradiated, and pulled immediately after reactor shutdown. Five Metlbond 302, five FM-1000, four Conolon, and four Epon 828/A specimens were tested in each irradiation run. These materials are tabulated in Table 4.16. Sample location and dosimetryare shown in Figures 4.19 and 4.20.

Ultimate tensile strengths, total nuclear radiation doses, and the number of specimens in control, in static irradiation, and in dynamic irradiation tests are shown in Tables 4.17 and 4.18. Stress-strain curves are given in Figures 4.21 through 4.37. The two stress-strain curves for the lap-shear specimens are plotted from crosshead-travel data measured by the LVDT. The elongation of the LVDT was

reduced to strain in a 2-inch gage length to give the abscissa of the curves. In the case of the stress-strain curves obtained from strain-gage measurements of the specimen strain, the curves are extrapolated (as indicated by a dashed line) from the breaking point of the strain gages to the breaking point of the specimens. Correlation of strain-gage and LVDT data is given in Figure 4.38.

The average ultimate tensile strength of all specimens showed a significant increasing trend from the control tests through the static irradiation tests to the dynamic irradiation tests. The sole exception to this trend is the ultimate strength of the FM-1000 specimens in dynamic Run 1. It should be pointed out, however, that the standard deviation of the ultimate strength of the FM-1000 specimens in Run 1 is 729 psi, which overlaps the trend. In addition, the stress-strain curves for the irradiated glass-cloth-laminates - with the exception of Specimen 1 of the static Conolon laminates - definitely show that the elastic moduli of the laminates have increased as a result of the combined effects of the vacuum and nuclear radiation. The increased elastic moduli and progressive increase of ultimate tensile strengths apparently can be attributed to a greater rate of crosslinking of the polymer networks relative to polymer chain scission by oxygen during irradiation. At the lower partial pressures of oxygen in the higher vacuum, the rate of oxygen-induced chain scission is decreased and, consequently, the relative rate of radiation-induced crosslinking is increased, leading to increased stiffness and strength of the polymers.

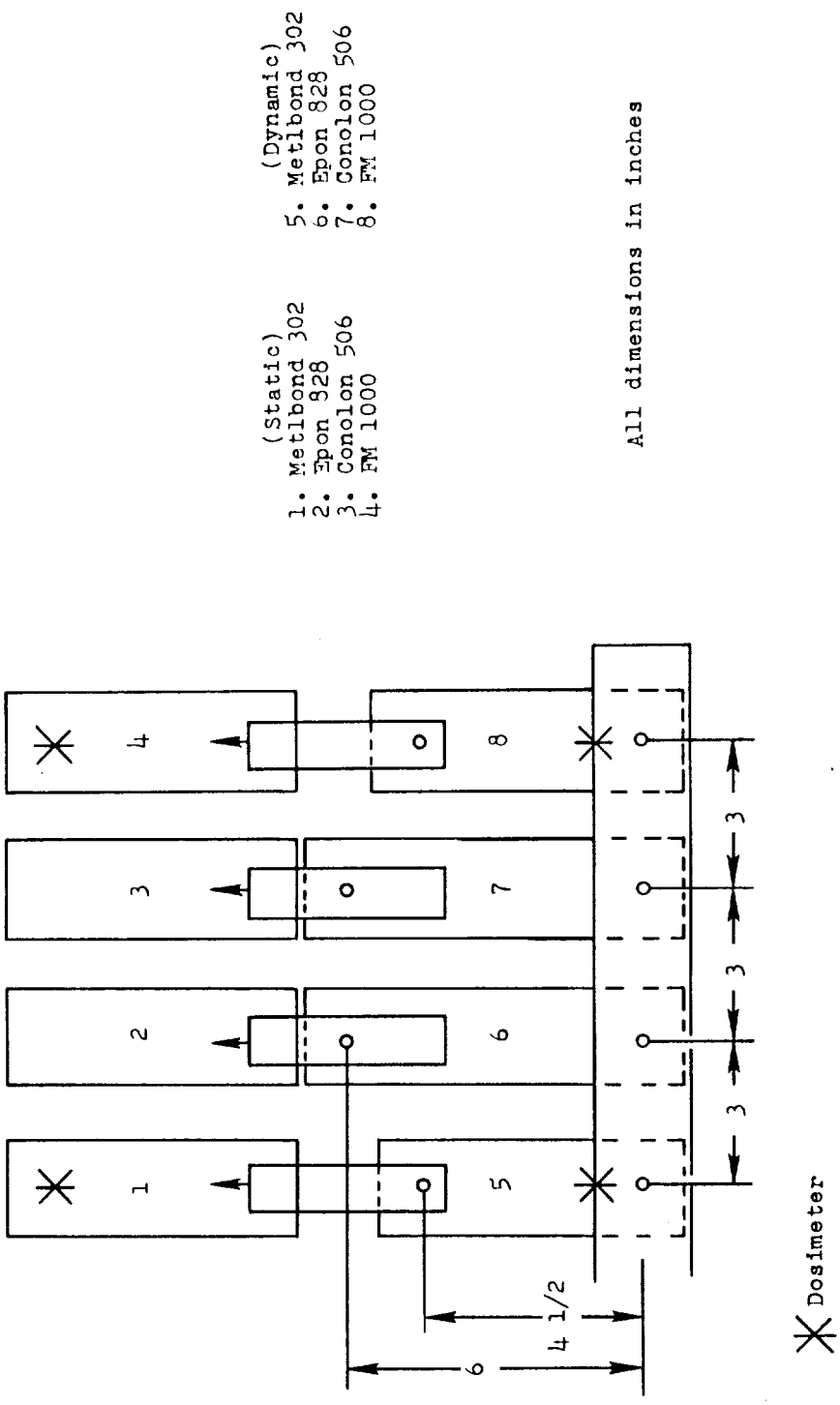

Figure 4.19 Location of Samples and Dosimeters for High-Force Dynamic Test: Run 1

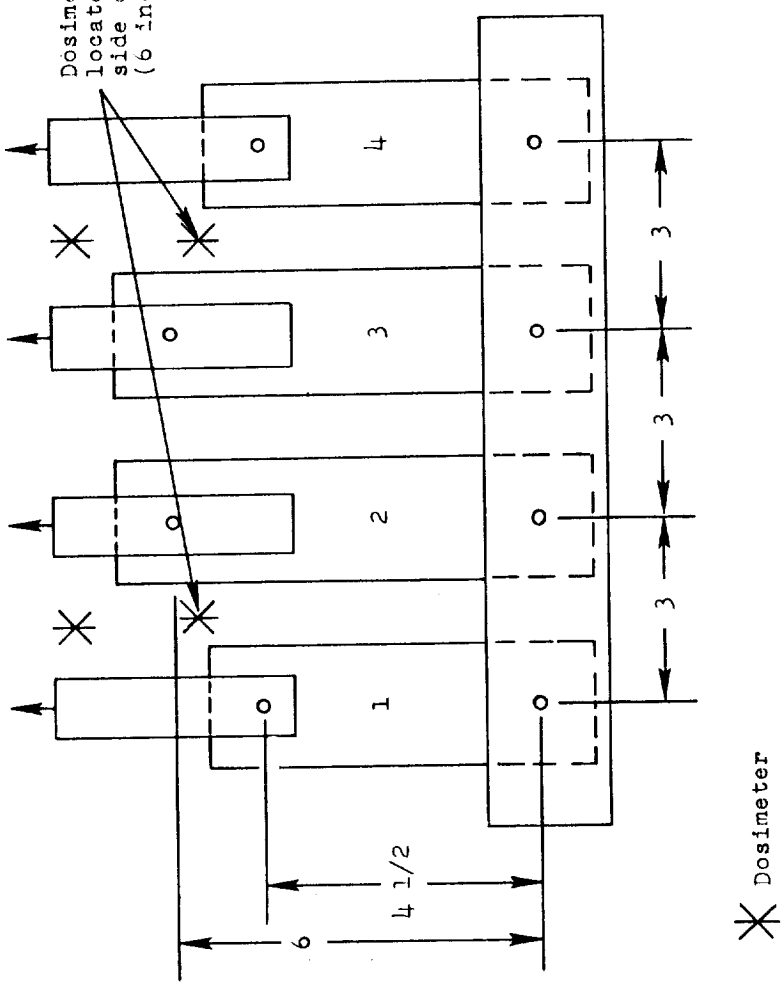

Figure 4.20 Location of Samples and Dosimeters for High-Force Dynamic Test: Run 2

Table 4.17

Test Environment and Results for High-Force Dynamic-Test Materials: Structural Adhesives

Material and Type of Test	Radiation Exposure				Ultimate Shear Strength (psi)	Temperature		Pressure	
	Gamma [ergs/gm(C)]	Neutrons (n/cm^2)				Avg (^oF)	Fig. No.	Avg (torr)	Fig. No.
		Thermal	E>2.9 Mev	E>8.1 Mev					
FM-1000	0	0 (control specimens)	0	0	6302 6117 6004 5946 5955 6065/153[a]	77	-	760	-
High-Force Tester	1.1(10)	1.82(14) (vacuum irradiation)	1.83(15)	7.0(13)	6050 6096 6525 4830 4977 5696/729	157	D-16	3	4.2
High-Force Tester	1.9(10)	5.1(14) (vacuum irradiation)	4.15(15)	1.7(14)	7016 6897 7689 7760 7340/419	-	-	5(-6)	4.3
Instron Tester	9.15(9)	1.34(14) (vacuum irradiation)	1.51(15)	5.95(13)	6082 6200 5900 6185 6442 6162/233	207	D-16	3	4.2
Metlbond 302	0	0 (control specimens)	0	0	2323 2510 2570 2526 2482/120[a]	77	-	760	
High-Force Tester	1.6(10)	1.0(14) (vacuum irradiation)	2.33(15)	8.8(13)	2984 2938 2949 2747 2660 2856 2856/139	157[b]	D-16	3	4.2
High-Force Tester	2.05(10)	4.57(14) (vacuum irradiation)	4.32(15)	1.98(14)	3613 3680 3310 3497 3455 3511/159	-	-	5(-6)	4.3
Instron Tester	9.15(9)	1.34(14) (vacuum irradiation)	1.51(15)	5.95(13)	2586 2415 2355 2536 2643 2507/140	207[b]	D-16	3	4.2

[a]Average value/standard deviation on an individual basis
[b]Estimated value based on temperature of FM-1000

Table 4.18

Test Environment and Results for High-Force Dynamic-Test Materials: Structural Laminates

Material and Type of Test	Radiation Exposure				Ultimate Tensile Strength (psi)	Ultimate Elongation (%)	Temperature		Pressure	
	Gamma [ergs/gm(C)]	Neutrons (n/cm^2)					Avg (^{o}F)	Fig. No.	Avg (torr)	Fig. No.
		Thermal	E>2.9 Mev	E>8.1 Mev						
Epon 828	0	0 (control specimens)		0	33,760 41,137 37,452/6534	1.3 1.5 1.40/.17[a]	77	-	760	-
High-Force Tester	1.33(10)	8.6(13)	2.0(115) (vacuum irradiation)	7.57(13)	46,700 46,000 47,267 50,893 47,715/2376	1.8 2.2 2.0/.34	153[b]	D-17	3	4.2
High-Force Tester	1.97(10)	4.83(14)	4.23(15) (vacuum irradiation)	1.84(14)	56,267 56,035 55,200 54,452 55,489/881	-	205	D-19	5(-6)	4.3
Instron Tester	8.6(9)	1.61(14)	1.45(15) (vacuum irradiation)	5.7(13)	42,034 40,830 41,699 44,000 42,141/1540	1.5 1.4 1.5 1.6 1.5/.097	158[b]	D-17	3	4.2
Conolon 506	0	0 (control specimens)		0	41,333	1.5	77	-	760	-
High-Force Tester	1.25(10)	7.81(13)	1.82(15) (vacuum irradiation)	6.88(13)	52,250 52,250 53,438 56,333 53,568/1983	2.2 2.3 2.25/.088	153	D-15	3	4.2
High-Force Tester	1.97(10)	4.83(14)	4.23(15) (vacuum irradiation)	1.84(14)	64,516 61,515 65,484 65,484 64,250/1928	-	-	-	5(-6)	4.3
Instron Tester	9.7(9)	1.07(14)	1.57(15) (vacuum irradiation)	6.2(13)	39,492 42,193 41,295 44,079 41,765/2228	1.4 1.4 1.4 1.6 1.45/.097	158	D-15	3	4.3
Instron Tester	1.0(10)	0	2.5(15) (air irradiation)	0	41,850/3	1.91/3	-	-	760	-
Instron Tester	6.7(10)	0	1.7(16) (air irradiation)	0	40,160/3	1.81/3	-	-	760	-

[a]Average value/standard deviation on an individual basis

[b]Estimated value based on temperature of Conolon 506

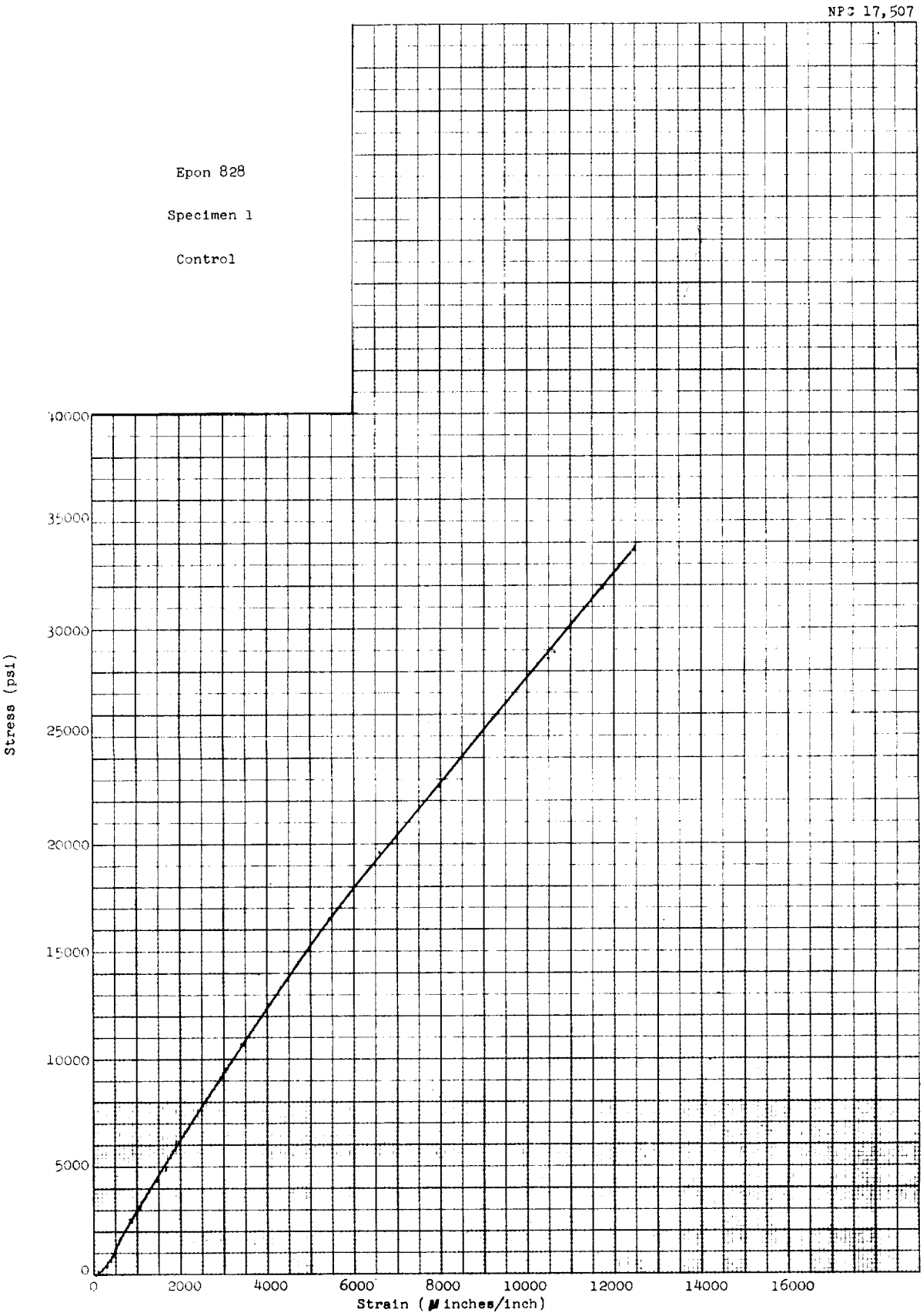

Figure 4.21 Stress-Strain Curve of Epon 828/A: Control Specimen 1

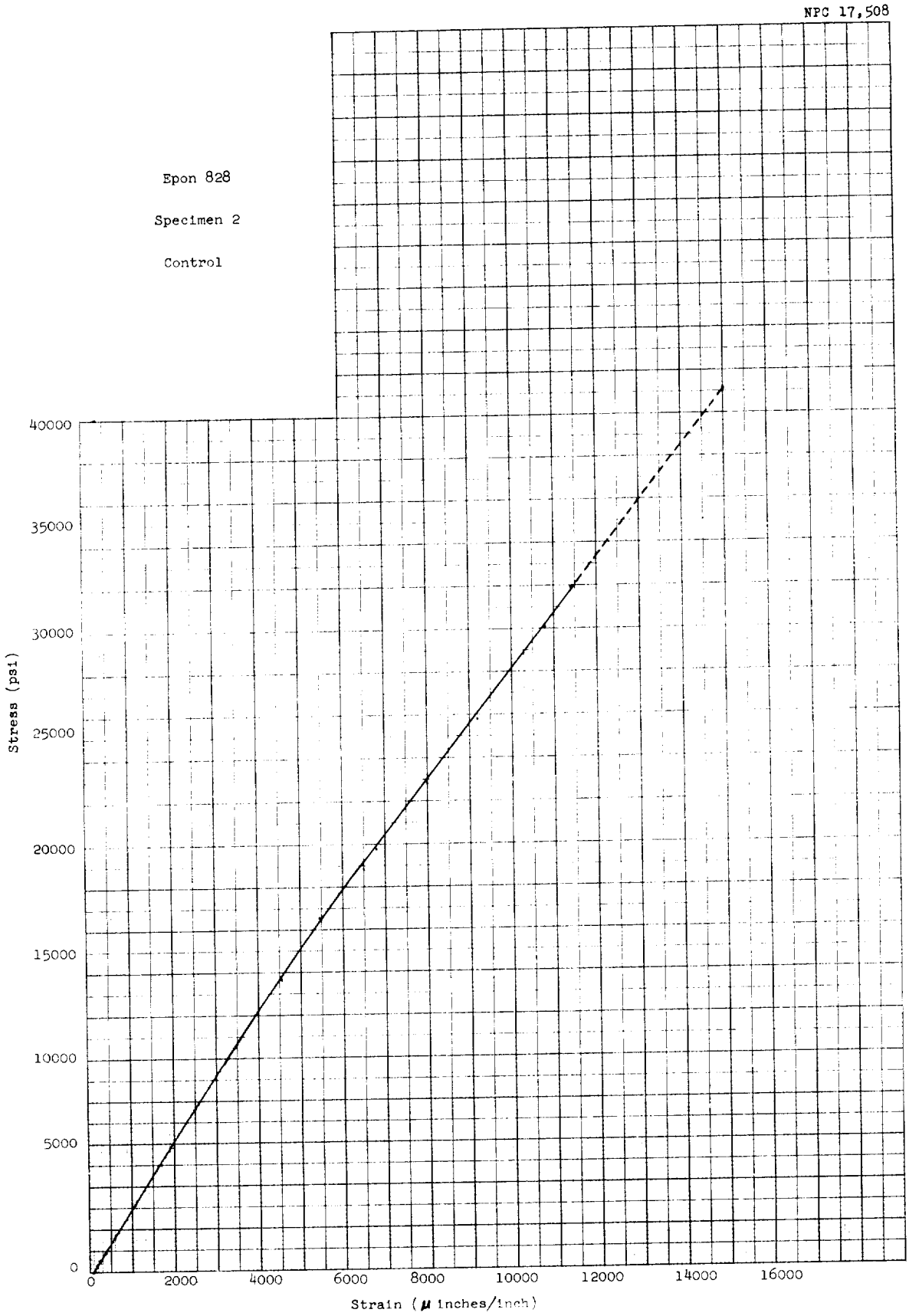

Figure 4.22 Stress-Strain Curve of Epon 828/A: Control Specimen 2

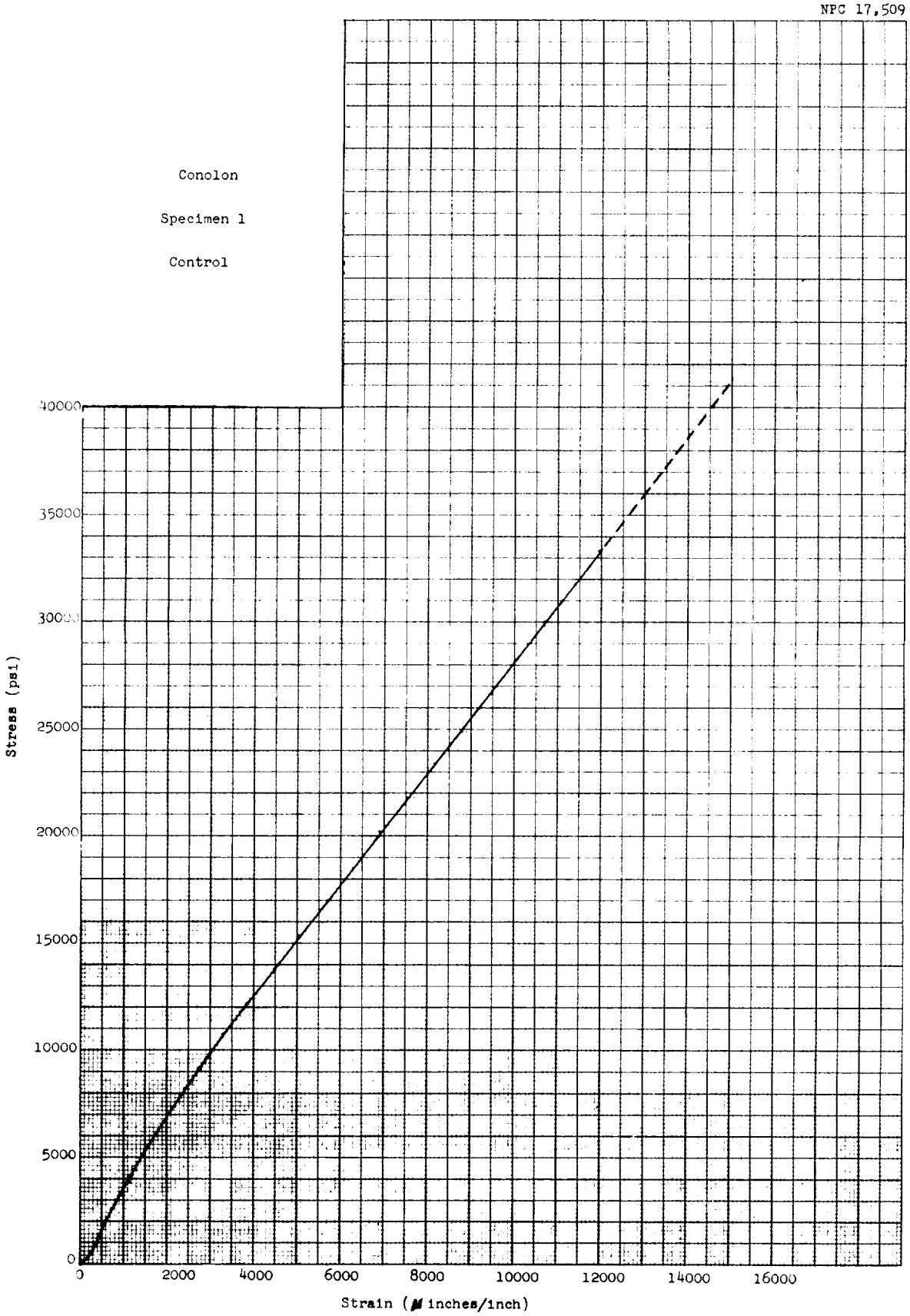

Figure 4.23 Stress-Strain Curve of Conolon: Control Specimen 1

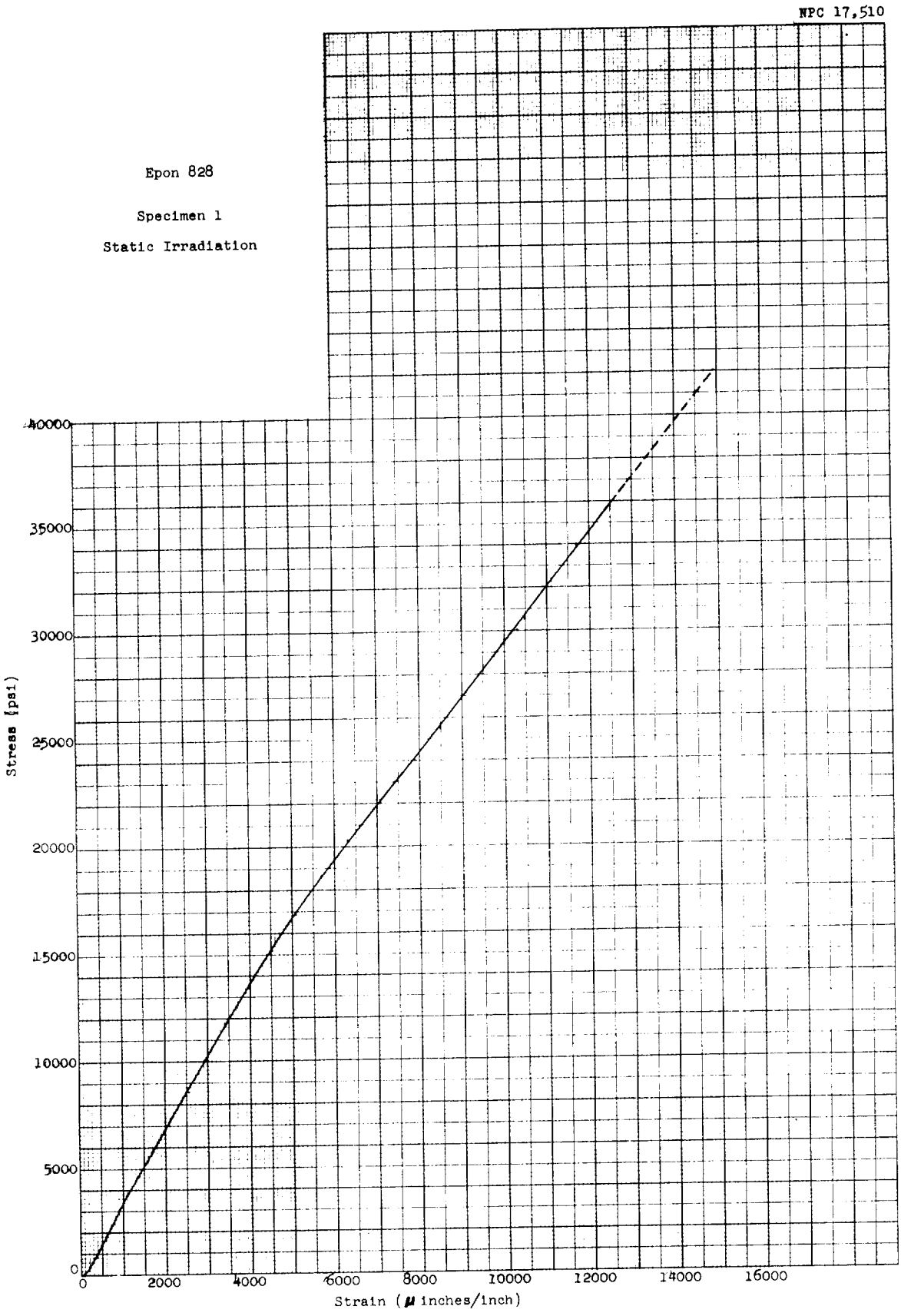

Figure 4.24 Stress-Strain Curve of Epon 828/A Irradiated in High-Force Tensile Test: Static Irradiation; Specimen 1

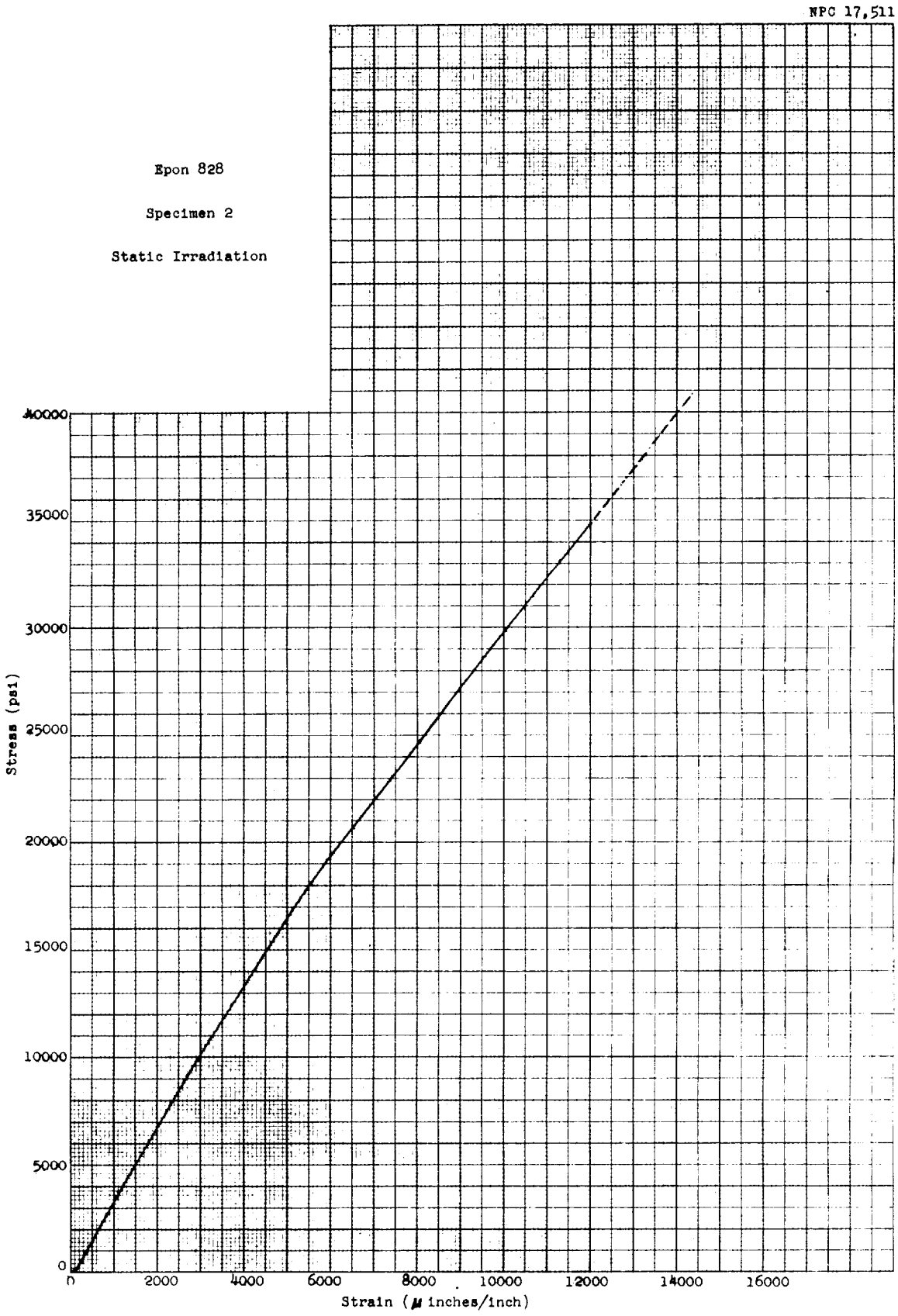

Figure 4.25 Stress-Strain Curve of Epon 828/A Irradiated in High-Force Tensile Test: Static Irradiation; Specimen 2

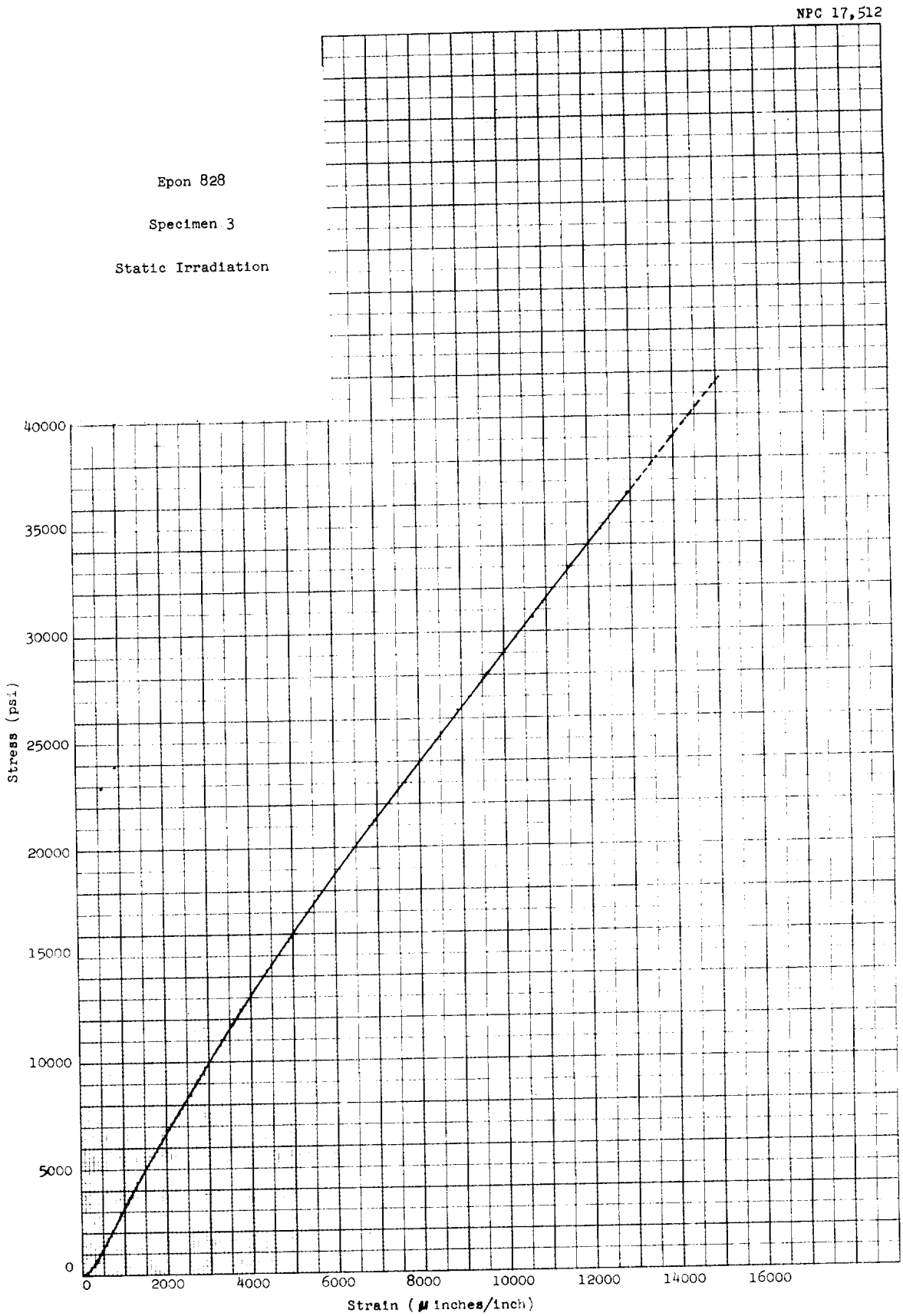

Figure 4.26 Stress-Strain Curve of Epon 828/A Irradiated in High-Force Tensile Test: Static Irradiation; Specimen 3

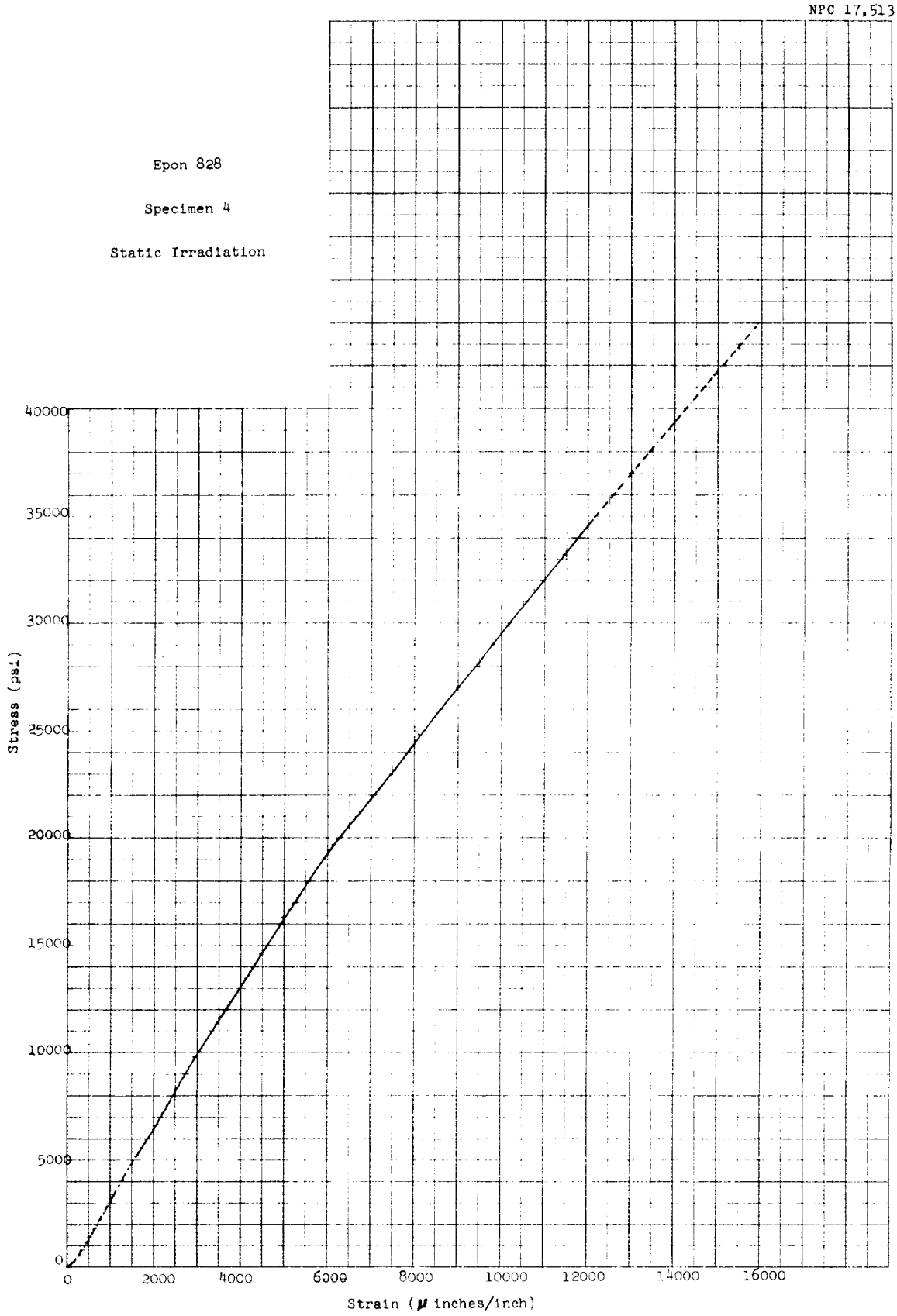

Figure 4.27 Stress-Strain Curve of Epon 828/A Irradiated in High-Force Tensile Test: Static Irradiation; Specimen 4

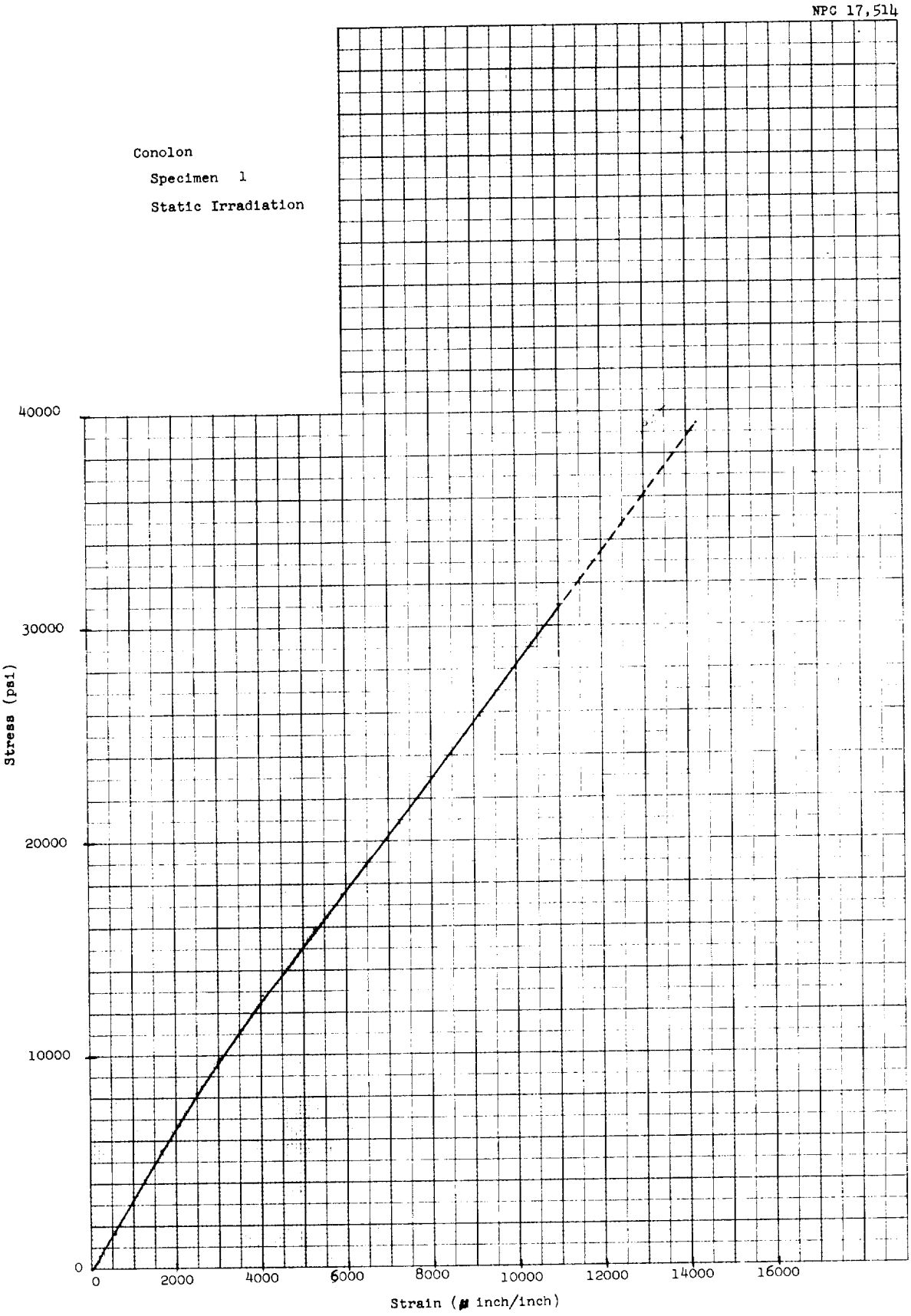

Figure 4.28 Stress-Strain Curve of Conolon Irradiated in High-Force Tensile Test: Static Irradiation; Specimen 1

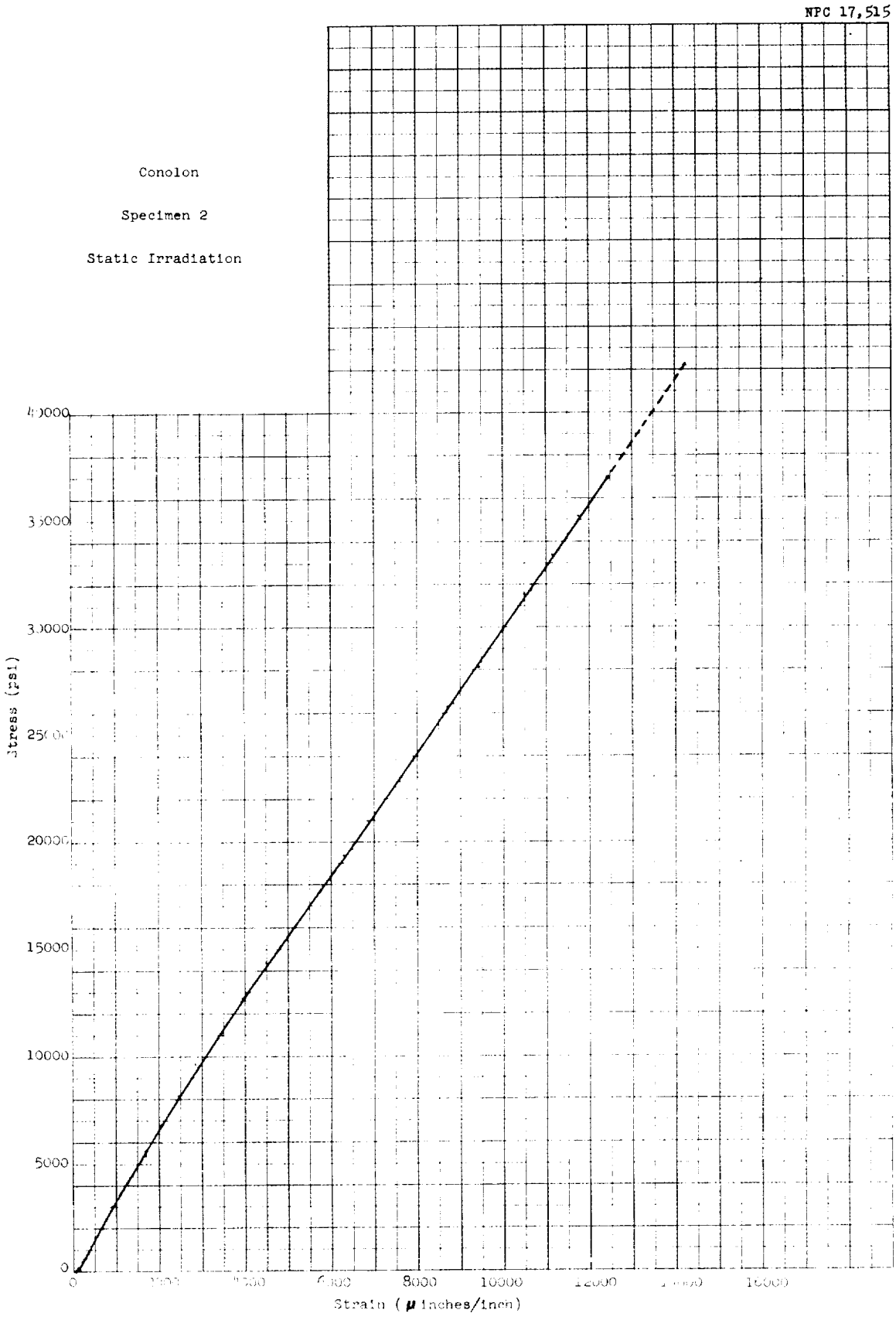

Figure 4.29 Stress-Strain Curve of Conolon Irradiated in High-Force Tensile Test: Static Irradiation; Specimen 2

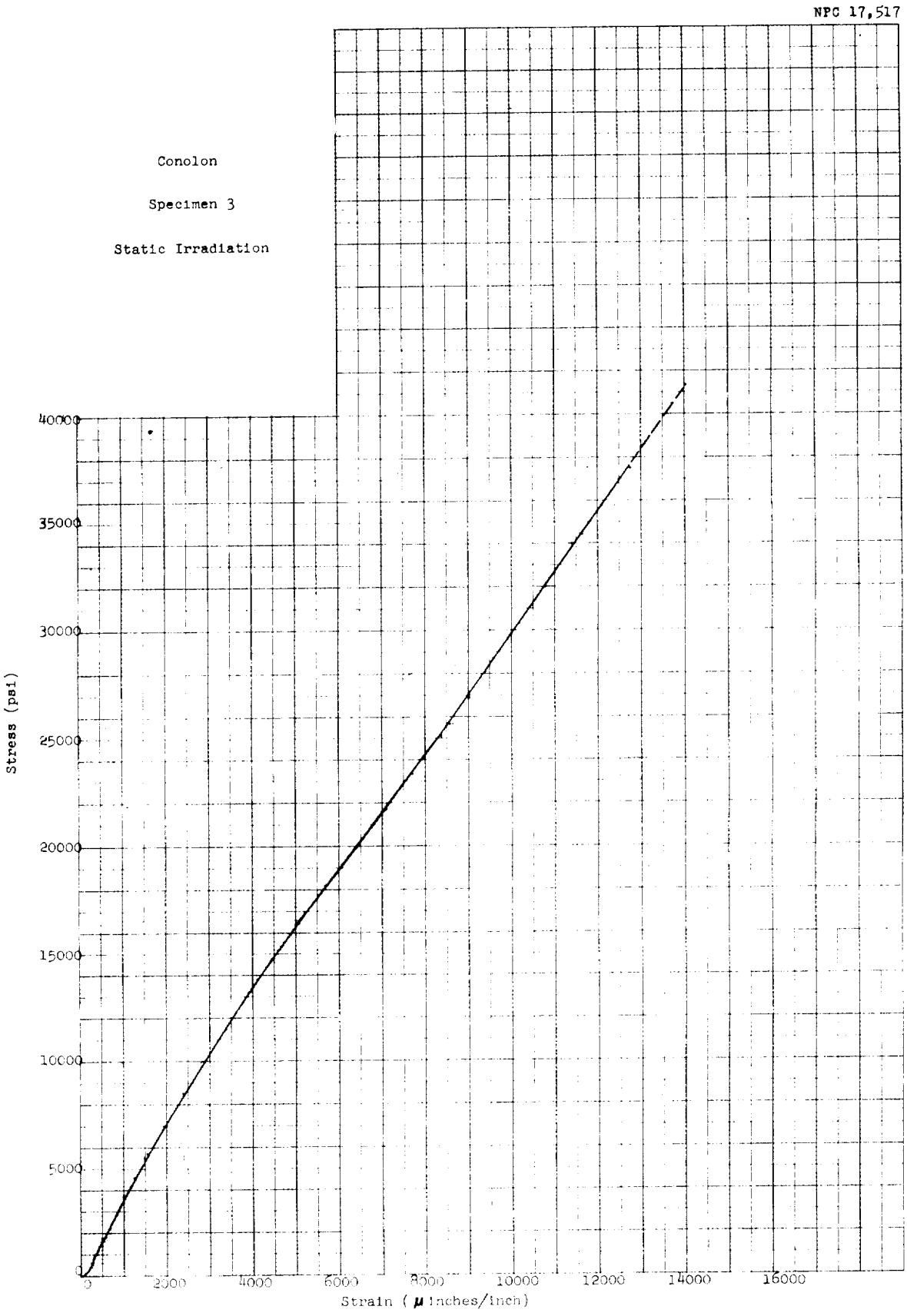

Figure 4.30 Stress-Strain Curve of Conolon Irradiated in High-Force Tensile Test: Static Irradiation; Specimen 3

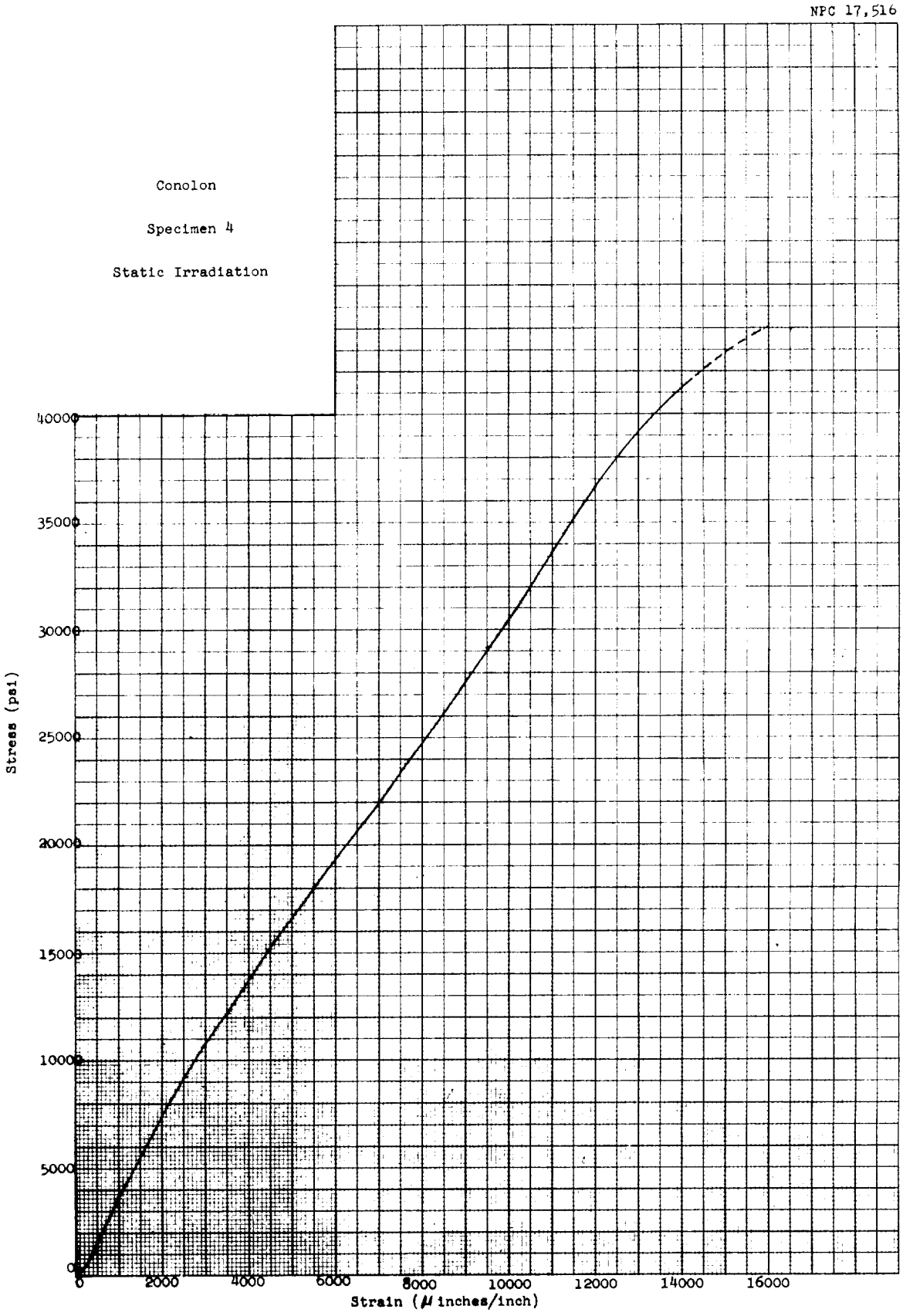

Figure 4.31 Stress-Strain Curve of Conolon Irradiated in High-Force Tensile Test: Static Irradiation; Specimen 4

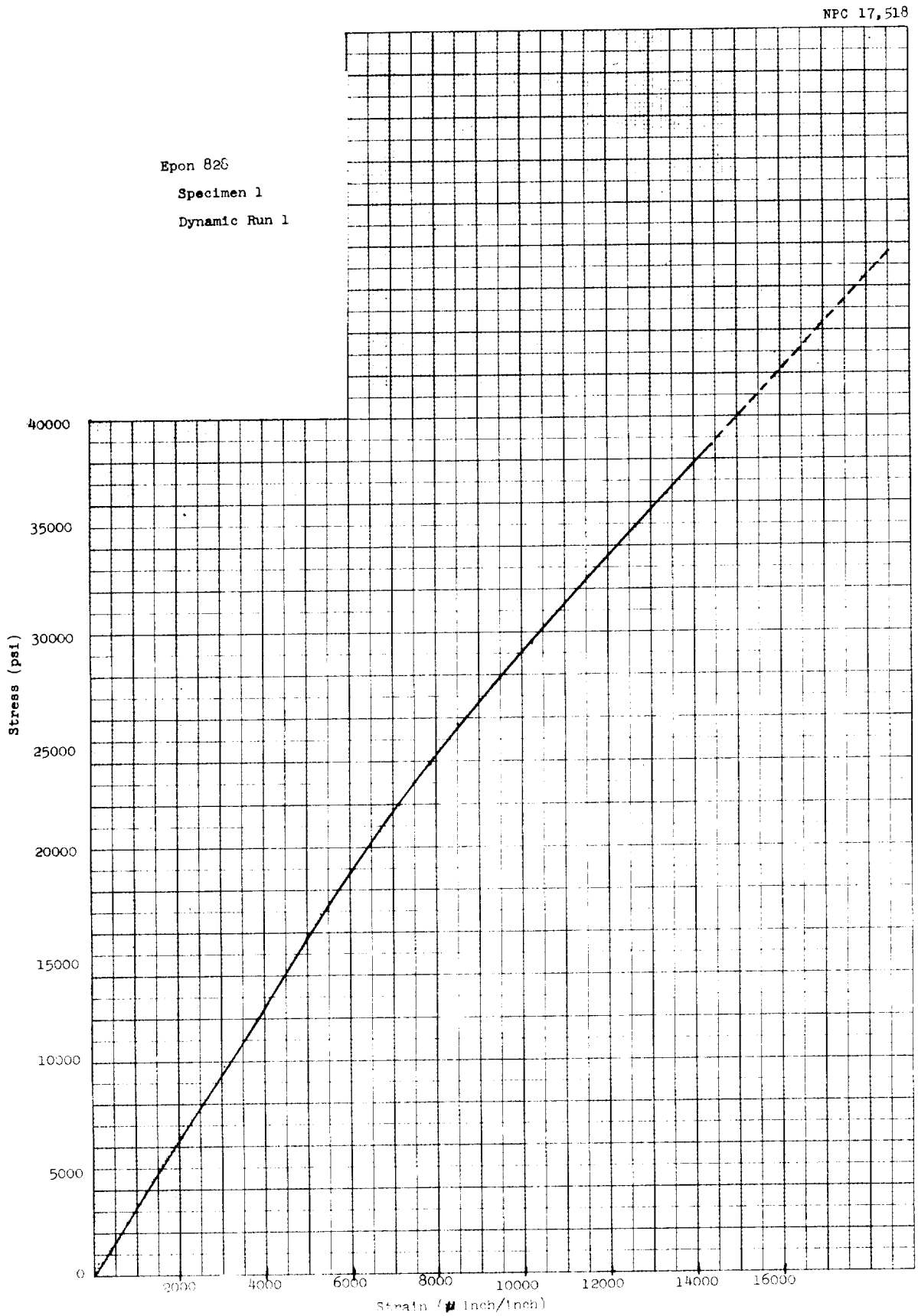

Figure 4.32 Stress-Strain Curve of Epon 828/A Irradiated in High-Force Tensile Test: Run 1: Specimen 1

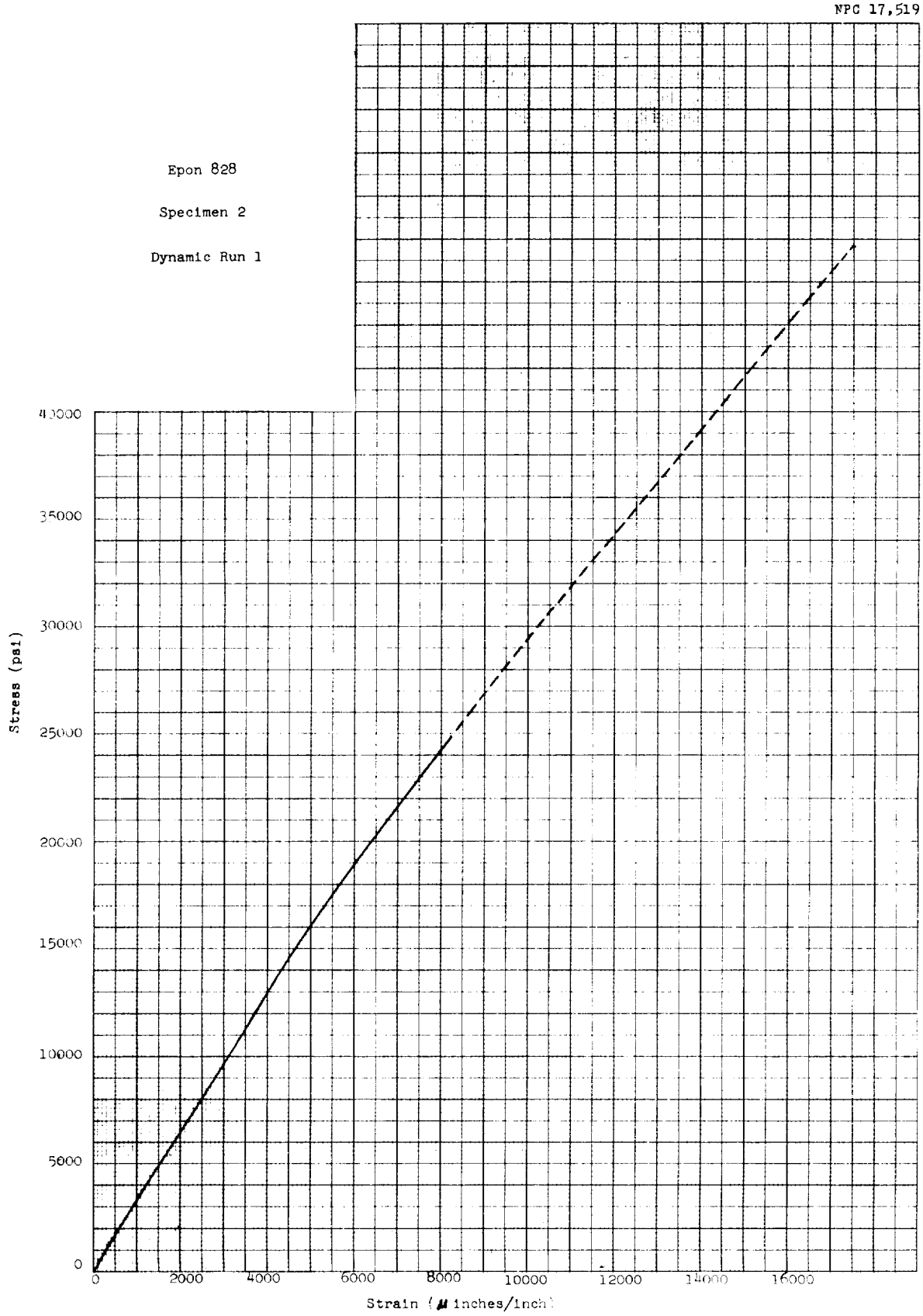

Figure 4.33 Stress-Strain Curve of Epon 828/A Irradiated in High-Force Tensile Test: Run 1; Specimen 2

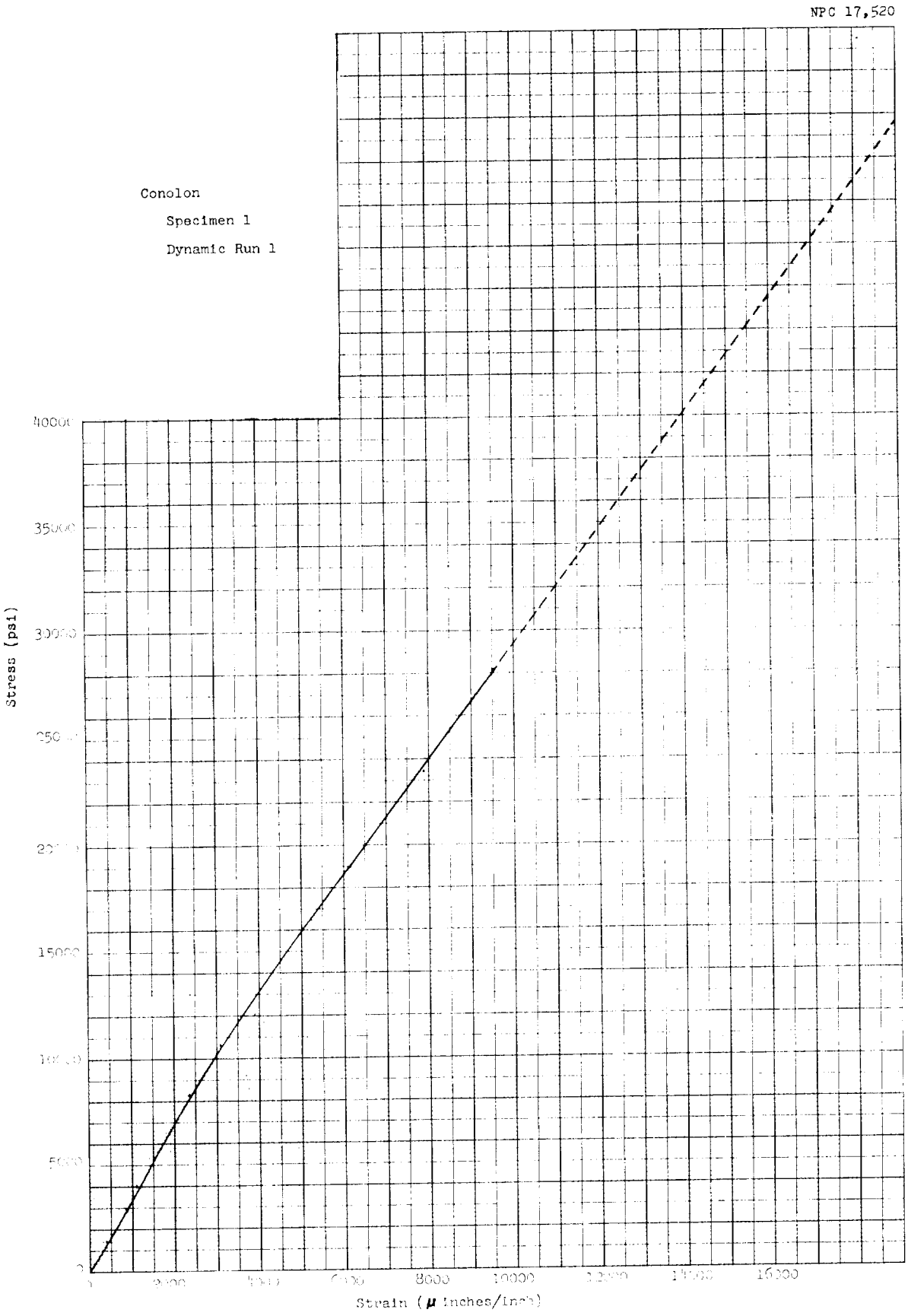

Figure 4.34 Stress-Strain Curve of Conolon Irradiated In High-Force Tensile Test: Run 1; Specimen 1

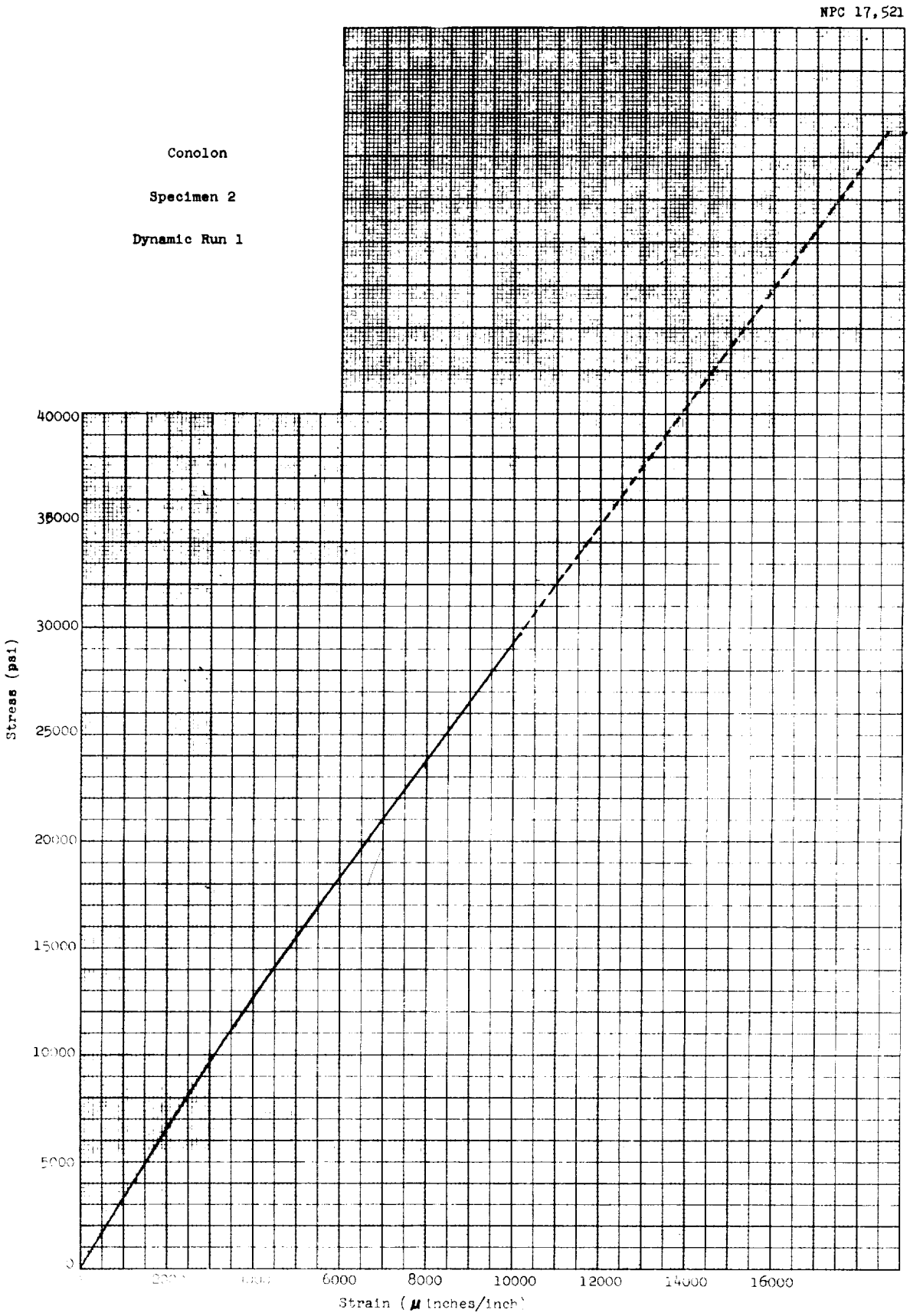

Figure 4.35 Stress-Strain Curve of Conolon Irradiated in High-Force Tensile Test: Run 1; Specimen 2

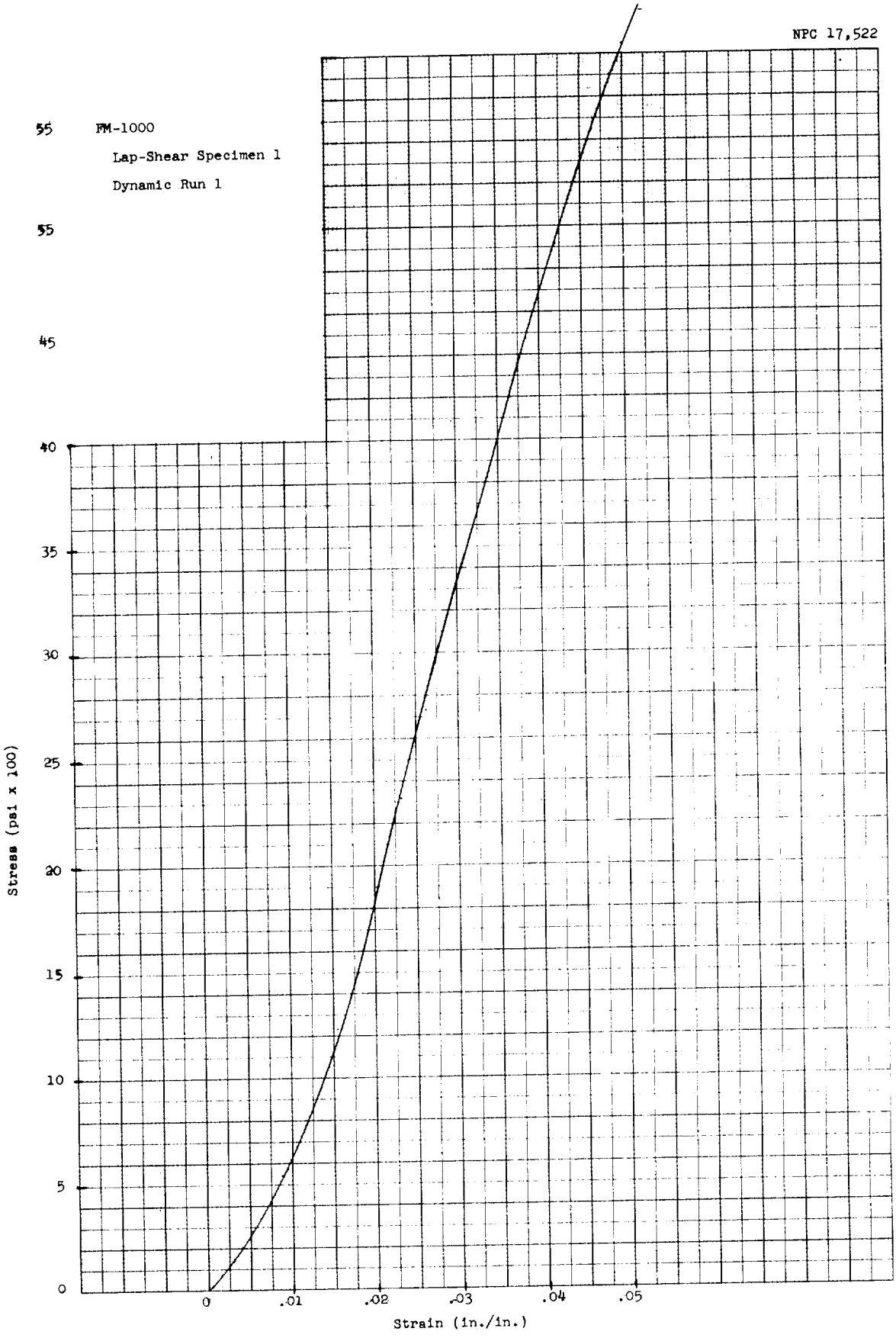

Figure 4.36 Stress-Strain Curve of FM-1000 Irradiated in High-Force Tensile Test: Run 1

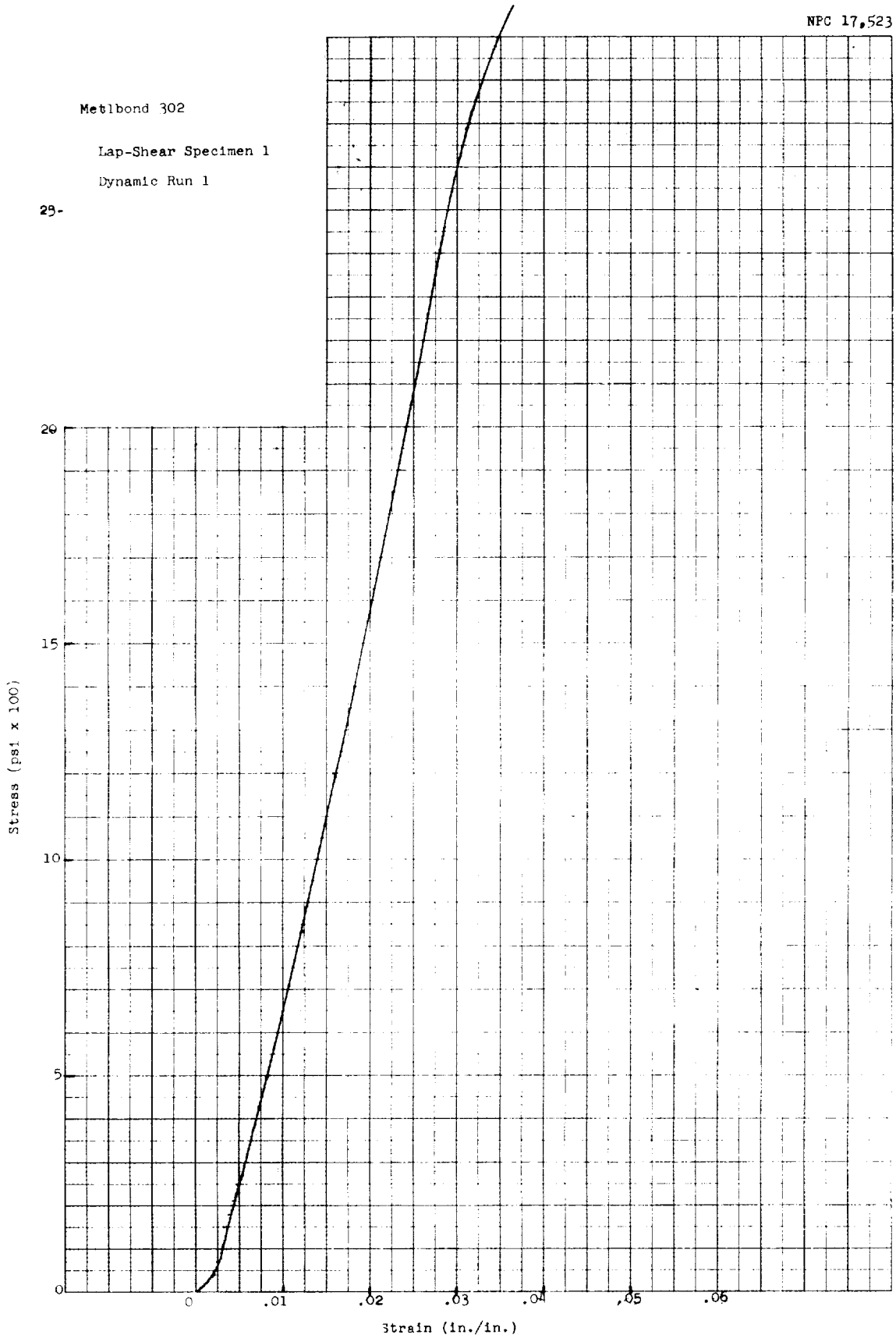

Figure 4.37 Stress-Strain Curve of Metlbond 302 Irradiated in High-Force Tensile Test: Run 1

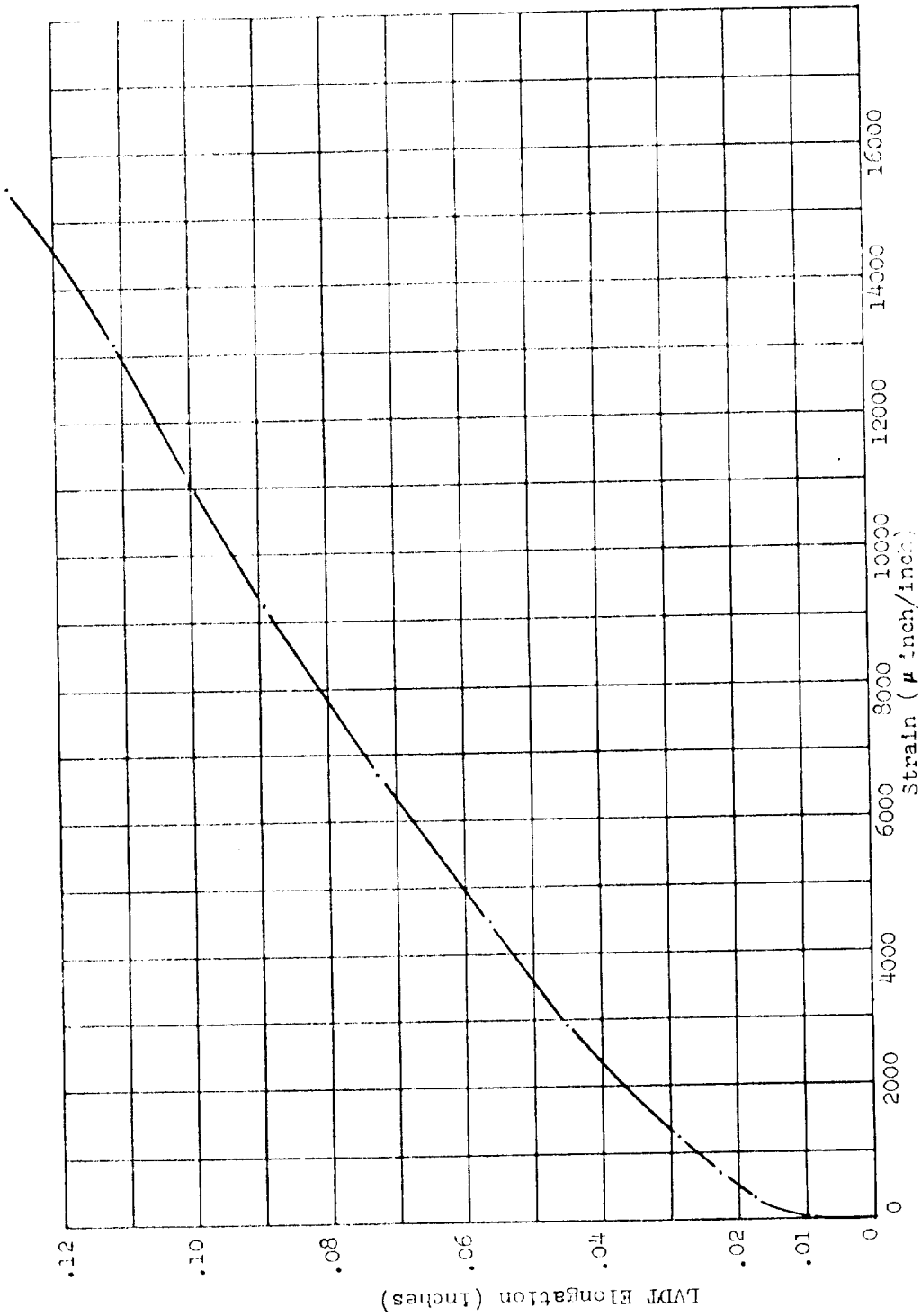

Figure 4.38 Correlation of LVDT Crosshead Travel with Strain-Gage Strain

4.5 Bearing Lubricant Test

In this test, the effects of vacuum-irradiation on the lubricity of four selected lubricants were investigated. The lubricants were tested by means of small servomotors, the bearings of which had been packed with the lubricants. The measurements taken during irradiation of the motors while inside the vacuum system included the time required for the motor rotors to coast down to zero rpm after electrical power shutoff, the no-load motor speeds, the bearing temperatures, the current drawn by the motors, the vacuum pressure, and the radiation exposure.

4.5.1 Experimental Equipment

The experimental equipment consisted of the following items: eight small servomotors specially fitted with bearings containing the particular lubricant to be tested; a rack to suspend the motors in the vacuum irradiation chamber, to support magnetic reed switches for measurement of motor rpm, and to support copper-constantan thermocouples for measurement of bearing temperatures; and electronic measuring circuits, which were connected to the sensing elements in the vacuum irradiation chamber by a 165-ft cable. A description of the prototype apparatus used in investigating this concept of measurement is given in the Third Quarterly Progress Report (Ref. 10). The apparatus used in the actual lubricant test differs in particulars from the prototype but is substantially the same. Figure 4.39 is a photograph of the test apparatus.

NPC 17,485
31-6752

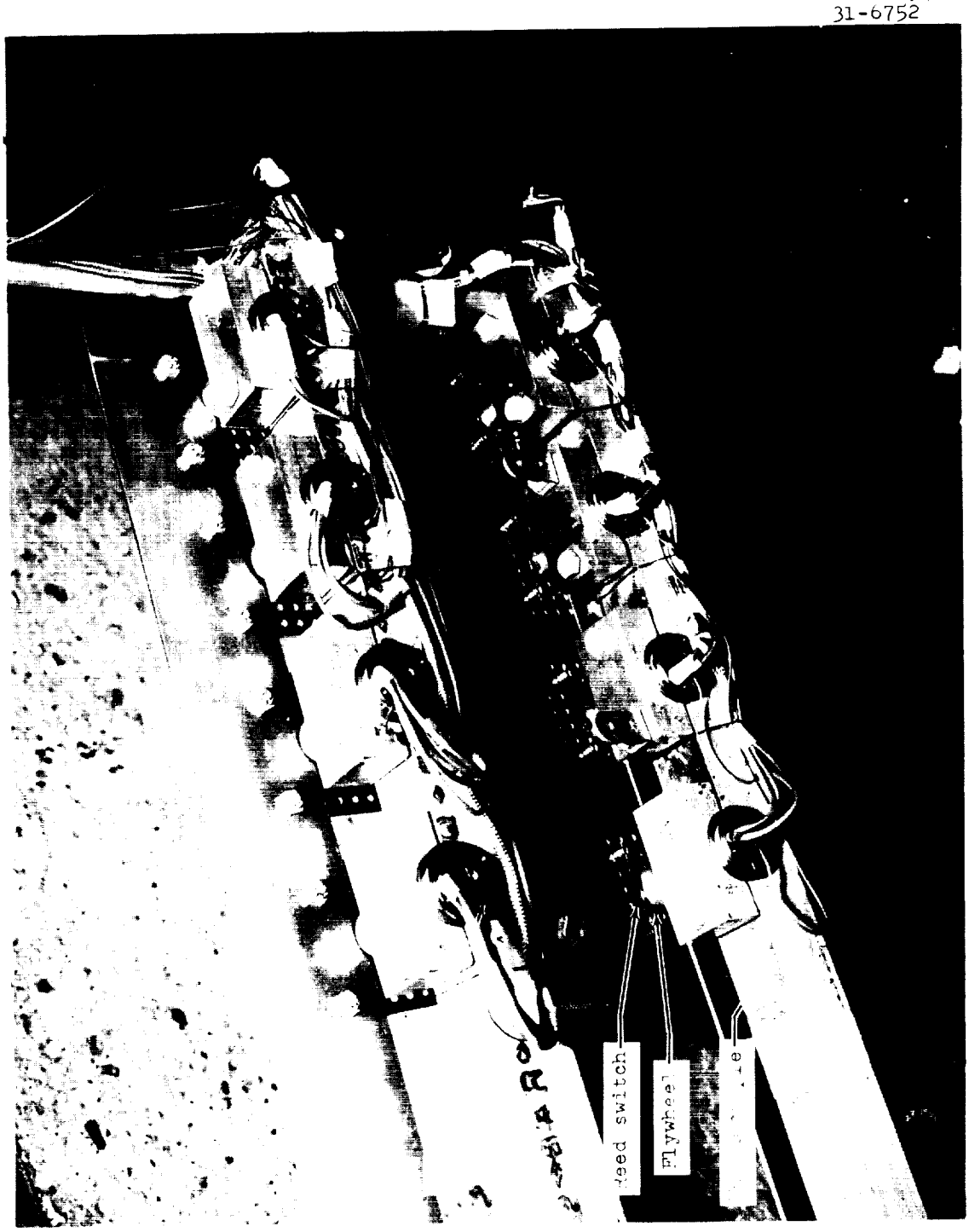

Figure 4.39 View of Bearing-Lubricant-Test Motors

Four types of lubricants were used in this test: GE Versilube F-50, an oil; Shell ETR-H, a grease; Molykote X-15, a dry-film lubricant with inorganic binder; and Electrofilm 66-C, a dry-film lubricant with organic binder. These lubricants have been described in Reference 10.

Each motor used in this test was specially fitted with miniature ball bearings which were packed with one of the four lubricants. The bearings were packed and installed in the motors at the Miniature Precision Bearing Company by engineers who also measured starting torque, radial clearance, and end-play of the bearings. The bearings were initially cleaned with acceptable solvents in a triple-spray wash under controlled rotation. Following cleaning, they were dried with forced air. The bearing surfaces were then examined for defects and a dirt count made. The average running torque of the bearings was checked with a Miniature Precision Bearing Company Model MB Mark 3 Torque Tester. Vibration of the bearings at 6000 rpm was tested with a Miniature Precision Bearing Company Model MB Vamp Tester. The lubricant was then applied and the running torque and vibration tests repeated. The bearings were assembled in the motors in a white room. Radial clearance of all bearings was held between 0.0002 and 0.0005 inch. The method of application of lubricants is given in Table C-2 (App. C).

All eight of the motors are Type R119-22E servomotors manufactured by the Kearfott Company. They are 2-phase 400-cps motors requiring 115 volts per phase. Measured at stall, the field current per phase is 53 milliamperes, the power input per phase is 3.5 watts, the power factor per phase is 0.575, and the effective

resistance per phase is 3800 ohms. The minimum no-load speed at both high and low temperature is 6200 rpm, with a typical value given as 6650 rpm. The minimum stall torque is 0.60 ounce-inch, with a typical value given as 0.62 ounch-inch. The moment of inertia of the rotor is 1.07 gm-cm^2, and the theoretical acceleration is 39,450 radians/sec^2. The typical temperature rise during operation of the motors is 99°F.

For purposes of measuring the motor speed and coast time, a small Alnico bar magnet was attached to the shaft of each motor by means of a cylindrical aluminum spindle. The spindle was pressed onto the motor shaft, so that the bar-magnet axis was perpendicular to the motor shaft. This magnet assembly increased the moment of inertia of the rotor by an additional 4.92 gm-cm^2.

The motors were mounted on a rack, illustrated in Figures 4.39 and 4.40, in positions that were symmetrical with respect to the centerline of the GTR core in order to obtain a high and uniform radiation dose rate. The rack itself was of lightweight but rigid construction, consisting entirely of aluminum alloy - a design which minimized structural heating by gamma rays. Opposite each motor on the rack was mounted a magnetic-reed switch, the position of which could be adjusted with respect to the bar magnet attached to the motor shaft. This design feature allowed elimination of a large portion of the contact bounce produced in the switches by the high speed of the motors.

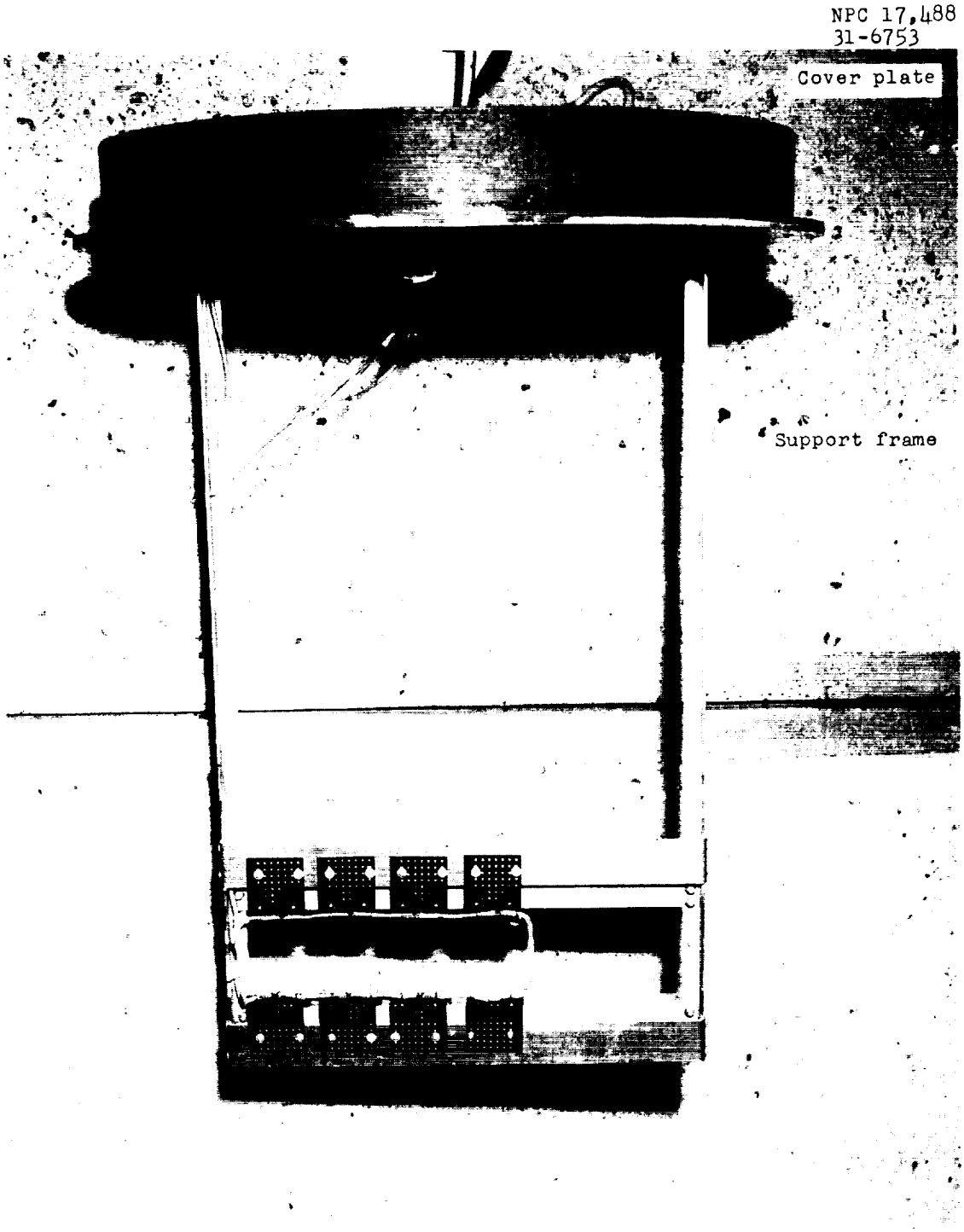

Figure 4.40 Bearing-Lubricant-Test Rack

Normally, the reed switches would be set at a distance of 1/8 inch from the poles of the magnets. All electrical wiring to the reed switches and motors was made from 24-gage magnet wire that was thoroughly coated with glyptal to reduce outgassing of the insulation while in the vacuum chamber. Two separate cables, consisting of wire bundles prepared in the above manner and covered with a single shield, led from Deutsch plugs on the cover plate of the vacuum-irradiation chamber down the motor rack - one to the reed switches, the other to the motors.

The electrical circuits were only slightly changed from the description given in Reference 10. The circuit diagram of the filter and amplifier through which signals from the reed switches passed in going to the Visicorder and Eput meter is shown in Figure 4.41. Connected to the output of the Eput meter was a printer which printed each reading of the Eput meter on a paper tape. Accessory to the Visicorder was a signal generator that produced a 100-cps signal which was recorded on a channel adjacent to that for motor speed and which served as a time signal. In addition, a fiducial mark for coast-time measurements was made on another Visicorder channel by means of a push-button micro-switch connected to the battery power supply of the filter-amplifier circuit. Power was supplied to run the motors by a circuit such as that shown in Figure 4.42. To supply 115-volt, 2-phase, 400-cps power in the nuclear reactor area, it was necessary to use two legs and a common ground of a 208-volt,3-phase, 400-cps line - which resulted in 115 volts phase to ground. This evidently

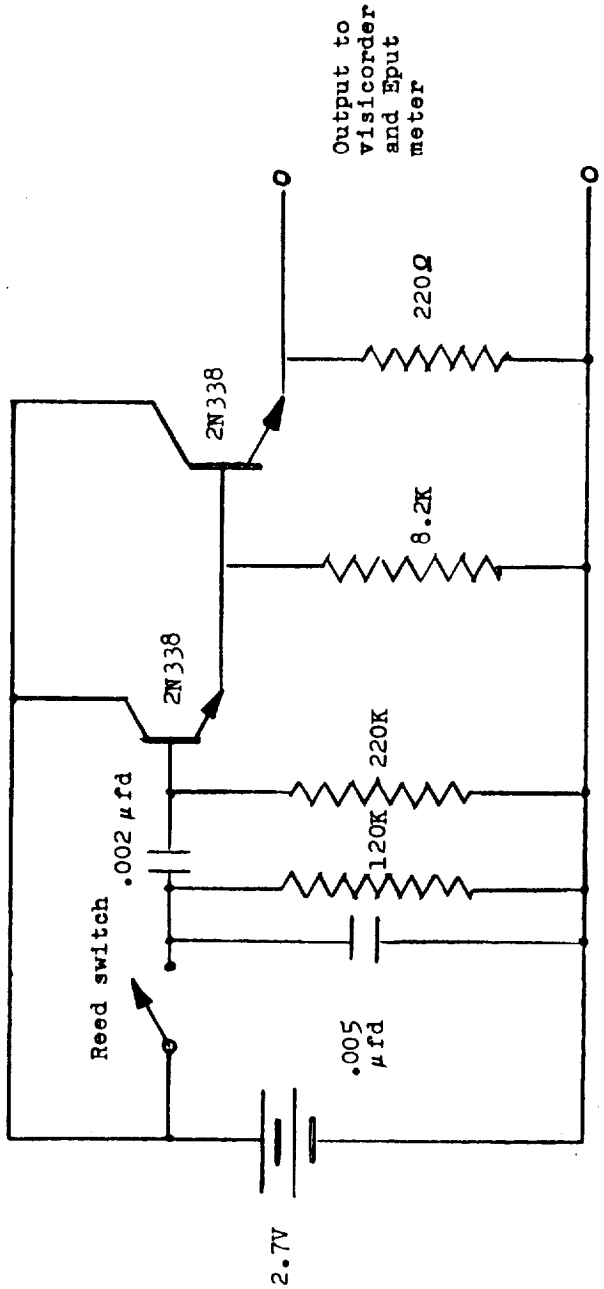

Figure 4.41 Circuit Diagram of Pulse Amplifier

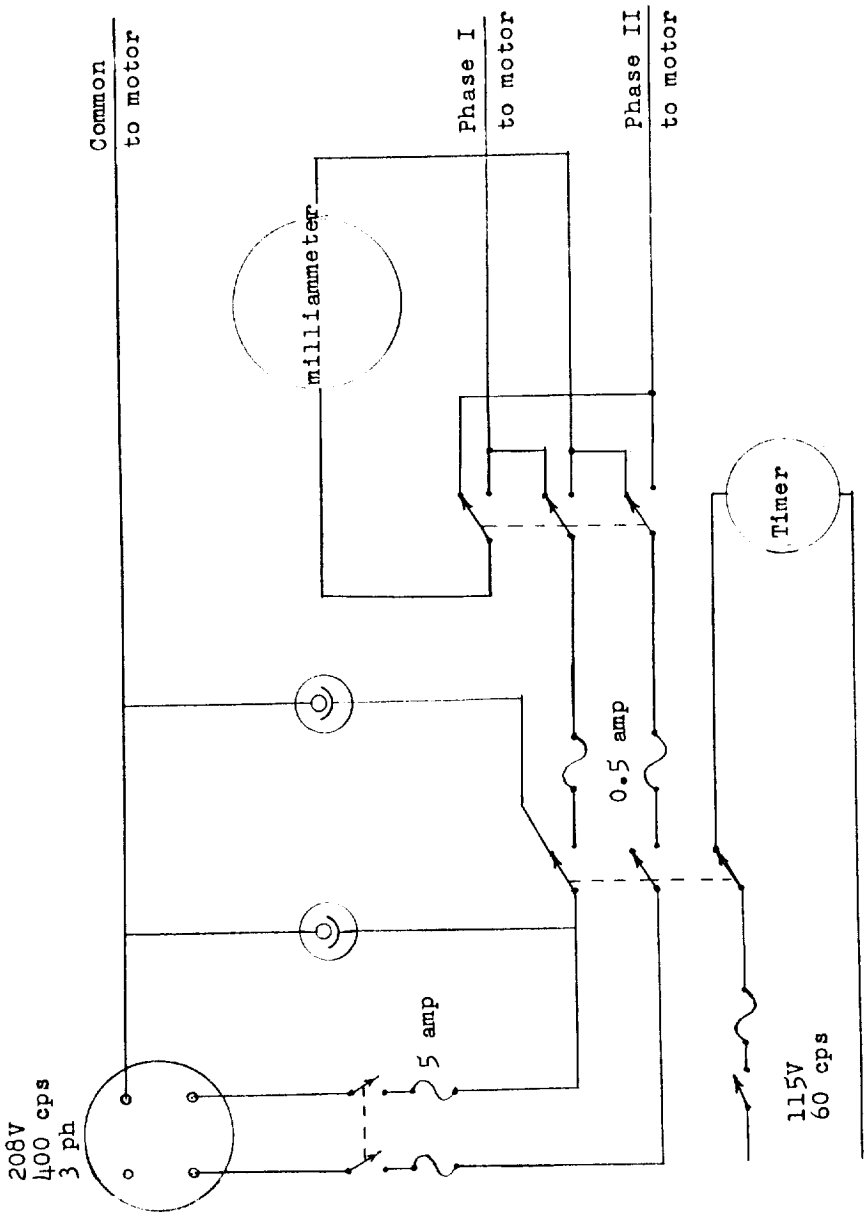

Figure 4.42 Circuit Diagram of Motor Power Supply

did not influence the no-load speed of the motors. In series with each servo motor was connected a 0-100-ma milliammeter which could be switched to read either the current in the fixed-phase winding or the current in the control-phase winding of the field coils. An electrical timer for use in measuring coast time of the motors was not used, because its operation resulted, in the 60-cycle line, in a transient which affected the Eput meter readings. A stop-watch was used satisfactorily in place of the electrical timer.

Temperature measurements were made by means of copper-constantan thermocouples securely clamped to the outer race of the bearing on the back of each motor. Temperature readings were obtained from the thermocouples by a Weston recorder. The Philips gage and the Hughes gage on the vacuum-irradiation chamber provided means of measuring pressure when the bearing-lubricant test assembly was pumped down. Two sets of dosimeters were attached to the servomotor rack in positions between and immediately adjacent to the two rows of motors and symmetrical with respect to the reactor centerline. Each dosimeter set consisted of a nitrous-oxide dosimeter, a cadmium-covered copper foil, a bare copper foil, a magnesium foil, an aluminum foil, and a sulfur pellet.

4.5.2 Experimental Results

Primarily, the variables measured in this test were the following: no-load speed of the motors, coast time and speed during coast-down of the motors, total running time of the

motors, fixed-phase current and control-phase current, temperature of the motor bearings, pressure in the vacuum chamber, and total reactor radiation dose received by the lubricants. The entire bearing-lubricant test may be divided into four parts, with the parts differing somewhat in the test procedures used and kinds of data taken: (1) preliminary measurements, (2) control measurements, (3) measurements during irradiation, and (4) postirradiation measurements. Data pertinent to the accuracy and precision of the instruments used are given in Table 4.19

Table 4.19

Experimental Precision of Bearing-Lubricant-Test Instruments and Accuracy of Measurements

Instrument	Variable Measured	Sensitivity	Maximum Error
Visicorder	Coast-Time Motor Speed (No Load)	0.01 sec	± 0.03 sec ± 30 rpm
Eput meter	Coast-Time Motor Speed (No Load)	1.0 sec	± 0.6 sec ± 50 rpm
Milliammeters	Field Current	2 ma	± 5 ma
Electrical timer	Total Running Time	0.1 min	± 5%
Hughes and Philips gages	Vacuum-Chamber Pressure	(see Section 4.1)	
Dosimeters	Radiation Dose	(see Section III)	

4.5.2.1 Preliminary Measurements

Preliminary measurements in air were conducted in both the IML and in the reactor control area. The 3-phase line frequency in the laboratory was 395 cps, while in the reactor control area it was 415.5 cps - which resulted in about a 5% increase of motor speed for tests conducted in the reactor area. Unfortunately, because of the late arrival of some of the servomotors, it was not possible to test the lubricants and apparatus as thoroughly as planned. In fact, the tight schedule necessitated carrying out control tests in the reactor area immediately prior to irradiation. Preliminary tests were made in the IML to compare no-load speed measured by Eput meter readings with no-load speed measured by a stroboscope, which was taken as a standard. These results are given in Table 4.20, along with the motor number, type of lubricant contained in the motor bearings, and current in the two field windings of the motors. The differences between the two speed measurements do not exceed 1%.

It was possible to measure by stopwatch and direct observation the coast time for Motor 8 and Motor 2 before the bearing test rig had to be moved to the reactor area and placed in the vacuum-irradiation chamber. Motor 8 had a coast time of 3.0 seconds in air, and Motor 2 had a coast time of 36.0 seconds. These values compare with 3.3 seconds and 37.2 seconds, respectively, obtained by means of the Eput meter after the test rig had been pumped down in the vacuum-irradiation chamber.

Table 4.20

No-Load Speed of Motors at 80°F Bearing Temperature

Motor Number	Lubricant Type	No-Load Speed (rpm)		Field Current (ma)	
		Stroboscope	Eput Meter	Phase I	Phase II
1	Molykote X-15	6425	6420	50	40
2	Electrofilm 66 C	6375	6330	48	39
3	Electrofilm 66 C	6125	6120	53	44
4	Molykote X-15	5872	5850	51	42
5	Shell ETR-H	5600	5600	55	46
6	Shell ETR-H	5500	5490	51	44
7	GE F-50	6575	6540	51	42
8	GE F-50	6200	6180	50	41

4.5.2.2 Control Measurements

After the bearing-lubricant test rig was installed in the vacuum-irradiation chamber, placed in the east position in the reactor pool, and pumped down to 5×10^{-7} torr, five control runs were made in which motor spped, coast time, field current, and speed during the coast down were measured. These data are given in Table 4.21. Four coast-down runs were made using the Eput meter and stopwatch and one run made using the Visicorder. These control data are plotted in Figures 4.43, 4.44, 4.45, and 4.46 along with the irradiation test data. The fourth control run made with the Eput meter

Table 4.21

Bearing-Lubricant Control Data

Control Run Number	Motor Number	Field Current (ma)		No-Load Speed (rpm)	Coast Time (sec)
		Phase I	Phase II		
1	1	47	37	6660	----
	2	44	36	6690	----
	3	50	41	6390	----
	4	48	40	5790	----
	5	44	42	6020	----
	6	49	41	5640	----
	7	48	39	6840	----
	8	48	39	6420	----
2	1	47	37	6600	4.2
	2	44	36	6690	37.2
	3	50	41	6360	42.3
	4	48	39	6090	27.0
	5	52	44	5760	3.0
	6	48	41	5610	2.7
	7	48	39	6840	3.0
	8	47	39	6480	3.3
3	1	47	37	6600	4.8
	2	44	36	6660	35.7
	3	50	41	6390	43.2
	4	48	40	6090	28.2
	5	52	44	5730	3.0
	6	48	41	5640	2.7
	7	48	40	6840	3.0
	8	47	39	6450	1.8
4	1	47	37	6630	4.8
	2	44	36	6690	40.2
	3	50	41	6360	42.6
	4	48	39	6090	29.1
	5	52	44	5790	3.0
	6	48	41	5610	2.4
	7	48	40	6780	4.2
	8	47	39	6390	3.0
5 (Visi-corder)	1	--	--	----	3.17
	2	--	--	----	33.99
	5	--	--	----	0.59
	6	--	--	----	1.13
	7	--	--	----	2.18
	8	--	--	6300	1.54

was carried out after the lubricants had been left overnight (8 hours, 23 minutes) in vacuum at an average temperature of about 65°F.

4.5.2.3 Measurements During Irradiation

Plots of the variables measured during irradiation are given in Figures 4.43 through 4.59.

The test procedure at first was to run the motors continuously, except when coast-time data were taken. However, four hours after start of the irradiation run, the temperature of the motors began to exceed the normal operating-temperature rise of 100°F. It was quite naturally thought that this excess temperature was due to gamma-ray heating. About 13 hours after the start, when the temperature became so excessive that it was felt that continuance of the test at full reactor power would be intolerable, the reactor was retracted from the closet. Examination of the data at this time did not reveal an obvious connection between coast-down time and the temperature increase, because the coast-down times of some motors were increasing while coast-down times of others were decreasing - indeed, it had not been expected that the small motors could generate enough heat to sustain a large temperature increase. However, because the temperature of the motors stabilized only ten degrees lower after retracting the reactor, it became apparent that the heating was due to friction drag in the motor bearings themselves. Accordingly, the motors were shut off, with the result that bearing temperature dropped about 25°F in ten minutes, indicating that the major source of heating was, in

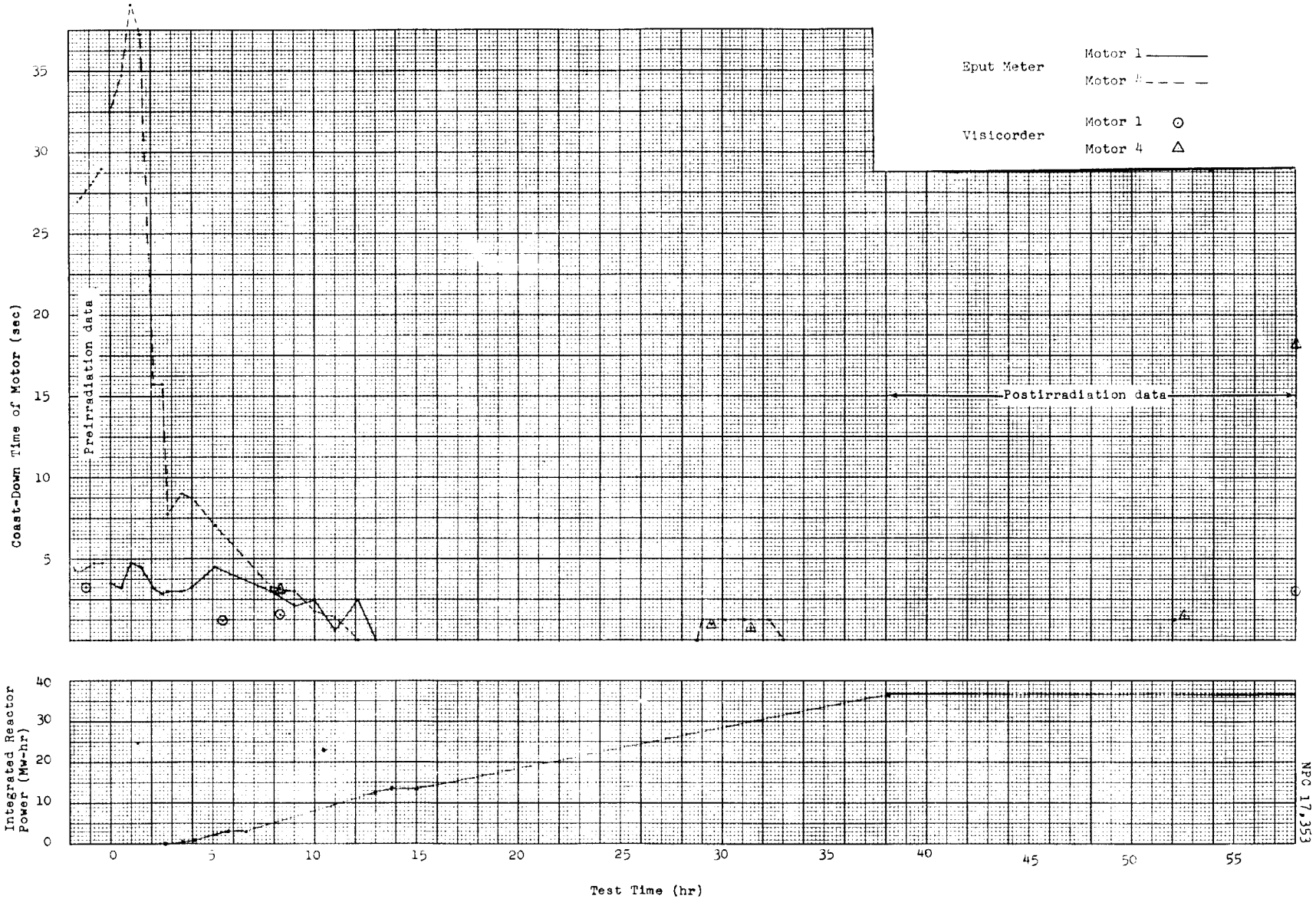

Figure 4.43 Motor Coast-Down Time as a Function of Radiation Exposure and Test Time: Molykote X-15

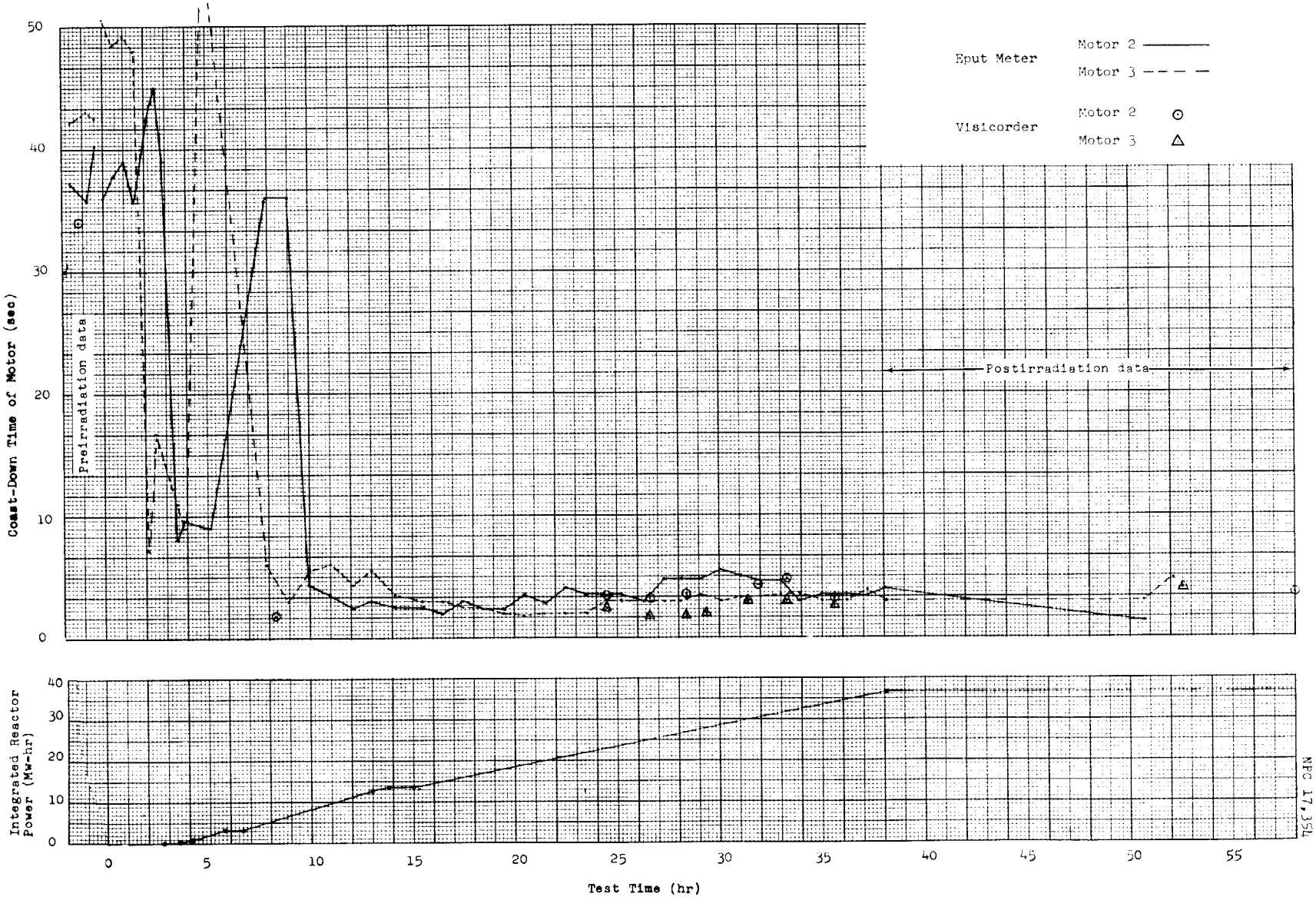

Figure 4.44 Motor Coast-Down Time as a Function of Radiation Exposure and Test Time: Electrofilm 66-C

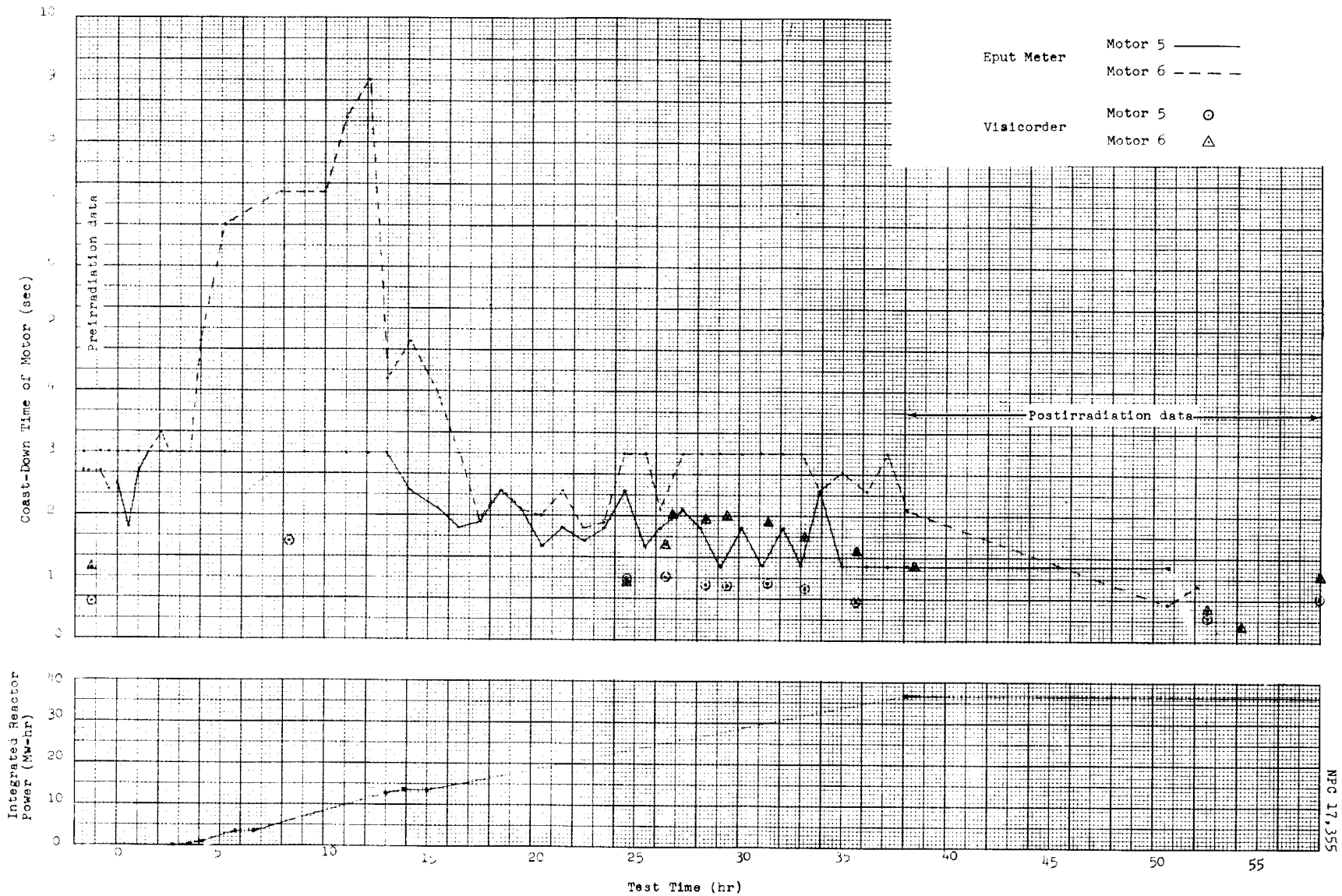

Figure 4.45 Motor Coast-Down Time as a Function of Radiation Exposure and Test Time: Shell ETR-H

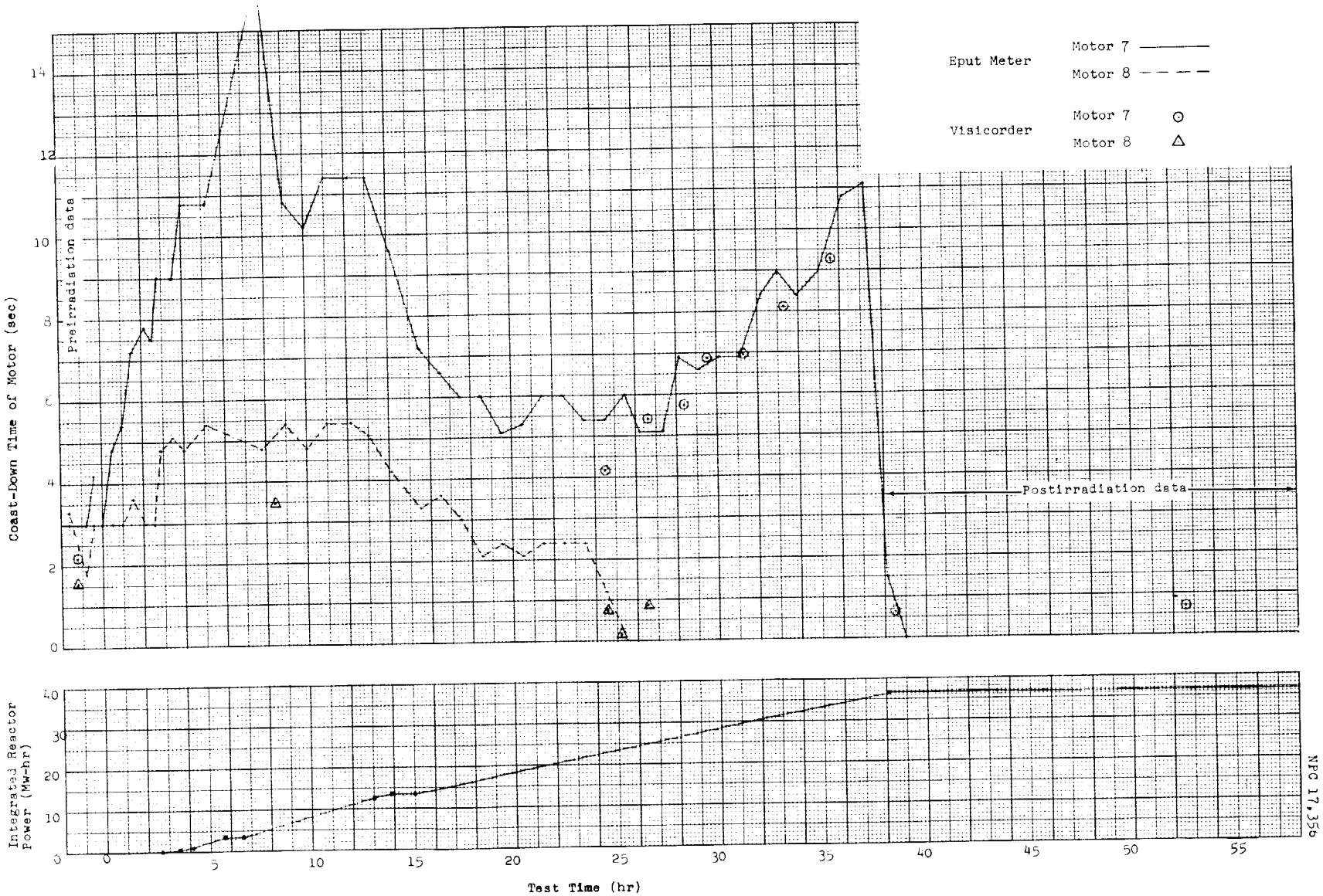

Figure 4.46 Motor Coast-Down Time as a Function of Radiation Exposure and Test Time: G E F-50

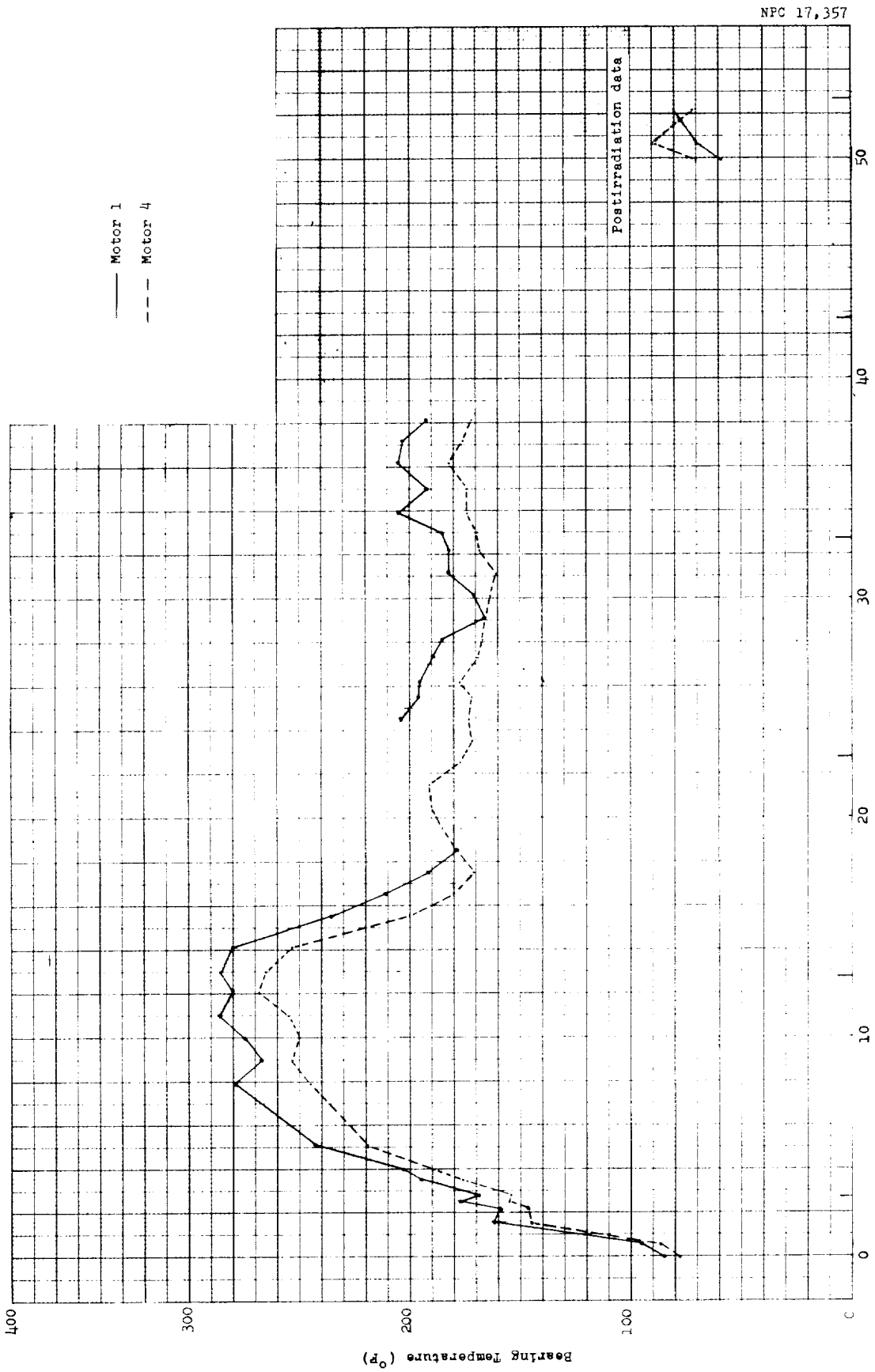

Figure 4.47 Bearing Temperature During Test: Molykote X-15

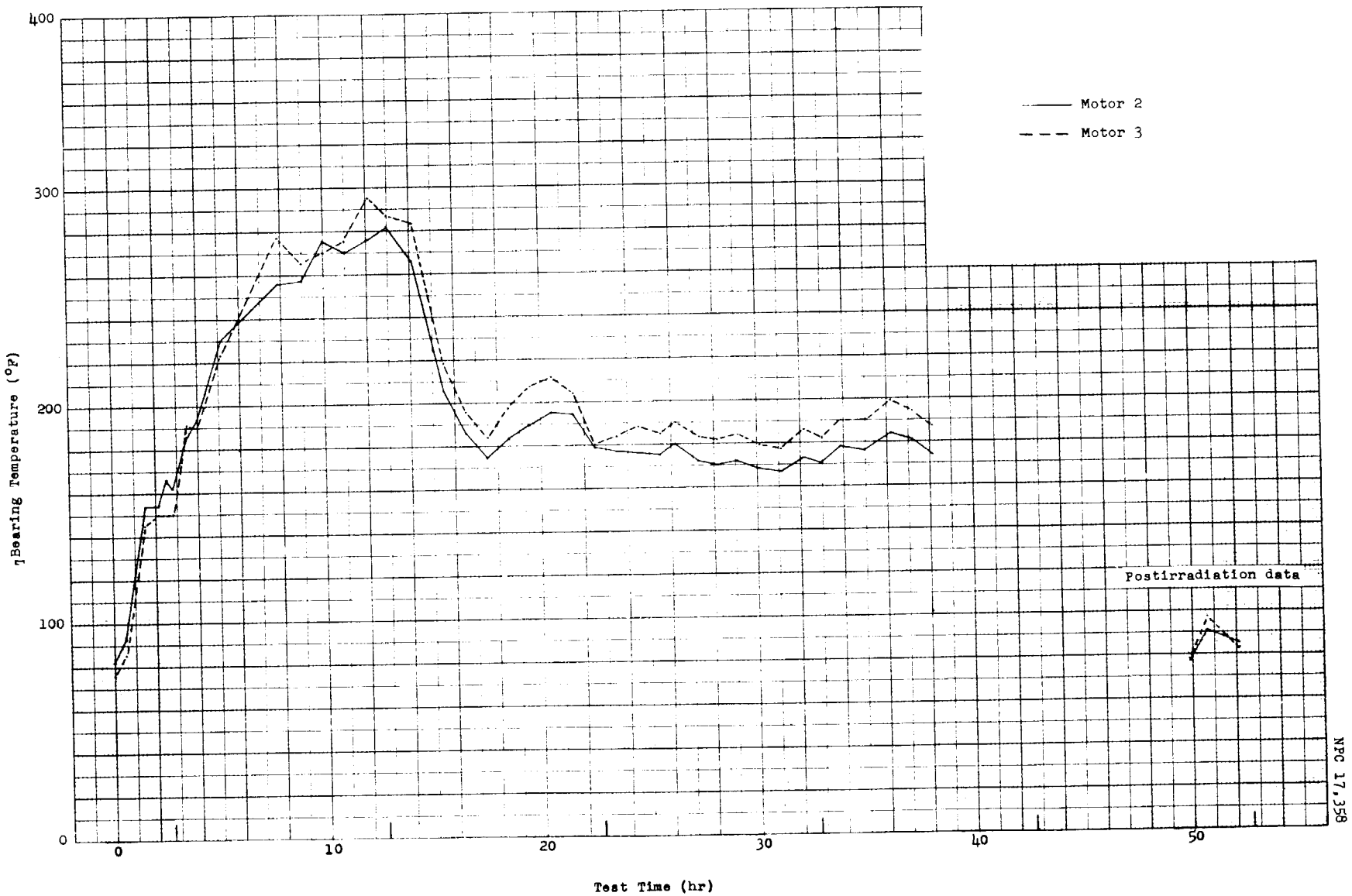

Figure 4.48 Bearing Temperature During Test: Electrofilm 66-C

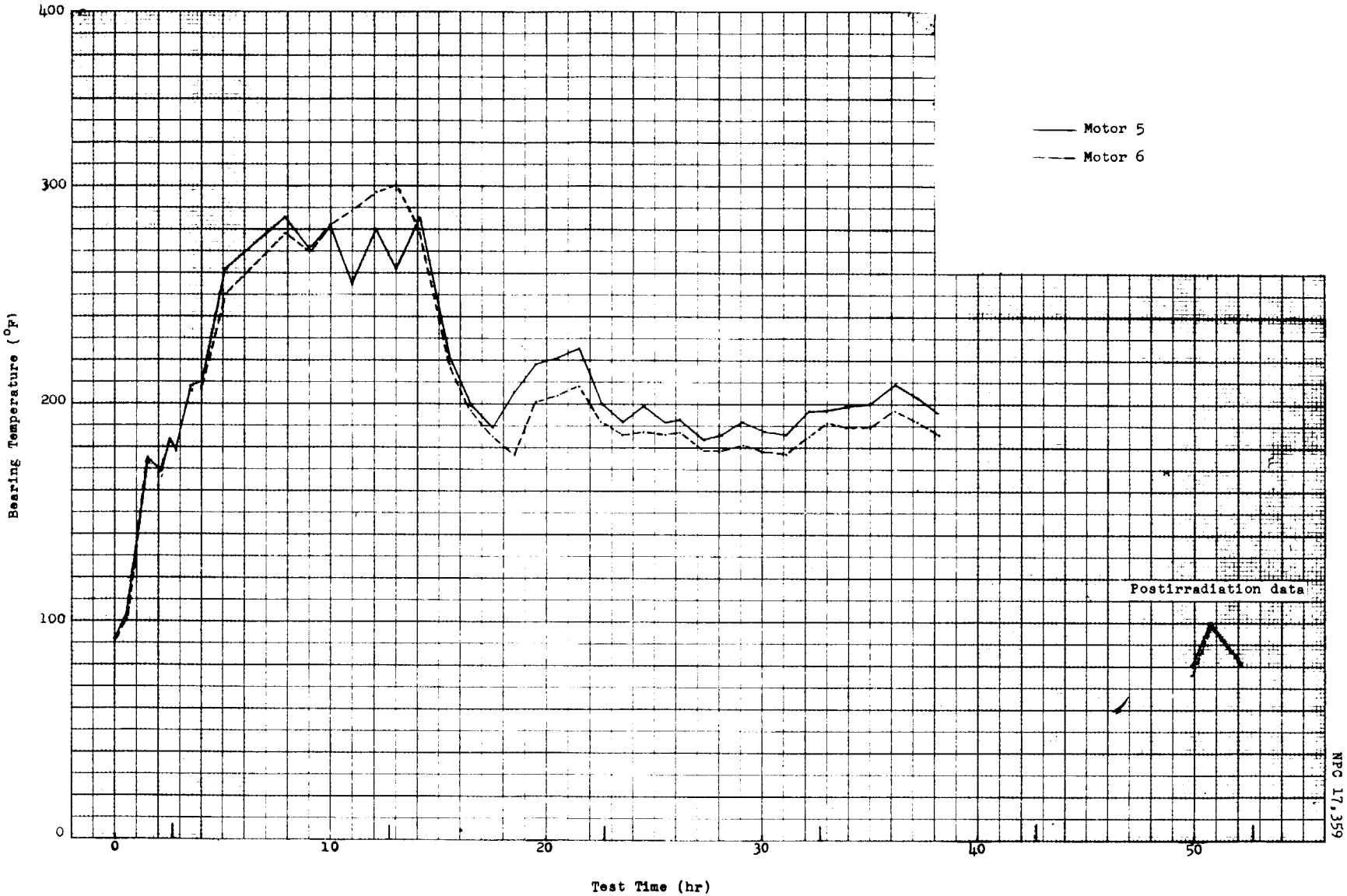

Figure 4.49 Bearing Temperature During Test: Shell ETR-H

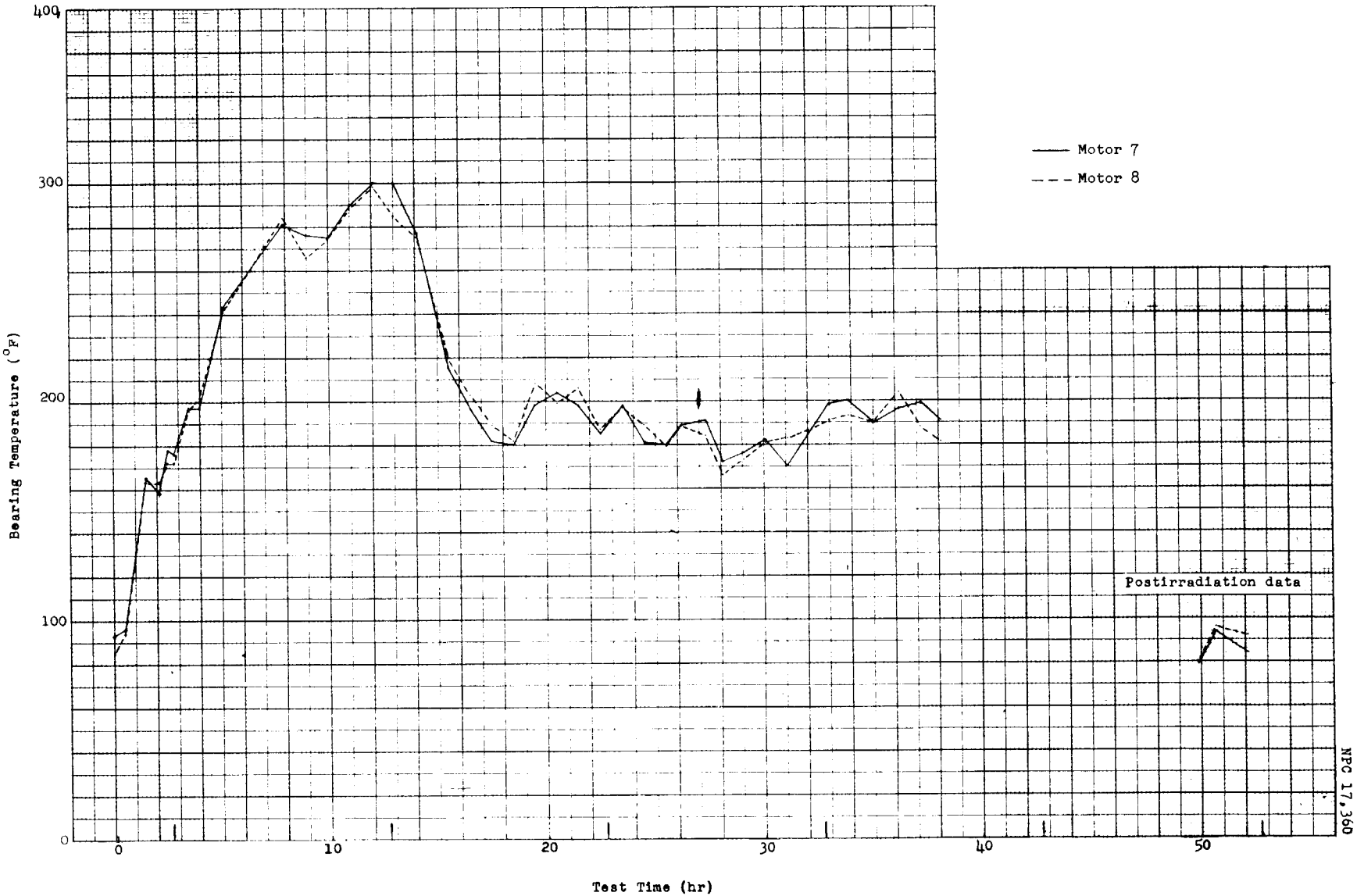

Figure 4.50 Bearing Temperature During Test: G E F-50

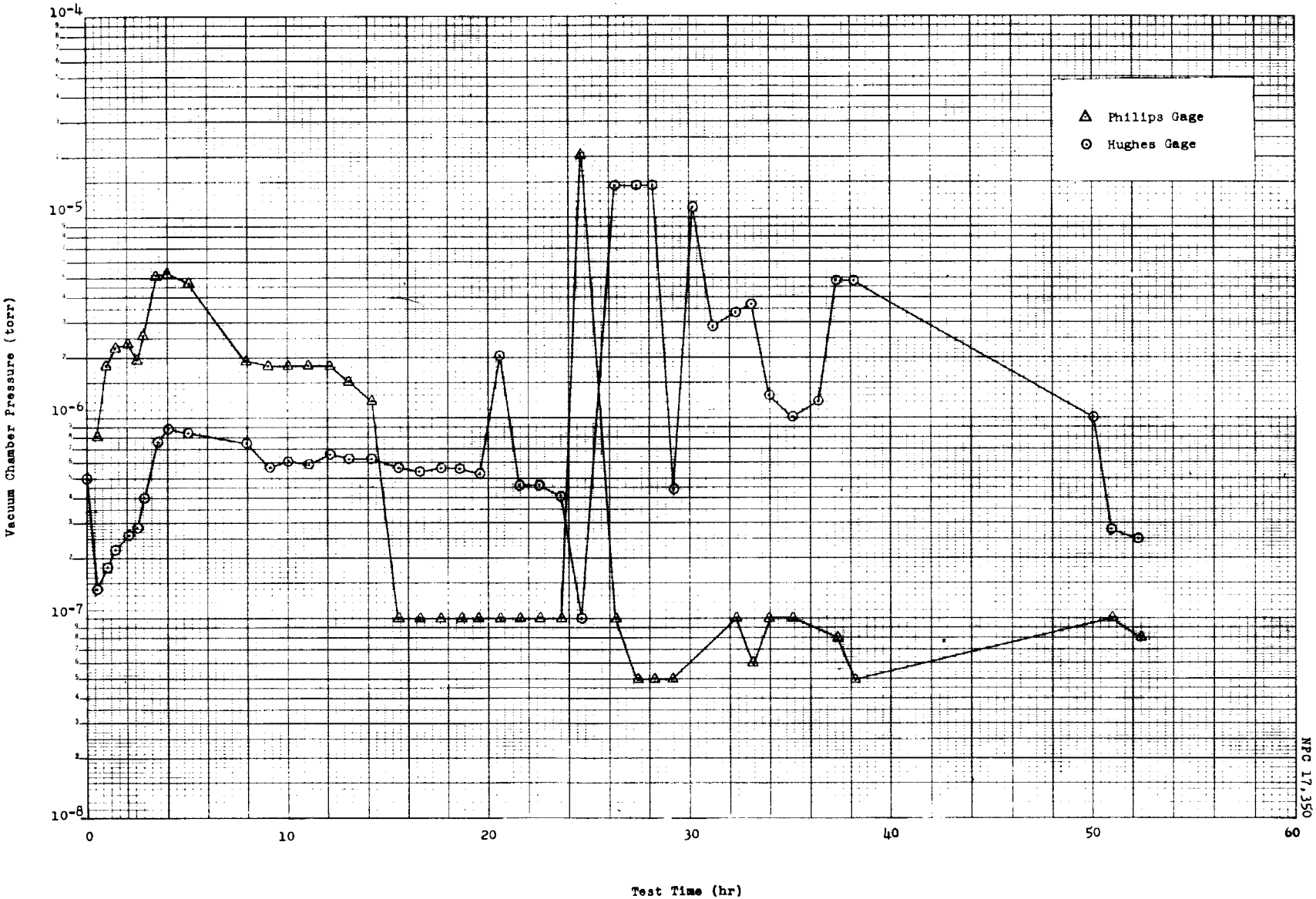

Figure 4.51 Vacuum-Chamber Pressure During Bearing-Lubricant Test

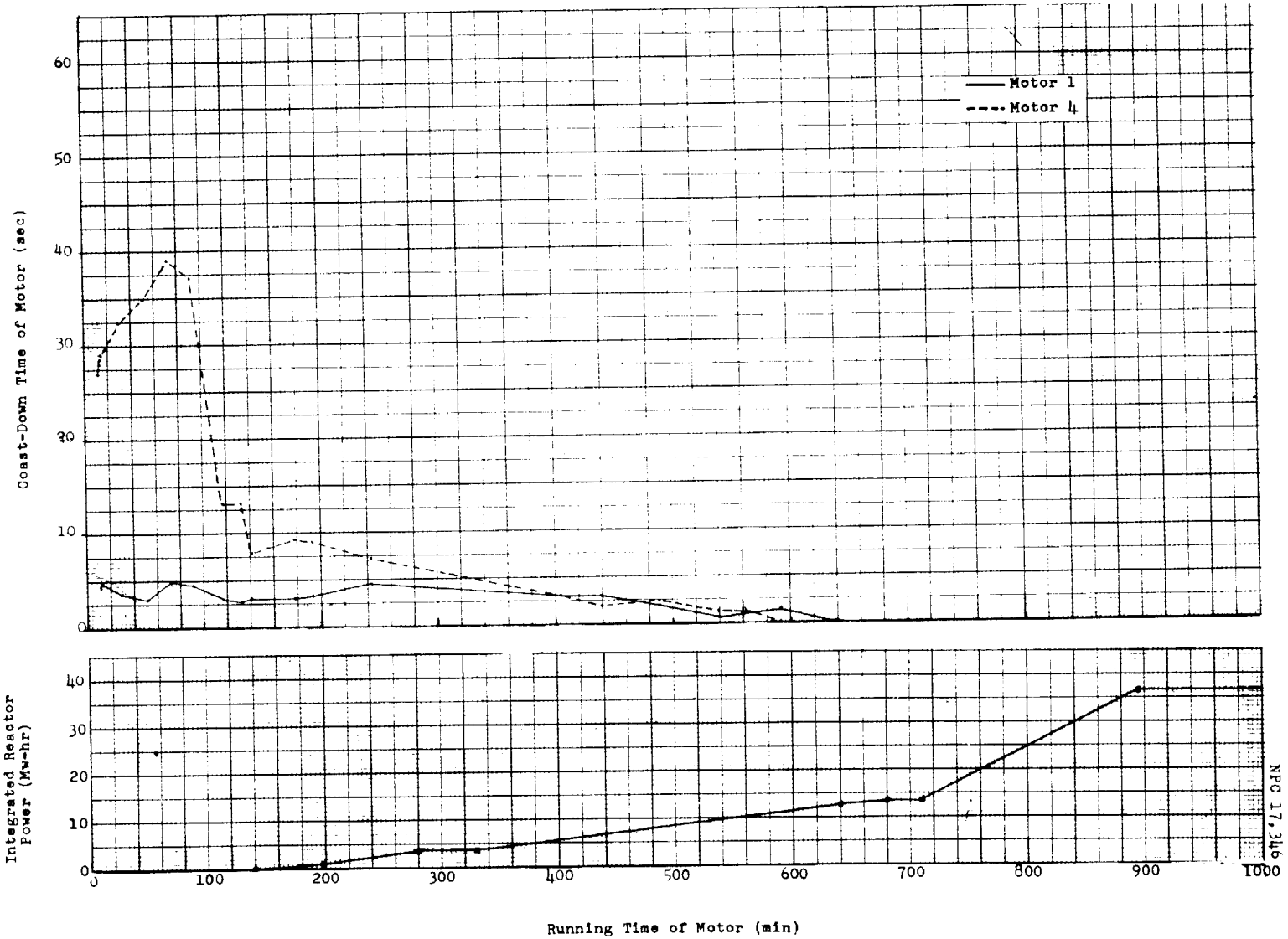

Figure 4.52 Motor Coast-Down Time as a Function of Radiation Exposure and Running Time of Motor: Molykote X-15

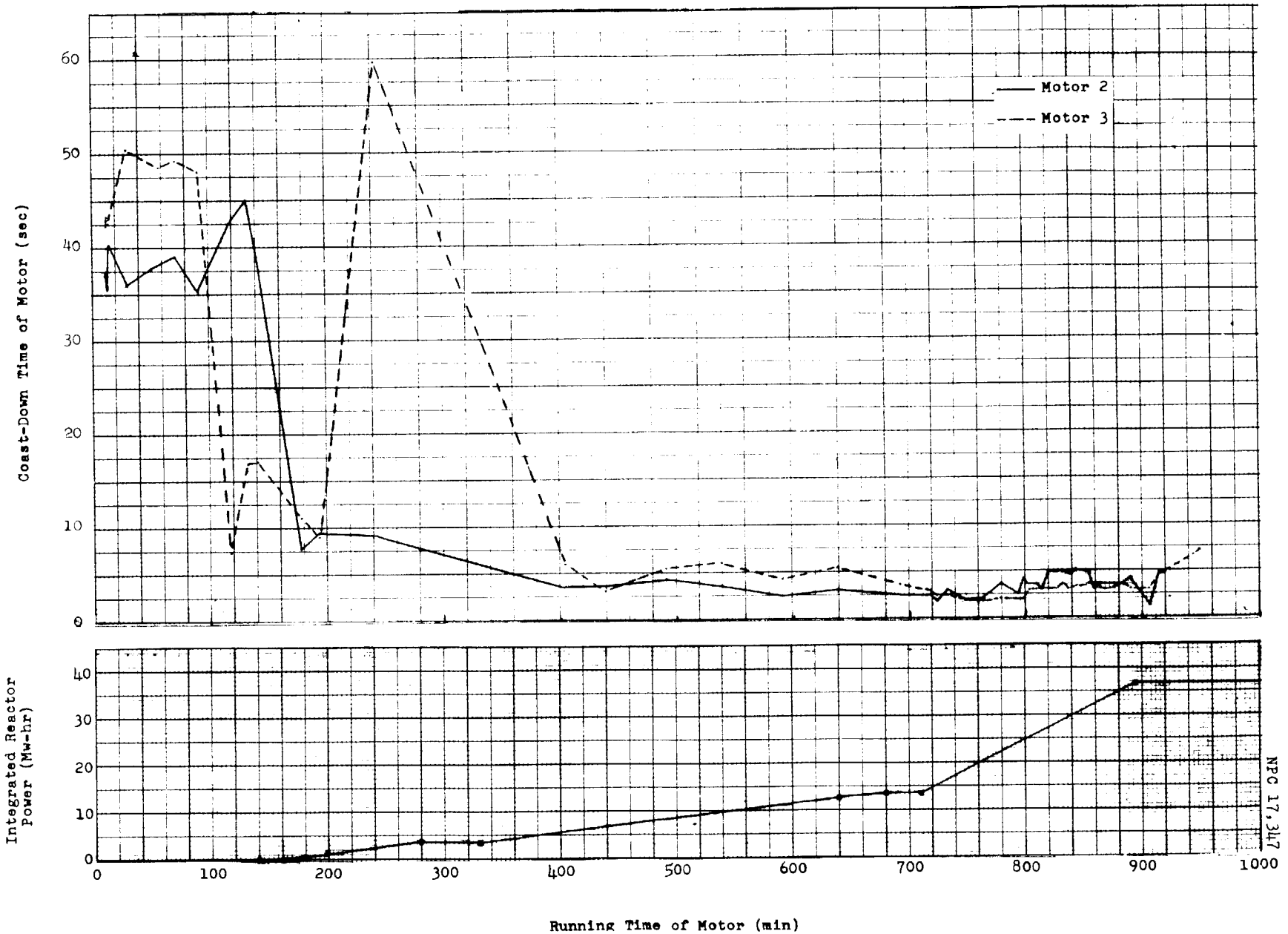

Figure 4.53 Motor Coast-Down Time as a Function of Radiation Exposure and Running Time of Motor: Electrofilm 66C

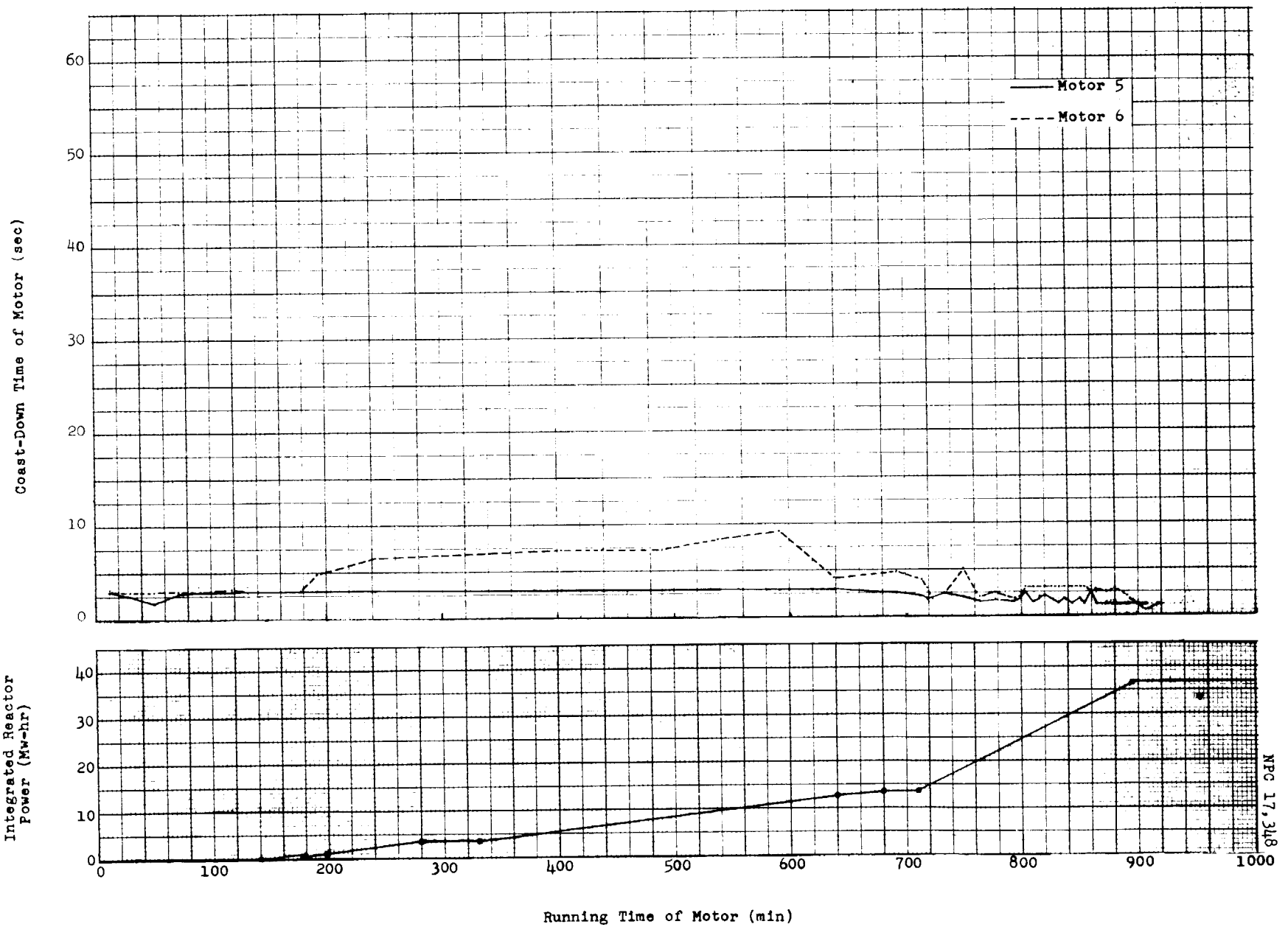

Figure 4.54 Motor Coast-Down Time as a Function of Radiation Exposure and Running Time of Motor: Shell ETR-H

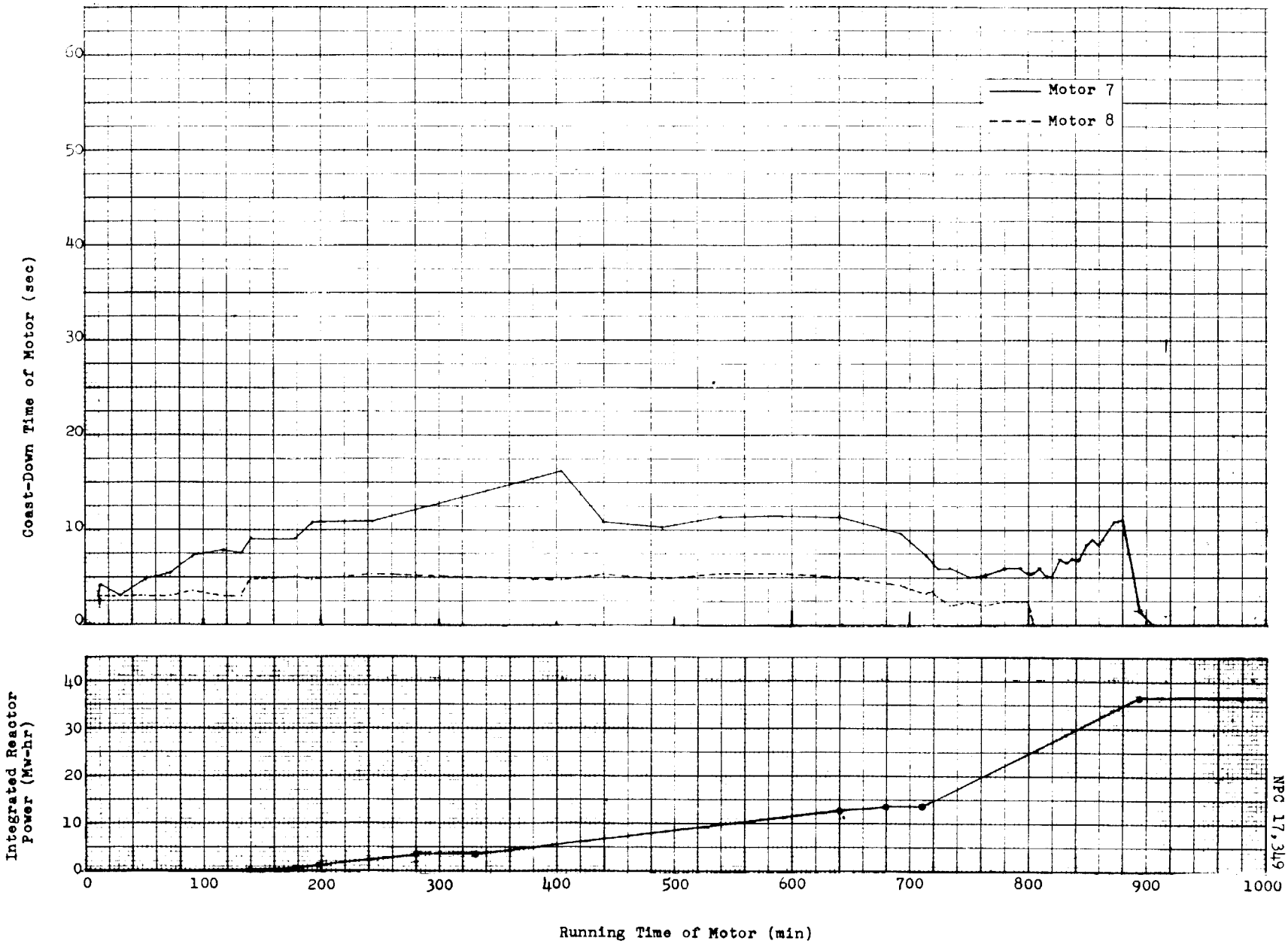

Figure 4.55 Motor Coast-Down Time as a Function of Radiation Exposure and Running Time of Motor: G E F-50

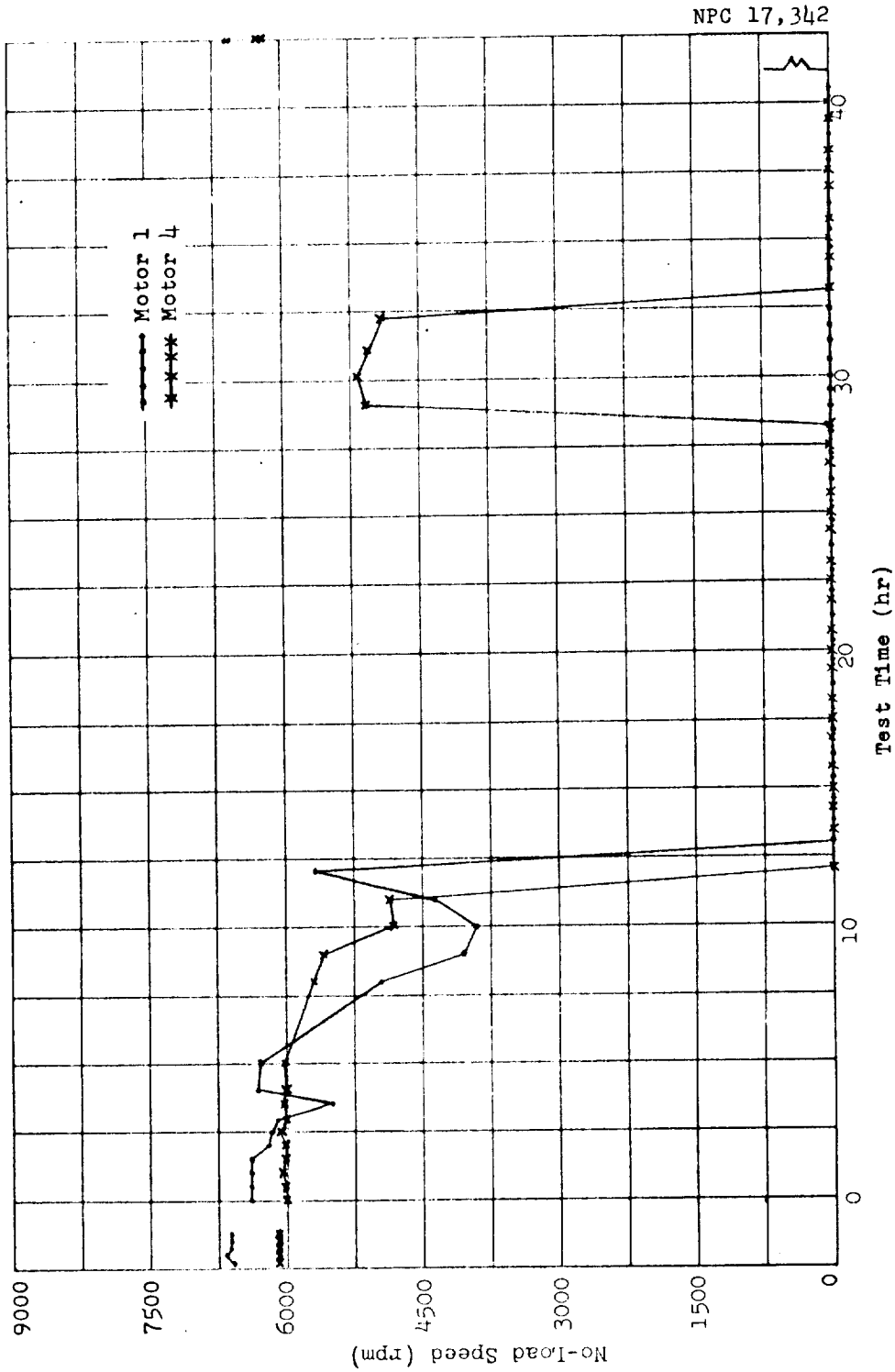

Figure 4.56 No-Load Speed of Motors During Test: Molykote X-15

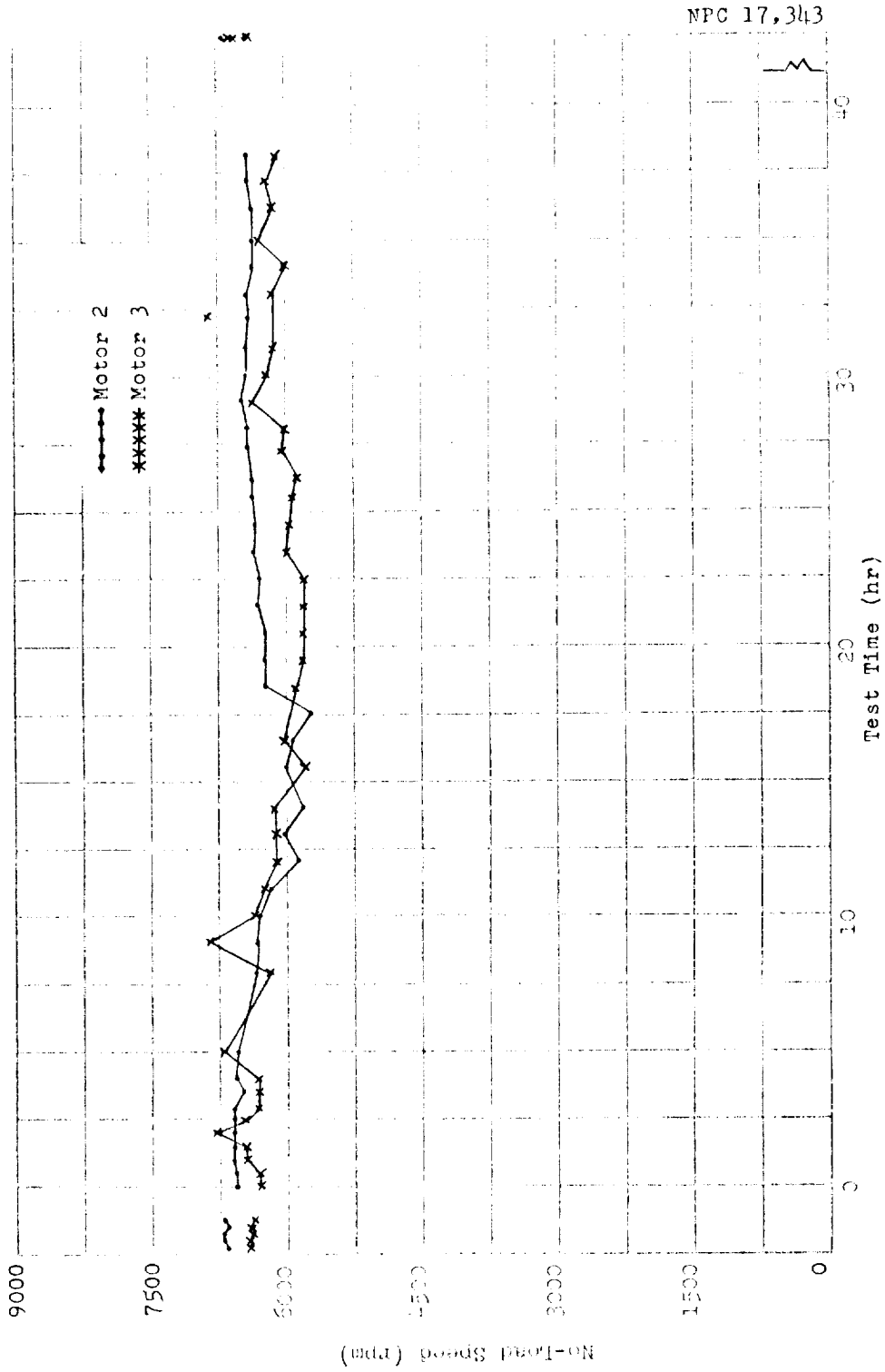

Figure 4.57 No-Load Speed of Motors During Test: Electrofilm 66-C

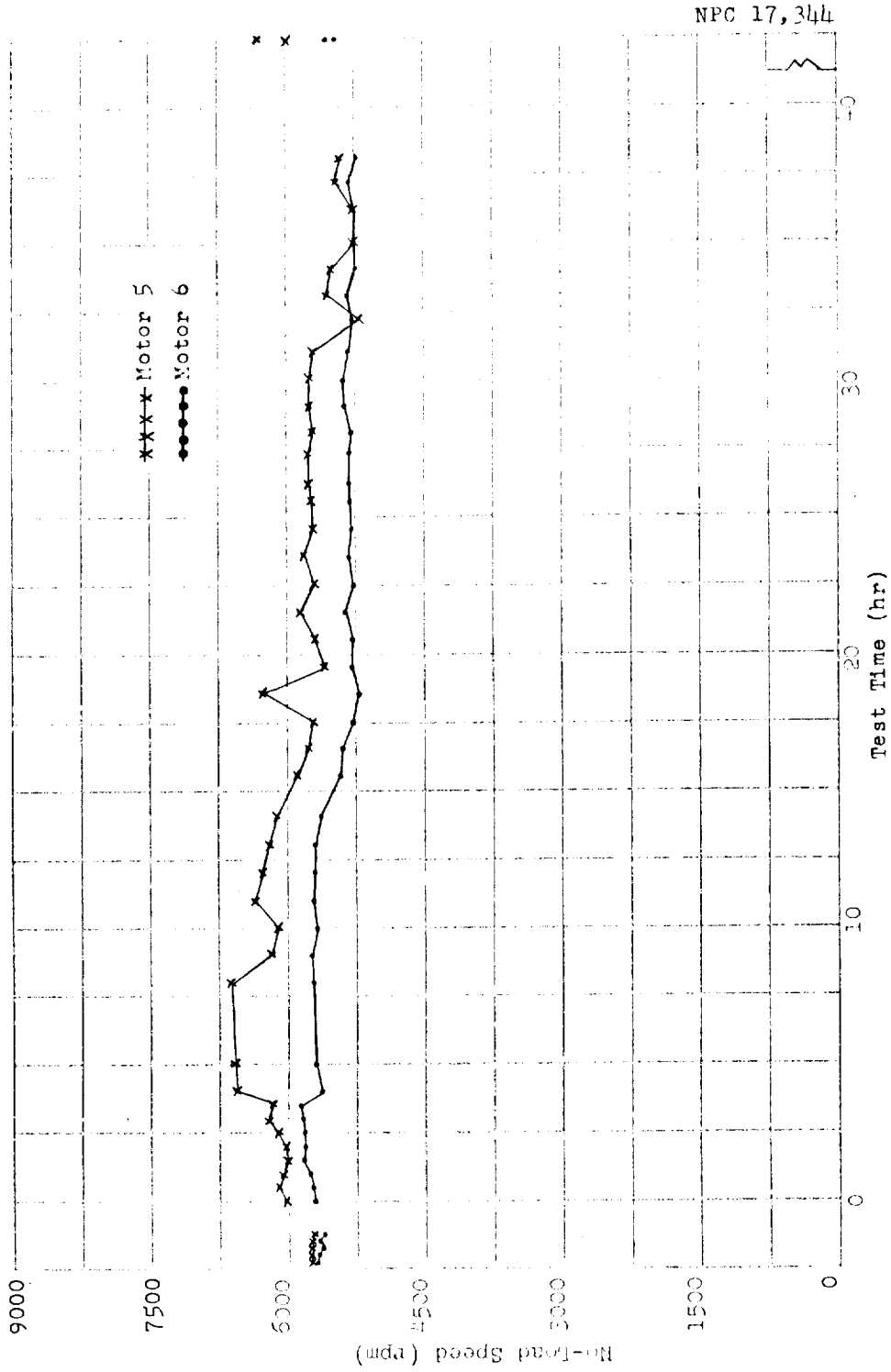

Figure 4.58 No-Load Speed of Motors During Test: Shell ETR-H

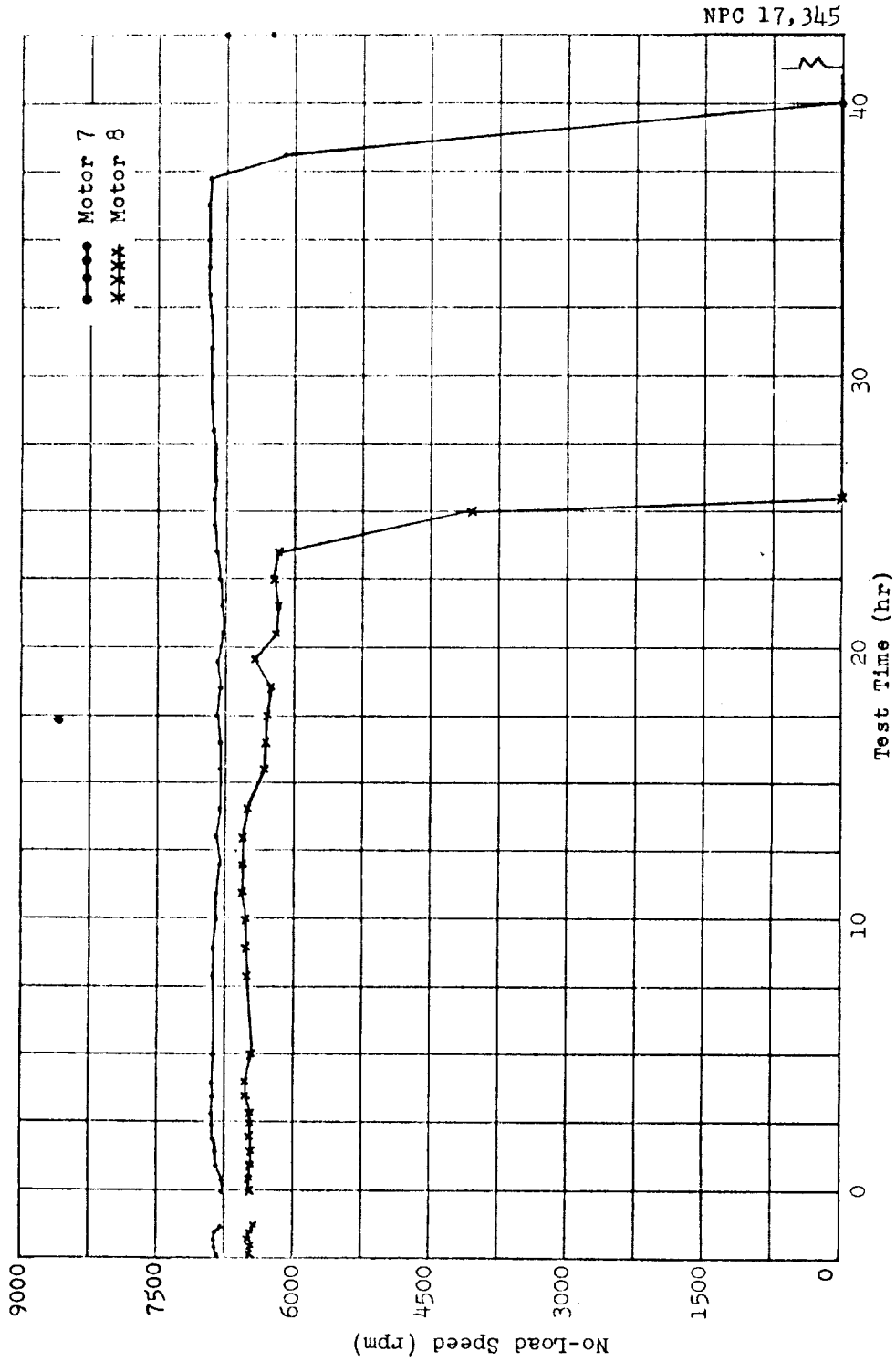

Figure 4.59 No-Load Speed of Motors During Test: G E F-50

fact, friction. Thus, the reactor was brought back to full power and the test procedure modified (starting 14.5 hours after beginning the test) so that all motors were turned off between hourly data cycles except for five minutes of running to warm them up immediately before a set of data was taken. In any case, each data cycle consisted of measurement of motor field current in both phases, coast time, bearing temperature, running time, motor speed during coast down, no-load speed, and pressure in the vacuum chamber.

At four hours from the beginning of the test, the current in Phase I of Motor 6 suddenly jumped from 48 ma to 65 ma, where it remained. There were no other changes, and it is not known what caused the phenomenon. At any rate, it did not have anynoticeable effect on the outcome of the test. At 5.1 hours, the amplifier used for matching impedance to the input of the Visicorder became inoperative, and two hours were required to repair the amplifier. In spite of these repairs, the amplifier gain never again became entirely satisfactory. Coast time could be accurately determined, although motor speed during coast down could be read only over a portion of the chart.

About 9.5 hours after the beginning of the irradiation run, Motor 1, which contained Molykote X-15, stopped running and would start only sporadically. At 13 hours, Motor 1 could no longer be started at all. Motor 4, also containing Molykote X-15, exhibited the same behavior and would no longer run after 12.1 hours. Motor 8, containing GE F-50, stopped running

after 24.5 hours, failing to run again for the remainder of the test. Motors 1 and 4, however, operated sporadically later in the test, and Motor 4 ran long enough for a few data cycles to be completed between 29.1 and 32.2 hours. At 38.1 hours, first Motor 7, containing GE F-50, and then, less markedly, Motor 6, containing Shell ETR-H, showed symptoms of failing. In all cases of this type of failure, the no-load speed and the coast time of the motors gradually decreased beforehand. The reactor was shut down and the irradiation run terminated at 38.1 hours after beginning of the irradiation-run measurements. This gave a total irradiation time of 35.3 hours and total exposures of about 7×10^9 ergs/gm(C) gammas and 1.05×10^{15} neutrons/cm^2 ($E > 2.9$ Mev) for the motors. The reactor schedule and total gamma and neutron exposures are listed in Table 4.22.

Table 4.22

Reactor Schedule for Bearing-Lubricant Test

Date	Time (hr)	Test Time (hr)	Reactor Power Level (Mw)	Total Exposure		
				Thermal Neutron (n/cm2)	Neutrons E>2.9 Mev (n/cm2)	Gammas [ergs/gm(C)]
10/15	11:41	2.7	0.3	0	0	0
	12:29	3.5	1.0	6.94(11)	6.87(12)	4.58(7)
	13:03	4.1	1.5	2.42(12)	2.40(13)	1.60(8)
	14:45	5.75	Scram	9.57(12)	9.48(13)	6.32(8)
	15:37	6.6	1.5	9.57(12)	9.48(13)	6.32(8)
	22:00	13.0	1.0	3.72(13)	3.69(14)	2.46(9)
	22:50	13.8	Retracted	3.97(13)	3.93(14)	2.62(9)
	23:57	15.0	1.0	3.97(13)	3.93(14)	2.62(9)
10/16	22:55	38.0	Shutdown	1.06(14)	1.05(15)	7.0 (9)

4.5.2.4 Postirradiation Measurements

The peculiar decrease of no-load speed mentioned above suggested an experiment which was performed near the end of the test during the postirradiation run. (The motors had been left all night in vacuum, and by this time - 52 hours after beginning the irradiation run - only Motors 2 and 3, containing Electrofilm 66-C, and Motors 5 and 6, containing Shell ETR-H, would run consistently.) The motors were turned on individually and allowed to run until their speed became zero. During this time, motor speed and bearing temperature were measured. The results are plotted against time in Figures 4.60 and 4.61. It is obvious from these results that none of the lubricants was performing satisfactorily, even though the motors initially ran at no-load speeds nearly as high as those run at the beginning of the test.

Postirradiation tests were made in order to verify the coast times recorded at the end of the irradiation run and in order to verify the Eput meter and Visicorder indications. Postirradiation data have been plotted in the figures for the irradiation-run data for purposes of direct comparison (Figs. 4.43-4.50 and 4.56-4.59). After the fourth postirradiation data cycle, only Motor 6 was operative and, then, only barely so. Therefore, the vacuum system was removed from the reactor pool to be opened for visual inspection of the servomotors. As soon as the chamber pressure had increased substantially near to atmospheric pressure, it was found that, with the exception of Motors 7 and 8, all the motors would operate again at essentially

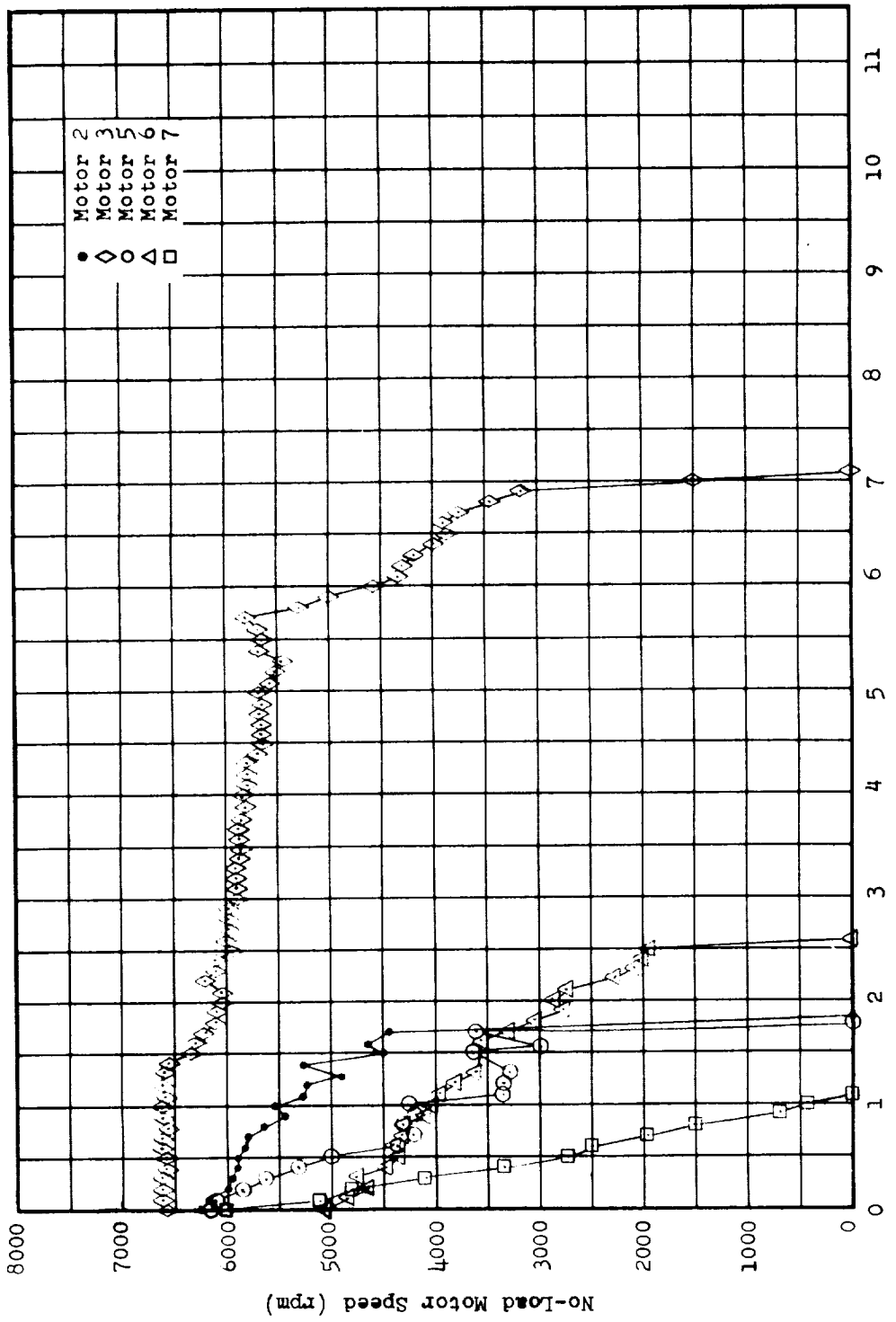

Figure 4.60 No-Load Motor Speed as a Function of Time for Motor Speed to Become Zero

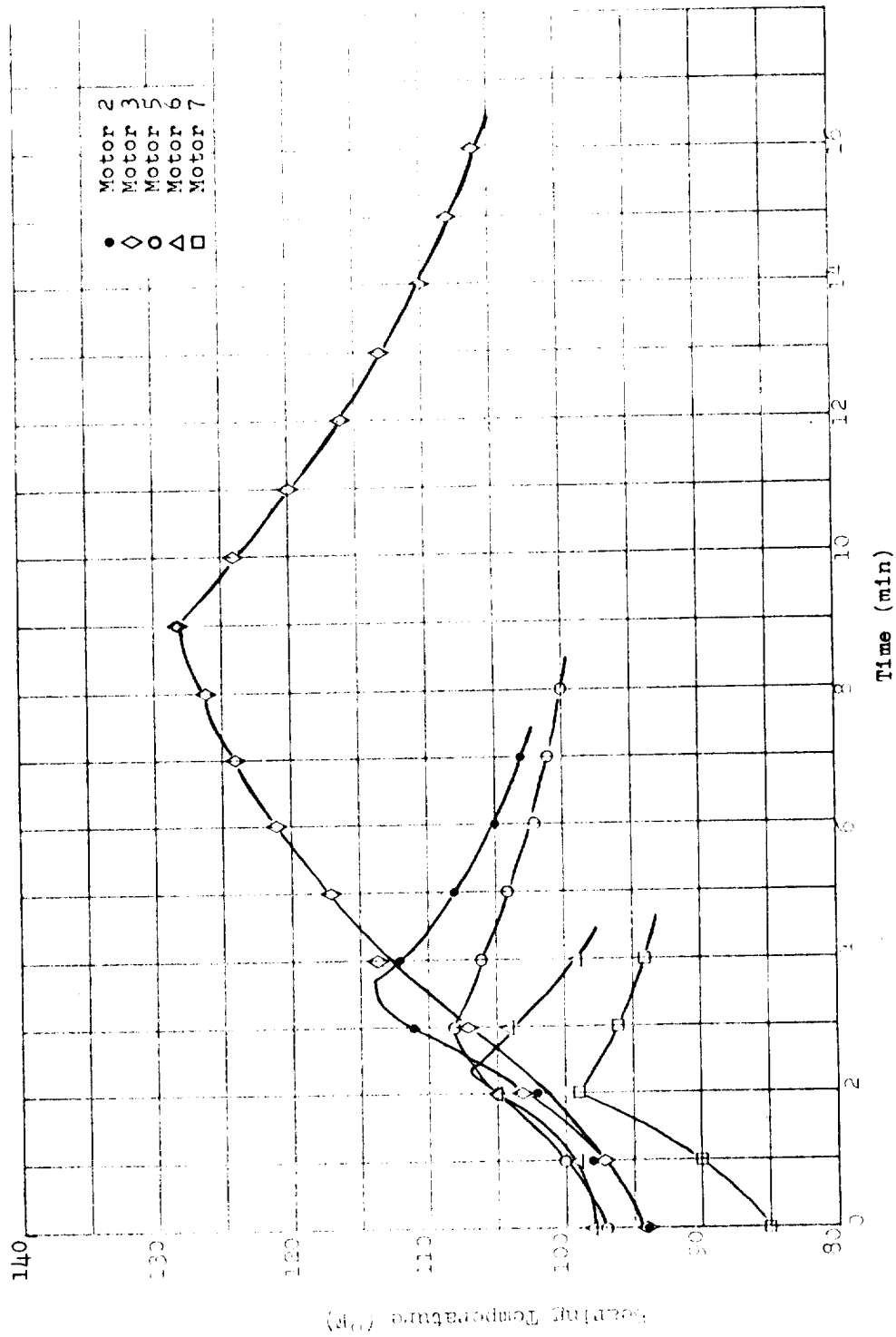

Figure 4.61 Motor-Bearing Temperature as a Function of Time for Motor Speed to Become Zero

the original no-load speed and higher coast times than observed at the end of the irradiation run. By the time the vacuum chamber was opened, all the motors were running except Motor 8. The actual operation of the motors was verified visually and Motor 8 was found to have frozen bearings.

4.5.2.5 Discussion of Measurements

The solid-film lubricants exhibited behavior different from that of the grease and oil lubricants. The motors containing solid-film lubricants, with the exception of Motor 1 (Molykote X-15), initially had exceptionally long coast times compared with the other motors (See Figures 4.43-4.46). Because control data were taken at intervals varying from 10.5 hours to 1 hour before testing was begun, they are not plotted on a real-time basis; all other such data are, however, plotted against actual test time. The above figures show that those motors with long coast times experienced a sudden drop in coast time, beginning at 2 hours after start of the test. Since the sudden drop for one of the motors occurred before the reactor was started, this drop cannot be entirely attributed to the effect of radiation; rather, it seems to be a result of continuous running of the motors in vacuum.

At this point, it is instructive to refer to the bearing-temperature curves shown in Figures 4.47 through 4.50, and to the pressure curves shown in Figure 4.51. From these curves it can be seen that bearing temperature for all motors rose continuously during the first 14 hours of the test and that the

vacuum-chamber pressure, as measured by both the Hughes and Philips gages, increased concomitantly, which indicates that outgassing of the lubricants was taking place during this period.

It is not possible to separate exactly the various phenomena occurring over this period with respect to cause and effect. However, it appears likely that, since the motors were first run continuously in vacuum for a relatively long period of time beginning with the irradiation run, the normal bearing-temperature rise led to additional outgassing and resultant deterioration of the lubricants, especially the dry-film lubricants. This deterioration of lubricating properties in turn caused (1) the sudden drop of coast time for the two Electrofilm 66-C motors and for the one Molykote X-15 motor with high initial coast time, and (2) the subsequent drastic increase of temperature. Following the rapid initial decrease, the coast time of the two motors containing Molykote X-15 decreased gradually until, at about nine hours (corresponding to a radiation dose of 2×10^9 ergs/gm(C)), the motors stopped running (Sec. 4.5.2.3). At this same time, the coast time of the two motors containing Electrofilm 66-C fluctuated between high values and low values, eventually reaching a low value of about five seconds at eight hours and remaining there throughout the irradiation run.

On the other hand, the motors containing Shell ETR-H and GE F-50 did not have high coast times during the control measurements and otherwise exhibited entirely different coast-time behavior. Within the first 14 hours of the irradiation run, the coast time of the motors containing Shell ETR-H and the motors containing GE F-50 slowly increased, as was verified for the motors having shorter coast times by Visicorder data shown in Figures 4.45 and 4.46. This increase presents the most puzzling aspect of the test, for, on the one hand, the increased coast time can reasonably result only from decreased bearing friction, while, on the other hand, the large increase of bearing temperature, as discussed previously, was evidently due to increased bearing friction. It is possible that all the heat was generated by friction in the bearings of the dry-film lubricant motors and conducted through the motor rack to the thermocouples in the bearings of the other motors, where the rise of temperature reduced the effective viscosities of the grease and oil. This latter contention is supported by bearing temperatures for Motors 1, 4, and 8, which continued to register high (even increasing) bearing temperatures over long portions of the irradiation run when the motors were not actually running. The bearing temperature of Motor 8 in particular shows that there must have been heat conduction through the rack from the other running motors. Motor 8 was not running at all after 25 hours; yet, in spite of this, its bearing temperature closely followed that of the other motors for the rest of the test, as can be seen from Figures 4.47 through 4.50.

It is possible that oil and grease breakdown due to nuclear radiation, as well as viscosity decrease due to the higher bearing temperatures, also contributed to the increased coast times observed during the first 14 hours. At the end of this period, the coast times for the Shell ETR-H motor exhibited slightly decreasing trends throughout the remainder of the run (Fig. 4.45), whereas the coast times of the GE F-50 motors at first slowly decreased until 24 hours after start of the run when Motor 8 failed but Motor 7 reversed its trend, increased its coast time steadily, and then preciptitously reduced its coast time at $\sim$ 37 hours (Fig. 4.46).

For convenience in determining the total operating time of any given motor at some particular event of coast time, temperature, no-load speed, etc., the coast time of the motors is plotted versus total running time in Figures 4.52 through 4.55. No-load speed as a function of test time is shown in Figures 4.56 through 4.59 for all motors. Impending failure of the motors was foreshadowed by a gradual decrease of no-load speed. Field current, which did not vary significantly throughout the entire test, is given in Table 4.23.

From the foregoing discussion, it is evident that, during the vacuum irradiation of the bearing lubricants, complicated environmental interactions were present. Radiation, vacuum, and temperature effects are definitely present, but they are not easy to separate. It is also difficult to determine exact

Table 4.23

Field Current During Bearing Lubricant Test

Test Time (hr)	Phase I Current (ma)							
	Motor 1	Motor 2	Motor 3	Motor 4	Motor 5	Motor 6	Motor 7	Motor 8
0	46	43	48	46	52	47	47	47
1.5	45	44	49	46	52	47	48	47
2.8	46	46	51	48	53	48	49	48
5.1	46	46	51	47	52	64	48	47
10.0	44	46	51	46	52	64	46	48
13.0	44	46	51	45	52	64	46	48
16.5	44	46	51	48	52	64	48	47
19.5	43	45	50	44	52	64	47	47
22.5	--	45	50	44	51	64	47	46
26.2	--	46	51	--	52	64	48	--
29.1	--	46	51	47	52	64	48	--
32.2	--	46	51	47	52	64	48	--
35.0	--	46	51	--	52	64	46	--
38.1	--	46	51	--	52	64	48	--
50.7	--	46	53	--	53	67	48	--
52.1	--	46	52	--	53	68	48	--

Test Time (hr)	Phase II Current (ma)							
	Motor 1	Motor 2	Motor 3	Motor 4	Motor 5	Motor 6	Motor 7	Motor 8
0	36	35	39	37	43	40	38	37
1.5	36	36	40	37	43	40	38	38
2.8	37	37	41	39	44	41	39	39
5.1	37	37	42	39	43	42	39	38
10.0	44	38	42	40	43	42	40	39
13.0	43	38	42	44	44	42	40	38
16.5	43	38	42	40	43	42	39	38
19.5	42	37	41	43	43	42	38	38
22.5	--	37	41	43	43	42	39	38
26.2	--	37	41	--	43	42	39	--
29.1	--	37	41	40	43	42	39	--
32.2	--	37	41	40	43	42	38	--
35.0	--	37	42	--	44	42	39	--
38.1	--	37	41	--	44	42	39	--
50.7	--	37	41	--	45	44	47	--
52.1	--	38	41	--	47	43	40	--

times for failure of the lubricants. Table 4.24 has been constructed to show, for the listed criteria, what one might accept for failure or unsatisfactory lubricant performance according to the time in vacuum at which failures apparently occurred.

Table 4.24

Failure Time of Lubricants

Criterion of Failure	Test Time of Failure of Lubricant (hr)							
	Molykote X-15		Electrofilm 66-C		Shell ETR-H		GE F-50	
	1	4	2	3	5	6	7	8
20% decrease of no-load speed	9.0	10.0	none	none	none	none	50.7	24.5
50% decrease of coast time	9.0	2.1	3.5	2.1	35.0	50.7	52.1	18.5
Failure of motor to restart	12.1	11.0	none	none	none	none	50.7	25.5

4.5.3 Specific Modifications

The following modifications in test procedure and apparatus will be incorporated in the next test:

1. Larger motors with coast times much longer than the resolution times of the measuring instruments will be used. The long coast time will have the advantage of enabling one to obtain effective viscosity of the lubricants by means of the equation

$$W = W_o \exp (-a \eta t) ,$$

where W is the motor speed during coast down, W_o is the no-load speed of the motor, η is the effective viscosity, a is a constant characteristic of the bearing and motor, and t is the time during coast down. The coast down of the motors obeys this equation in the range $W_o \geq W \geq 1/2W_o$. In the present test it is possible to apply this equation only to Motors 2, 3, and 4, since all the other motors have coast times too short to resolve this initial range. Furthermore, larger motors will be less subject to bearing damage during shipment.

2. The test rack will be equipped with means for either cooling or thermally isolating the motors so that the temperature may be held constant enough to allow more direct observation of vacuum and radiation effects.

3. More control measurements will be taken. An independent set of motors will be used to test the lubricants in vacuum only for a period of time at least comparable to that of the irradiation. With the motors and their lubricants in vacuum, measurements will be made, if scheduling permits, at a number of temperatures higher than ambient.

4. Finally, the pulse filter and amplifier circuit will be modified to give better performance, and lower-speed motors will be used to reduce contact bounce in the reed switches to an even greater extent.

4.6 Weight-Loss Test

The weight-loss test apparatus is a sensitive electrostatic balance designed to dynamically measure small weight losses of such organic materials as greases, plastics, elastomers, electrical and thermal insulations, and adhesives while subjected to the combined effects of high vacuum and reactor radiation. Unfortunately, due to malfunction of the apparatus, the irradiation run scheduled for the last quarter could not be made with the weight-loss apparatus. Instead, the high-force test apparatus was substituted. The problems associated with the failure of the weight-loss apparatus are discussed later in this section of the report.

4.6.1 Experimental Equipment

The experimental equipment for this test consisted primarily of a set of 15 electrostatic balances mounted on the same rack. A photograph of the setup is shown in Figure 4.62. These electrostatic balances were somewhat modified from the prototype balance reported in Reference 4, the Second Quarterly Progress Report. Specific modifications are listed below.

1. The material cup was replaced by a free-hanging weight pan.
2. The fixed condenser plate was made larger to increase the uniformity of the electric field.
3. The voltage on the indicator-light contacts was increased from 1.5 to 3.0 volts to guarantee that the indicator light would be turned on every time the arm was in an up or down position.
4. The length of the balance arm on the weight-pan side of the pivot was increased, so that the ratio of that length to the length of the arm from condenser plate to pivot was 2:1.

NPC 17,484
31-6750

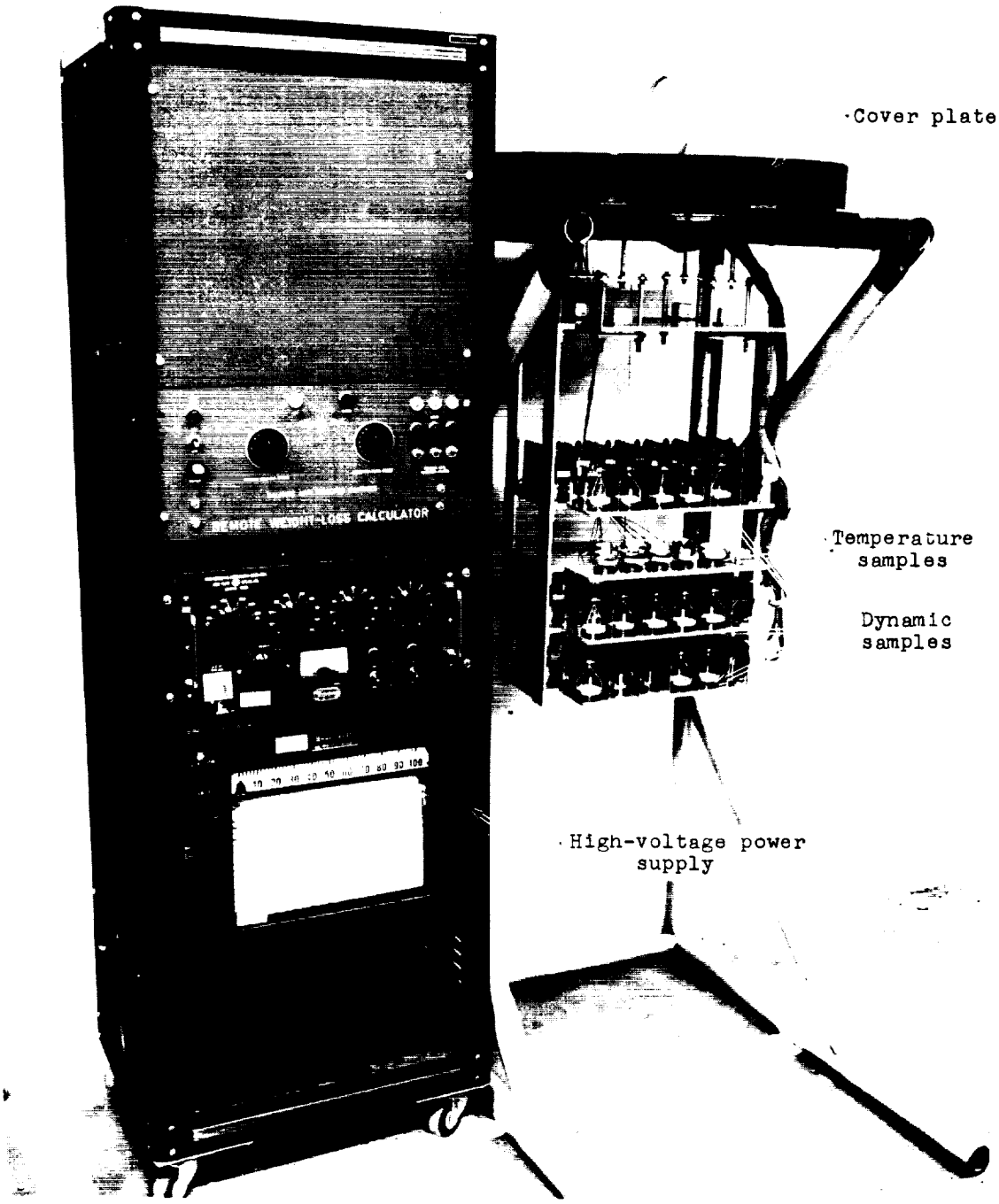

Figure 4.62 Weight-Loss Equipment

5. The sliding balance weight on the condenser side of the arm was removed.

6. The device to raise the arm off the pivot support was removed and replaced by a mechanism that would cage the arm by means of a set of alignment plates mounted on a shaft rotated by a 1-rpm motor.

Otherwise the balance mechanism was the same as that reported previously. The balance arm pivoted on an agate knife-edge resting on a flat agate plate. The arm was held loosely to the remainder of the balance by a very fine wire threaded through a small hole in the knife-edge holder and attached on both sides of the pivot support. This arrangement gave a very good sensitivity of approximately 0.2 mg/volt for each arm. Also, the rack holding the arms was fitted with holders for 15 specimens on which copper-constantan thermocouples were mounted for temperature measurement.

Auxiliary equipment consisted of a high-voltage power supply and a control console described in Reference 4. The technique of weight measurement with this apparatus is identical to that delineated on pages 73 through 76 of Reference 4.

4.6.2 Apparatus Calibration

Calibration of all the balance arms was accomplished by use of a set of ten weights weighing about 20 milligrams apiece. These weights were determined to one-tenth of a milligram on a precision laboratory balance before calibration of each arm. There was no significant change in the weights due to handling. During a calibration run, these weights were consecutively added to the weight pan of the electrostatic balance and voltage readings taken to give voltage as a function of weight over a range of about 200 milligrams.

Four such calibration runs were made for each arm. At first, the arms were calibrated in air. It was then found that the balance was particularly susceptible to small random forces, such as air drafts and mechanical vibration in the laboratory building. This susceptibility arises from two sources. The first of these, mentioned in the last progress report (Ref. 10), is the starting friction of the knife-edge, which causes the balance arm to have more than one position of balance.

The second source of susceptibility is the increase in force on the balance arm as the distance between the electrically charged condenser plates decreases. This affects the balancing of the arms in a particular way. If the voltage across the condenser plates has been increased to a point where the arm is nearly ready to balance, the electrostatic force on the arm resting in the up position is not large enough to overcome the weight on the arm. However, if the arm is displaced downward by vibration, the increased electrostatic attraction exceeds the force due to the weight, so that the arm rotates to the down position at a voltage lower than that necessary had there been no vibration.

As a consequence of these two phenomena, whose effects would be more marked in the evidently greater vibration of the vacuum system, and in spite of the damped apparatus supports, it was necessary even after careful leveling to recalibrate the weight-loss apparatus while it was inside the IML vacuum system. An example of the calibration curves obtained is shown in Figure 4.63.

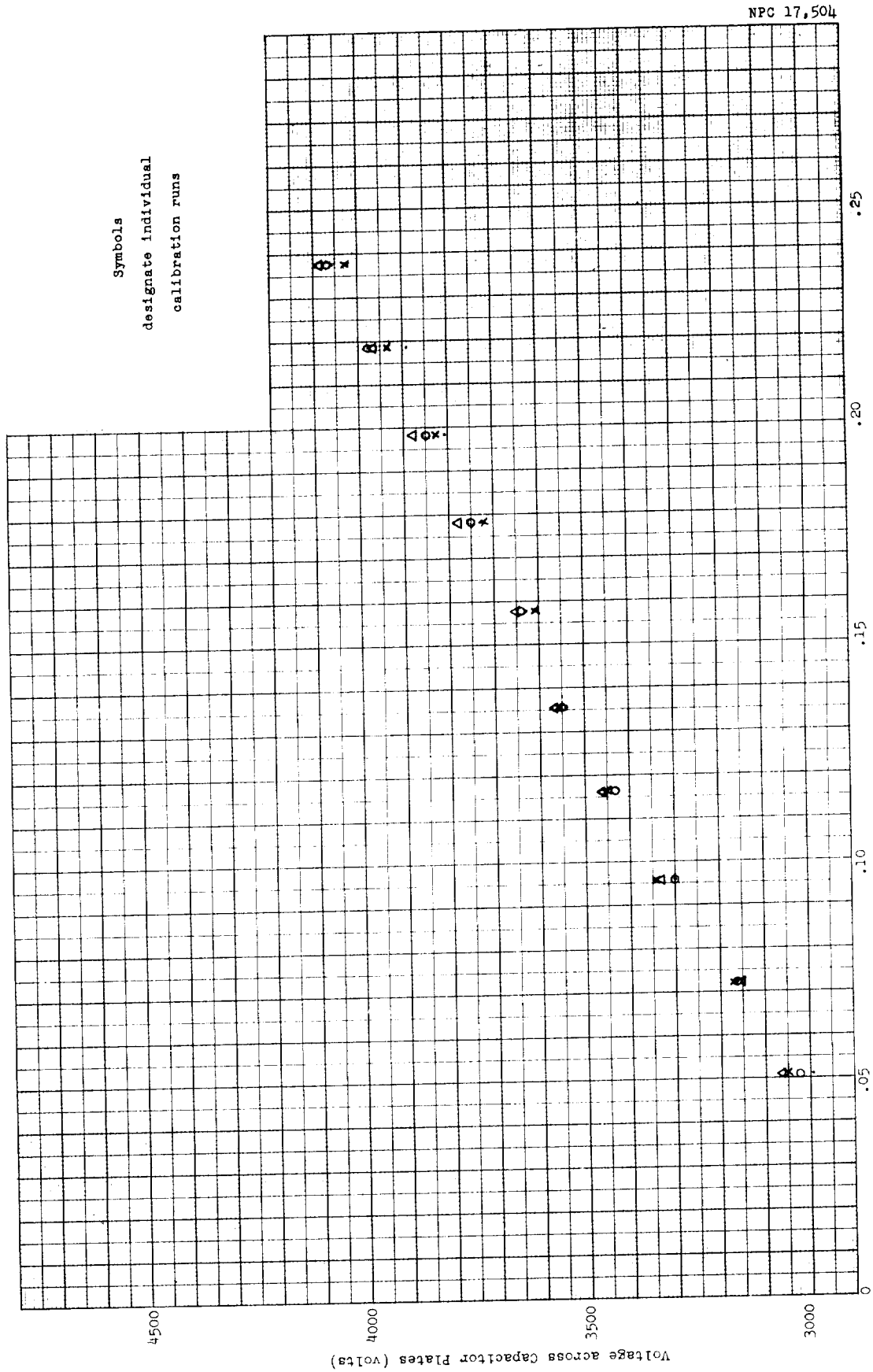

Figure 4.63 Sample Calibration Curve for Weight-Loss Apparatus

Following calibration, 200-mg samples of benzoic acid were added to several of the balance arms and the system pumped down to a pressure of 2.6×10^{-4} torr. The time rate of weight loss of benzoic acid was then measured. Results are shown in Figure 4.64.

4.6.3 Experimental Procedure

A 39-hour control run with specimens of the materials listed in Table A-9 of Reference 4 was then conducted in the IML vacuum chamber at 7.1×10^{-6} torr. The results showed that practically no significant change in weight occurred for any of the materials. These control data are given in Table 4.25.

During the two days immediately preceding the scheduled vacuum irradiation of the weight-loss specimens, three successive malfunctions of the weight-loss apparatus occurred, making continuance of the test impossible. Approximately 45 hours before reactor startup and during final checkout of the weight-loss apparatus, a relay which limits the rotation of the balance-arm alignment plates on the bottom row of arms failed to shut off the drive motor, with the result that the alignment plates were driven all the way around until they crushed two balance-arm agate supports. Additional checkout indicated possible damage to the agate supports of the remaining arms. At this time (about midnight of the same day) the high-voltage power supply failed. The next morning (Sunday), a new power supply was obtained and installed and an attempt was made to operate the balance. High-voltage arcing now began to occur and was traced to the vicinity of the high-voltage plug on the rear of the control-console chassis.

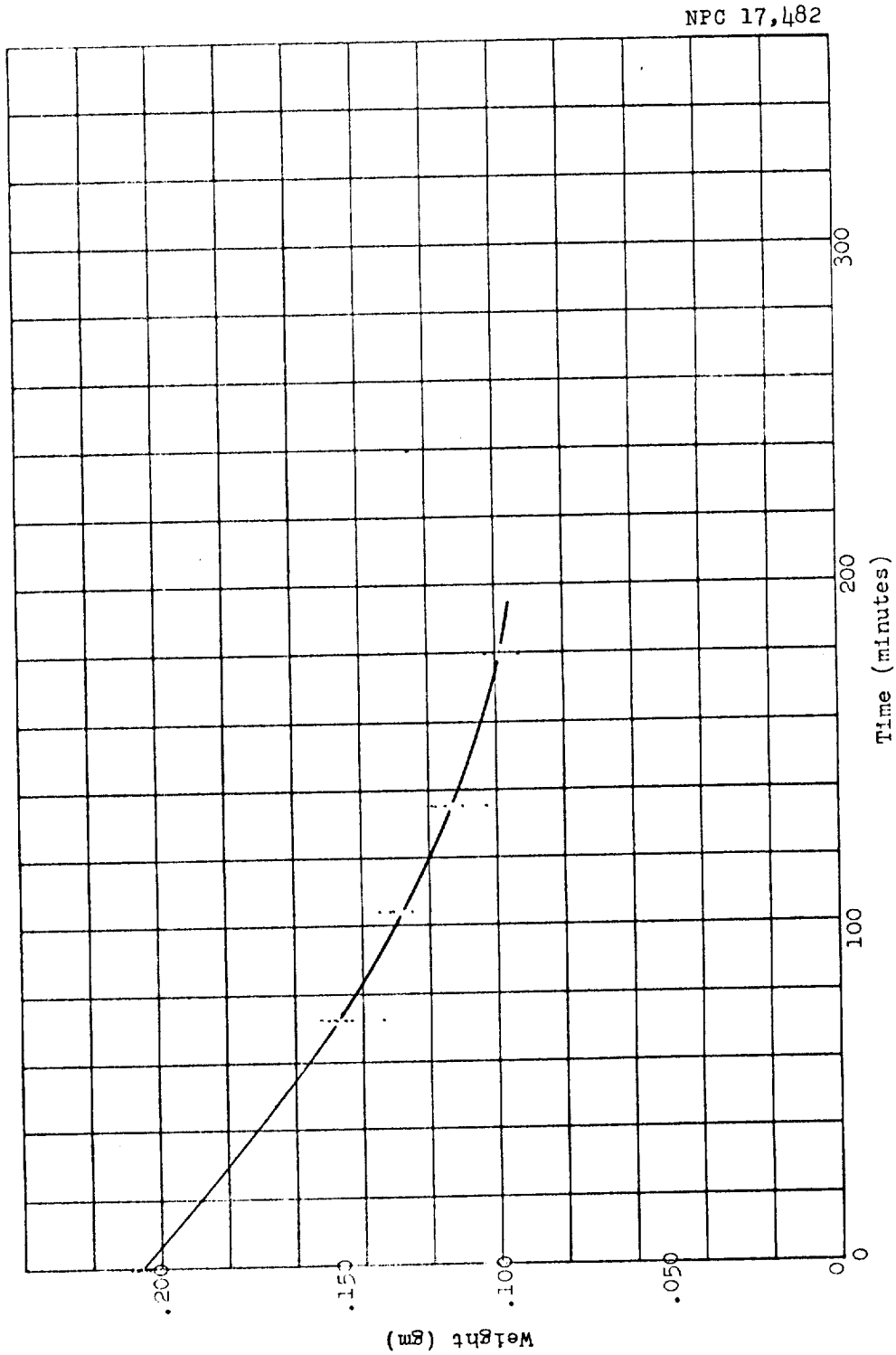

Figure 4.64 Weight Loss of Benzoic Acid in Vacuum

Table 4.25

Control Data for Weight-Loss Test

Time (min)	Stafoam		Kel-F-81		RTV-60		Teflon		Styrofoam 22	
	Voltage (v)	Weight (gm)	Voltage (v)	Weight (gm)	Voltage (v)	Weight (gm)	Voltage (v)	Weight (gm)	Voltage (v)	Weight (gm)
0	3230	0.3150	3810	2.0523	4030	2.0086	3770	2.0038	4070	0.2476
65	3270	0.3189	3790	2.0415	4070	2.0285	3810	2.0244	4080	0.2482
130	3250	0.3169	3760	2.0254	4070	2.0285	3800	2.0191	4090	0.2488
190	3250	0.3169	3770	2.0307	3950	1.9687	3760	1.9979	4080	0.2482
251	3250	0.3169	3780	2.0361	3970	1.9787	3750	1.9926	4090	0.2488
310	3260	0.3179	3780	2.0361	3970	1.9787	3770	2.0032	4100	0.2494
370	3280	0.3199	3800	2.0469	3980	1.9837	3800	2.0191	4100	0.2494
490	3220	0.3140	3790	2.0415	3970	1.9787	3780	2.0085	4090	0.2488
610	3200	0.3121	3760	2.0254	3970	1.9787	3750	1.9926	4080	0.2482
730	3210	0.3130	3880	2.0900	3960	1.9737	3750	1.9926	4030	0.2452
853	3200	0.3121	3860	2.0792	3950	1.9687	3740	1.9872	4000	0.2434
970	3230	0.3150	3850	2.0738	3940	1.9637	3750	1.9926	4030	0.2452
1120	3240	0.3160	3890	2.0954	3950	1.9687	3730	1.9819	4050	0.2464
1300	3230	0.3150	3850	2.0738	3950	1.9687	3740	1.9872	4050	0.2464
1500	3220	0.3140	3770	2.0307	3960	1.9737	3760	1.9979	4070	0.2476
1698	3230	0.3150	3780	2.0361	3940	1.9637	3770	2.0032	4050	0.2464
1882	3220	0.3140	3790	2.0415	3950	1.9687	3760	1.9979	4030	0.2452
2020	----	------	3830	2.0631	3920	1.9538	3760	1.9979	4060	0.2470
2172	3250	0.3169	3900	2.1008	3940	1.9637	3770	2.0032	4040	0.2458
2350		0.3086		2.0537		2.0056		2.0036		0.2428

Table 4.25 (cont'd)

Time (min)	Polyamid H-Film		Mylar		Epon 828		Metlbond 302A		Conolon	
	Voltage (v)	Weight (gm)	Voltage (v)	Weight (gm)	Voltage (v)	Weight (gm)	Voltage (v)	Weight (gm)	Voltage (v)	Weight (gm)
0	4030	1.0117	4160	0.6046	3640	2.0175	4060	2.0571	3910	2.0143
65	4070	1.0216	4220	0.6132	3670	2.0341	4080	2.0672	3890	2.0040
130	4060	1.0191	4250	0.6175	3680	2.0397	4080	2.0672	3870	1.9937
190	4020	1.0090	4250	0.6175	3620	2.0064	4060	2.0571	3880	1.9989
251	4010	1.0065	4250	0.6175	3630	2.0120	4060	2.0571	3880	1.9989
310	4030	1.0117	4210	0.6117	3640	2.0175	4080	2.0672	3890	2.0040
370	4070	1.0216	4210	0.6117	3670	2.0341	4100	2.0773	3880	1.9989
490	4030	1.0117	4160	0.6046	3650	2.0230	4070	2.0621	3850	1.9834
610	4000	1.0040	4150	0.6029	3620	2.0064	4070	2.0621	3830	1.9731
730	4000	1.0040	4080	0.5928	3660	2.0286	4080	2.0672	3900	2.0092
853	4020	1.0090	4040	0.5870	3630	2.0120	4060	2.0571	3880	1.9987
970	4020	1.0090	4050	0.5885	3640	2.0175	4070	2.0621	3870	1.9937
1120	----	------	4070	0.5914	3640	2.0175	4080	2.0672	3880	1.9989
1300	----	------	4050	0.5885	3630	2.0120	4080	2.0672	3850	1.9834
1500	----	------	4080	0.5928	3640	2.0175	4080	2.0672	3880	1.9989
1698	----	------	4180	0.6074	3640	2.0175	4090	2.0723	3870	1.9937
1882	----	------	4200	0.6102	3640	2.0175	4060	2.0571	3860	1.9886
2020	----	------	4190	0.6088	3650	2.0230	4050	2.0520	3870	1.9937
2172	----	------	----	------	3670	2.0341	4030	2.0419	3860	1.9886
2350		1.0051		0.6040		2.0171		2.0564		2.0088

Table 4.25 (cont'd)

Time (min)	GE F-50		Neoprene		Buna N		Viton B		GE F-50	
	Voltage (v)	Weight (gm)	Voltage (v)	Weight (gm)	Voltage (v)	Weight (gm)	Voltage (v)	Weight (gm)	Voltage (v)	Weight (gm)
0	4000	2.0250	3730	2.0701	3690	2.0603	3630	2.0101	2880	2.0194
65	4020	2.0351	3760	2.0868	3710	2.0715	3650	2.0212	2880	2.0194
130	4020	2.0351	3770	2.0923	3710	2.0715	3650	2.0212	2860	2.0054
190	3990	2.0199	3740	2.0757	3660	2.0436	3650	2.0212	2850	1.9984
251	4030	2.0402	3730	2.0701	3660	2.0436	3630	2.0101	2840	1.9914
310	4040	2.0453	3740	2.0757	3670	2.0491	3630	2.0101	2850	1.9934
370	4040	2.0453	3750	2.0812	3700	2.0659	3680	2.0378	2870	2.0124
490	4030	2.0402	3710	2.0590	3670	2.0491	3650	2.0212	2840	1.9914
610	4030	2.0402	3690	2.0479	3660	2.0436	3610	1.9990	2800	1.9633
730	----	------	3700	2.0535	3650	2.0380	3620	2.0046	2810	1.9703
853	4080	2.0655	3700	2.0535	3660	2.0436	3630	2.0101	2820	1.9773
970	4100	2.0756	----	------	3710	2.0715	3680	2.0378	----	------
1120	----	------	----	------	3670	2.0491	3630	2.0101	2840	1.9914
1300	----	------	----	------	3670	2.0491	3620	2.0046	2840	1.9914
1500	3990	2.0199	3900	2.1645	3680	2.0547	3630	2.0101	2840	1.9914
1698	4010	2.0301	3920	2.1756	3670	2.0491	3640	2.0157	2840	1.9914
1882	4010	2.0301	3970	2.1034	3660	2.0436	3630	2.0101	2830	1.9843
2020	4000	2.0250	----	------	3670	2.0491	3600	1.9935	2800	1.9633
2172	4040	2.0453	----	------	3680	2.0547	3630	2.0101	2840	1.9914
2350		2.0244		2.0651		2.0488		2.0096		2.0188

Since these three malfunctions had cast considerable doubt on the possibility of obtaining valid results with the apparatus, and since there remained only sufficient time for transporting equipment to the reactor area and securing the vacuum-irradiation systems in place in the reactor pool, the weight-loss test was abandoned.

The high-force test equipment, which had been kept on a standby basis, was substituted for the weight-loss apparatus. It is hoped that it will be possible to reschedule the weight-loss test for a future irradiation. At the present time, plans for modification of the weight-loss apparatus to prevent such malfunctions are under consideration.

4.7 Optical Properties of Thermal-Control Coatings

The effects of vacuum irradiation on the optical properties of four thermal-control coatings were investigated. The four test coatings picked for this test are representative of the types of organic paint that would be considered for nuclear-vehicle application.

4.7.1 Experimental Operation

The coatings tested in this experiment are listed in Table 4.26. Fabrication of the test samples and determination of the optical properties was done by the Space Science Laboratory at General Dynamics/Astronautics prior to shipment to General Dynamics/Fort Worth for vacuum irradiation.

The samples were prepared by applying several coats of sample paint onto 15/16-in.-diam aluminum disks (Al 2024). The thickness of the disks was 0.041 inch. Before application of the paint, the disks were cleaned with MEK and then with a naptha cleaner. Care was taken to spray enough paint onto the disks to obtain opaque coatings.

Six test samples of each coating material were fabricated and measured to establish a base-line value before shipment to Fort Worth. Three test samples of each coating were exposed during vacuum irradiation, while the other three samples were stored in a dry chamber to establish if changes in the coatings' optical properties occurred during transit or storage.

Table 4.26

Thermal-Control Coatings Tested in the Vacuum-Irradiation

Number of Samples	Basic Polymer Type	Name of Primer and Material	Manufacturer	Number of Coats	Average Thickness (0.001 in.)
12	Epoxy (white)	Epoxy Primer SA 9184 (white), Skyspar A-423 SA 9185 (untinted white color)	Andrew Brown	4	5.4
12	Silicone (white)	W. P. Fuller 517-W-1 high-gloss, heat-resistant TiO_2 pigment	W. P. Fuller	3	3.6
12	Silicone (aluminum)	No primer, W. P. Fuller 172-A-1 silicone-aluminum filled	W. P. Fuller	3	3.3
12	Acrylic (black)	Lacquer, pretreatment primer P40GCL Kemacryl lacquer, black No. W49BC12	Sherwin-Williams	2	2.0

The specimens were irradiated in the west vacuum chamber during Run 1, along with the organic materials listed in Section 4.2. These samples were mounted on the static holders shown in Figure 4.4.

The temperature of a representative specimen was recorded and is presented in Figure D-5 of Appendix D. The vacuum-chamber pressure during irradiation is shown in Figure 4.1.

After irradiation the samples were returned to General Dynamics/Astronautics in a metal can that was flushed with nitrogen before sealing. The optical-property measurements that are described below were made at General Dynamics/Astronautics.

The optical properties were measured with a Cary Model 14 spectrometer having an integrating sphere attachment and with a Perkin-Elmer Model 13 double-beam photometer which incorporates a hohlraum as a light source. The sample was placed inside the holhlraum, or the integrating sphere, where it was isotropically irradiated with the light. The intensity of the normal, monochromatic component of the reflected radiation was compared to the monochromatic intensity of a blackbody. The ratio of these two intensities, which is equal to the monochromatic reflectance, was displayed on a recording instrument as a function of wavelength. The measurements were made over a wavelength region of from 0.30 to 33 microns.

From the measured monochromatic reflectance, ρ_λ, the monochromatic values of emittance, ϵ_λ, and absorptance, α_λ were obtained as follows:

$$\epsilon_\lambda = \alpha_\lambda = 1 - \rho_\lambda$$

The reflectance of the sample was measured at one temperature (100°F) only. Assuming that the monochromatic emittance will show only second-order variations with temperature, the total emittance was calculated for 100°, 300°, and 500°K.

A detailed description of the experimental arrangement is discussed in Reference 14. Reference 15 includes an analysis of errors due to self-emission of source and detector. The radiation sources, prisms, filters, and detectors used for different wavelength regions are given in Table 4.27.

4.7.2 Experimental Results

The total emittance resulting from the normal spectral reflectivity measurement is presented in Table 4.28. Values are presented for the solar absorptance and the total normal emittance at 100°, 300°, and 500°K. The normal spectral reflectivity measurements are given in Appendix E.

The accuracy of the Cary Model 14 spectrometer, which works in the wavelength region of from 0.3 to 2 microns, is better than 2%. Since 95% of the solar energy is contained in this wavelength region, the error in the solar absorptance will not exceed 2%. The reproducibility of the Perkin-Elmer Model 13 spectrometer is approximately 3% of the full-scale pen deflection. This implies a relative error in the reflectance of 0.03 for the wavelength region between 2 and 33 microns. Since the blackbody energy peaks for 100°, 300°, and 500°K all fall within that wavelength interval, the emittances shown in Table 4.28 may deviate within the limits of $\pm$ 0.015. The error of the ratio of solar absorptance to

Table 4.27

Equipment Used in Optical-Property Determination of Thermal-Control Coatings

Source	Spectrograph Prism	Detector	Diagonal	Filter	Wavelength Coverage (microns)
Integrating Sphere, Tungsten (1000° K)	Cary Model 14	Phototube	None	None	0.3 to 0.6
		Lead Sulfide	None	None	0.6 to 2.0
Hohlraum (820° C)	Perkin-Elmer Model 13 Cs Br	Thermo-couple with Cs Br window	Mirror	None	1.36 to 12.0
			Scatterplate	None	12.0 to 19.1
			Scatterplate	Ag Cl/Ag S	19.1 to 24.4
			Restrahlen plate	None	24.4 to 33.0

Table 4.28

Optical Properties of Thermal-Control-Coatings Test Samples

Material and Test Condition	Radiation Exposure				Solar Absorptance α	Calculated Total Normal Emittance at Sample Temperature					
						100°K		300°K		500°K	
	Gamma [ergs/gm(C)]	Neutrons (n/cm²)				Emissivity ε	α/ε	Emissivity ε	α/ε	Emissivity ε	α/ε
		Thermal	E>2.9 Mev	E>8.1 Mev							
Acrylic black (GD/A)[a]	0	0	0	0	0.944	0.884	1.07	0.909	1.04	0.925	1.02
(controls)	0	0	0	0	0.947	0.832	1.14	0.886	1.07	0.920	1.02
	0	0	0	0	0.947	0.801	1.18	0.875	1.08	0.913	1.04
	0	0	0	0	0.947	0.832	1.14	0.886	1.07	0.920	1.03
					0.947	0.822	1.15	0.882	1.07	0.918	1.03
(irradiated)	2.4(10)	3.7(14)	2.2(15)	8.4(13)	0.947	0.832	1.14	0.886	1.07	0.920	1.02
	1.7(10)	3.4(14)	1.9(15)	7.1(13)	0.947	0.832	1.14	0.886	1.07	0.920	1.02
	1.0(10)	3.1(14)	1.6(15)	5.8(13)	0.947	0.832	1.14	0.886	1.07	0.920	1.02
					0.947	0.832	1.14	0.886	1.07	0.920	1.02
Epoxy white (GD/A)[a]	0	0	0	0	0.303	0.906	0.334	0.905	0.335	0.906	0.334
(controls)	0	0	0	0	0.301	0.865	0.348	0.891	0.338	0.888	0.339
	0	0	0	0	0.300	0.866	0.346	0.886	0.339	0.875	0.343
	0	0	0	0	0.300	0.866	0.346	0.873	0.344	0.872	0.344
					0.300	0.866	0.347	0.883	0.340	0.883	0.342
(irradiated)	2.4(10)	3.7(14)	2.2(15)	8.4(13)	0.382	0.873	0.438	0.896	0.426	0.890	0.429
	1.7(10)	3.4(14)	1.9(15)	7.1(13)	0.382	0.873	0.438	0.896	0.426	0.890	0.429
	1.0(10)	3.1(14)	1.6(15)	5.8(13)	0.382	0.873	0.438	0.896	0.426	0.890	0.429
					0.382	0.872	0.438	0.896	0.426	0.890	0.429
Silicone white (GD/A)[a]	0	0	0	0	0.336	0.835	0.402	0.874	0.384	0.789	0.426
(controls)	0	0	0	0	0.330	0.853	0.387	0.889	0.371	0.791	0.417
	0	0	0	0	0.330	0.853	0.387	0.893	0.370	0.810	0.407
	0	0	0	0	0.301	0.853	0.353	0.886	0.340	0.778	0.387
					0.320	0.853	0.375	0.889	0.360	0.800	0.404
(irradiated)	2.4(10)	3.7(14)	2.2(15)	8.4(13)	0.342	0.830	0.412	0.873	0.392	0.808	0.423
	1.7(10)	3.4(14)	1.9(15)	7.1(13)	0.341	0.829	0.411	0.870	0.392	0.783	0.436
	1.0(10)	3.1(14)	1.6(15)	5.8(13)	0.342	0.829	0.413	0.871	0.393	0.793	0.431
					0.342	0.829	0.412	0.871	0.392	0.795	0.430
Silicone aluminum (GD/A)[a]	0	0	0	0	0.280	0.307	0.912	0.296	0.946	0.272	1.03
(controls)	0	0	0	0	0.283	0.288	0.983	0.278	1.02	0.261	1.08
	0	0	0	0	0.283	0.288	0.983	0.278	1.02	0.261	1.08
	0	0	0	0	0.283	0.288	0.983	0.278	1.02	0.261	1.08
					0.283	0.288	0.983	0.278	1.02	0.261	1.08
(irradiated)	2.4(10)	3.7(14)	2.2(15)	8.4(13)	0.301	0.312	0.965	0.299	1.01	0.274	1.10
	1.7(10)	3.4(14)	1.9(15)	7.1(13)	0.301	0.312	0.965	0.299	1.01	0.274	1.10
	1.0(10)	3.1(14)	1.6(15)	5.8(13)	0.288	0.299	0.963	0.278	1.04	0.250	1.15
					0.296	0.309	0.964	0.292	1.02	0.266	1.12

[a]Representative value before shipment from General Dynamics/Astronautics

emittance is given by

$$\pm \frac{\alpha}{\epsilon} \left(\frac{\Delta\alpha}{\alpha} + \frac{\Delta\epsilon}{\epsilon} \right),$$

where $\Delta\alpha/\alpha = 0.01$, and $\Delta\epsilon = 0.015$.

In addition to these instrumental errors, different surface roughness and contamination may result in a slight change of optical properties among apparently equal paint samples.

The vacuum-irradiation exposure produced very little detectable change in the reflectivity of the acrylic black samples over the measured wavelength region, because the reflectivity is quite small in this region. Since the relative changes of reflectance, absorptance, and emittance are equal ($\Delta\rho = -\Delta\alpha = -\Delta\epsilon$), the changes in the solar absorptance and total normal emittance are also small. The results in Table 4.28 show that the changes in the optical properties of acrylic black paint are less than the instrumental errors given above. This can also be observed from the monochromatic reflectivity curves given in Appendix E.

Vacuum irradiation of the epoxy white samples tends to lower the reflectivity in the visible and near-infrared region of the spectrum. The reflectivity of epoxy white paint is quite small for wavelengths longer than 3.6 microns. Since the emission of radiative energy from bodies at 100°, 300°, and 500°K occurs primarily at wavelengths greater than 3.6 microns, an appreciable change in the emissivity does not occur. However, the solar absorptance changes considerably, as can be observed in Table 4.28.

No detectable change in optical properties was noted for the silicone white and silicone aluminum paints subjected to the vacuum-irradiation exposures.

V. CONCLUSIONS AND RECOMMENDATIONS

The first known engineering tests for evaluating the effects of the combined environments of high vacuum and nuclear-reactor radiation on nonmetallic materials have been successfully completed. These tests, conducted at NARF during 1962, are part of a continuing program of basic engineering studies to be conducted on nine major material-application categories.

5.1 General Discussion

During the launch and powered flight of a chemically powered spacecraft, the materials in the vehicle are subjected to a complex of interacting forces in a changing environment. During the ascent from the prelaunch environment of high humidity and salt air to the outer-space environment of high vacuum and cryotemperatures, the spacecraft experiences acceleration loads, vibration, heating due to friction, and rapid pressure changes. Although the problems of material selection and engineering design arising from such conditions have been largely overcome, the addition of radiation to the complex creates new problems to be identified and resolved. Ideally, a program to study these problems would provide for materials to be tested under conditions that would exactly simulate those encountered in a nuclear-powered-vehicle flight. However, existing technology in the fields of high-vacuum and nuclear-radiation testing has not yet reached the level where full execution of this type of program is possible.

In an actual flight, the ascent time of a space vehicle to a low earth orbit is in the neighborhood of a few minutes, with the vacuum pressure after attaining orbit being approximately 10^{-6} torr. The vacuum equipment used in these tests (the most advanced that was available in December 1961) required two hours to achieve a comparable vacuum in the environmental chamber. Nevertheless, the fact that the experiment is not an exact analog of the changing environmental conditions experienced by the vehicle does not invalidate the usefulness of the data in materials selection, since most of the materials tested have successfully withstood the rigors of rocket flight.

Another matter for consideration in using these data in the selection of materials for spacecraft is the difference between the dose rates of the Ground Test Reactor used in this experiment and those of the vehicle's nuclear-heat-exchanger rocket engine. Although the mechanical properties of organic materials have not yet been shown to be significantly affected by the magnitude of the dose rate, it is the opinion of the author that the effects of high dose rate and vacuum should be investigated when the Kiwi reactors are being tested. This opinion is based in part on the fact that a dose-rate problem does exist for electrical components, such as transistors, diodes, vacuum tubes, and capacitors and because of the large differences between the dose rates of the GTR and the vehicle reactors. Before the dose-rate problems can be investigated, however, materials must be found that will sustain the damaging effects of the combination environment of vacuum and radiation.

The remaining area of concern in applying these data directly to spacecraft materials selection is that of radiation-induced heating in the materials and components. The effects of high vacuum on organic materials has been shown to be aggravated by high temperatures (Ref. 16). This has not yet been shown to be true for the vacuum-radiation environments, but should still be a major consideration for study. As shown by Hill and Kerlin in Reference 17, the heating rates for dense materials from reactor radiation are very high. This heating effect is also shown for the test materials by the temperature plots in Appendix D. By the use of empirical heating data and standard heat-transfer techniques, the temperatures of the materials in the vehicles can be controlled. This control will be necessary, for many of the existing materials are temperature sensitive.

All of the desired types of data could not be obtained in the laboratory with the present equipment and techniques. However, considerable data have been obtained in the present tests and sufficient correlation of these data can be made to permit initial selection of materials for use in a nuclear-powered space vehicle.

5.2 Experimental Test Equipment

Although lack of pertinent information in several areas was a handicap to the design and construction of the vacuum equipment, the tests showed that, by judicious engineering, standard vacuum equipment could be used in a nuclear-reactor radiation field. The design of the vacuum chambers and the vacuum-pump shields proved to be adequate: the measured vacuum pumping speed more than

satisfied the design value, and the radiation dose at the diffusion pump remained below the critical value.

An evaluation of the effects of gamma radiation on the vacuum-pumping-speed characteristics of DC-704 diffusion-pump oil, which was performed by O. H. Hill of GD/FW and D. L. Stevenson, of CVC, showed that the change in pumping characteristics after the irradiation was smaller than expected. A complete discussion of this investigation is given in Appendix A. Also, there was no appreciable change in vacuum pressure noted during the reactor radiation that could be attributed to radiation effects on the vacuum-punp oil.

The radiation-induced gassing from the materials in the vacuum environment had a smaller effect on the chamber pressure than had been previously calculated. The vacuum systems were designed around the gassing rates for polyethylene (Ref. 18). On the basis of these rates, the quantity of material that could be accommodated in each system was 50 grams. However, it was found during the tests that a large quantity of test samples ($\sim$ 250 grams) could be irradiated in the vacuum chamber without raising the pressure above 10^{-6} torr. This suggests that the effective pumping speeds of the systems are considerably in excess of the conservative estimate utilized in the design.

The effect of radiation on the vacuum gages was found to be lower than predicted. Although some operational problems were encountered with the vacuum gages, good service was generally provided.

In a few cases a data point was compromised by the low signal-to-noise ratio in the electronics of the dynamic testers; in general, however, this equipment operated satisfactorily. A few modifications and improvements that should eliminate this problem will be made in the dynamic testers during the second year of operation.

5.3 Experimental Test Results

In this test program, 47 materials were evaluated during seven vacuum-chamber irradiations. Because of the large number of materials involved, a few did not receive the optimum dose to produce medium damage. The materials that showed no detectable change in properties after the vacuum irradiation are grouped together and presented in tabular form in the Report Summary. These materials could probably be used safely in a nuclear-powered spacecraft, providing that they are not exposed to higher doses than those listed in the table and that their properties are compatible with other design criteria. The other materials tested would have a very low reliability if exposed to the indicated doses; however, most of these materials would be usable at a lower total radiation exposure. Many of the materials will be tested at lower and/or higher doses during the second year of these experiments to determine 10% and/or 50% damage thresholds.

Photographs of the test samples showing a change in color between the vacuum-irradiated samples and the control samples were made. Copies of the photographs are on file at NASA in Huntsville. Because of the difficulty involved in reproducing

true color in photographs, these pictures are not included in this report. The color changes that occurred in these specimens are noted in the results section pertaining to each material. These are color changes visible to the eye and are not the result of colorimetric analysis.

5.3.1 Static Tests

5.3.1.1 Mechanical Property Tests

Table 5.1 presents a summary of the results of tests conducted on the materials after the following exposures: (1) vacuum and no radiation, (2) vacuum and radiation, and (3) air and radiation. The materials were subsequently tested in air in the Instron testing machine located in the IML at the NARF facility in Fort Worth.

The results of these tests performed on materials irradiated in both air and vacuum show that general predictions of the property changes due to irradiation in a vacuum cannot be made on the basis of air-irradiation results. Examples of the validity of this conclusion are presented below for select materials.

Buna N (Parker Rubber Co.)

One of the compounds tested in both environments was Parker Rubber Company's O-ring compound 66-581. The original ultimate elongation of 493% for this Buna N compound decreased to 78% after a vacuum irradiation of 8.1×10^9 ergs/gm(C). For the air irradiations of 3.2×10^9 ergs/gm(C) and 1×10^{10} ergs/gm(C), the ultimate elongation values were 246% and 104%, respectively. The ultimate tensile strength of this compound increased with increasing dose for both the air and vacuum irradiations. The vacuum irradiation produced more changes in the mechanical properties of this compound than the air irradiation.

Table 5.1

Summary of Property Changes for Materials
Irradiated in Vacuum and Air and Tested in Air

Category	Trade Name	Gamma Dose [ergs/gm(C)]	Vacuum (torr)	Specimen Configuration	Measured Property	Percent Change in Measured Property
Adhesives	FM-1000	1.7×10^{10}	5×10^{-7}	Lap shear	Ult. shear strength	0
	Metlbond 406	9.2×10^{9}	3×10^{-1}	Lap shear	Ult. shear strength	0
		1.7×10^{10}	5×10^{-7}	Lap shear	Ult. shear strength	0
		1.1×10^{10}	Air Irrad.	Lap shear	Ult. shear strength	0
		4.9×10^{10}	Air Irrad.	Lap shear	Ult. shear strength	-86.5
	Metlbond 302	9.2×10^{9}	3×10^{-1}	Lap shear	Ult. shear strength	0
	Epon 422-J	3.9×10^{10}	2×10^{-6}	Lap shear	Ult. shear strength	0
	AF-6	3.9×10^{10}	2×10^{-6}	Lap shear	Ult. shear strength	0
	Metlbond 408	3.9×10^{10}	2×10^{-6}	Lap shear	Ult. shear strength	-78
	Epon VIII	1.7×10^{10}	5×10^{-7}	Lap shear	Ult. shear strength	-12
	FM-47	3.9×10^{10}	2×10^{-6}	Lap shear	Ult. shear strength	-42
Seals	Parker Compound 66-581 (Buna N)	8.1×10^{9}	2×10^{-6}	O-Rings	Ult. shear strength Ult. elongation Weight change	+37 -85 - 1.27
		8.1×10^{9}	2×10^{-6}	Tensile (ASTM-D-412-51T, Die C)	Ult. tensile strength Ult. elongation Weight change	+25 -85 - 1.32
		3.2×10^{9}	Air Irrad.	O-Rings	Ult. tensile strength Ult. elongation	+15 -50
		1.1×10^{10}	Air Irrad.	O-Rings	Ult. tensile strength Ult. elongation	+56 -79.5

Table 5.1 (cont'd)

Category	Trade Name	Gamma Dose [erg/gm(C)]	Vacuum (torr)	Specimen Configuration	Measured Property	Percent Change in Measured Property
Seals (cont'd)	Natural Rubber	0 Vacuum Controls	1×10^{-6}	O-Rings	Ult. tensile strength Ult. elongation Weight change	0 0 + 1
		9.0×10^{9}	2×10^{-6}	O-Rings	Ult. tensile strength Ult. elongation Weight change	-48 -75 0
	Viton B PRP 19007	9.0×10^{9}	3×10^{-7}	O-Rings	Ult. tensile strenth Ult. elongation	-21 -88
Thermal Insulation	Urethane DS-620	1.1×10^{10}	3×10^{-7}	Compression disks	Comp. strength @ 25% deflection Weight change	0 ~- 4
	Stafoam AA-402	0 Vacuum Controls	1×10^{-6}	Compression disks	Comp. strength @ 25% deflection Ult. comp. strength Weight change	- 9.6 - 4.2 - 1.96
		8.9×10^{9}	3×10^{-7}	Compression disks	Comp. strength @ 25% deflection Ult. comp. strength Weight change	-13 ~- 9 ~- 1
		5.0×10^{9}	Air Irrad.	Compression disks	Comp. strength @ 25% deflection Ult. comp. strength	-65 -64
		8.0×10^{9}	Air Irrad.	Compression disks	Comp. strength @ 25% deflection Ult. comp. strength	-63.5 -66.5
	Refrasil Batting B-100 (silicone oxide)	5.4×10^{9}	5×10^{-6}	Compression stacks	Comp. strength @ 80% deflection Comp. strength @ 40% deflection	-24 -31

Table 5.1 (Cont'd)

Category	Trade Name	Gamma Dose [erg/gm(C)]	Vacuum (torr)	Specimen Configuration	Measured Property	Percent Change in Measured Property
Thermal Insulation (cont'd)	Styrofoam 22	0 Vacuum Controls	1×10^{-6}	Compression disks	Comp. strength @ 25% deflection Weight change	- 9.25 - 1.97
		1×10^{10}	2×10^{-6}	Compression disks	Comp. strength @ 25% deflection Weight change	0 - 0.66
		5.0×10^{9}	Air Irrad.	Compression disks	Comp. strength @ 25% deflection	-52.5
		1.0×10^{10}	Air Irrad.	Compression disks	Comp. strength @ 25% deflection	-65.5
Structural Laminates	Silicone DC-2106	4.5×10^{10}	5×10^{-7}	Tensile (ASTM-D-638-58T, Type I)	Ult. tensile strength Ult. elongation Weight change	0 0 - 0.19
	CTL-91-LD	4.5×10^{10}	5×10^{-7}	Tensile (ASTM-D-638-58T, Type I)	Ult. tensile strength Ult. elongation Weight change	0 0 - 0.60
	Epon 828	8.6×10^{9}	3×10^{-1}	Tensile, mod. (ASTM-D-638-58T, Type I)	Ult. tensile strength Ult. elongation	0 0
		7.5×10^{9}	3×10^{-7}	Straight flexural specimens	Ult. flexural strength Ult. deflection Weight change	0 0 0
	Conolon 506	9.7×10^{9}	3×10^{-1}	Tensile, mod. (ASTM-D-638-58T, Type I)	Ult. tensile strength Ult. elongation	0 0
	Mobiloy AH-81 (phenolic)	1.7×10^{10}	5×10^{-7}	Straight tensile specimens	Ult. tensile strength	-15.6

Table 5.1 (cont'd)

Category	Trade Name	Gamma Dose [erg/gm(C)]	Vacuum (torr)	Specimen Configuration	Measured Property	Percent Change in Measured Property
Electrical Insulation	KEL-F-81	1.5×10^{10}	2×10^{-6}	Tensile (ASTM-D-638-58T, Type I)	Ult. tensile strength Ult. elongation Weight change	-100 -100 - 0.29
		5.5×10^{9}	Air Irrad.	Tensile (ASTM-D-638-58T, Type I)	Ult. tensile strength Ult. elongation	- 70 -100
		8.0×10^{9}	Air Irrad.	Tensile (ASTM-D-638-58T, Type I)	Ult. tensile strength Ult. elongation	-100 -100
	Mylar (10 mil) (polyester)	2.4×10^{10}	2×10^{-6}	Straight tensile specimens	Ult. tensile strength Ult. elongation Weight change	0 -100 0
	Mylar A (3 mil) (polyester)	1.3×10^{9}	5×10^{-6}	Straight tensile specimens	Ult. tensile strength Ult. elongation Weight change	+150 + 51 0
		7.0×10^{9}	5×10^{-6}	Straight tensile specimens	Ult. tensile strength Ult. elongation Weight change	+150 + 51 0
	Mylar C (1 mil) (polyester)	1.3×10^{9}	5×10^{-6}	Straight tensile specimens	Ult. tensile strength Ult. elongation Weight change	0 0 0
		5.4×10^{9}	5×10^{-6}	Straight tensile specimens	Ult. tensile strength Ult. elongation Weight change	0 0 0
	Mylar C	4.9×10^{9}	Air Irrad.	Straight tensile specimens	Ult. tensile strength Ult. elongation	+116 + 28
		8.0×10^{9}	Air Irrad.	Straight tensile specimens	Ult. tensile strength Ult. elongation	- 4.5 - 15.5

Table 5.1 (cont'd)

Category	Trade Name	Gamma Dose [ergs/gm(C)]	Vacuum (torr)	Specimen Configuration	Measured Property	Percent Change in Measured Property
Electrical Insulation (cont'd)	DuPont H-Film	0 Vacuum Controls	1×10^{-6}	Straight tensile specimens	Tensile strength @ 25% Tensile strength @ 50% Ult. tensile strength Ult. elongation	- 2.2 - 3.2 - 8.3 - 1.4
		8.8×10^{9}	3×10^{-7}	Straight tensile specimens	Tensile strength @ 25% Tensile strength @ 50% Ult. tensile strength Ult. elongation	0 0 0 0
	Silicone DC 7-170	9.0×10^{9}	2×10^{-6}	Tensile (ASTM-D-412-51T, Die C)	Ult. tensile strength Ult. elongation Weight change	+144 - 83.5 - 0.2
Potting Compounds	Epon 828/Z	1.0×10^{-10}	2×10^{-6}	Compression disks	Ult. comp. strength Weight change	+ 5.8 0
	DC R-7521	9.0×10^{9}	2×10^{-6}	Compression disks	Ult. comp. strength Weight change	0 0
	RTV-60	8.6×10^{9}	3×10^{-7}	Compression disks	Comp. strength @ 25% Comp. strength @ 0.02 in. Weight change	+667 +405 0
Dielectric Material	Teflon TFE (40 mil)	1.9×10^{9}	5×10^{-6}	Straight tensile specimens	Ult. tensile strength Ult. elongation Weight change	- 44.5 - 96 0
	Teflon TFE (10 mil)	0 Vacuum Controls	1×10^{-6}	Straight tensile specimens	Ult. tensile strength Ult. elongation Weight change	0 0 0
		1.7×10^{9}	5×10^{-6}	Straight tensile specimens	Ult. tensile strength Ult. elongation Weight change	- 42 - 98 0

Table 5.1 (cont'd)

Category	Trade Name	Gamma Dose [ergs/gm(C)]	Vacuum (torr)	Specimen Configuration	Measured Property	Percent Change in Measured Property
Dielectric Material (cont'd)	Teflon FEP (40 mil)	8.6×10^{9}	5×10^{-7}	Straight tensile specimens	Ult. tensile strength Ult. elongation Weight change	- 40.5 ≈- 99 - 0.26
	Marlex 6002	1.1×10^{10}	5×10^{-7}	Straight tensile specimens	Ult. tensile strength Ult. elongation Weight change	+ 37 - 94.5 0
	Teslar	1.3×10^{9}	5×10^{-6}	Straight tensile specimens	Ult. tensile strength Ult. elongation Weight change	0 0 0
		6.2×10^{9}	5×10^{-6}	Straight tensile specimens	Ult. tensile strength Ult. elongation Weight change	0 0 0
Elastomers	Buna N (RA 30760)	0 Vacuum Controls	1×10^{-6}	Tensile (ASTM-D-412-51T, Die C)	Ult. tensile strength Ult. elongation Weight change	0 0 0
		1.7×10^{9}	5×10^{-6}	Tensile (ASTM-D-412-51T, Die C)	Ult. tensile strength Ult. elongation Weight change	- 91.5 - 34.3 0
		7.0×10^{9}	5×10^{-6}	Tensile (ASTM-D-412-51T, Die C)	Ult. tensile strength Ult. elongation Weight change	- 92 - 71 0
		1.9×10^{9}	Air Irrad.	Tensile (ASTM-D-412-51T, Die C)	Ult. tensile strength Ult. elongation	- 11.6 - 39
		2.1×10^{10}	Air Irrad.	Tensile (ASTM-D-412-51T, Die C)	Ult. tensile strength Ult. elongation	+ 43 - 84.5
	Neoprene (RA 24160)	1.9×10^{9}	5×10^{-6}	Tensile (ASTM-D-412-51T, Die C)	Ult. tensile strength Ult. elongation Weight change	- 94 - 49 0

Table 5.1 (cont'd)

Category	Trade Name	Gamma Dose [erg/gm(C)]	Vacuum (torr)	Specimen Configuration	Measured Property	Percent Change in Measured Property
Elastomers (cont'd)	Neoprene (RA 24160) (cont'd)	5.4×10^{9}	5×10^{-6}	Tensile (ASTM-D-412-51T, Die C)	Ult. tensile strength Ult. elongation Weight change	- 96 - 77 0
	Viton A (RA 26360)	0 Vacuum Controls	1×10^{-6}	Tensile (ASTM-D-412-51T, Die C)	Ult. tensile strength Ult. elongation Weight change	0 0 0
		1.6×10^{10}	5×10^{-7}	Tensile (ASTM-D-412-51T, Die C)	Ult. tensile strength Ult. elongation Weight change	0 - 84 - 1.2
		1.9×10^{9}	Air Irrad.	Tensile (ASTM-D-412-51T, Die C)	Ult. tensile strength Ult. elongation	- 21.3 - 43
		2.1×10^{10}	Air Irrad.	Tensile (ASTM-D-412-51T)	Ult. tensile strength Ult. elongation	+ 39 - 83

Buna N (NASA)

Buna N formulation compounded by NASA (RA-30760) was tested as tensile specimens. From the data in Table 5.1, a significant change in the ultimate tensile strength is evident between those specimens irradiated in vacuum to a dose of 1.7×10^9 ergs/gm(C) and those irradiated in air to a dose of 1.9×10^9 ergs/gm(C). The average value for the vacuum-irradiation specimens was 203 psi, whereas that for the air-irradiation specimens was 2174 psi - a factor of 10 difference. The effect of a higher dose, 7×10^9 ergs/gm(C), on specimens in a vacuum was not significantly different from that of the lower dose. However, an increase in dose to 2.1×10^{10} ergs/gm(C) in air caused the tensile strength to increase 43% (or to 3512 psi).

The changes in ultimate elongation produced by the vacuum irradiation were less than those produced by the air irradiation. At the lower doses, the percent ultimate elongation of the vacuum-irradiation specimens was higher than the value for the air-irradiation specimens (450% and 391%, respectively.)

Viton A (NASA)

A Viton A formulation compounded by NASA (RA-26360) and tested in both air and vacuum shows a different trend. The Viton A elastomers retained the same tensile strength, conversely to the Buna N compound (RA-30760), while the elongation properties of Viton A were more severely affected by the vacuum irradiation than those of the Buna N.

Because of the large sheet-to-sheet variation in the test platens, only general trends are indicated here. The ultimate tensile strength showed no significant change after the vacuum irradiation of 1.8×10^{10} ergs/gm(C), while the ultimate elongation decreased significantly. After a 2.1×10^{10}-erg/gm(C) dose in air the material showed a significant increase in tensile strength and a significant decrease in elongation.

Styrofoam 22 (Dow Corning Corp.)

Samples from the same batch of Styrofoam 22 (polystyrene) were irradiated in vacuum during this phase of the experiment and in air during the cryogenic phase (Ref. 1). The results from tests on samples exposed to vacuum, to vacuum irradiation, and to air irradiation are given in Table 5.1. Samples placed in a vacuum for the same period of time as those irradiated in a vacuum showed a 9.3% decrease in compression strength and 7.0% decrease in weight. The samples irradiated in a vacuum to a dose of 1.0×10^{10} ergs/gm(C) showed no significant change in compression strength and only a small (0.66%) decrease in weight. This indicates that while the vacuum alone had a softening effect on the material, the addition of radiation to the vacuum tended to counteract it with a hardening effect. The hardening produced by radiation in vacuum, however, was not nearly so pronounced as that produced by radiation in air: The compression strength of samples irradiated in air to 5.0×10^{9} ergs/gm(C) decreased 52% and those irradiated to a higher dose of 1.0×10^{10} ergs/gm(C) decreased 66%.

Stafoam AA-402 (American Latex Products)

Samples from the same batch of Stafoam AA-402 (polyurethane) were irradiated in vacuum during this test and in air during the cryogenic section (Ref. 1) of these experiments. The results from the tests after the vacuum control, vacuum irradiation, and air irradiation are given in Table 5.1. These results are very similar to those of Styrofoam 22, given above. The compression strength at 25% deflection decreased 9.6%, 13%, and 65% for the control, vacuum irradiated [5.0×10^{9} ergs/gm(C)], and air irradiated [5.0×10^{9} ergs/gm(C)] samples, respectively. The ultimate compression strength values showed the same trend: a decrease of 4.2%, 9%, and 64%, for the control, vacuum irradiated, and air irradiated samples, respectively. Both the vacuum and vacuum irradiation had a small softening effect, while the air irradiation had a hardening effect on the material.

DC 7-170 (Dow Corning)

A summary of the results of the tests performed on samples of vacuum irradiated DC 7-170 (silicone) is given in Table 5.1. After a dose of 9.0×10^9 ergs/gm(C), the tensile strength increased 144% while the elongation decreased 83.5%.

Newell (Ref. 13) reports the changes in DC 7-170 mechanical properties after an air irradiation of 1×10^{10} ergs/gm(C). These data show a decrease of only 45% in elongation and an increase of 38% in tensile strength. A comparison of the vacuum- and air-irradiation data shows that the mechanical properties were more severely affected by the vacuum-irradiation environment than by the air-irradiation environment.

Marlex 6002 (Philips Petroleum)

Samples of Marlex (polyester) were irradiated in the vacuum chamber to 1.0×10^{10} ergs/gm(C). The resulting data presented in Table 5.1 show an increase of 37% in ultimate tensile strength and a decrease of 94.5% in ultimate elongation.

Harrison and Giberson (Ref. 12) report that Marlex rapidly deteriorated at low exposures in air and was extremely brittle and crumblyafter a dose of 5×10^9 ergs/gm(C). Exclusion of air helped considerably since the material was not brittle after being irradiated in a vacuum to 1×10^{10} ergs/gm(C). It lost most of its elongation under these conditions, but retained a substantial amount of its tensile strength. The data presented in Table 4.8 for Marlex 6002 show an increase in tensile strength and retention of 55% elongation after a 1.1×10^{10}-erg/gm(C) dose, indicating that these materials are benefitted by the exclusion of oxygen during irradiation.

Teflon

Although the radiation environments which produced the changes reported in Table 5.1 for Teflon TFE are different from the ones reported by DuPont for the same material (Ref. 18), they are close enough to warrant a comparison of the results. After an irradiation by a cobalt-60 source (gamma-ray emission of 1.3×10^6 rad/hr) in a vacuum of 1×10^{-6} torr for a total dose of 5.3×10^9 ergs/gm(C), the specimens tested by DuPont had an ultimate elongation of 38% and a tensile strength of 1,462 psi; after a gamma dose of 1.6×10^{10} ergs/gm(C), the specimens had an ultimate elongation of 16% and a tensile strength of 800 psi. DuPont's tests were conducted on 0.010-in.-thick film samples of Telon TFE, the same thickness as the NARF samples. However, the values for the NARF samples are much lower than those from DuPont; after a gamma dose of 1.7×10^9 ergs/gm(C), the ultimate elongation was 2.5% and the tensile strength was 1275 psi. The differences in environments between the two experimental setups are (1) the use of a nuclear-reactor radiation source versus a cobalt-60 source and (2) a higher pressure during the reactor radiation.

Teflon FEP irradiated at a factor-of-10 lower pressure (5×10^{-7} torr) to a dose of 8.6×10^9 ergs/gm(C) showed only $\sim$ 1% elongation. DuPont stated that the values for Teflon FEP should be higher than the reported values for Teflon TFE. The difference in values from the two test programs is larger than one would expect. Effort will be spent during the next year to resolve this difference.

5.3.1.2 Optical Property Test

The results of optical tests conducted on organic thermal-control coatings is given in Table 5.2. The materials were irradiated in the vacuum chamber and then shipped to General Dynamics/Astronautics in San Diego, California, for the optical property determinations. These data show that the acrylic black was the least affected by the combined environments. The silicone aluminim compound changed in both absorptivity and emissivity, which resulted in no net change of the α/ϵ ratio.

Table 5.2

Summary of Optical Changes for Thermal-Control Coatings
Irradiated in Vacuum and Tested in Air

Category	Material	Gamma Dose [ergs/gm(C)]	Vacuum (torr)	Percent Change in Solar Absorbance (α)	Percent Change in Emissivity (ϵ) at 300°K	Percent Change in α/ϵ at 300°K
Thermal-Control Coatings	Acrylic, Black	1.7×10^{10}	2×10^{-6}	0	+ 0.454	0
	Epoxy, White	1.7×10^{10}	2×10^{-6}	+ 27	+ 1.47	+ 0.794
	Silicone, White	1.7×10^{10}	2×10^{-6}	+ 6.44	- 2.03	+ 8.9
	Silicone, Aluminum	1.7×10^{10}	2×10^{-6}	+ 4.6	+ 5.04	0

5.3.2 Dynamic Tests

5.3.2.1 Mechanical Property Tests

The materials presented in Table 5.3 were irradiated statically and tested after irradiation with special dynamic testers while still in the vacuum chamber. For the adhesives and laminates, two tests were performed at different pressures: 3×10^{-1} and 5×10^{-6} torr. The average ultimate tensile strength for the specimens in these two classes showed a significant increasing trend from the "as received" control tests to the dynamic tests. The sole exception to this trend is the ultimate strength of the FM-1000 specimens in dynamic Run 1. It should be pointed out, however, that the standard deviation of the ultimate strength of the FM-1000 specimens in Run 1 is 720 psi, which overlaps the trend. In addition, the stress-strain curves for the irradiated glass-cloth laminates - with the exception of Specimen 1 of the static Conolon laminates - definitely show that the elastic moduli of the laminates increase as a result of the combined effects of the vacuum and nuclear radiation. The increased elastic moduli and progressive increase of ultimate tensile strengths apparently can be attributed to a greater rate of crosslinking of the polymer chain scission by oxygen during irradiation. At the lower partial pressures of oxygen in the higher vacuums, the rate of oxygen-terminated chain scission is decreased, and, consequently, the relative rate of radiation-induced crosslinking is increased, leading to increased stiffness and strength of the polymers.

Table 5.3

Summary of Property Changes for Materials
Irradiated and Tested in Vacuum

Category	Trade Name	Gamma Dose [ergs/gm(C)]	Vacuum (torr)	Specimen Configuration	Measured Property	Percent Change in Measured Property
Adhesive	FM-1000	1.1×10^{10}	3×10^{-1}	Lap shear, modified	Ult. shear strength	0
		1.9×10^{10}	5×10^{-6}	Lap shear, modified	Ult. shear strength	+ 21
	MB-302	1.6×10^{10}	3×10^{-1}	Lap shear, modified	Ult. shear strength	+ 15
		2.1×10^{10}	5×10^{-6}	Lap shear, modified	Ult. shear strength	+ 41.5
Structural Laminate	Conolon 506	1.3×10^{10}	3×10^{-1}	Tensile, modified (ASTM-D-638-58T)	Ult. tensile strength Ult. elongation	+ 29.6 + 50
		2.0×10^{10}	5×10^{-6}	Tensile, modified (ASTM-D-638-58T)	Ult. tensile strength	+ 55
	Epon 828/A	1.4×10^{10}	3×10^{-1}	Tensile, modified (ASTM-D-638-58T)	Ult. tensile strength Ult. elongation	+ 27 + 43
		2.0×10^{10}	5×10^{-6}	Tensile, modified (ASTM-D-638-58T)	Ult. tensile strength	+ 48
Seal	Viton B (PRP 19007)	9.0×10^{9}	3×10^{-7}	O-Rings	Ult. tensile strength Ult. elongation	+ 7 - 79
Potting Compound	RTV-60	8.6×10^{9}	3×10^{-7}	Compression disks	Compressive strength @ 0.02-in. deflection	+ 76
Thermal Insulation	Stafoam AA-402	8.9×10^{9}	3×10^{-7}	Compression disks	Compressive strength @ 25% deflection Ult. comp. strength Weight change	+ 30 + 22 - 2.0

The effects of oxygen can also be shown from the data for the air irradiation on Conolon 506. Samples from the same batch of material were irradiated in air during the cryogenic section of these tests (Ref. 1). These data show that for 1 x 10^{10} ergs/gm(C) the ultimate tensile strength decreased 3%, and for a higher dose of 6.7 x 10^{10} ergs/gm(C) the ultimate tensile strength decreased 6%. The vacuum-irradiation results presented in Table 5.3 for the 2 x 10^{10}-erg/gm(C) dose show an increase of 55% in the ultimate tensile strength.

Strain gages used for the elongation measurement of the structural laminates performed satisfactorily. These gages (AB-3-513) were manufactured by Baldwin-Lima-Hamilton Corporation. The only discernable change in the bakelite-backed gages from the combined environments was a reduction of the total strain to which the gage could be subjected before the backing and wire grid broke.

The glass-cloth laminate specimens used in the high force tensile test were highly uniform in mechanical properties, as attested to by the stress-strain curves. The stress-strain curves for specimens in a given run correspond closely and, consequently, the effect of the vacuum-irradiation can readily be determined. For example, the average elastic moduli of the Epon 828/A control, static, and dynamic Run 1 specimens were 2.80 $\pm$ 0.032 x 10^6 psi, 2.95 $\pm$ 0.028 x 10^6 psi, and 2.93 $\pm$ 0.022 x 10^6 psi, respectively, and the average elastic moduli of the Conolon control, static, and dynamic Run 1 specimens were 2.81 x 10^6 psi (one specimen), 2.96 $\pm$ 0.11 x 10^6 psi, and 2.94 $\pm$ 0.007 x 10^6 psi, respectively.

Thus, the vacuum-irradiation produced about a 5% increase in elastic modulus.

The ultimate tensile strengths for the specimens (including lap-shear specimens) irradiated in dynamic Run 1 and dynamic Run 2 increased at the higher doses and higher vacuums in the range of radiation exposure of the test.

5.3.2.2 Bearing Lubricant Test

Results of the bearing lubricant test, while not showing any clear-cut trends, do show that lubrication of small motors in a combined vacuum-irradiation environment will be a serious problem. In this test, the effects of vacuum irradiation on properties of lubricants packed in miniature ball-bearings were investigated. A summary of the results of this test is given in Table 5.4, where the two measurements most indicative of lubricity changes, coast-down time and no-load speed, are given for each lubricant.

The decreases in no-load speed and coast-down time given in the table were computed with respect to the control values obtained at the beginning of the test. All lubricants were irradiated for a total time of 35.3 hours and total radiation exposure of 7×10^9 ergs/gm(C) and 1.05×10^{15} neutrons/cm^2 ($E > 2.9$ Mev) while in a vacuum that averaged 2×10^{-6} torr. As shown by the data in Table 5.4, even the dry-film lubricants do not appear to provide completely satisfactory lubrication in the test environment. On the other hand, no particular lubricant tested can be definitely ruled out as completely unsatisfactory.

Of the two dry-film lubricants tested, Electrofilm 66C performed better, although at higher radiation exposure this situation might be reversed because of the damaging effect of radiation on the organic binder utilized in Electrofilm 66C. Both motors containing Alpha Molykote X-15 lubricant froze at a dose of approximately 2 x 10^9 ergs/gm(C) and suffered relatively large changes in no-load speed and coast-down time before this point.

Of the two silicone lubricants tested (GE Versilube F-50 oil and Shell ETR-H grease), the grease performed better. One of the motors lubricated with the Versilube F-50 failed to restart after a dose of 5 x 10^9 ergs/gm(C), a running time of 800 minutes, and a total time in vacuum of 35 hours. The second motor failed after a dose of 7 x 10^9 ergs/gm(C), a running time of 900 minutes, and a total time in vacuum of 60 hours. None of the motors containing Shell ETR-H grease or Electrofilm 66C failed to restart at any time during the test, although they exhibited large changes in coast-down time. In addition, the no-load speed of the Electrofilm 66C motors had decreased 6 to 7% by the end of the test. Thus, deterioration of these lubricants during the test is also evident.

5.4 Experiment Evaluation

The overall results of the tests are considered to be satisfactory, particularly in view of the new testing techniques tried for the first time. Improvement in these techniques will be made during the continuation of this program to eliminate most of the small difficulties encountered during the dynamic tests.

Table 5.4

Summary of Lubricant Changes of Small Servomotor Bearings During the Vacuum Irradiation Test (Pressure = 2 x 10^{-6} torr)

Category	Trade Name	Gamma Dose at Time of Change [ergs/gm(C)]	Lubricant Change Indicator	Percent Change from Original Value
Solid-film lubricant (inorganic binder)	Alpha Molykote X-15 (Sample 1)	1.32 x 10^9	Coast-down time[a]	- 50
		1.32 x 10^9	No-load speed	- 20
		2.20 x 10^9	Motor failed to restart	
	Alpha Molykote X-15 (Sample 2)	0[b]	Coast-down time	- 50
		1.60 x 10^9	No-load speed	- 20
		1.89 x 10^9	Motor failed to restart	
Solid-film lubricant (organic binder)	Electrofilm 66-C (Sample 1)	4.58 x 10^7	Coast-down time	- 50
		7.0 x 10^9	No-load speed	- 4.5
	Electrofilm 66-C (sample 2)	0	Coast-down time	- 50
		7.0 x 10^9	No-load speed	- 5.2

[a]Time required for the miniature servomotors to coast to a stop from 6000 rpm.
[b]Coast-down time decreased 50% during the preirradiation vacuum operation.

Table 5.4 (cont'd)

Category	Trade Name	Gamma Dose at Time of Change [ergs/gm(C)]	Lubricant Change Indicator	Percent Change from Original Value
Silicone lubricating oil	General Electric Versilube F-50 (Sample 1)	7.0×10^9	Coast-down time	- 50
		7.10×10^9	No-load speed	- 20
		7.0×10^9	Motor failed to restart	
	General Electric Versilube F-50 (Sample 2)	3.79×10^9	Coast-down time	- 50
		4.93×10^9	No-load speed	- 20
		5.12×10^9	Motor failed to restart	
Silicone lubricating grease	Shell ETR-H (Sample 1)	6.93×10^9	Coast-down time	- 50
		7.00×10^9	No-load speed	- 6.3
	Shell ETR-H (Sample 2)	7.00×10^9	Coast-down time	- 50
		7.00×10^9	No-load speed	- 7

Most of the organic materials tested in this experiment will be subjected to three different doses during the succeeding tests. This will be done for both air and vacuum to give a clearer picture of radiation damage as a function of dose.

APPENDIX A

EFFECTS OF GAMMA RADIATION ON THE PUMPING-SPEED CHARACTERISTICS OF DC-704 DIFFUSION-PUMP OIL

APPENDIX A

EFFECTS OF GAMMA RADIATION ON THE PUMPING-SPEED CHARACTERISTICS OF DC-704 DIFFUSION-PUMP OIL

A-1 Introductory Remarks

The design of a Vacuum-Irradiation Assembly for use with the GTR employs oil diffusion pumps to achieve a vacuum of less than 10^{-6} mm-Hg at gas loads extending above 3.0 micron-liters/second. Oil diffusion pumps were employed because of their low cost (as compared to equivalent ion pumps) and their more adaptable geometry. In operation in the GTR environment, these pumps are shielded from the direct reactor flux by a shield consisting of four inches of lead and six inches of water. However, the scattered exposed dose rate at the pump stack was calculated to be approximately 1.75×10^6 ergs/gm(C)-Mw-hr in a preliminary analysis made by the NARF Shielding Group (Ref. 20). These calculations are substantiated by data developed during the first run with the vacuum units, when gamma dose rates of from 1.75×10^6 to 6.13×10^6 ergs/gm(C)-Mw-hr were measured with trichloroethylene dosimeters mounted in the vicinity of the diffusion pumps.

Irradiation programs requiring continuous exposures extending to 300 Mw-hr called for further information of the effects of radiation on the pumping-speed characteristics of the diffusion-pump oils, because of the general tendency of materials to alter their physical and chemical properties in a radiation environment.

Preceding page blank

The only data available on this topic was a Dow Corning brochure on DC-704 fluids, which indicated a change in ultimate pressure of from 2 to 3 x 10^{-6} mm-Hg. However, since this pressure was obtained with a single-stage glass diffusion pump after being subjected to a Co^{60} gamma dose of approximately 1.46 x 10^{10} ergs/gm(C) (Ref. 21), these results were not applicable to the problem under consideration.

Since Consolidated Vacuum Corporation received the contract to build the vacuum assemblies and since it is also the fabricator of the pumping units, Frank M. Jenner, president of the corporation, was approached about performing pumping-speed experiments on DC-704 samples irradiated to appropriate doses with the GD/FW Co^{60} unit to qualify the fluids for use in the GTR environment. Mr. Jenner graciously agreed to provide this service, and the data presented in the following text is the result of a cooperative effort between GD/FW and CVC.

A-2 Experimental Procedure and Results

A true analog of the vacuum assemblies used in the GTR environment would require that the diffusion-pump oils be subjected to the same thermal and vacuum experience as that associated with these units during actual operation. Since it was not feasible to construct such an analog for use with the GD/FW Co^{60} Irradiator, it was decided as a first approximation to subject irradiated samples to postirradiation dynamic testing.

The effect of radiation on the oil should, qualitatively at least, include the production of (1) low-molecular-weight volatives via chain scission, with vapor pressures higher than that characteristic of the parent fluid, and (2) higher-molecular-weight species through crosslinking. The former will be pumped as ordinary gases and removed from the system. The latter could conceivable affect the pumping speed, since these species will effectively decrease the intensity of the molecular beam at the nozzle outlets and increase the molecular weight of the vapor. The collision probability of a vapor molecule, and hence the pumping speed, should qualitatively be proportional to the square root of the molecular weight of the vapor molecule and to the intensity of the vapor stream. This suggests that the pumping speed of a fluid, rather than the so-called ultimate pressure, should be examined in a particular pumping assembly.

A-2.1 Irradiation Procedure and Results

Four samples, approximately 500 cc each and taken from the same batch of DC-704, were tested. One was used as a control and three were irradiated to nominal exposed doses of 10^8, 10^9, and 10^{10} ergs/gm(C) in the GD/FW Co^{60} Irradiator. Each sample to be irradiated was placed in a 3-in.-OD x 5-in.-long stainless-steel container fitted with a silver-soldered brass bottom plate and a top shoulder with gasket groove. A lead gasket was used for sealing. A top plate was then attached to the container with Allen screws and fitted with a coiled 1/4-in.-OD copper tube attached to an exhaust line to permit the gases liberated by the fluid to be exhausted by a Welch Duo-Seal 1402B vacuum pump

during irradiation. A CO_2-acetone trap was placed between the sample container and the vacuum pump to prevent contamination of the sample by backstreaming fore-pump oil.

Upon completion of each sample irradiation, dry nitrogen was bled into the sample container, the copper tube was crimp-sealed, and the samples were shipped to Consolidated Vacuum Corporation, Rochester, New York.

The dosimetry consisted for four trichloroethylene dosimeters attached to the sample container. A sketch of the sample container and dosimeter arrangement is given in Figure A-1. The temperature of the sample was not monitored during irradiation, but previous experience suggests a temperature of 28-35°C. For these irradiation runs, the centerline of the source rods in the Co^{60} Irradiator were on a 4.0-in. circle, but the center of the sample volume was displaced inadvertently approximately two inches vertically down from the center of the source-rod configuration. This conclusion is based upon the results of the trichloroethylene dosimeters (Table A-1). Ordinarily, the dosimetry can be more rigorously defined from the description of the geometry of the irradiator.

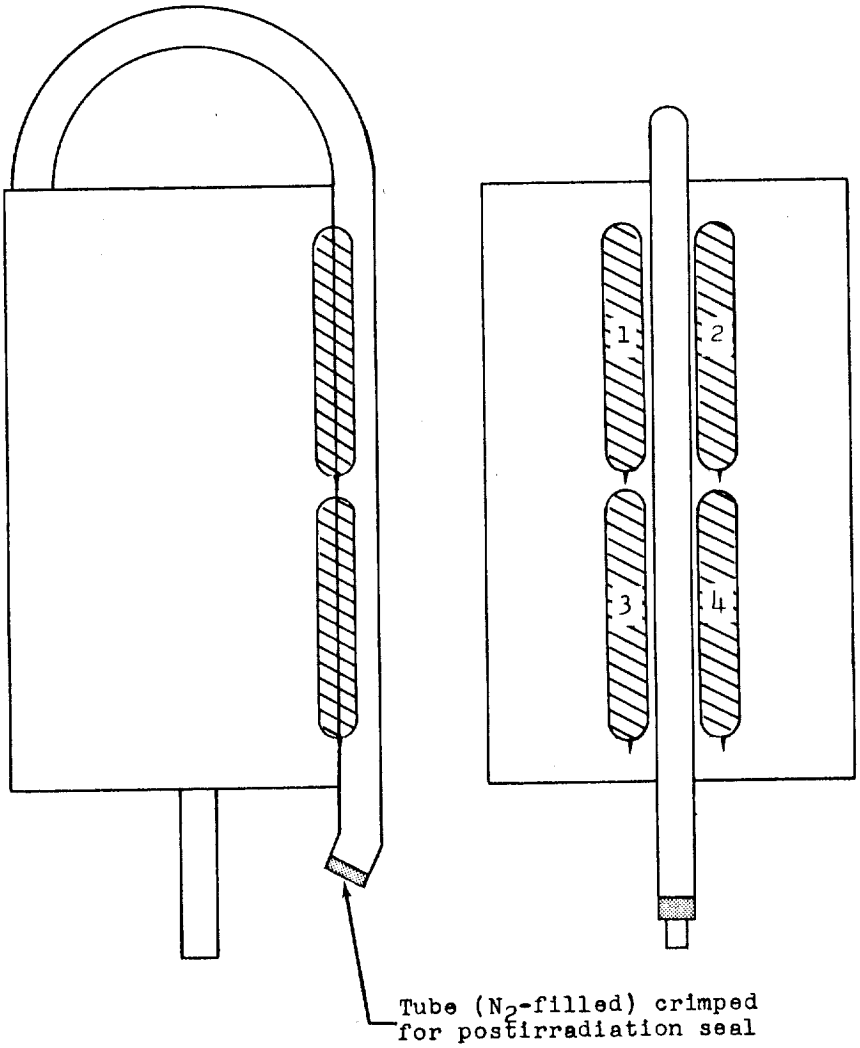

Figure A-1 Views of Sample Holder with Dosimetry Packets: Co^{60} Irradiation; T≅30°C

Table A-1

Dosimetry Data for DC-704 Irradiation

Dose Designation	Gamma Dose [ergs/gm(C)]			
	Position No. 1	Position No. 2	Position No. 3	Position No. 4
A	8.77 (8)	8.77 (8)	2.19(7)	2.28(7)
B	1.40 (9)	1.40 (9)	5.35(8)	4.47(8)
C	1.40(10)	1.49(10)	6.23(9)	5.87(9)

A-2.2 Pumping-Speed Evaluation

The quantity of oil in a given irradiated sample was chosen to maximize the utilization of the Co^{60} unit and to supply a sufficient amount for the CVC PMC-720 diffusion pump series, which is the second smaller size below the PMC-4100 employed by GD/FW. The operational characteristics and parameters are similar, with the exception of geometry and speed.

A preliminary evaluation of small samples of Doses A [$\sim 10^8$ ergs/gm(C)], B [$\sim 10^9$ ergs/gm(C)], and C [$\sim 10^{10}$ ergs/gm(C)] of the irradiated DC-704 in a G4 glass pump indicated little or no deterioration of the pump fluid as might be reflected in the ultimate pressure of a non-fractionating single-stage glass pump. It was, therefore, elected to eliminate Dose A from the speed-measurement program.

The speed measurements made with Dose B and Dose C samples in the PMC-720 are shown in Figure A-2 relative to the control test made with a sample of unradiated DC-704 from the same manufacturing lot.

The measured speed plateau with a Bayard Alpert ion gage was about 800 liters per second in test runs made on two different days. The system pumped at least 24 hours before any measurements were made. A McLeod gage used for a separate test on the Dose C sample indicated a plateau speed of 750 liters per second in the 10^{-5}- to 10^{-4}-torr range.

In CVC's normal procedure, a McLeod gage is used to determine the speed plateau in this range, with the ion gage being calibrated against the McLeod on the pump test dome. The ion gage is then assumed to be linear in response down to gage readings approaching the x-ray limit of the gage tube (2×10^{-10} torr).

With the irradiated Dc-704 tests, it was not desirable to risk contaminating the test setup with mercury vapor from the McLeod gage, because of the need to make careful measurements in the 10^{-8} to 10^{-6} torr range. Therefore, the McLeod gage was not installed until later. The apparent discrepancy between the two types of gages is thus the result of having to accept the calibration of the ion tube from an "oil free" system for use on a system where the change in sensitivity due to the pump-fluid vapors in the test dome could not immediately be taken into account.

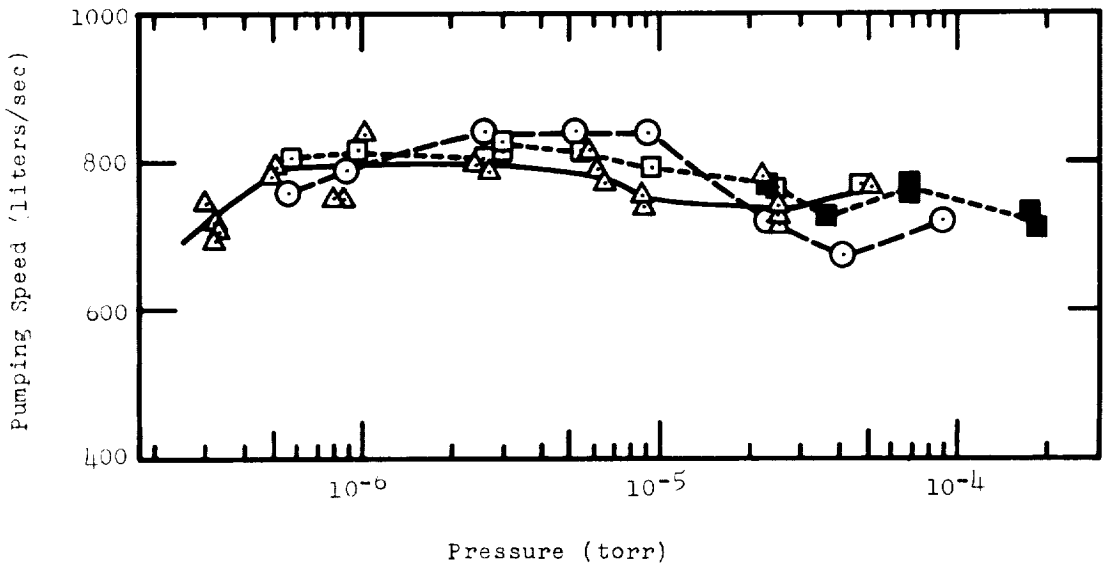

Figure A-2 Effects of Co^{60} Irradiation on the Air Pumping Speed of DC-704 in the CVC PMC-720 Pump

The range variation in the ultimate pressures at each dose was relatively small except in one case (Dose B), where an abnormally high room temperature was noted. The variations are as follows:

Control oil	6.6×10^{-8} torr
Dose B oil	$8.0 \times 10^{-8} - 1.6 \times 10^{-7}$ torr
Dose C oil	$8.0 \times 10^{-8} - 8.8 \times 10^{-8}$ torr

One cannot, at this time, place any great significance in the variation or in the fact that ultimate pressure did not reach as low a value as that shown in the CVC catalog.

The oils appeared to have experienced some discoloration as a result of the irradiation. Compared to the water-white color of the unirradiated fluid, the samples irradiated to Dose A [$\sim 10^{8}$ ergs/gm(C)], Dose B [$\sim 10^{9}$ ergs/gm(C)], and Dose C [$\sim 10^{10}$ ergs/gm(C)] were, within the limitations of observation, light amber, amber, and dark amber, respectively. This discoloration is mentioned because, after about 108 megawatt-hours of reactor irradiation, it was noted that the DC-704 removed from the vacuum-irradiation chambers showed only a faint discoloration when compared to the control fluid. This observation tends to confirm what one would anticipate from the amount of scattered radiation measured at the pump location (see Section A-1).

A-3 Conclusions

Within the limitations set by the compromise inherent in the analog chosen for these studies, one may draw the following conclusions:

1. DC-704 diffusion pump oil may be expected to perform satisfactorily without any detectable depreciation of pumping-speed characteristics when subjected to an exposed radiation dose of at least 10^{10} ergs/gm(C).

2. On the basis of information available regarding the scattered-radiation level in the GTR facility and the color appearance of the DC-704 after 108 megawatt-hours of radiation exposure, it is anticipated that the fluids should exhibit a useful radiation life in excess of 800 megawatt-hours exposure.

APPENDIX B

EFFECTS OF REDUCED PRESSURE ON MATERIALS AT VARIOUS TEMPERATURES

APPENDIX B

EFFECTS OF REDUCED PRESSURE ON MATERIALS AT VARIOUS TEMPERATURES

The George C. Marshall Space Flight Center has recently conducted tests to determine the effects of reduced pressure on materials at various temperatures. The results of tests performed on coupons from the same batch of material as tested during the vacuum-irradiation tests are presented in Tables B-1 through B-9.

The effects of reduced pressure on materials at various temperatures was determined by the General Chemistry Section, Engineering Materials Branch, Structures and Mechanics Division, of the George C. Marshall Space Flight Center, Huntsville, Alabama. The procedures followed for weight-loss and tensile-strength tests during the vacuum-temperature tests were similar to the procedures described in NASA Report No. ARPA Order 92-59 Compatibility of Engineering Materials with Space Environment by Riehl, Looney, and Caruso.

The data presented here, along with data generated on other materials, will be published by NASA.

Preceding page blank

Table B-2

Effect of Vacuum and Elevated Temperatures on Metlbond 406-1
(Data from George C. Marshall Space Flight Center)

Sample Code	Bond Dimensions (in.)			Surface Area ($in.^2$)	Tensile Data		Sample Treatment Data
	Thickness	Length	Width		Break Load (lb)	Shear (psi)	
MR-1	0.138	0.50	0.995	0.4975	2550	5126	Control samples submitted by Rubber Section
MR-2	0.138	0.50	1.000	0.5000	2780	5560	
MR-3	0.138	0.50	0.980	0.4900	2520	5143	
MR-4	0.138	0.50	1.000	0.5000	2540	5080	
MR-5	0.138	0.50	1.000	0.5000	2590	5180	
					Avg	5218	
A-1	0.138	0.50	0.990	0.4950	2820	5697	Control samples submitted by Vacuum Lab
A-2	0.138	0.50	1.000	0.5000	2730	5460	
A-3	0.138	0.50	1.000	0.5000	2965	5930	
A-4	0.138	0.50	1.000	0.5000	2645	5290	
A-5	0.138	0.50	1.000	0.5000	2930	5860	
					Avg	5647	
B-1	0.138	0.50	1.000	0.5000	2520	5040	Exposed 24 hours in vacuum at ambient temperature
B-2	0.138	0.50	0.990	0.4950	2620	5293	
B-3	0.138	0.50	0.980	0.4900	2615	5337	
B-4	0.138	0.50	0.985	0.4925	2740	5563	
B-5	0.138	0.50	1.000	0.5000	2860	5720	
					Avg	5391	
C-1	0.138	0.50	0.995	0.4975	3030	6090	Exposed 24 hours in vacuum at 200°C
C-2	0.138	0.50	0.995	0.4975	2800	5628	
C-3	0.138	0.50	0.985	0.4925	2940	5970	
C-4	0.138	0.50	0.980	0.4900	3260	6653	
C-5	0.138	0.50	0.985	0.4925	2840	5796	
					Avg	6027	
D-1	0.138	0.50	0.995	0.4575	2120	4634	Exposed 24 hours in oven at 200°C and atm pressure
D-2	0.138	0.50	0.985	0.4925	2380	4832	
D-3	0.138	0.50	0.995	0.4975	2395	4814	
D-4	0.138	0.50	0.985	0.4925	2120	4305	
D-5	0.138	0.50	0.995	0.4975	2160	4386	
					Avg	4594	

Preceding page blank

Table B-3

Effect of Vacuum and Elevated Temperatures on Epon VIII Adhesive Bond
(Data from George C. Marshall Space Flight Center)

Sample Code	Bond Dimensions (in.)			Surface Area ($in.^2$)	Tensile Data		Sample Treatment Data
	Thickness	Length	Width		Break Load (lb)	Shear (psi)	
MR-1	0.143	0.50	0.985	0.493	1440	2920	Control samples submitted by M-P&VE-MR
MR-2	0.143	0.50	0.990	0.495	1470	2969	
MR-3	0.143	0.50	0.955	0.478	1380	2887	
MR-4	0.143	0.50	0.940	0.470	1340	2851	
MR-5	0.143	0.50	0.970	0.485	1340	2762	
					Avg	2878	
A-1	0.140	0.50	0.950	0.475	1120	2357	Control samples submitted by Vacuum Lab
A-2	0.140	0.50	0.985	0.493	1350	2738	
A-3	0.140	0.50	1.045	0.522	1350	2586	
A-4	0.140	0.50	0.975	0.487	1270	2608	
A-5	0.140	0.50	0.970	0.485	1200	2474	
					Avg	2552	
B-1	0.140	0.50	1.000	0.500	1380	2760	Exposed 24 hours in vacuum at 26°C
B-2	0.140	0.50	1.000	0.500	1260	2520	
B-3	0.140	0.50	1.000	0.500	1580	3160	
B-4	0.140	0.50	0.990	0.495	1235	2494	
B-5	0.140	0.50	0.990	0.495	1240	2505	
					Avg	2688	
C-1	0.140	0.50	0.980	0.490	1200	2448	Exposed 24 hours in vacuum at 200°C
C-2	0.140	0.50	0.995	0.498	1405	2821	
C-3	0.140	0.50	0.945	0.473	1195	2526	
C-4	0.140	0.50	1.005	0.502	1433	2848	
C-5	0.140	0.50	0.995	0.498	1235	2479	
					Avg	2624	
A-1	0.140	0.50	0.955	0.4775	1145	2398	Control samples
A-2	0.140	0.50	0.980	0.4900	1000	2041	
A-3	0.140	0.50	1.000	0.5000	895	1790	
A-4	0.140	0.50	1.010	0.5050	1170	2317	
A-5	0.140	0.50	0.990	0.4950	1360	2747	
					Avg	2259	
B-1	0.140	0.50	1.010	0.5050	900	1782	Exposed 24 hours in oven at 200°C and atmospheric pressure
B-2	0.140	0.50	0.975	0.4875	660	1354	
B-3	0.140	0.50	0.990	0.4950	800	1616	
B-4	0.140	0.50	1.005	0.5025	800	1592	
B-5	0.140	0.50	1.015	0.5075	980	1931	
					Avg	1655	

Table B-4

Effect of Vacuum and High Temperature on FM-1000 Adhesive Film
(Data from George C. Marshall Space Flight Center)

Sample Code	Bond Dimensions (in.)			Surface Area ($in.^2$)	Tensile Data		Sample Treatment Data
	Thickness	Length	Width		Break Load (lb)	Shear (psi)	
MR-1	0.133	0.470	1.00	0.470	2955	6290	Control samples submitted by -MR
MR-2	0.134	0.510	1.005	0.508	3000	5900	
MR-3	0.134	0.495	0.980	0.485	2870	5920	
MR-4	0.133	0.495	1.00	0.495	2905	5880	
MR-5	0.134	0.520	0.995	0.517	3150	6100	
					Avg	6018	
A-1	0.133	0.50	0.995	0.497	2440	6922	Control samples submitted by Vacuum Lab
A-2	0.133	0.50	1.005	0.502	3390	6753	
A-3	0.133	0.50	0.995	0.497	3385	6811	
A-4	0.133	0.50	1.005	0.502	3220	6414	
A-5	0.133	0.50	1.000	0.500	3270	6540	
					Avg	6688	
B-1	0.133	0.50	0.990	0.495	3580	7232	Exposed 24 hours in vacuum at ambient temperature
B-2	0.133	0.50	1.005	0.502	2580	7131	
B-3	0.133	0.50	0.985	0.492	3430	6972	
B-4	0.133	0.50	1.010	0.505	3540	7010	
B-5	0.133	0.50	0.995	0.497	3525	7093	
					Avg	7088	
C-1	0.133	0.50	0.985	0.492	2780	7683	Exposed 24 hours in vacuum at 200°C
C-2	0.133	0.50	1.005	0.502	4360	8685	
C-3	0.133	0.50	1.005	0.502	3860	7689	
C-4	0.133	0.50	0.985	0.492	4280	8699	
C-5	0.133	0.50	0.995	0.497	3670	7384	
					Avg	8028	
A-1	0.134	0.50	0.995	0.4975	3085	6201	Control samples
A-2	0.134	0.50	0.990	0.4950	3120	6303	
A-3	0.134	0.50	0.990	0.4950	3180	6426	
A-4	0.134	0.50	1.005	0.5025	3195	6358	
A-5	0.134	0.50	0.980	0.4900	2950	6020	
					Avg	6261	
B-1	0.134	0.50	1.010	0.5050	3470	6871	Exposed 24 hours in oven at 200°C and atm pressure
B-2	0.134	0.50	1.000	0.5000	2490	6980	
B-3	0.134	0.50	0.995	0.4975	3480	6995	
B-4	0.134	0.50	1.000	0.5000	3430	6860	
B-5	0.134	0.50	0.985	0.4925	3540	7188	
					Avg	6979	

Table B-5

Effect of Vacuum and Elevated Temperatures on Epon 422J
(Data from George C. Marshall Space Flight Center)

Sample Code	Bond Dimensions (in.)			Surface Area ($in.^2$)	Tensile Data		Sample Treatment Data
	Thickness	Length	Width		Break Load (lb)	Shear (psi)	
A-1	0.142	0.50	0.995	0.4975	1160	2332	Control samples
A-2	0.142	0.50	0.990	0.4950	1050	2121	
A-3	0.142	0.50	1.000	0.5000	1020	2040	
A-4	0.142	0.50	0.995	0.4975	1130	2260	
A-5	0.142	0.50	1.000	0.5000	1120	2240	
					Avg	2199	
B-1	0.142	0.50	0.990	0.4950	710	1434	Exposed 24 hours
B-2	0.142	0.50	1.000	0.5000	695	1390	in oven at 200°C
B-3	0.142	0.50	1.000	0.5000	900	1800	and atm pressure
B-4	0.142	0.50	1.000	0.5000	895	1790	
B-5	0.142	0.50	1.000	0.5000	760	1520	
					Avg	1587	

Table B-6

Effect of Vacuum and Elevated Temperatures on FM-47 Adhesive Bond
(Data from George C. Marshall Space Flight Center)

Sample Code	Bond Dimensions (in.)			Surface Area ($in.^2$)	Tensile Data		Sample Treatment Data
	Thickness	Length	Width		Break Load (lb)	Shear (psi)	
MR-1	0.138	0.50	1.015	0.507	2350	4635	Control samples submitted by M-P&VE-MR
MR-2	0.138	0.50	0.963	0.482	1940	4024	
MR-3	0.138	0.50	-	-	-	-	
MR-4	0.138	0.50	1.025	0.513	1940	3781	
MR-5	0.138	0.50	1.025	0.513	2305	4493	
					Avg	4232	
A-1	0.141	0.50	1.020	0.506	1995	3942	Control samples submitted by Vacuum Lab
A-2	0.141	0.50	1.025	0.513	2070	4035	
A-3	0.141	0.50	1.020	0.510	2175	4264	
A-4	0.141	0.50	1.020	0.510	2130	4176	
A-5	0.141	0.50	0.125	0.513	2285	4454	
					Avg	4174	
B-1	0.139	0.50	1.025	0.513	2275	4434	Exposed 24 hours in vacuum at 26°C
B-2	0.139	0.50	1.040	0.520	1980	3807	
B-3	0.139	0.50	1.030	0.515	2045	3970	
B-4	0.139	0.50	1.020	0.510	2300	4509	
B-5	0.139	0.50	1.025	0.513	2255	4395	
					Avg	4222	
C-1	0.141	0.50	1.020	0.510	2270	4450	Exposed 24 hours in vacuum at 200°C
C-2	0.141	0.50	1.020	0.510	1880	3686	
C-3	0.141	0.50	1.040	0.520	2380	4576	
C-4	0.141	0.50	1.020	0.510	2530	4960	
C-5	0.141	0.50	1.020	0.510	2230	4372	
					Avg	4408	
A-1	0.143	0.50	1.010	0.5050	2375	6696	Control samples
A-2	0.143	0.50	0.960	0.4800	1940	4041	
A-3	0.143	0.50	1.025	0.5125	2240	4435	
A-4	0.143	0.50	1.010	0.5050	2045	4051	
A-5	0.143	0.50	1.010	0.5050	1880	3724	
					Avg	4589	
B-1	0.143	0.50	1.020	0.5100	1700	3333	Exposed 24 hours in oven at 200°C and atm pressure
B-2	0.143	0.50	0.950	0.4750	1470	3094	
B-3	0.143	0.50	1.020	0.5100	1680	3296	
B-4	0.143	0.50	1.015	0.5075	1480	2916	
B-5	0.143	0.50	1.015	0.5075	1470	2898	
					Avg	3107	

Table B-7

Effect of Vacuum and Elevated Temperatures on Metlbond 302A
(Data from George C. Marshall Space Flight Center)

Sample Code	Bond Dimensions (in.)			Surface Area ($in.^2$)	Tensile Data		Sample Treatment Data
	Thickness	Length	Width		Break Load (lb)	Shear (psi)	
MR-1	0.138	0.50	0.940	0.470	1160	2468	Control samples
MR-2	0.138	0.50	0.995	0.498	1350	2710	submitted by
MR-3	0.138	0.50	0.945	0.473	1220	2579	M-P&VE-MR
MR-4	0.138	0.50	0.965	0.483	1190	2463	
MR-5	0.138	0.50	0.995	0.498	1200	2410	
					Avg	2526	
A-1	0.139	0.50	0.930	0.465	1195	2570	Control samples
A-2	0.139	0.50	0.967	0.485	1330	2742	submitted by
A-3	0.139	0.50	1.018	0.509	1365	2681	Vacuum Lab
A-4	0.139	0.50	1.020	0.510	1340	2627	
A-5	0.139	0.50	1.021	0.511	1380	2700	
					Avg	2670	
B-1	0.149	0.50	0.910	0.455	1325	2912	Exposed 24 hours
B-2	0.149	0.50	0.960	0.480	1265	2635	in vacuum at
B-3	0.149	0.50	0.956	0.478	1320	2761	26°C
B-4	0.149	0.50	0.976	0.488	1130	2315	
B-5	0.149	0.50	1.010	0.505	1400	2772	
					Avg	2680	
C-1	0.143	0.50	0.938	0.469	1185	2526	Exposed 24 hours
C-2	0.143	0.50	0.987	0.494	1290	2611	in vacuum at
C-3	0.143	0.50	0.984	0.492	1345	2733	200°C
C-4	0.143	0.50	1.031	0.516	1495	2897	
C-5	0.143	0.50	0.933	0.466	1240	2660	
					Avg	2686	
A-1	0.138	0.50	0.940	0.4700	1040	2213	Control samples
A-2	0.138	0.50	0.940	0.4700	1030	2189	
A-3	0.138	0.50	0.960	0.4800	1110	2313	
A-4	0.138	0.50	0.990	0.4950	1120	2263	
A-5	0.138	0.50	0.990	0.4950	1105	2232	
					Avg	2242	
B-1	0.138	0.50	0.915	0.4575	960	2098	Exposed 24 hours
B-2	0.138	0.50	0.925	0.4625	930	2011	in oven at 200°C
B-3	0.138	0.50	0.970	0.4850	920	1897	and atm pressure
B-4	0.138	0.50	0.970	0.4850	980	2021	
B-5	0.138	0.50	0.940	0.4700	860	1830	
					Avg	1971	

Table B-8

Effect of Vacuum and Elevated Temperatures on AF-6 Adhesive
(Data from George C. Marshall Space Flight Center)

Sample Code	Bond Dimensions (in.)			Surface Area ($in.^2$)	Tensile Data		Sample Treatment Data
	Thickness	Length	Width		Break Load (lb)	Shear (psi)	
MR-1	0.136	0.515	1.00	0.515	855	-	Control samples submitted by Rubber Lab
MR-2	0.136	0.510	0.992	0.506	1410	2790	
MR-3	0.136	0.510	0.997	0.507	1360	2690	
MR-4	0.136	0.520	0.984	0.511	1225	2400	
MR-5	0.136	0.520	0.980	0.510	1345	2640	
					Avg	2630	
MG-1	0.136	0.520	0.990	0.514	1170	2276	Control samples submitted by Vacuum Lab
MG-2	0.136	0.525	0.987	0.510	1425	2751	
MG-3	0.136	0.505	1.00	0.505	1495	2960	
MG-4	0.136	0.510	0.995	0.507	1152	2272	
MG-5	0.136	0.515	0.990	0.510	1515	2971	
					Avg	2646	
A-1	0.136	0.500	1.05	0.525	1020	1942	Exposed 24 hours in vacuum at ambient temperature
A-2	0.136	0.505	1.00	0.505	1700	3366	
A-3	0.136	0.525	0.960	0.504	932	2301	
A-4	0.136	0.520	0.997	0.518	1475	2874	
A-5	0.136	0.510	0.992	0.506	990	1956	
					Avg	2488	
B-1	0.136	0.510	0.970	0.495	1500	3030	Exposed 24 hours in vacuum at 100°C
B-2	0.136	0.512	0.995	0.509	1055	2073	
B-3	0.136	0.510	1.00	0.510	1555	3049	
B-4	0.136	0.530	0.985	0.522	1352	2590	
B-5	0.136	0.500	0.987	0.494	1102	2231	
					Avg	2594	
C-1	0.135	0.505	0.960	0.485	2190	4515	Exposed 24 hours in vacuum at 200°C
C-2	0.135	0.480	0.990	0.475	2200	4631	
C-3	0.135	0.485	1.005	0.487	2220	4559	
C-4	0.135	0.490	1.005	0.492	2260	4593	
C-5	0.135	0.500	0.990	0.495	1760	3556	
					Avg	4371	
D-1	0.135	0.510	0.995	0.507	1580	3116	Control samples not treated
D-2	0.135	0.525	0.985	0.517	1160	2244	
D-3	0.135	0.510	0.995	0.507	1610	3176	
D-4	0.135	0.525	0.990	0.520	1520	2923	
D-5	0.135	0.540	0.975	0.527	1414	2685	
					Avg	2829	

Table B-9

Effect of Vacuum and Elevated Temperatures on Metlbond 408
(Data from George C. Marshall Space Flight Center)

Sample Code	Bond Dimensions (in.)			Surface Area ($in.^2$)	Tensile Data		Sample Treatment Data
	Thickness	Length	Width		Break Load (lb)	Shear (psi)	
A-1	0.138	0.50	1.000	0.5000	2730	5460	Control samples
A-2	0.138	0.50	1.000	0.5000	2610	5220	
A-3	0.138	0.50	1.000	0.5000	2720	5440	
A-4	0.138	0.50	1.005	0.5025	2640	5254	
A-5	0.138	0.50	1.000	0.5000	2490	4980	
					Avg	5271	
B-1	0.138	0.50	1.000	0.5000	2580	5160	Exposed 24 hours in oven at 200°C and atm pressure
B-2	0.138	0.50	0.995	0.4975	2420	4864	
B-3	0.138	0.50	1.000	0.5000	2740	5480	
B-4	0.138	0.50	0.995	0.4975	2620	5266	
B-5	0.138	0.50	1.000	0.5000	2460	4920	
					Avg	5138	

APPENDIX C

DESCRIPTION OF MATERIALS IRRADIATED IN A VACUUM

Table C-1

Materials Used in Structural-Adhesive Tests

Trade Name and Manufacturer	Material Description and Preparation
Scotchweld AF-6 (nitrile phenolic) Minnesota Mining & Manufacturing Co.	Samples were prepared and supplied by NASA. Sample preparation was as follows: No primer was used. The samples were rinsed and air-dried, and the adhesive was applied as a $\frac{1}{2}$" bond width. The samples were cured in a modified Carvar Press, removed at once, cooled, and cut to 1" wide test specimens on a band saw. About 3/8" was cut from each sample width and discarded. The excess adhesive was removed from all bond edges and the bond area was measured to $\pm$.005" for each test specimen. All test specimens were selected at random for each test. Cure Data Time: 1 hour Temperature: 350°F Pressure: 125 psi
Epon VIII (epoxy base) Shell Chemical Company	Samples were prepared and supplied by NASA. Samples were prepared as follows: No primer was used. The test pieces were rinsed and air-dried, and the adhesive was applied as a $\frac{1}{2}$" bond width. The samples were cured in a hot-air oven. The adhesive mixture was 100 parts of Epon VIII mixed with 6 parts of Shell Chemical activator "A". All samples were prepared from

Note: Prior to bonding, the base metal for all of the structural adhesives listed in Table C-1 were cleaned as follows: 4" x 6" x 1/8" aluminum sheets (2024-T3) were degreased by wiping with toluene and soaking in warm water containing Alconox detergent. After thorough rinsing and air drying, the bond areas were cleaned by a solution containing the following:

330 g sodium dichromate ($2H_2O$)
2740 ml distilled water
525 ml 95% sulphuric acid

This solution was kept at 150-160°F for 20 minutes.

Preceding page blank

Table C-1 (cont'd)

Trade Name and Manufacturer	Material Description and Preparation
Epon VIII (cont'd)	one batch of the adhesive and were cured at the same time. After cooling, a 3/8" strip was removed before cutting to 1" wide test specimens. The excess adhesive was removed from the bond edges before testing. Cure Data Time: 1½ hours Temperature: 200° F (hot-air oven) Pressure: contact
Metlbond 302A (epoxy phenolic) Narmco Materials Division	Samples were prepared and supplied by NASA. Sample preparation was as follows: No primer was used. The samples were rinsed and air-dried, and the adhesive was applied as a 1/2" bond width. The samples were cured in a modified Carvar Press, removed at once, cooled, and cut to 1" wide test specimens on a band saw. About 3/8" was cut from each sample width and discarded. The excess adhesive was removed from all bond edges and the bond area was measured to ± .005" for each test specimen. Cure Data Time: 1 hour Temperature: 350° F Pressure: 25 psi
Bloomingdale FM-47 film (vinyl phenolic) Bloomingdale Rubber Company	Samples were prepared and supplied by NASA. Sample preparation was as follows: Primer was liquid FM-47. The test pieces were rinsed and air-dried. The bond area of all pieces was coated with liquid FM-47 applied with a brush. This coat was air-dried a minimum of two hours. A strip of the FM-47 film was applied to one side of the test sample and placed in a hot air oven at 105° C for 1 hour. This piece was used with a primed, air-dried half and was overlapped 1/2". The excess adhesive film was removed and sample was placed in a modified Carvar Press at about 5 psi for 5 minutes at 300° F. The pressure was released after about 30 seconds; then sample was cured for 1 hour. The sample was removed, a 3/8" strip was

Table C-1 (cont'd)

Trade Name and Manufacturer	Material Description and Preparation
Bloomingdale FM-47 film (cont'd)	cut from the side and discarded. Sample was cut to 1" wide strips for test specimens. The excess adhesive was removed from all bond edges and the bond area was measured to ± .005". Cure Data Time: 1 hour Temperature: 325° F Pressure: 100 psi
FM-1000 Film (epoxy nylon) Bloomingdale Rubber Co.	Samples were supplied and prepared by NASA. Sample preparation was as follows: No primer was used. The samples were rinsed and air-dried, and the adhesive was applied as a 1/2" bond width. The samples were cured in a modified Carvar Press, removed at once, cooled and cut to 1" wide test specimens on a band saw. About 3/8" was cut from each sample width and discarded. The excess adhesive was removed from all bond edges and the bond area was measured to ± .005" for each test specimen. All test specimens were selected at random for each test. Cure Data Time: 1 hour Temperature: 350° F Pressure: 125 psi
Metlbond 406-1 (epoxy polyamide) Narmco Industries	Samples were prepared and supplied by NASA. Sample preparation was as follows: No primer was used. After cleaning, the pieces were thoroughly rinsed and dried, and the adhesive was applied as a 1/2" bond width. The samples were cured in a press for 1 hour at 350° F and 25 psi. After cooling, the samples were cut to 1" wide test specimens. Initial control results for shear tensile were made at room temperature on a Reihle machine set at 10,000 pounds at 0.1"/minute pull rate. The specimens used for the initial control results were random selections, five specimens, which had all excess adhesive removed from the bond edges. The bond areas were measured to ± .005".

Table C-1 (cont'd)

Trade Name and Manufacturer	Material Description and Preparation
Metlbond 406-1 (cont'd)	Cure Data Time: 1 hour Temperature: 350° F Pressure: 25 psi
Epon 422J (epoxy phenolic) Shell Chemical Corp.	Samples were supplied and prepared by NASA. Samples were prepared as follows: The test pieces were rinsed and air-dried. The bond area of all pieces was coated with liquid Epon 422J applied with a brush. This coat was air-dried a minimum of 2 hours. A strip of the Epon 422J film was applied to one side of the test material and placed in a hot oven at 105° C for 1 hour. This piece was used with a primed air-dried half and was placed in a modified Carvar Press at about 5 psi for 5 minutes at 300° F. The pressure was released for about 30 seconds; then the sample was cured for 1 hour. The sample was removed; a 3/8" strip was cut from the side and discarded. The sample was cut into 1" wide strips for test specimens. The excess adhesive was removed from all bond edges and the bond area was measured to ± .005". Cure Data Time: 35 minutes Temperature: 340° F Pressure: 100 psi
Metlbond 408 (modified vinyl epoxy nylon) Narmco Materials Division	Samples were supplied and prepared by NASA. Sample preparation was as follows: No primer was used. The test pieces were rinsed and air-dried. The bond area of all pieces was coated with liquid Metlbond 408, applied with a brush. This coat was air-dried a minimum of 2 hours. A strip of the Metlbond 408 was applied to one side of the test sample and placed in a hot air oven at 105° C for 1 hour. This piece was used with a primed air-dried half and was overlapped 1/2". The excess adhesive film was removed and sample was placed in a modified Carvar Press at about 5 psi for 5 minutes at 300° F. The pressure was released for about 30 seconds; then

Table C-1 (cont'd)

Trade Name and Manufacturer	Material Description and Preparation
Metlbond 408 (cont'd)	sample was cured for 1 hour. The sample was removed, a 3/8" strip was cut from the side and discarded. Sample was cut to 1" wide strips for test specimens. The excess adhesive was removed from all bond edges and the bond area was measured to ± .005". Cure Data Time: 1 hour Temperature: 350° F Pressure: 25 psi

Table C-2

Materials Used in Lubricant Tests*

Trade Name and Manufacturer	Type Lubricant, Method of Application to Bearings, and Motor Specifications
Alpha Molykote X-15 (molybdenum disulfide-graphite-sodium silicate) The Molykote Corp.	Type of lubricant: solid-film (inorganic binder). Bearings were cleaned and passivated according to Mil Spec S-5002. Lubricant was thinned with water and, while bearings were being rotated, sprayed on the bearing races with an air brush until a film 0.002 to 0.003 inches thick was formed. Then, the lubricant was air dried and cured at 190°C for 1 hour. Starting voltage of motors: Motor 1: As Assembled 8.0 volts; After 5-Minute Run 6.5 volts Motor 4: As Assembled 4.0 volts; After 5-Minute Run 3.0 volts End-play of bearings (8-oz reversing load): Motor 1: As Assembled .0025 inch Motor 4: As Assembled .0023 inch
Electrofilm 66C (assumed to be molybdenum disulfide plus additive. An epoxy resin is the binder.) Electrofilm, Inc.	Type of lubricant: solid-film (organic binder). Bearings were cleaned and lubricant was applied in exactly the same manner described for Molykote X-15, except that dioxane solvent was used to thin the lubricant for spraying. Starting voltage of motors: Motor 2: As Assembled 4 volts; After 5-Minute Run 2 volts Motor 3: As Assembled 4.5 volts; After 5-Minute Run 2.5 volts End-play of bearings (8-oz reversing load): Motor 2: As Assembled 0.0021 inch Motor 3: As Assembled 0.0017 inch

* Bearing lubrication and test reported here were performed by Miniature Precision Bearing, Inc.

Table C-2 (cont'd)

Trade Name and Manufacturer	Type Lubricant, Method of Application to Bearings, and Motor Specifications
G. E. Versilube F-50 (chlorophenyl-methyl polysiloxane) The General Electric Company	Type of lubricant: lubricating oil Bearings were cleaned and the lubricant applied to the bearings with a sterile hypodermic syringe so that Motor 7 had 6.3 milligrams in its front and 6.4 milligrams in its rear bearing, and Motor 8 had 7.5 milligrams in its front and 8.1 milligrams in its rear bearing. Starting voltage of motors: Motor 7: As Assembled < 0.5 volt; After 5-Minute Run < 0.5 volt Motor 8: As Assembled < 0.5 volt; After 5-Minute Run < 0.5 volt End-play of bearings (8-oz reversing load) Motor 7: As Assembled 0.002 inch Motor 8: As Assembled 0.002 inch
Shell ETR-H (G. E. Versilube F-50 silicone fluid plus Blue Indanthrene vat dye thickener) Shell Oil Company	Type of lubricant: lubricating grease. Bearings were cleaned and packed to certain percentage of void space such that Motor 5 had 20.7 milligrams in its front and 21.4 milligrams in its rear bearing, and Motor 6 had 24.8 milligrams in its front and 24.0 milligrams in its rear bearing. Starting voltage of motors: Motor 5: As Assembled 1.5 volts; After 5-Minute Run 1 volt Motor 6: As Assembled 4 volts; After 5-Minute Run 1.5 volts End-play of bearings (8-oz reversing load). Motor 5: As Assembled 0.0025 inch Motor 6: As Assembled 0.004 inch

Table C-3

Materials Used in Seal Tests

Trade Name and Manufacturer	Material Description and Preparation
Parker 66-581 (Buna-N) Parker-Hannfin Co.	A compound developed to seal Mil-O-7808 in accordance with FMS-0026A, which specifies a temperature service range of -65° F to +300° F.
Natural Rubber, RA 33860 George C. Marshall Space Flight Center, Rubber and Plastics Section	Recipe: Rubber — 100 parts by weight Zinc oxide — 5 SRF black — 70 Stearic acid — 1 Phenyl-beta-napththylamine — 1 Sulfur — 3 Captax — 0.6 Cure: 25 minutes at 292° F
Viton B, Precision 19007 Precision Rubber Products Corp.	Samples were in the shape of O-rings of uniform size No. 215 and compression-set buttons which were 0.5 in. thick with an O.D. of 1.129 in.

Table C-4

Materials Used in Thermal-Insulation Tests

Trade Name and Manufacturer	Material Description and Preparation
Refrasil Batt B-100 (inorganic soft batting) H. I. Thompson Co.	This material is a low-sodium-content SiO_2 fiberglass, which does not become highly activated when subjected to nuclear radiation.
Eccofoam Q (inorganic rigid foam) Emerson & Caming, Inc.	This is a ceramic-type foam insulation. Test specimens were cut from a 1.0-in.-thick sheet.
Urethane DS-620 (organic non-rigid foam) American Latex Products Corp.	This is a polyester resin urethane. Samples were 0.5 in. thick.
Stafoam AA-402 (organic rigid foam) American Latex Products Corp.	This material is a freon blown, polyether-based polyurethane foam. Test materials were obtained with a thickness of 0.5 in. The density of this material ranges from 1.5 lb to 2 lb per cu ft.
Styrofoam 22 (organic rigid foam) Dow Chemical Corp.	Sheets 0.5 in. thick with a density of 1.6-2.0 lb per cu ft were obtained from Kirkland-Weber, Inc. This is a polystyrene-based foam.

Table C-5

Materials Used in Structural-Laminate Tests

Trade Name and Manufacturer	Material Description and Preparation
Conolon 506 (phenolic) Narmco Materials Division	Samples were prepared in accordance to vendor recipe by NASA.
Mobiloy AH-81 Cordo Moulding Products	Samples were prepared in accordance to vendor recipe by NASA.
DC-2106 Silicone Dow Corning Corp.	The test material was prepared by the Eldon Fiberglas Co. in Compton, California, per the following specifications: 1. Reinforcement: 181 glass fabric, 12-ply thickness 2. Finish: 112 neutral ph 3. Resin: DC2106-Mfg. Midland, Ohio 4. Resin Content" 42% 5. Lot: C-4554-1 6. Catalyst: XY-15 7. Press Cure: 30 min at 350°F with line pressure of 4 tons 8. Post Cure: 16 hr at 195°F 2 hr at 260°F 2 hr at 300°F 2 hr at 350°F 2 hr at 390°F 2 hr at 435°F 12 hr at 480°F
CTL-91-LD (phenolic) Coast Mfg. Co.	Test material prepared by Eldon Fiberglas Co., in Compton, California, per the following specifications: 1. Resin: CTL-91-LD (high pressure) 2. Curing Agent: none 3. Reinforcement: 181 Volan A, twelve plies thick 4. Specification Requirements: Mil-R-9299 5. Batch No.: S7-1 6. Resin Manufacturer: Ironside Resins Inc., 270 West Mound St., Columbus 16, Ohio 7. Press Cure: 1/2 hr at 300° F and 1/2 hr at 325° F with 20 tons on Dake press which applies 150 psi on part.

Table C-5 (cont'd)

Trade Name and Manufacturer	Material Description and Preparation
CTL-91-LD (cont'd)	8. **Post Cure:** 1 hr at each of following temperatures: 200° F, 250° F, 300° F, and 2 hrs at 350° F 9. **Laminate Thickness:** 0.125"
Epon 828/A	The test material was prepared by the Shell Chemical Co., Plastics and Resins Division, Houston, Texas, per the following specifications: 1. Reinforcement: 181 glass fabric, glass fabric finish 2. Finish: Volan A 3. Resin: Epon 828 4. Resin Content: 30% by weight 5. Catalyst: Shell A 6. Press Cure: 30 min at 240°F at 25 psi

Table C-6

Materials Used in Electrical Insulation Tests

Trade Name and Manufacturer	Material Description and Preparation
Mylar A E. I. duPont de Nemoursand Co.	Type A is a general purpose and electrical film. It is a polyester-type material. Test samples were prepared from 1000-gage (10-mil) and 300-gage (3-mil) material.
Mylar C E. I. duPont de Nemours and Co.	Type C is a capacitor-grade film used in the capacitor industry. The samples were prepared from 100-gage material.
Kel-F-81, Amorphous (fluorocarbon) Minnesota Mining and Manufacturing Company	The test material was obtained from Tube Turn Plastic, Inc., in Garland, Texas, in the form of sheets which were 0.125 in. thick. This material possesses the following properties: 1. Temperature stability of -400° F to +400° F 2. Insensitive to LO4 3. Excellent abrasion resistance
Silastic 7-170 (silicone) Dow Corning Corp.	The test specimens were 0.075 in. thick. The composition of this material was designated as follows: Constituent — % (wt) silicone-dimethyl — 52.5 silicone dioxide — 48.0 mercuric oxide — 1.0

Table C-7

Material Used in Potting-Compound Tests

Trade Name and Manufacturer	Material Description and Preparation
Epon 828/Z (rigid organic) Shell Chemical Co.	Test specimens were prepared in accordance with ASTM D695-54, Section 5, and ASTM D785-51, Section 4. This potting compound is prepared with Type Z curing agent.
DC-R-7521 (rigid organic silicone) Dow Corning Corp.	The product was obtained from Dow Corning and the test specimens were prepared at GD/FW in accordance with ASTM D695-54, Section 5, and ASTM D785-51. This product is prepared with a solventless silicone resin and a zirconium ortho-silicate filler.
RTV-60 (non-rigid organic silicone resin) Castable General Electric Co.	Test specimens were prepared at GD/FW in accordance with ASTM D575-46, Section 4, and ASTM D676-58T, Section 3. The compound has a two-part room-temperature curing system. Available information on the specific batch for the test specimens included the following: Color: red Catalyst: 1% silicure L-24 Date: Use before 6-1-62 Lot No.: 458

Table C-8

Materials Used in Dielectric-Material Tests

Trade Name and Manufacturer	Material Description and Preparation
Polyamid H Film E. I. duPont de Nemours and Co.	This film has a unique blending of physical, electrical, and thermal properties. At this time it is not commercially available. Manufacturer's property data are presented in the following table:

Property	Temperature 25° C	Temperature 200° C
Tensile Strength (psi)	20,000	12,000
Tensile Modulus (psi)	400,000	250,000
Break Elongation (%)	70	70
Tear Strength (g/mil)	8	-
Impact Strength (kg-cm/mil)	5-7	-
Dimensional Stability	-	Excellent
Thermal Conductivity ($Btu/ft^2/in/sec/^oF$)	0.8×10^{-4}	-
Dielectric Constant (10^3 cps)	3.5	3.2
Dissipation Factor (%)	0.3	0.3
Dielectric Strength [v/mil ($\frac{1}{4}$")] electrode)	6,000	-
Volume Resistivity (ohm-cm)	10^{17}	10^{13}

Results from experimental data indicate that A film is stable to γ-exposures in the order of 1×10^{11} ergs/gm(C).

Teflon FEP (fluoroethylene) (Teflon 100) E. I. duPont de Nemours and Co.	Sheets of .04-in.-thick Type C film were supplied by duPont. This film was cementable on both sides.
Teflon TFE (fluoroethylene) E. I. duPont de Nemours and Co.	Virgin Teflon sheets of Grade A, Type T-7 were obtained from John L. Dore Co. The sheets were 0.04 in. thick and 0.01 in. thick.
Marlex 6002 (polyethylene) Phillips Chemical Co.	This material is representative of the "linear" or high-density-type polyethylene. It is more crystalline than the low-density-type polyethylene.
Teslar (polyvinyl fluoride) E. I. duPont de Nemours and Co.	This was a film prepared by duPont. The samples were prepared from 200-gage material.

Table C-9

Materials Used in Thermal-Control-Coatings Tests

Trade Name and Manufacturer	Material Description and Preparation
Glossy white silicone, Fuller 517-W-1, no primer W. P. Fuller Co.	Samples were prepared by GD/Astronautics. Sample size is 0.994 ± 0.003 in. diameter and no greater than 0.250 in. thick, including coating and substrate. The coatings were bonded to 2024 aluminum. The thickness of the coating was not sufficient to be opaque.
Skyspar A-423, SA 9185 (untinted white color) Eopxy primer SA9184 (white) Andrew Brown Co	Samples were prepared by GD/Astronautics. Sample size is 0.994 ± 0.003 in. diameter and no greater than 0.250 in. thick, including coating and substrate. The coatings were bonded to 2024 aluminum. The thickness of the coating was not sufficient to be opaque.
Silicone Al filled, Fuller 172-A-1, no primer W. P. Fuller Co.	Samples were prepared by GD/Astronautics. Sample size is 0.994 ± 0.003 in. diameter and no greater than 0.250 in. thick, including coating and substrate. The coatings were bonded to 2024 aluminum. The thickness of the coating was sufficient to be opaque.
Lacquer, pretreatment primer P40GC1 Kemacryl lacquer Black No. M49BC12 Sherwin-Williams	Samples were prepared by GD/Astronautics. Sample size is 0.994 ± 0.003 in. diameter and no greater than 0.250 in. thick, including coating and substrate. The coatings were bonded to 2024 aluminum. The thickness of the coating was sufficient to be opaque.

Table C-10

Materials Used in Elastomer Tests

Trade Name and Manufacturer	Material Description and Preparation
Viton A George C. Marshall Space Flight Center, Rubber and Plastics Section	Sheet stock obtained from MSFC. Viton A (Fluoro elastomer) 100.0 Zinc Oxide 10.0 Dyphos (Dibasic Lead Phosphite) 10.0 Tri- (2-Ethylhexyl Phosphite) 5.0 Hexamethylenediamine Carbamate 2.0 127.0
Buna N George C. Marshall Space Flight Center, Rubber and Plastics Section	Sheet stock obtained from MSFC. Paracril D (Butadiene-Acrylonitrile Copolymer) 100.0 Zinc Oxide 5.0 Stearic Acid 1.0 Age Rite Resin D (Polymerized Trimethyl Dihydroquinoline) 2.0 Sterling NS (Carbon Black) 23.0 Pine Tar 3.0 Methyl Tuads (Tetramethylthiuram Disulfide) 3.0 Santocure (N-Cyclohexyl-2-Benzothiazole Sulfenamide) 3.0 140.0

Table C-10 (cont'd)

Trade Name and Manufacturer	Material Description and Preparation
Neoprene George C. Marshall Space Flight Center, Rubber and Plastics Section	Sheet stock obtained from MSFC. Constituent — Parts Neoprene Type W (Chloroprene Polymer) 100.0 Neozone A (Phenyl-Alpha-Napthylamine) 2.0 Stearic Acid 0.5 Sterling NS (Carbon Black) 37.5 Magnesium Oxide 2.0 Zinc Oxide 5.0 NA-22 (2-Mercaptoimidazoline) 0.5 147.5
Parker 66-581 (Buna N) Parker-Hannfin Co.	A compound developed to seal Mil-O-7808 in accordance with FMS-00264A, which specifies a temperature service range of -65°F to -300°F.

APPENDIX D

TEMPERATURES OF MATERIALS DURING VACUUM IRRADIATIONS

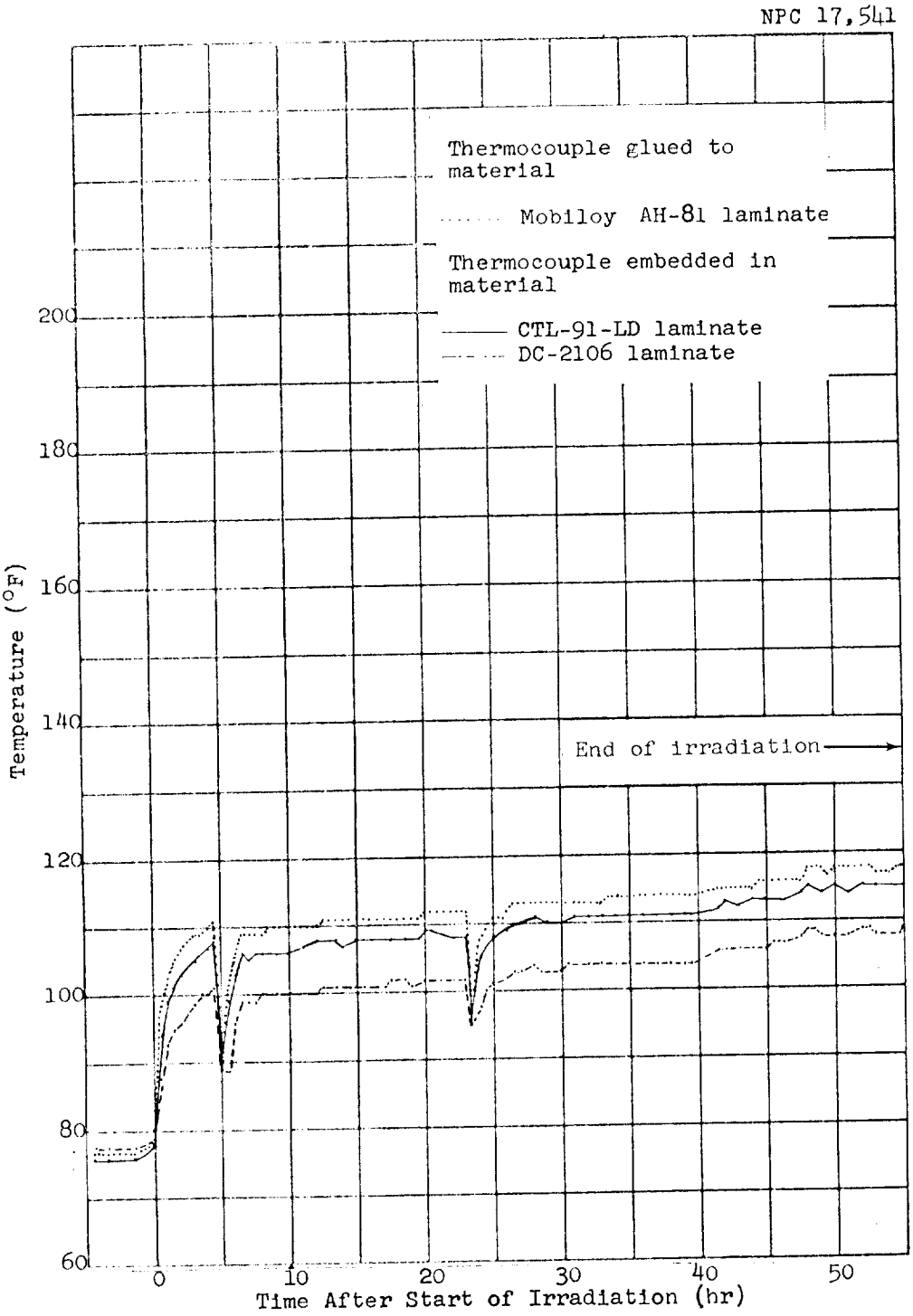

Figure D-1 Specimen Temperatures During Static Test: Mobiloy AH-81 CTL-91-LD, and DC-2106

Preceding page blank

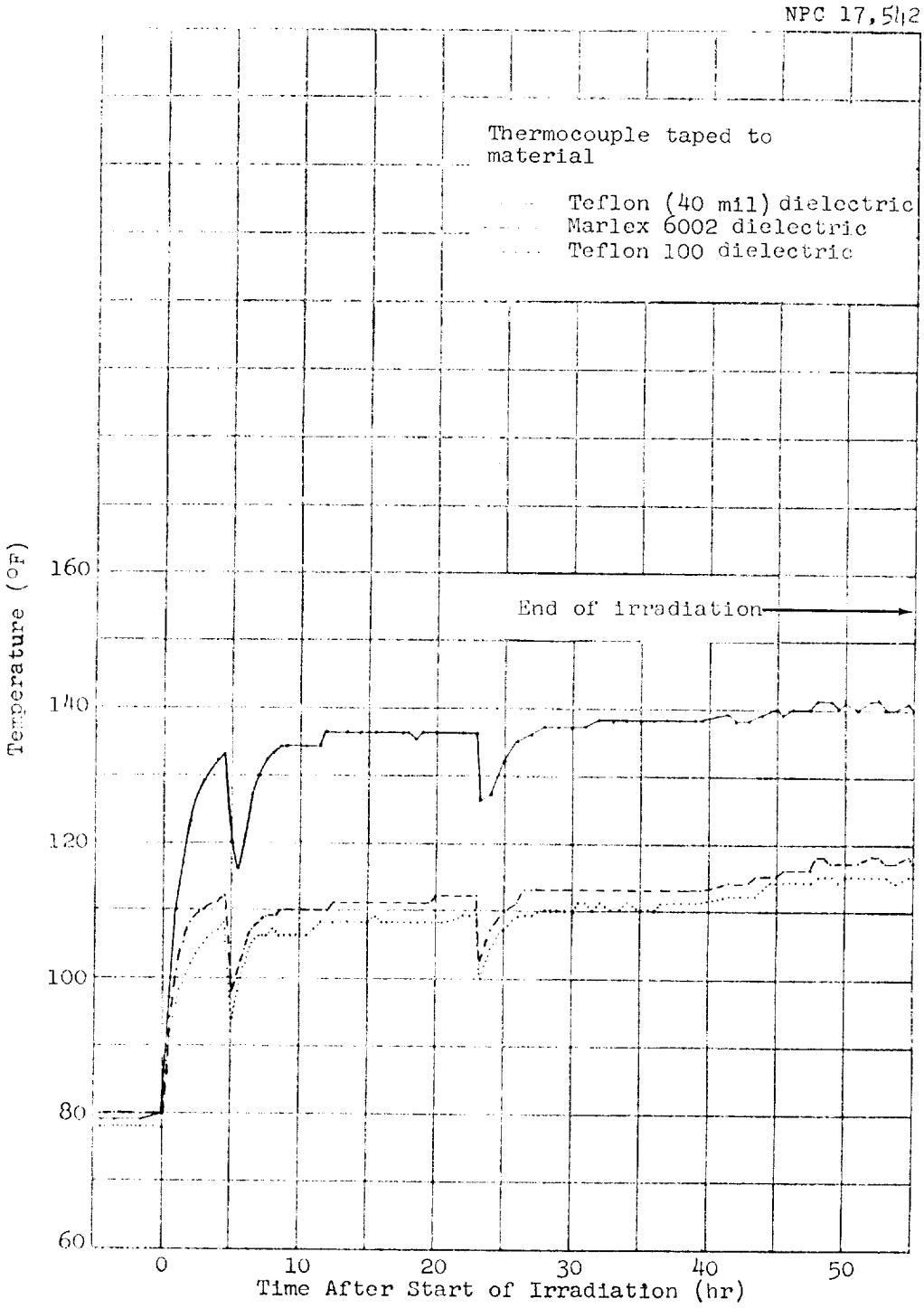

Figure D-2 **Specimen Temperatures During Static Test: Teflon (40 mil), Marlex 6002, and Teflon 100**

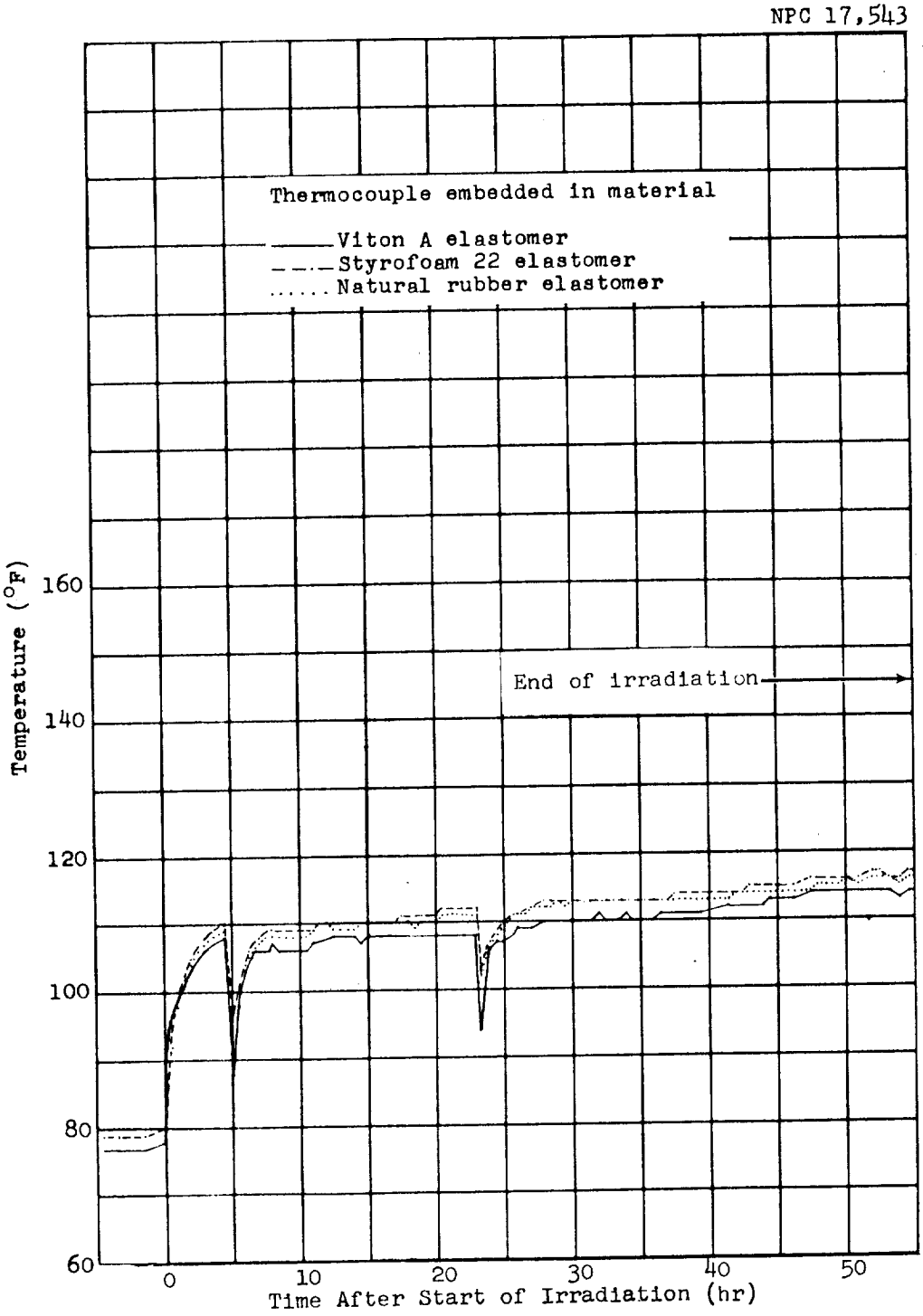

Figure D-3 Specimen Temperatures During Static Test: Viton A, Styrofoam 22, and Natural Rubber

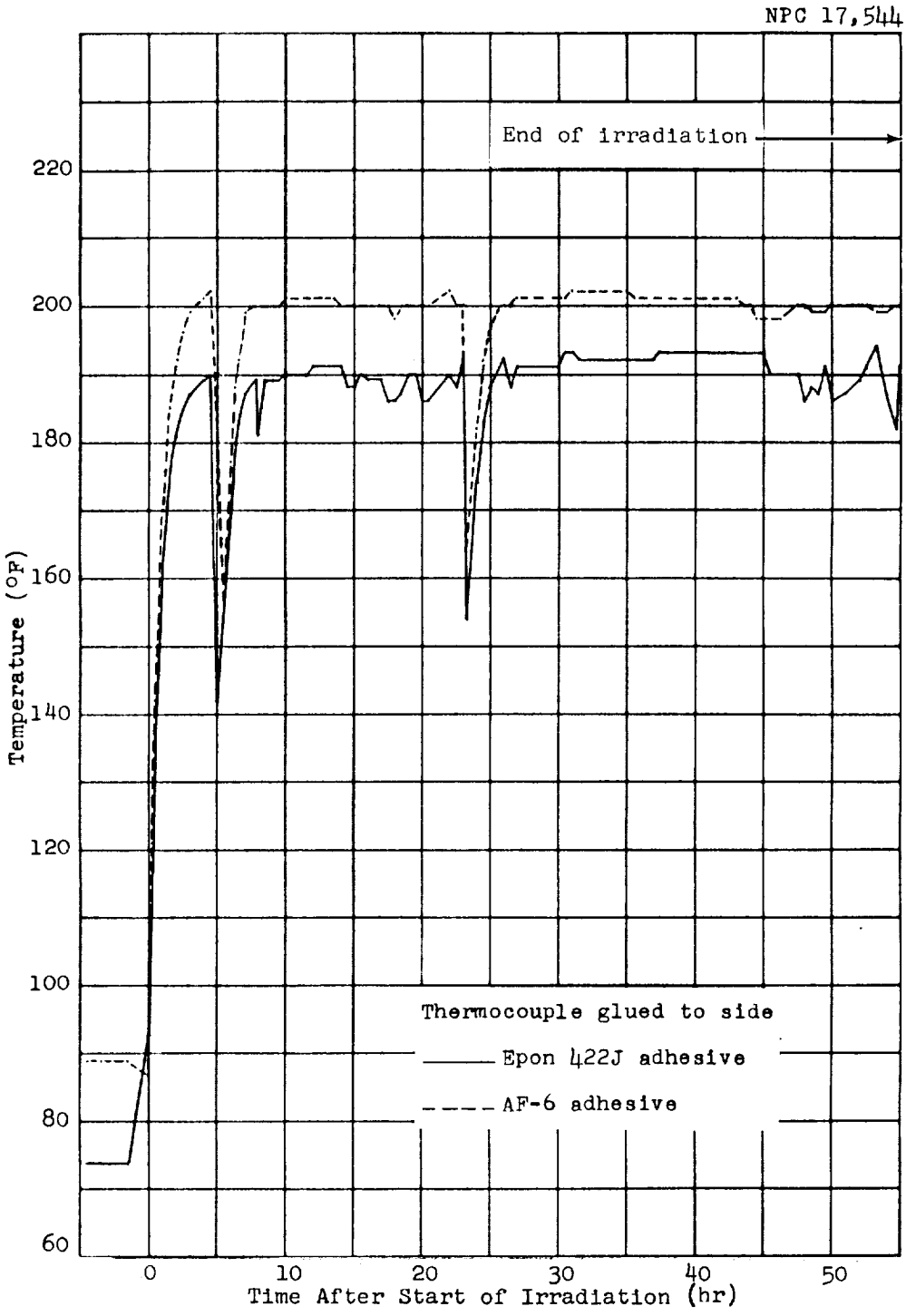

Figure D-4 Specimen Temperatures During Static Test: Epon 422J and AF-6

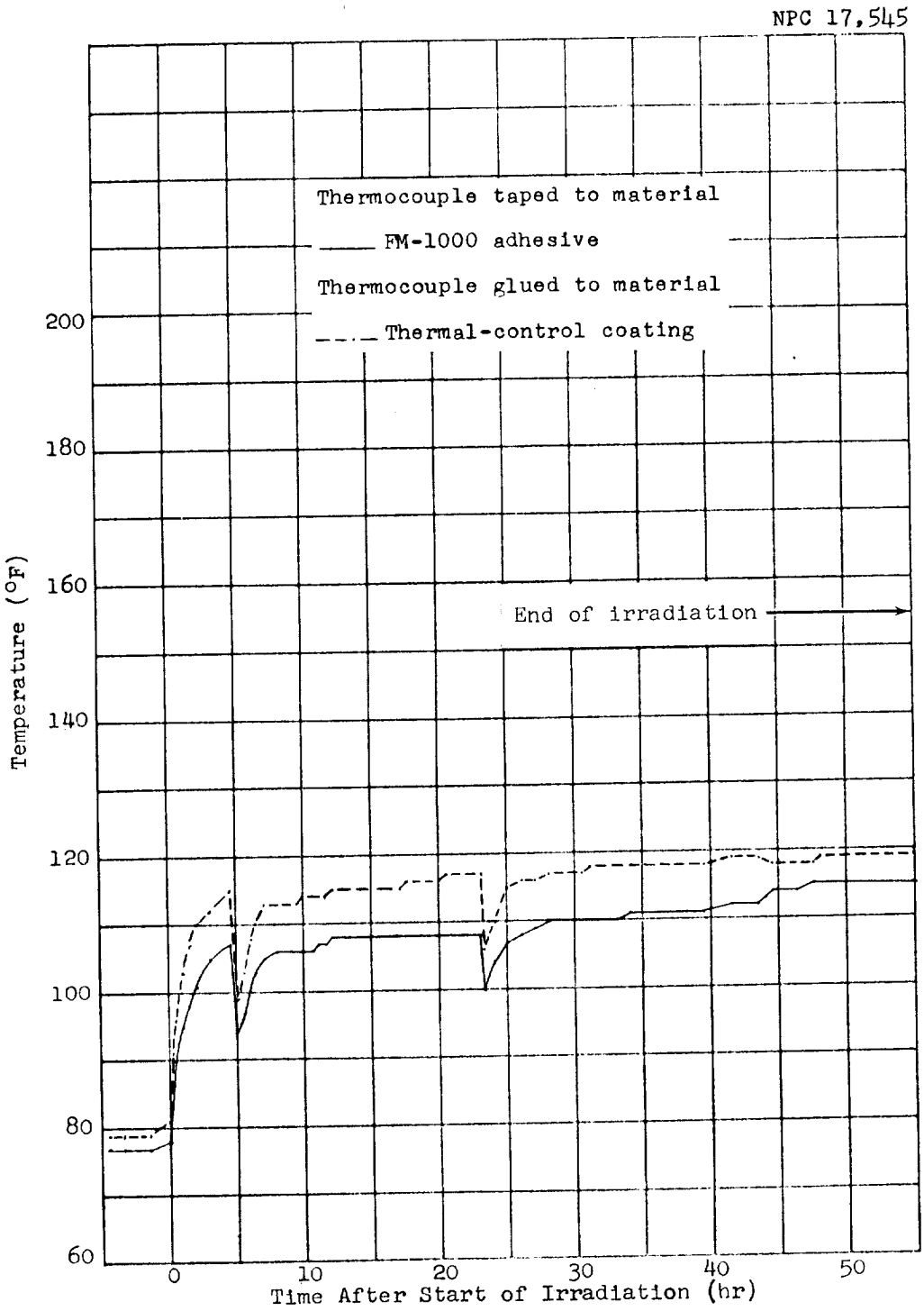

Figure D-5 Specimen Temperatures During Static Test: FM-1000 and Thermal Coating

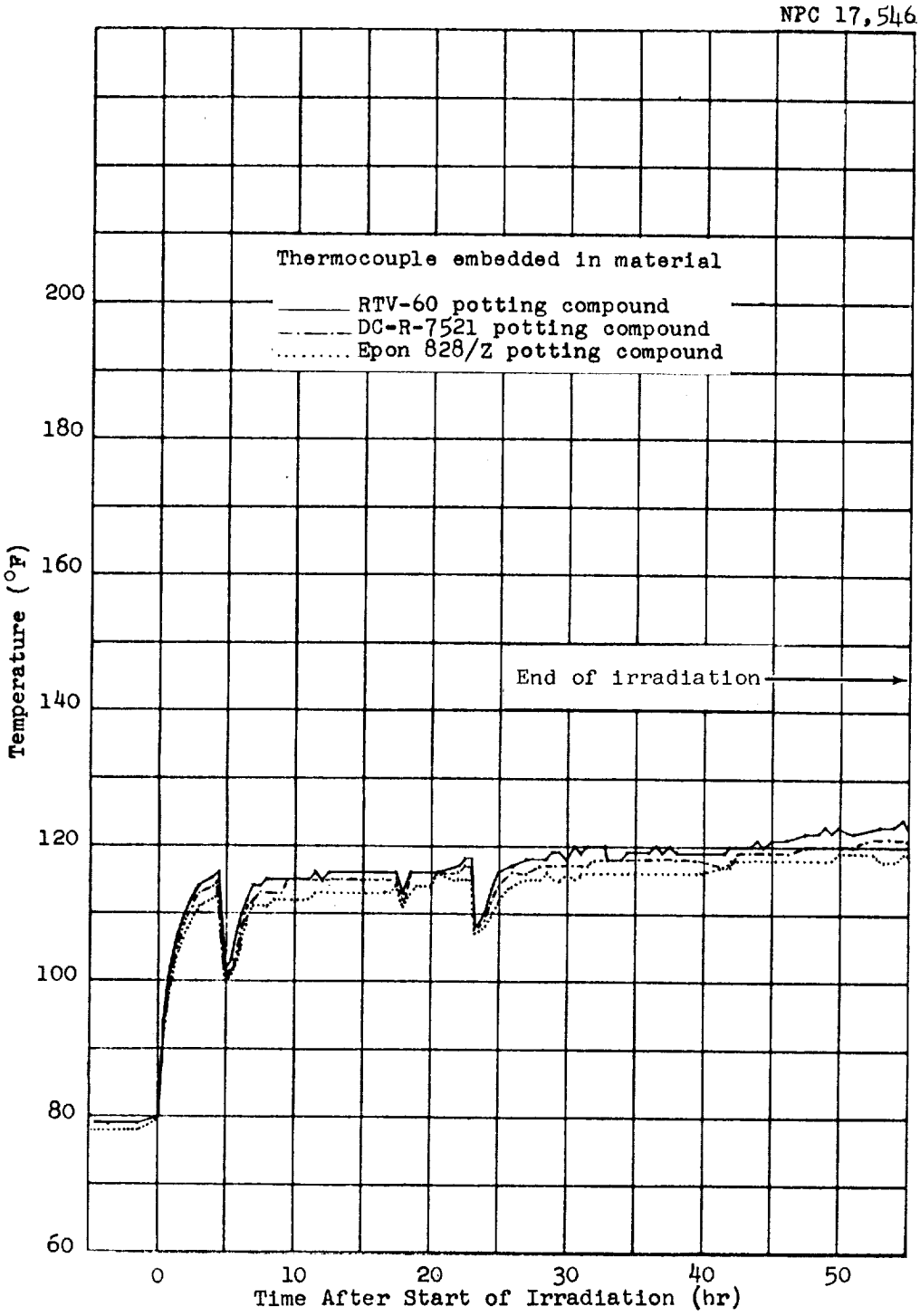

Figure D-6 Specimen Temperatures During Static Test: RTV-60, DC-R-7521, and Epon 828/Z

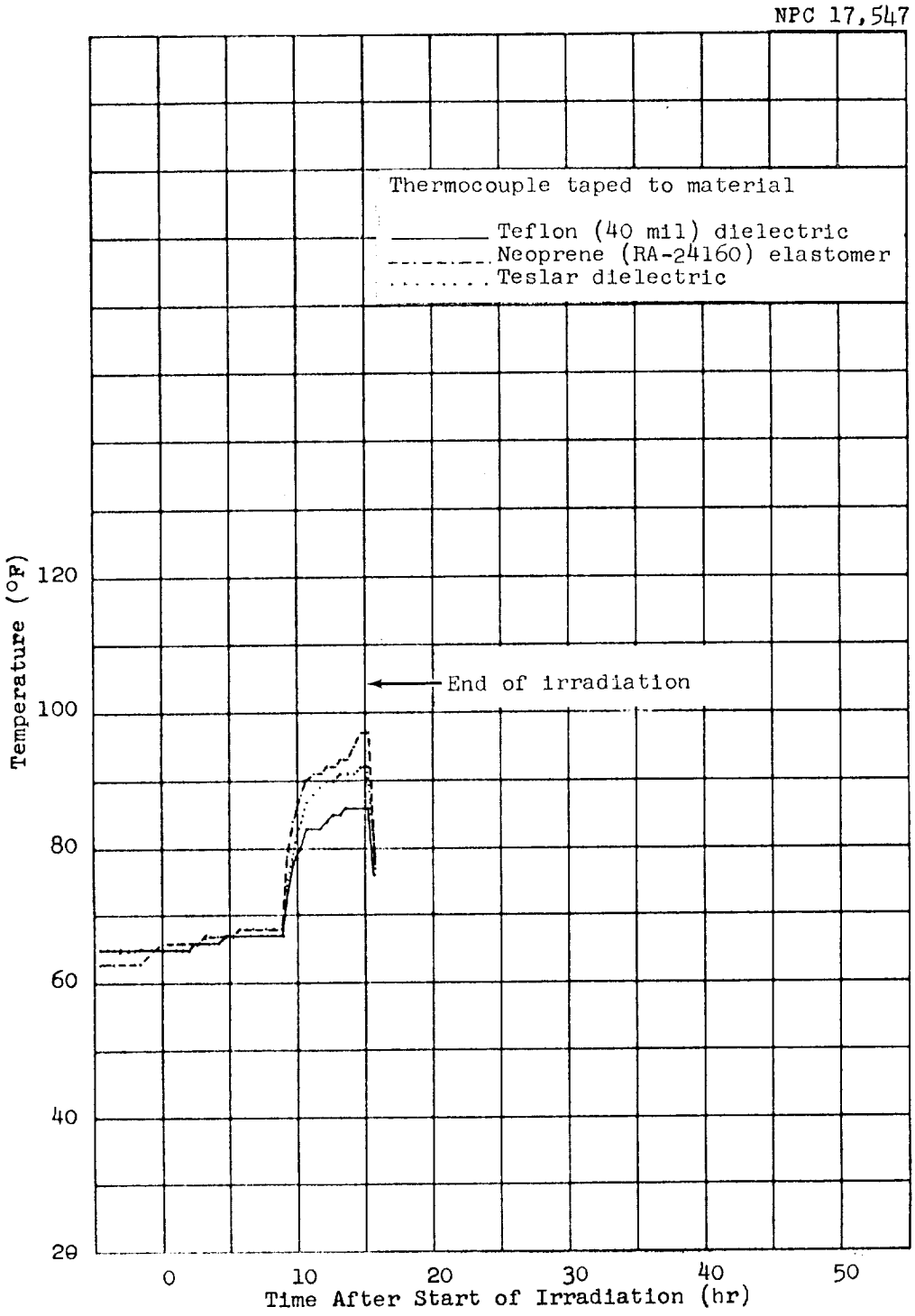

Figure D-7 Specimen Temperatures During Static Test: Teflon (40 mil), Neoprene (RA-24160), and Teslar

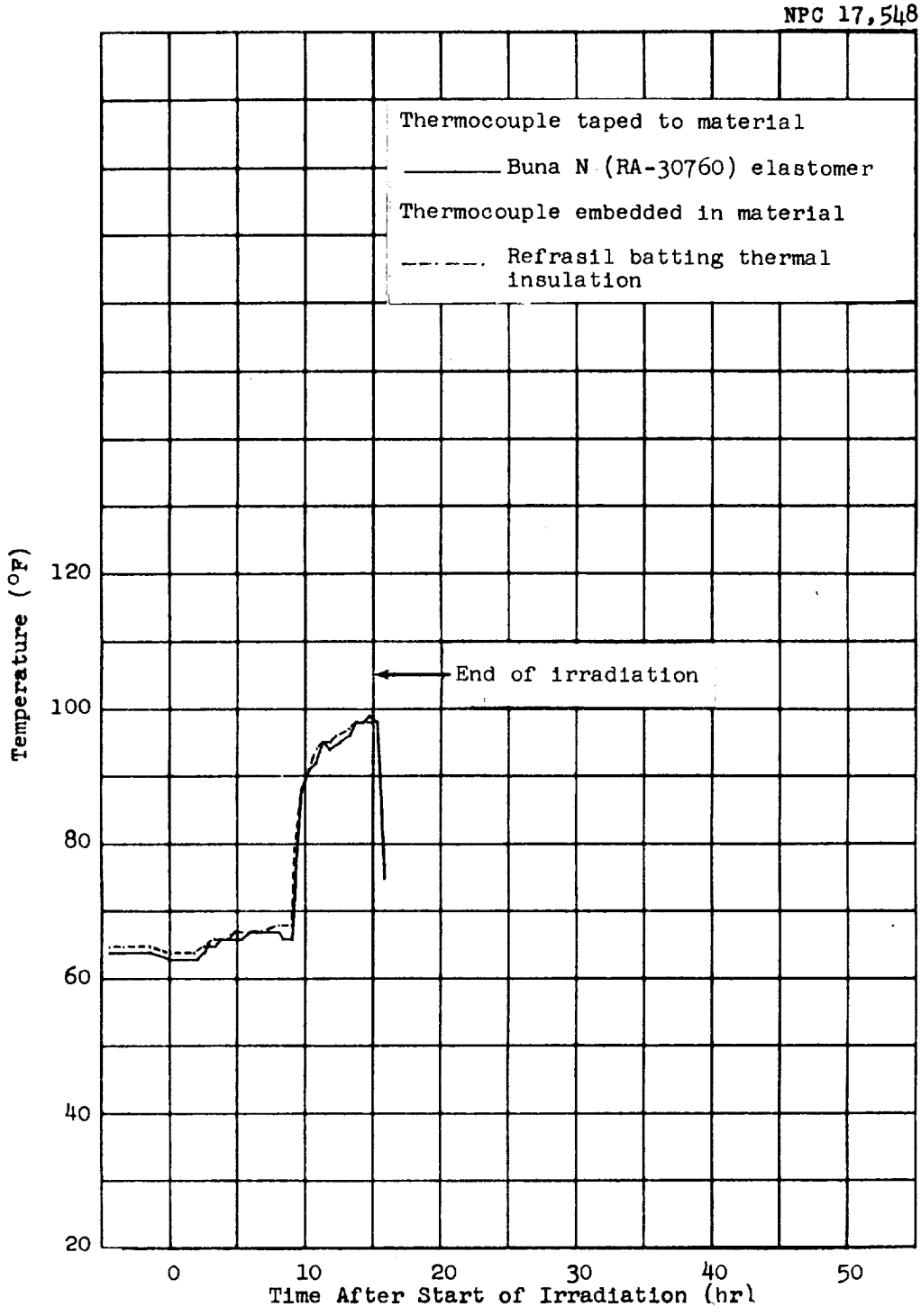

Figure D-8 Specimen Temperatures During Static Test: Buna N (RA-30760) and Refrasil Batting (B-100)

NPC 17,549

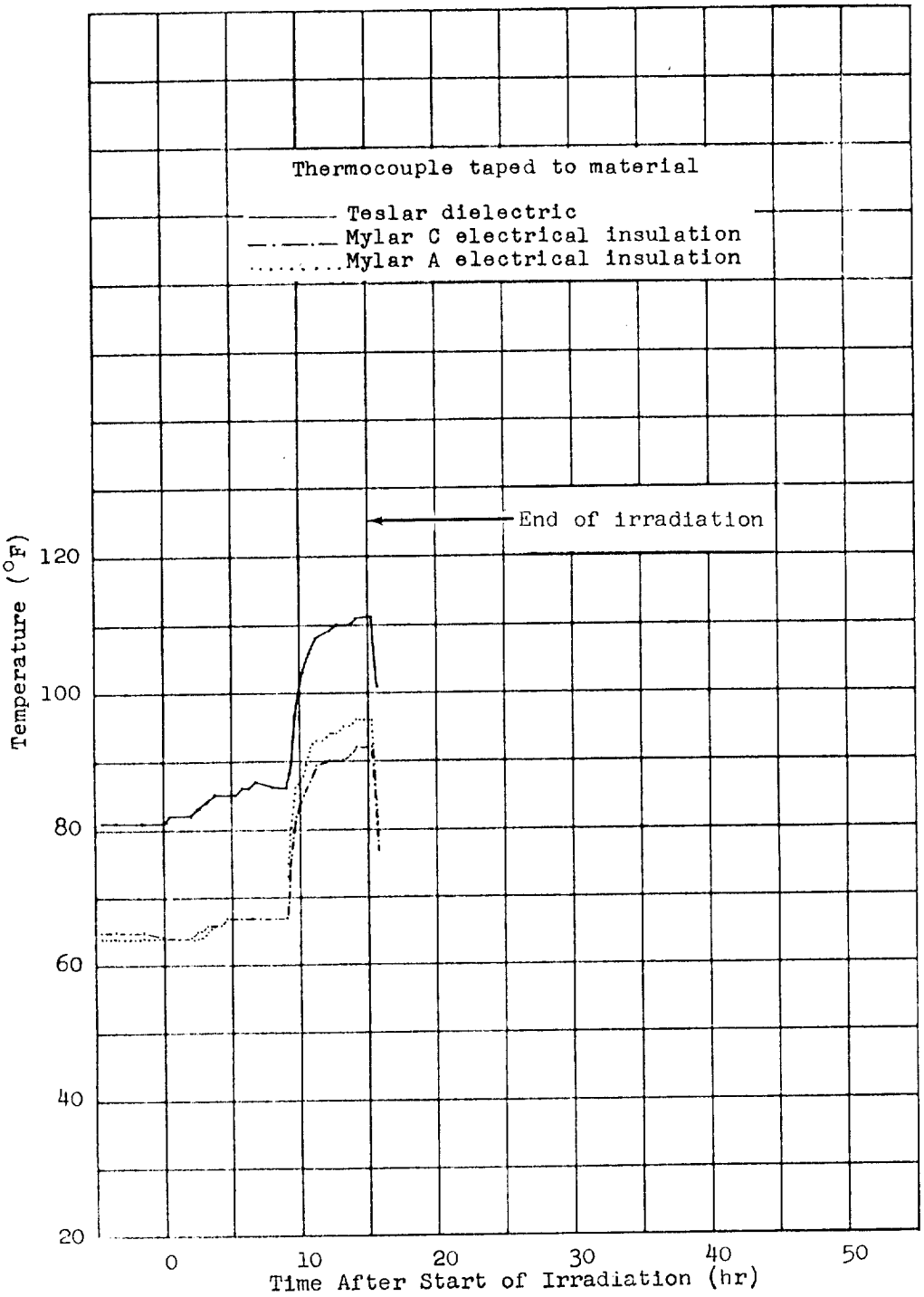

Figure D-9 Specimen Temperatures During Static Test: Teslar, Mylar C, and Mylar A

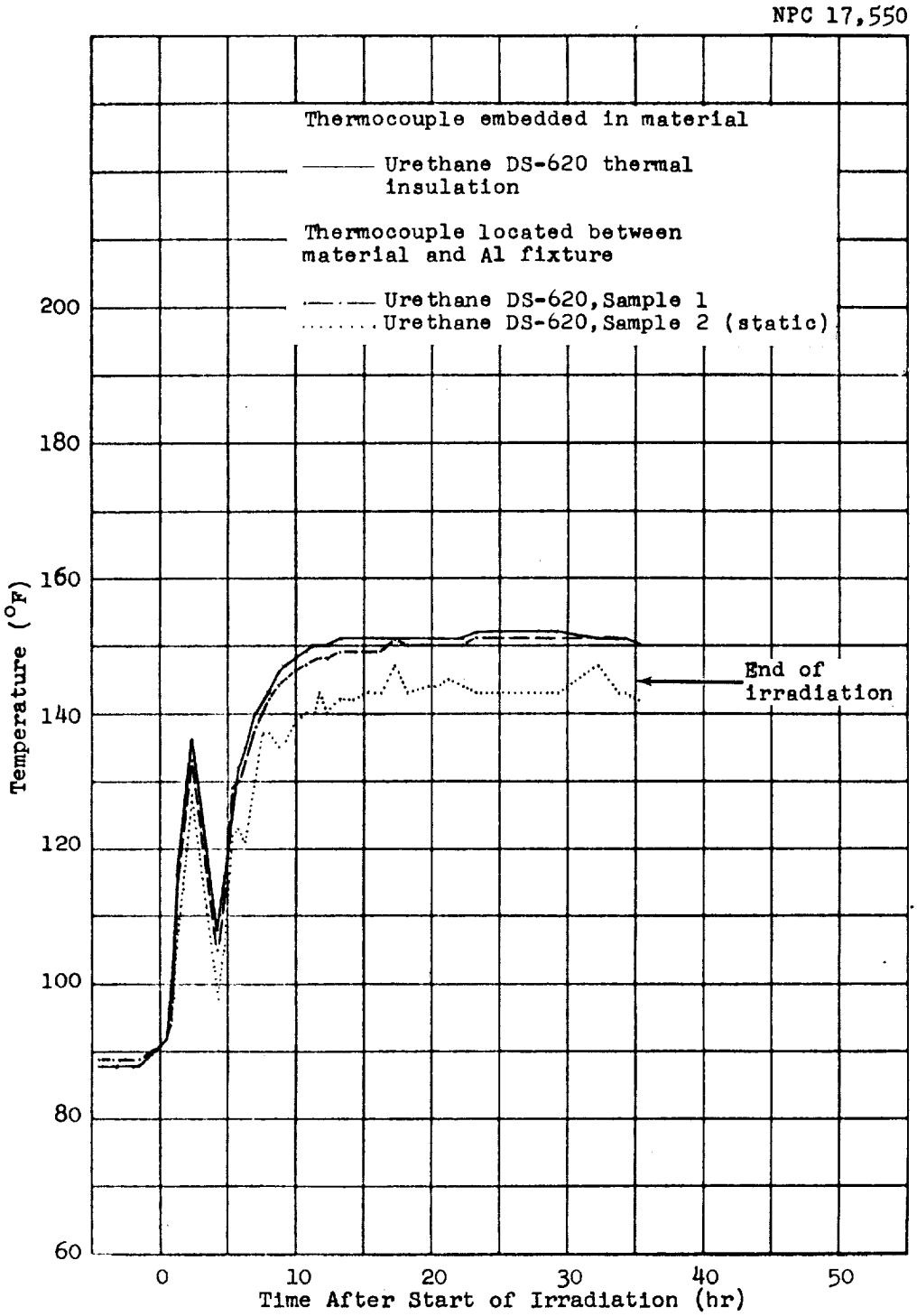

Figure D-10 Specimen Temperatures During Low-Force Dynamic Test: Urethane DS-620

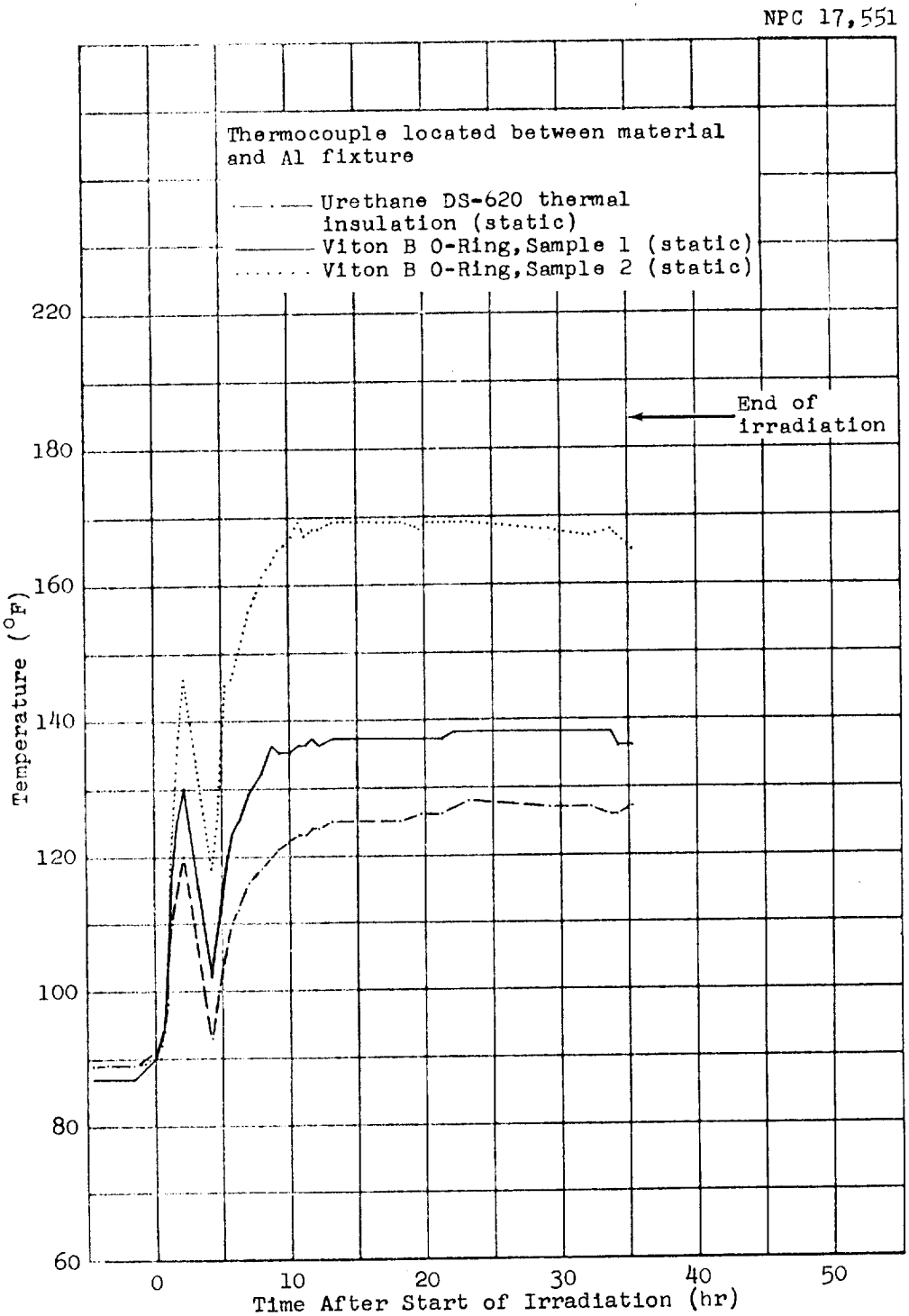

Figure D-11 **Specimen Temperatures During Low-Force Dynamic Test: Urethane DS-620 and Viton B**

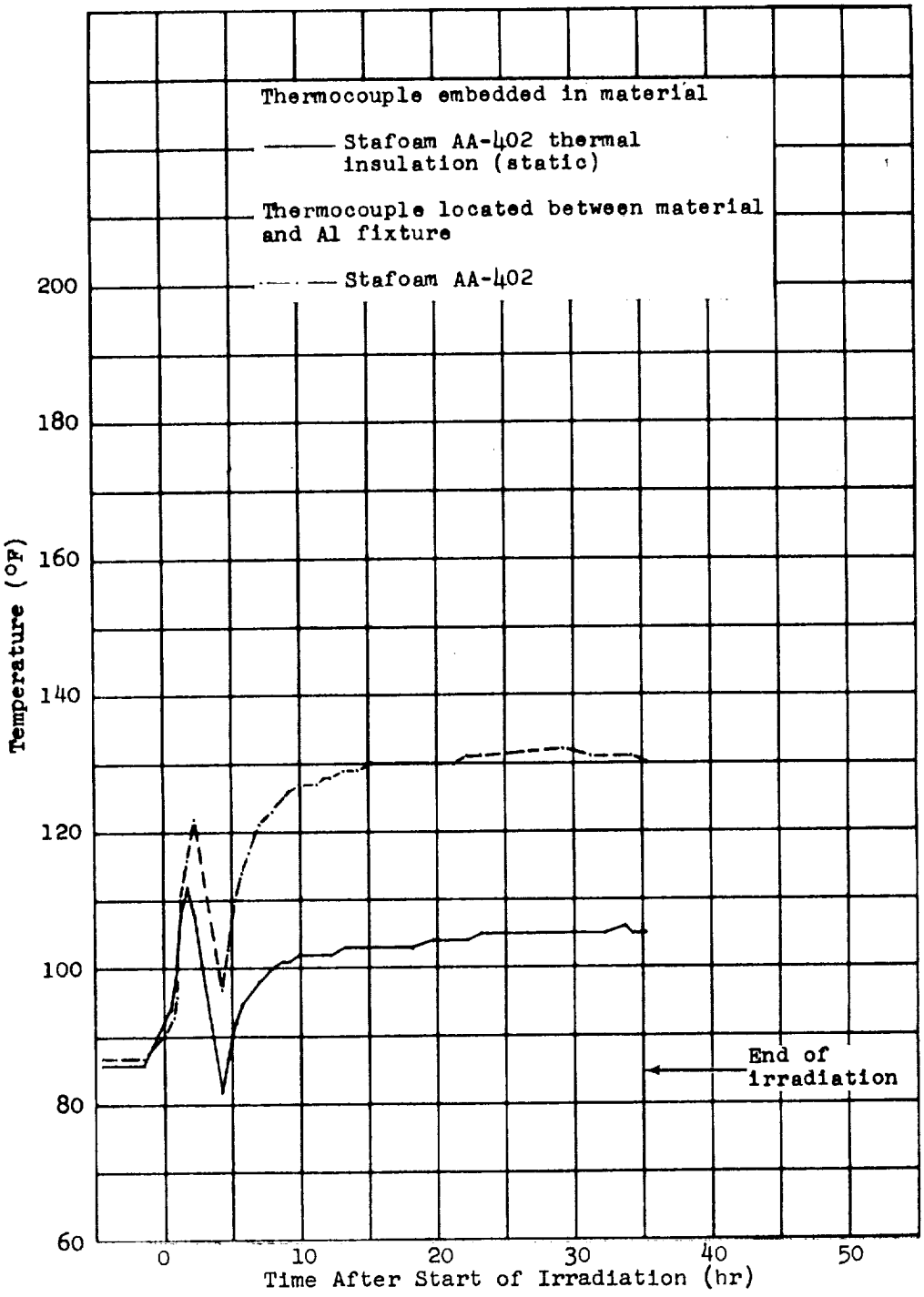

Figure D-12 **Specimen Temperatures During Low-Force Dynamic Test: Stafoam AA-402**

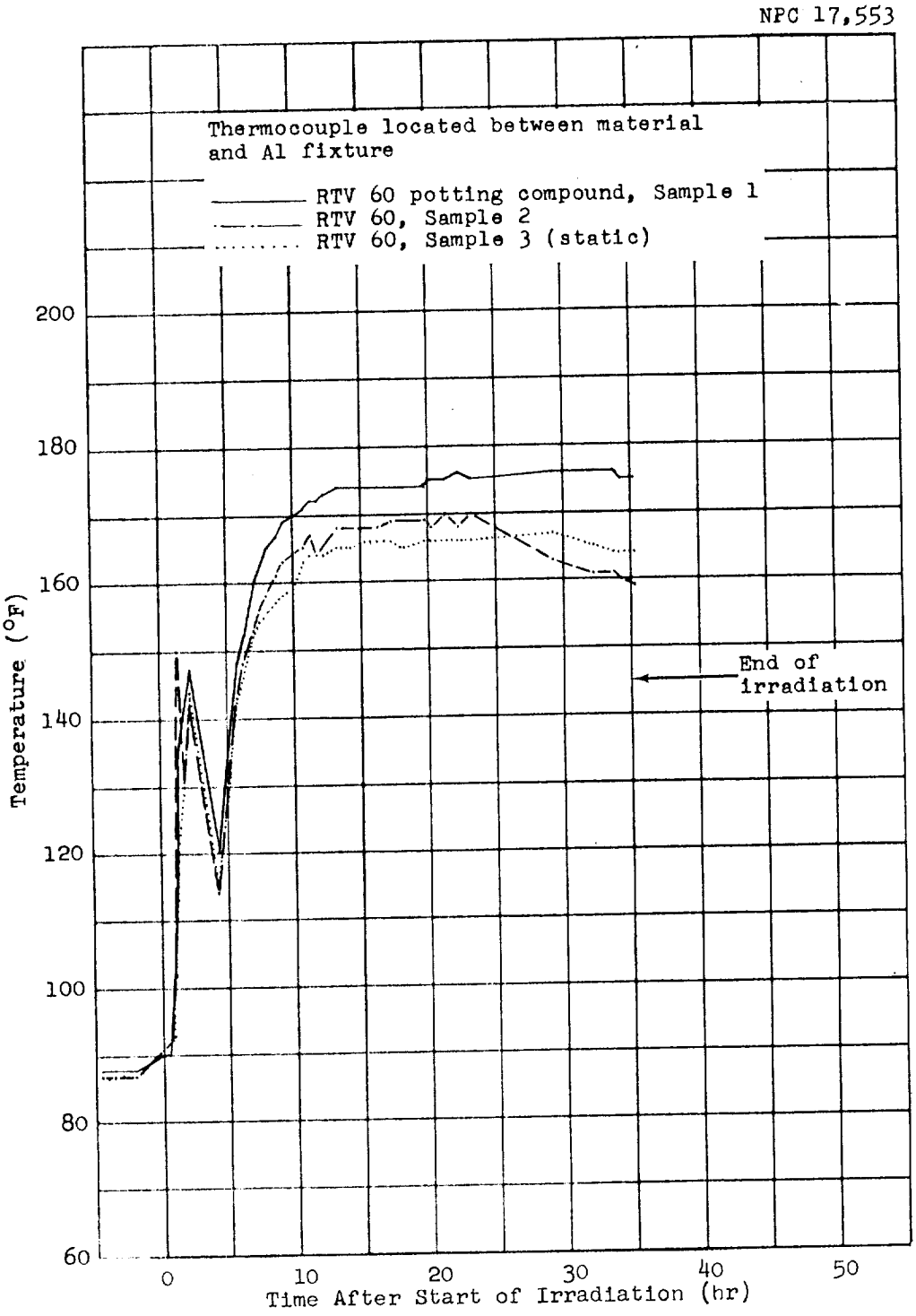

Figure D-13 **Specimen Temperatures During Low-Force Dynamic Test: RTV-60**

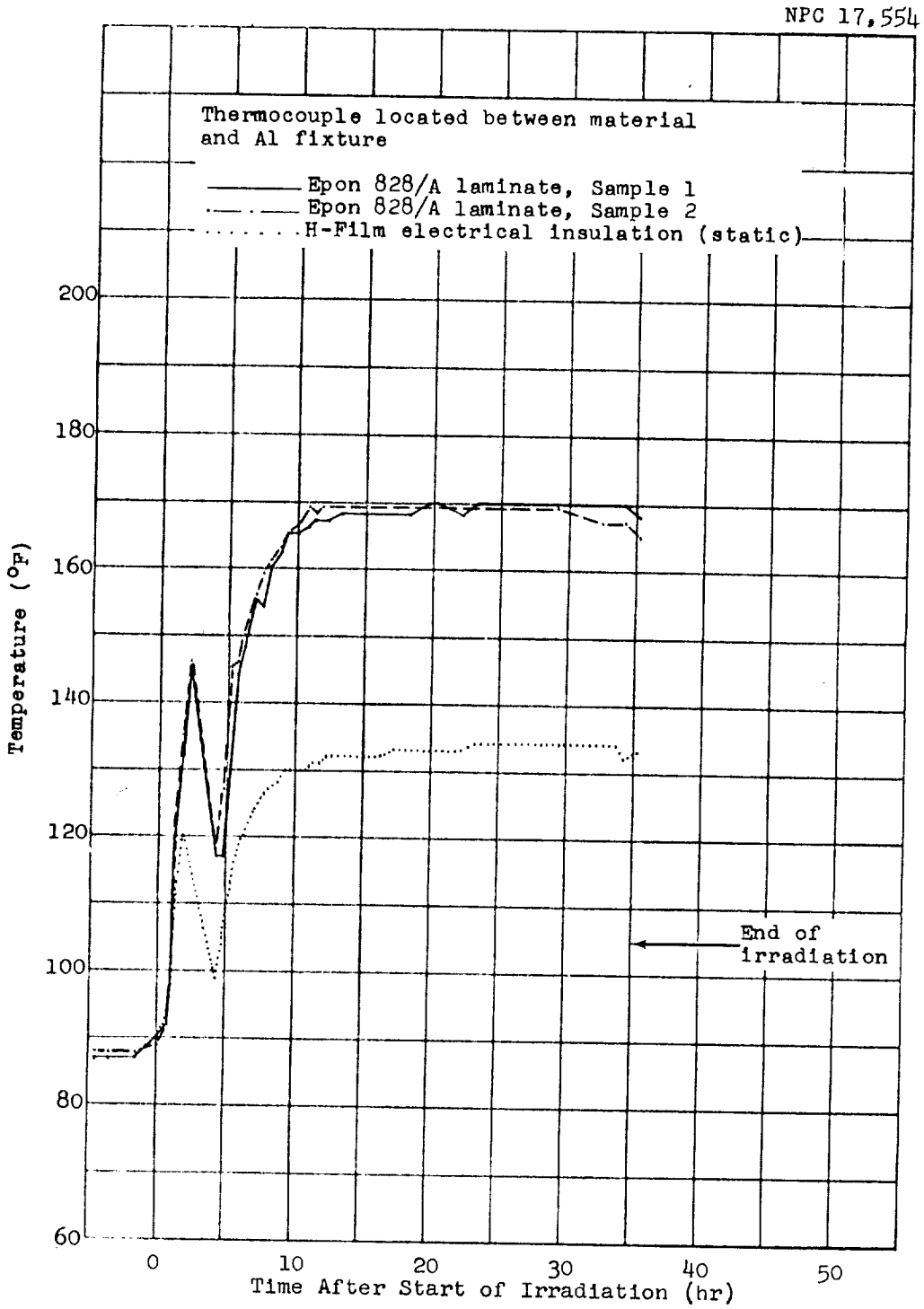

Figure D-14 **Specimen Temperatures During Low-Force Dynamic Test: Epon 828/A and DuPont H-Film**

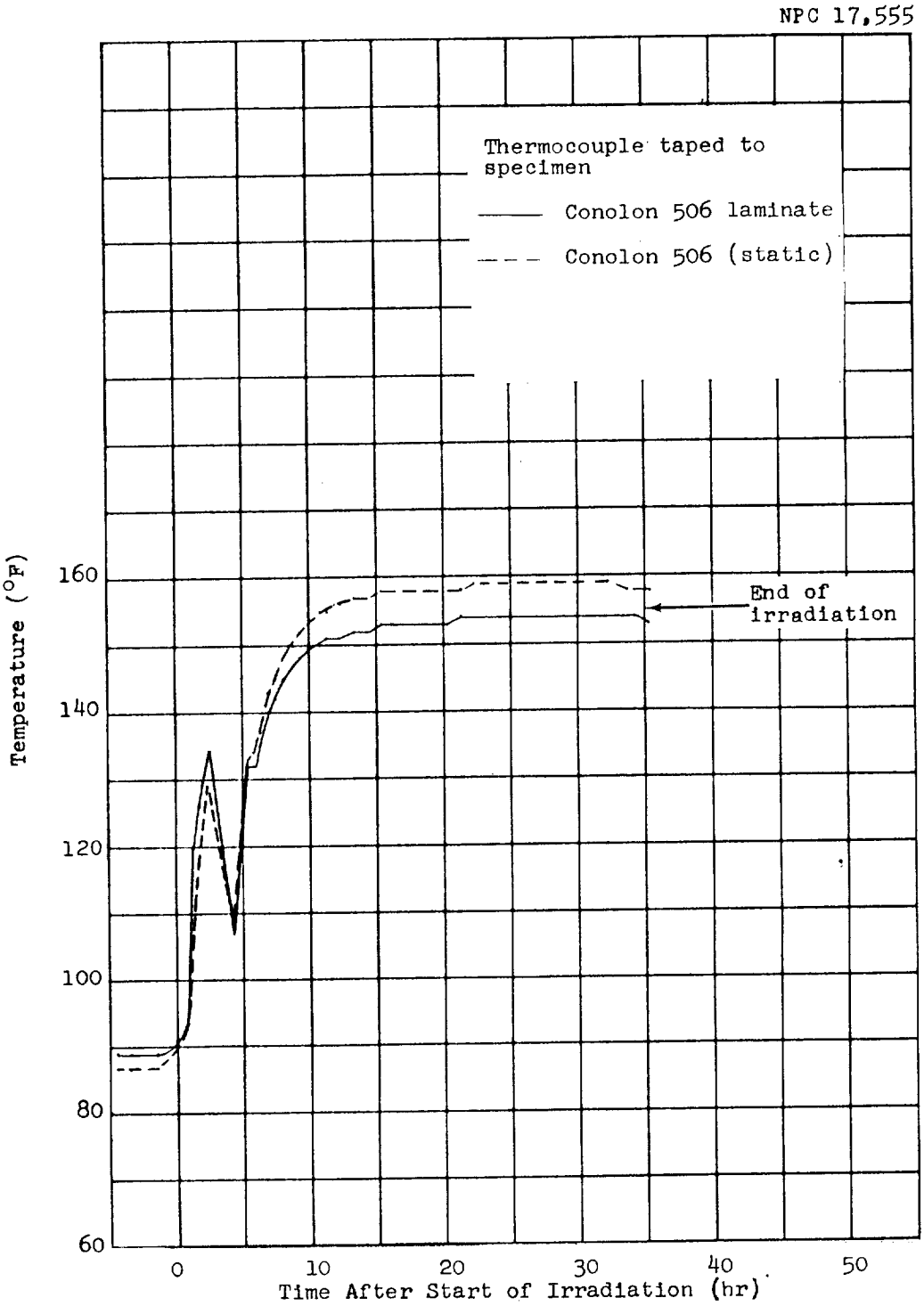

Figure D-15 **Specimen Temperatures During High-Force Dynamic Test: Conolon 506**

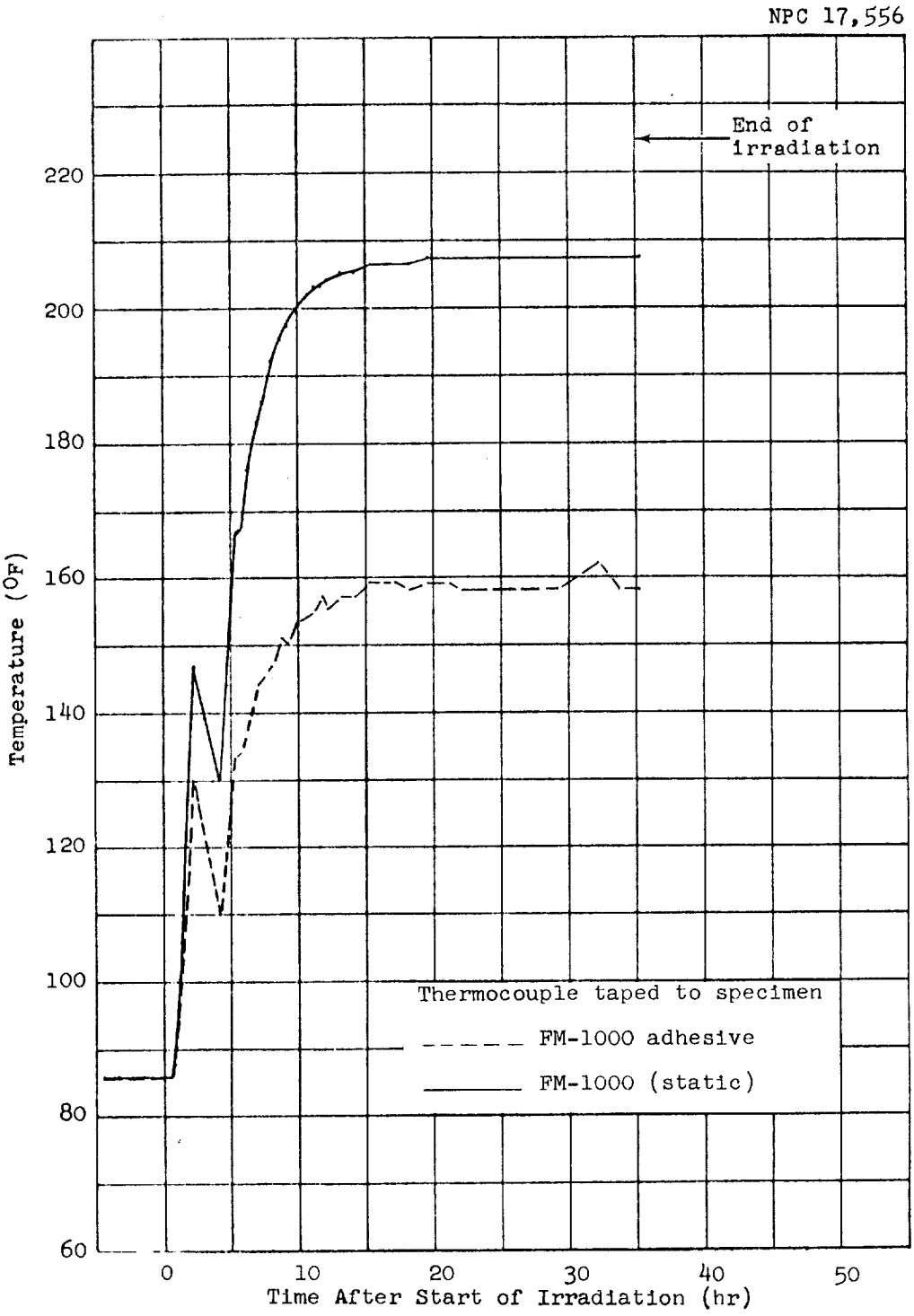

Figure D-16 Specimen Temperatures During High-Force Dynamic Test: FM-1000

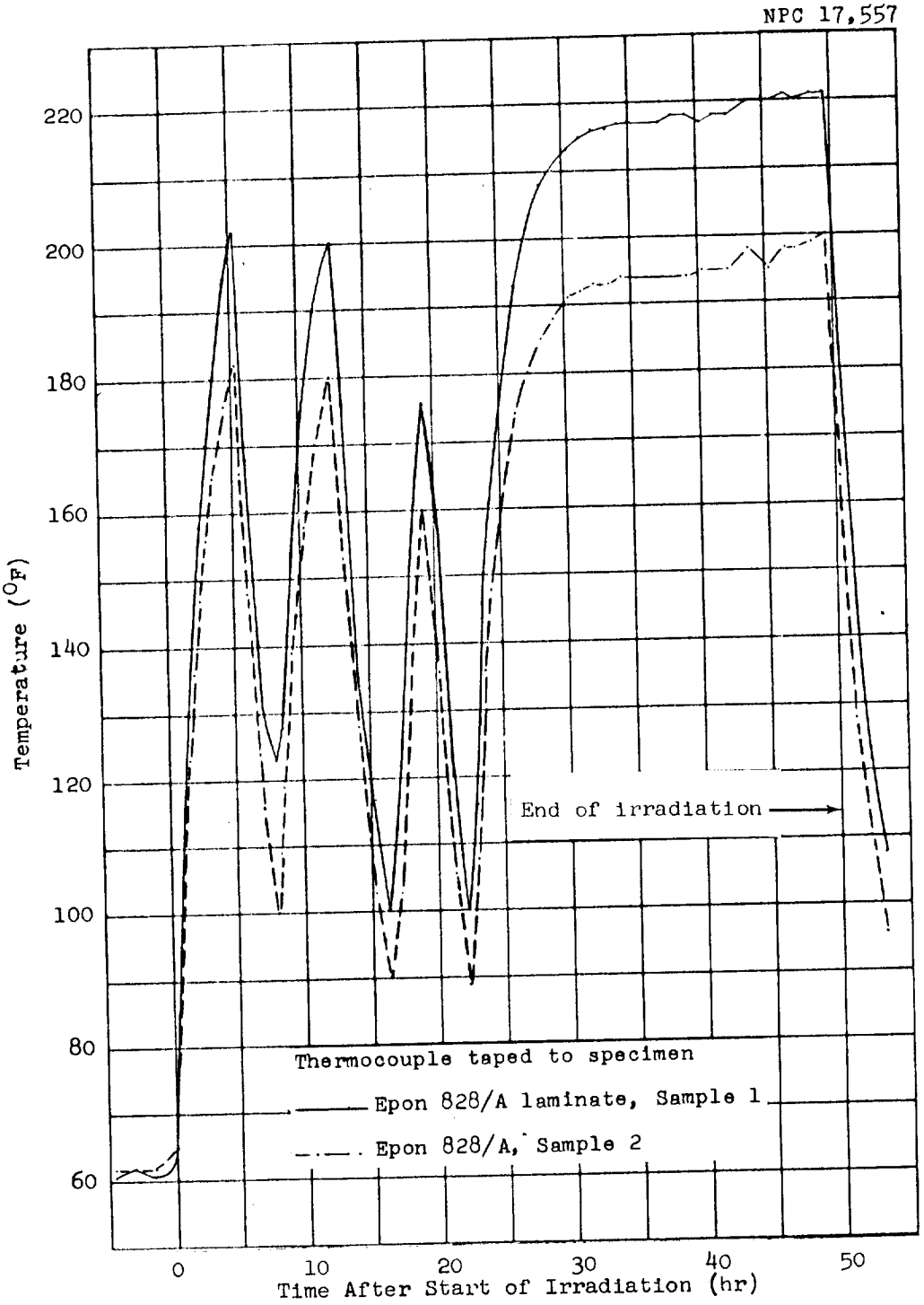

Figure D-17 Specimen Temperatures During High-Force Dynamic Test: Epon 828/A

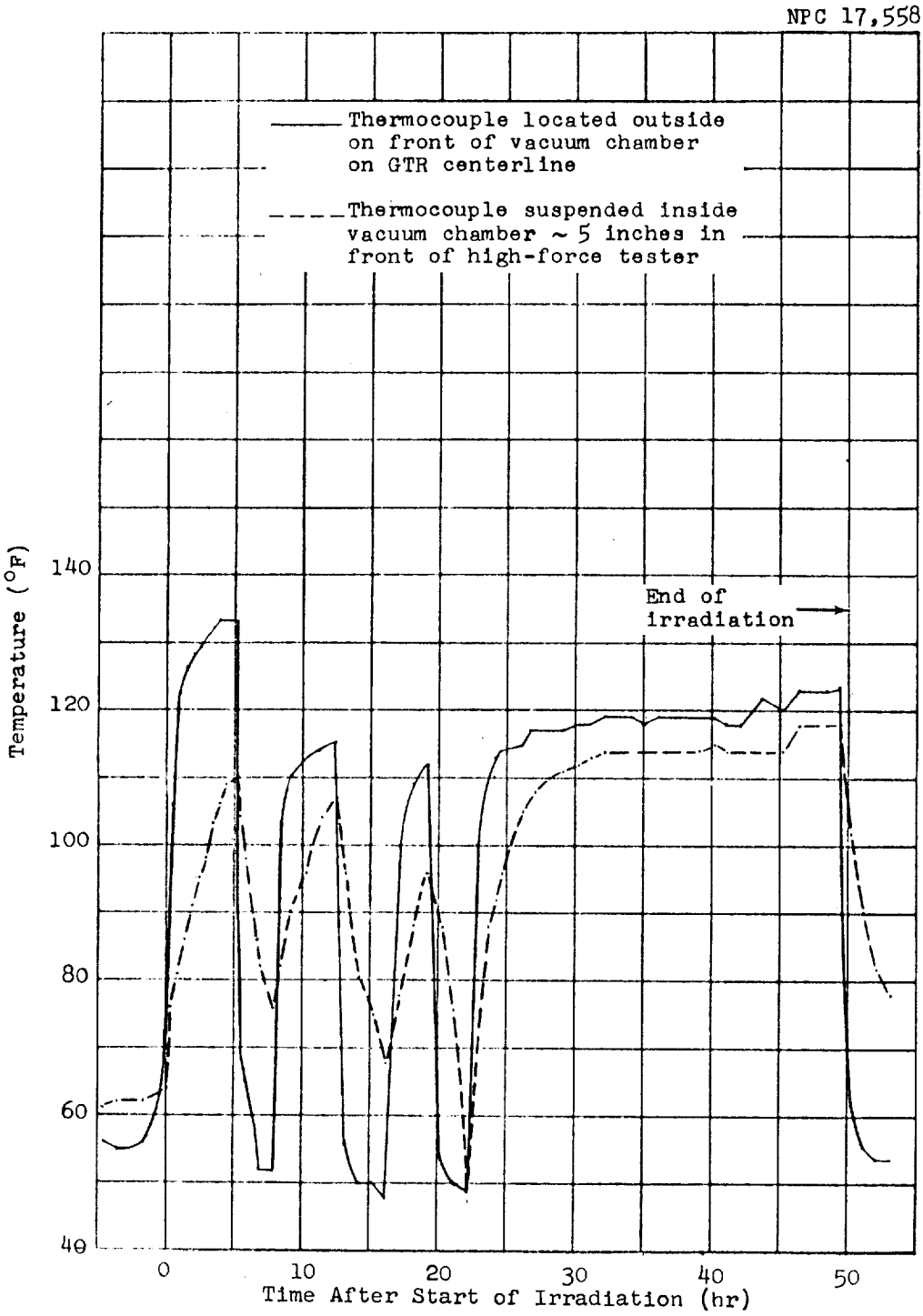

Figure D-18 Vacuum-Chamber Temperatures During High-Force Dynamic Test

APPENDIX E

MONOCHROMATIC REFLECTIVITY AND ABSORPTIVITY CURVES FOR THERMAL-CONTROL-COATING SAMPLES

(Values Determined by the Space Science Laboratory of General Dynamics/Astronautics)

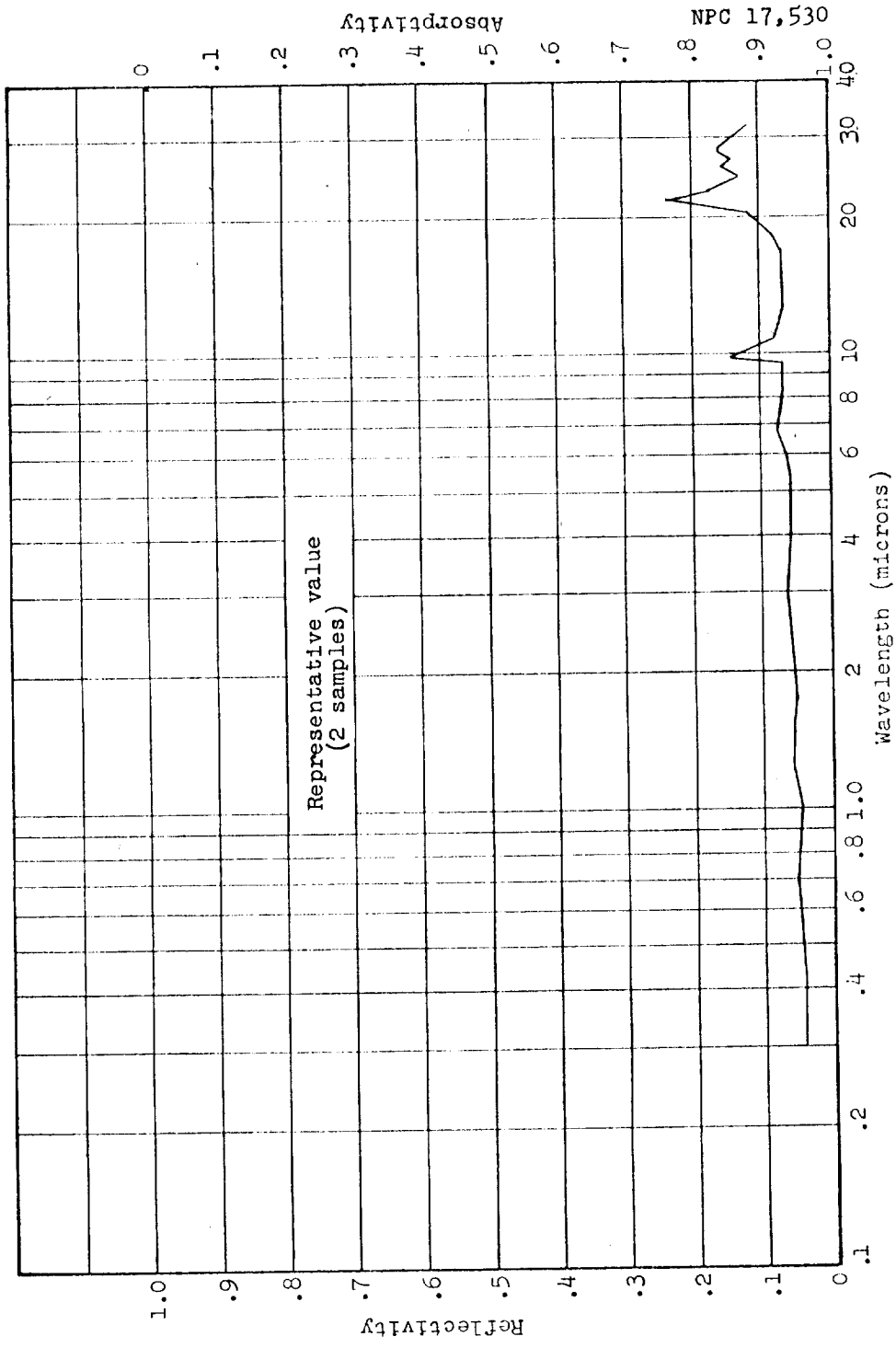

Figure E-1 Monochromatic Reflectivity and Absorptivity: Acrylic Black; Preshipment Control Samples

Preceding page blank

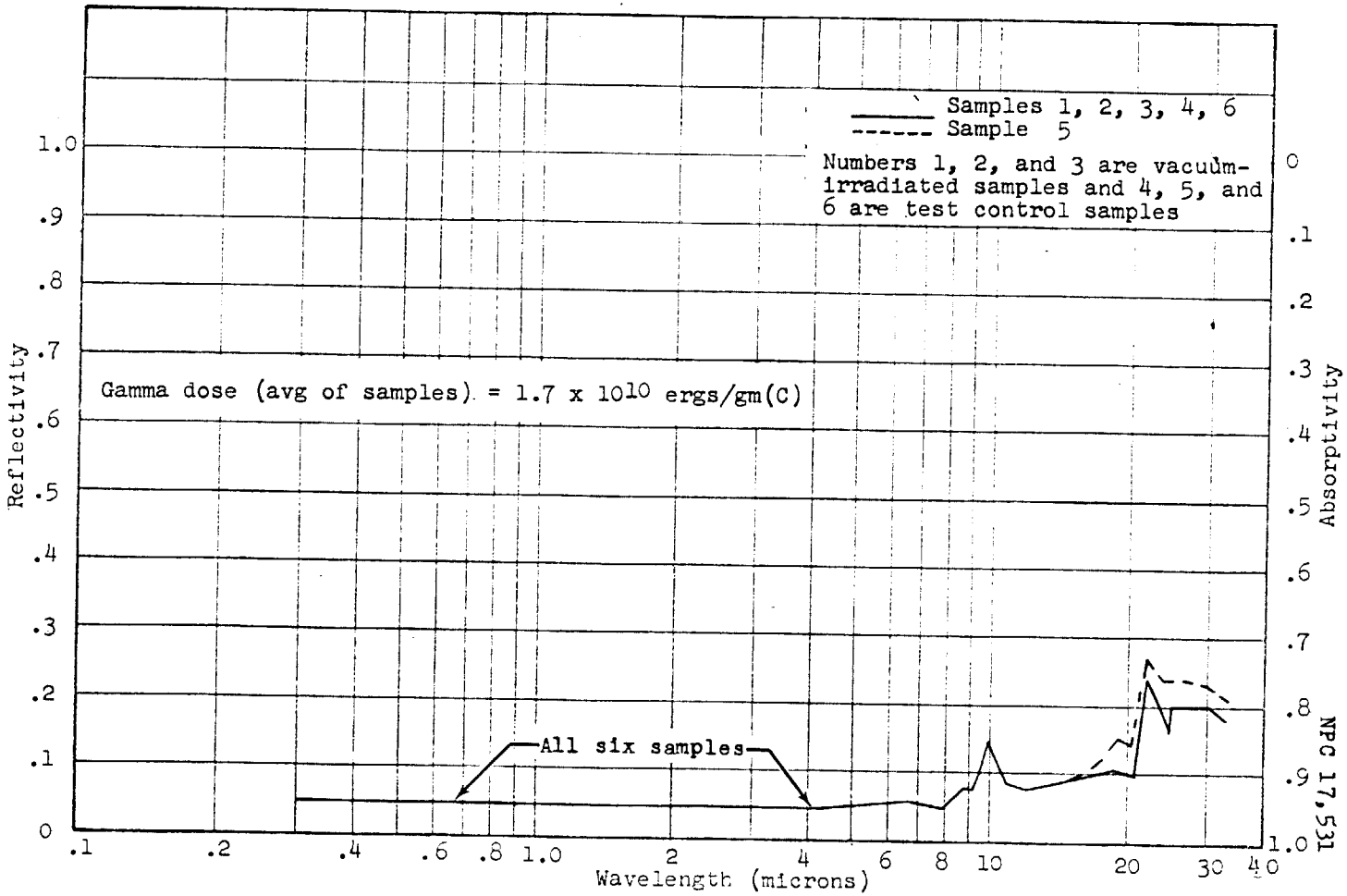
Samples 1, 2, 3, 4, 6
Sample 5
Numbers 1, 2, and 3 are vacuum-irradiated samples and 4, 5, and 6 are test control samples
Gamma dose (avg of samples) = 1.7 x 10^10 ergs/gm(C)
All six samples
Reflectivity
Absorptivity
Wavelength (microns)
NPC 17,531

Figure E-2 Monochromatic Reflectivity and Absorptivity: Acrylic Black; Test Control Samples and Vacuum-Irradiated Samples

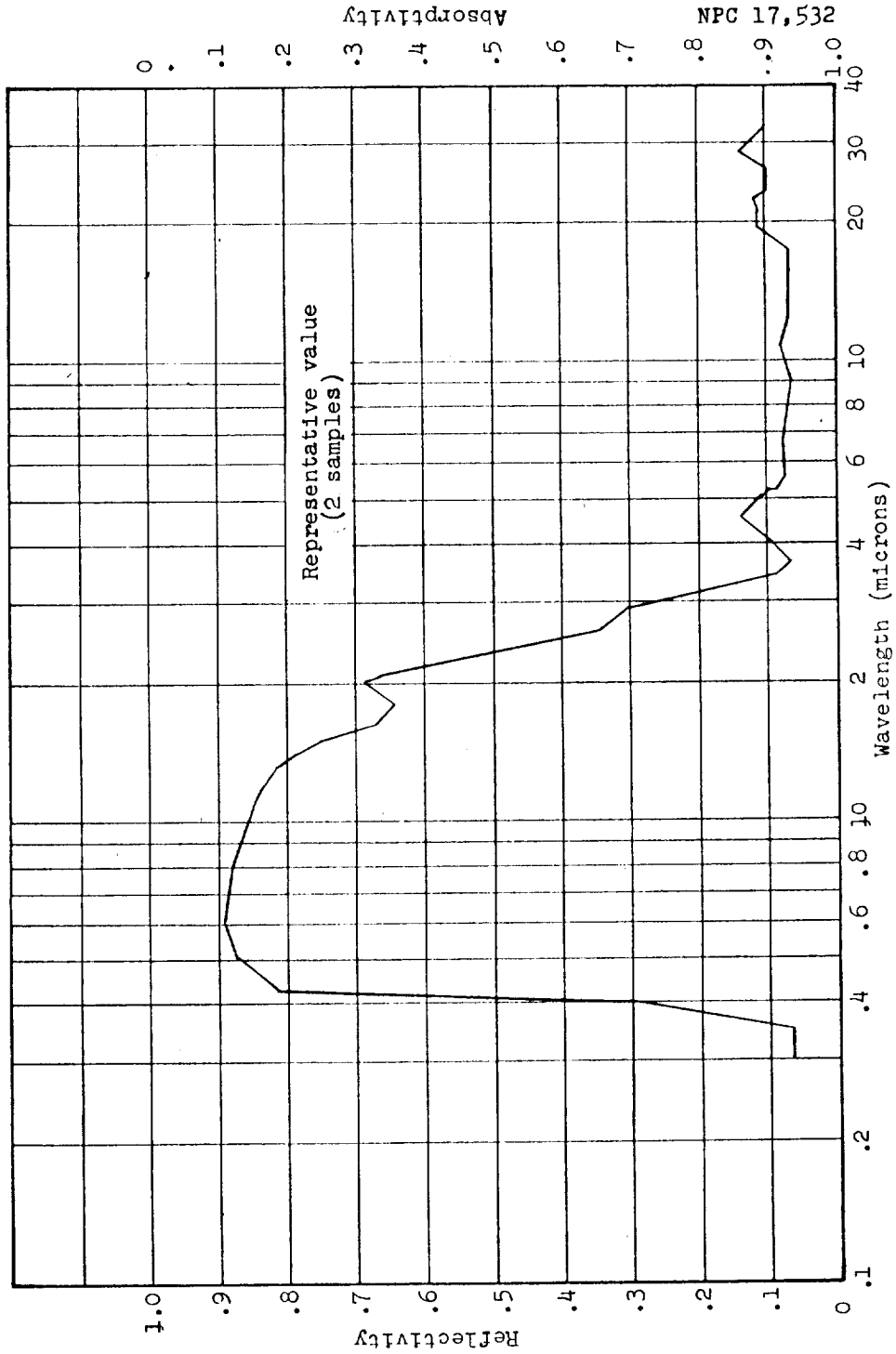

Figure E-3 Monochromatic Reflectivity and Absorptivity: Epoxy White; Preshipment Control Samples

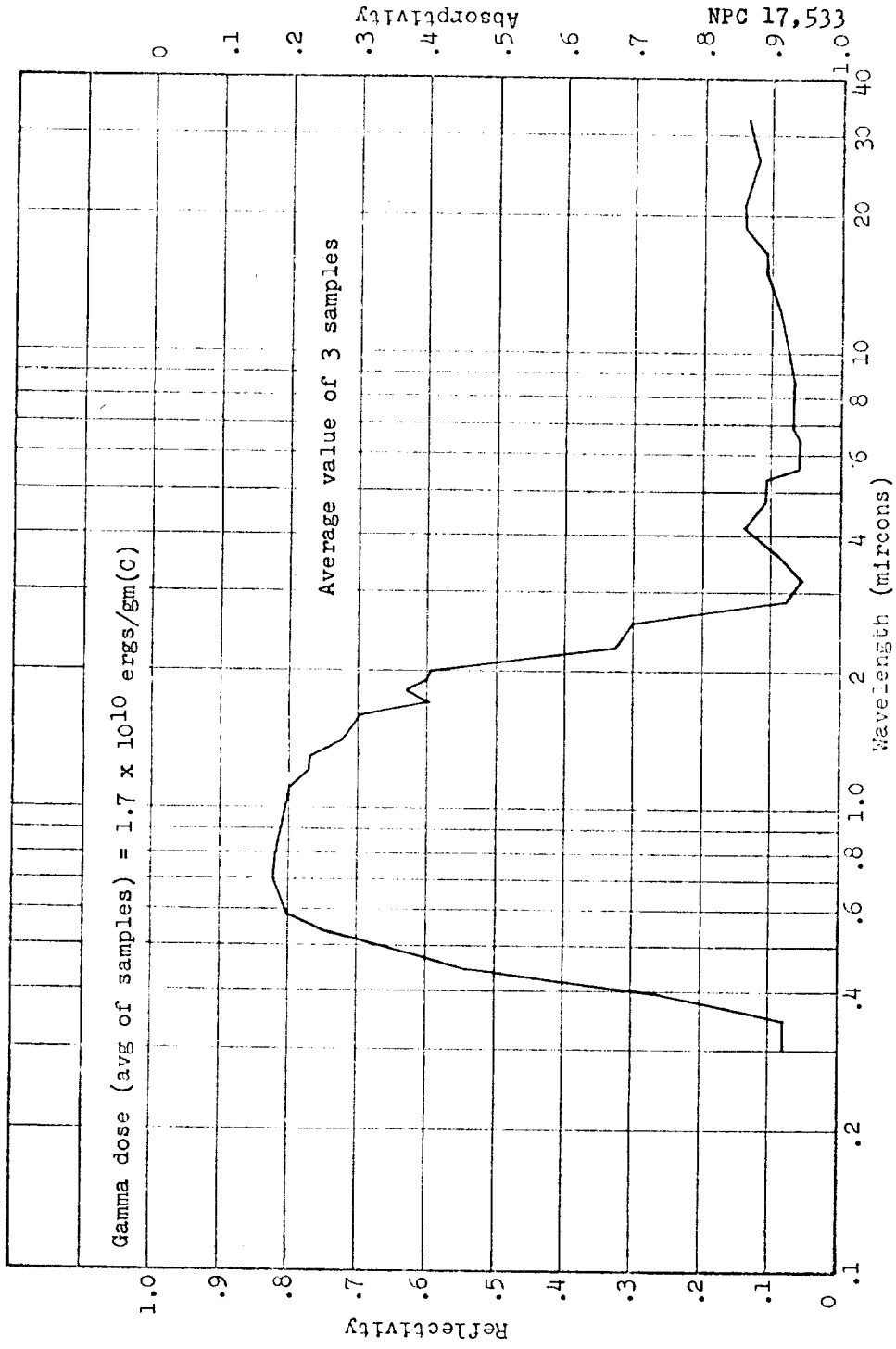

Figure E-4 Monochromatic Reflectivity and Absorptivity: Epoxy White; Vacuum-Irradiated Samples

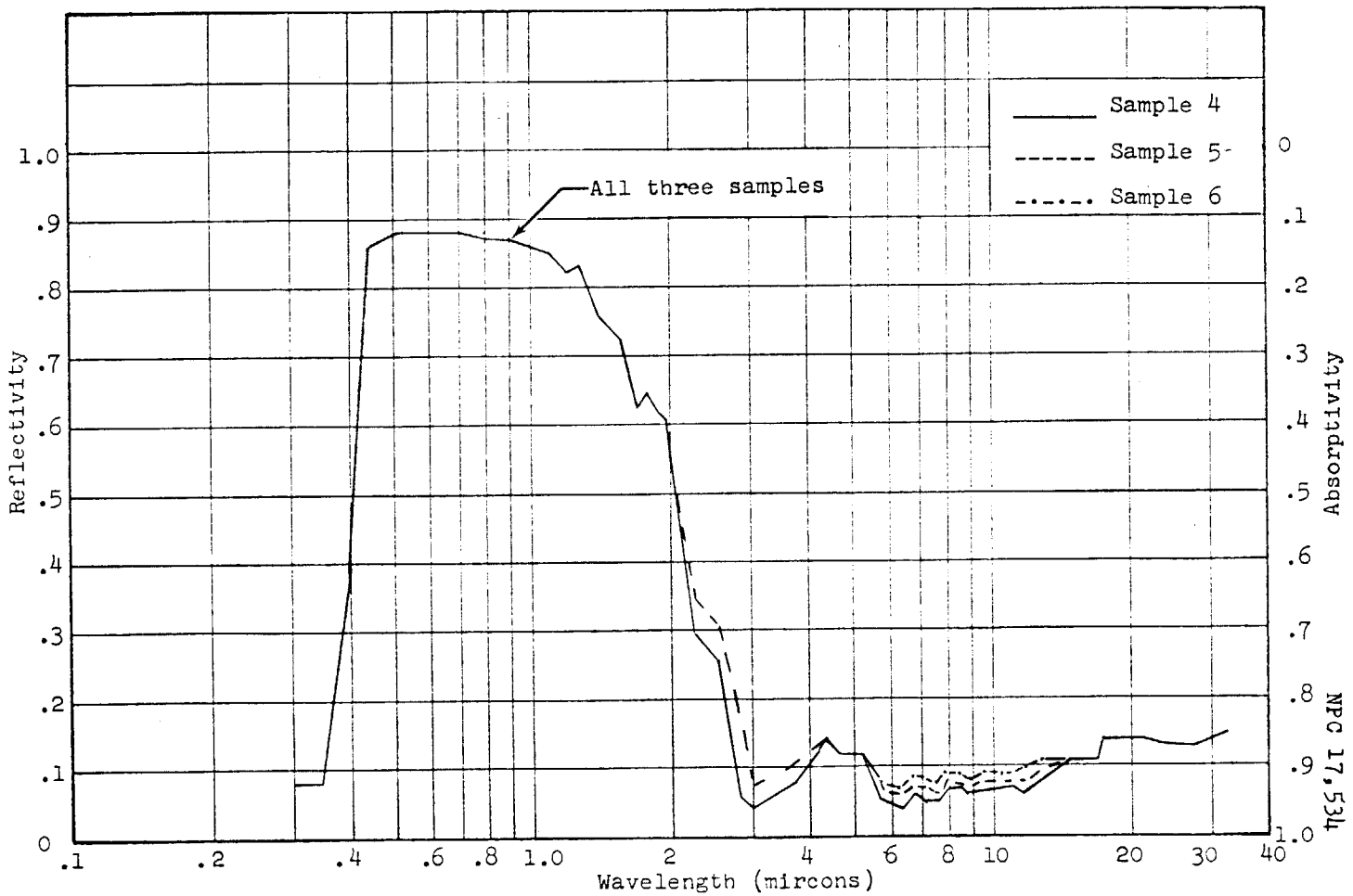

Figure E-5 Monochromatic Reflectivity and Absorptivity: Epoxy White; Test Control Samples

NPC 17,534

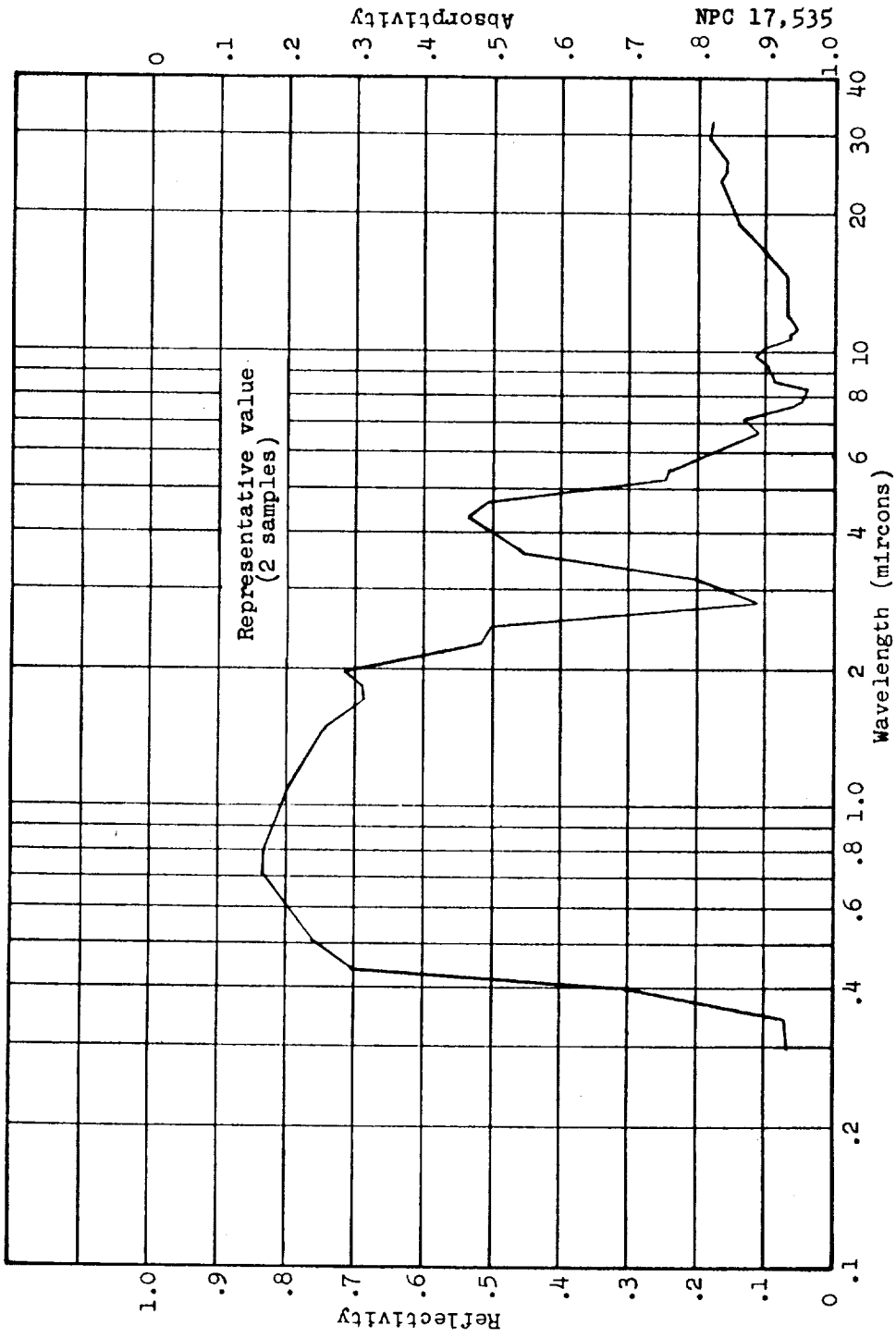

Figure E-6 Monochromatic Reflectivity and Absorptivity: Silicone White; Preshipment Control Samples

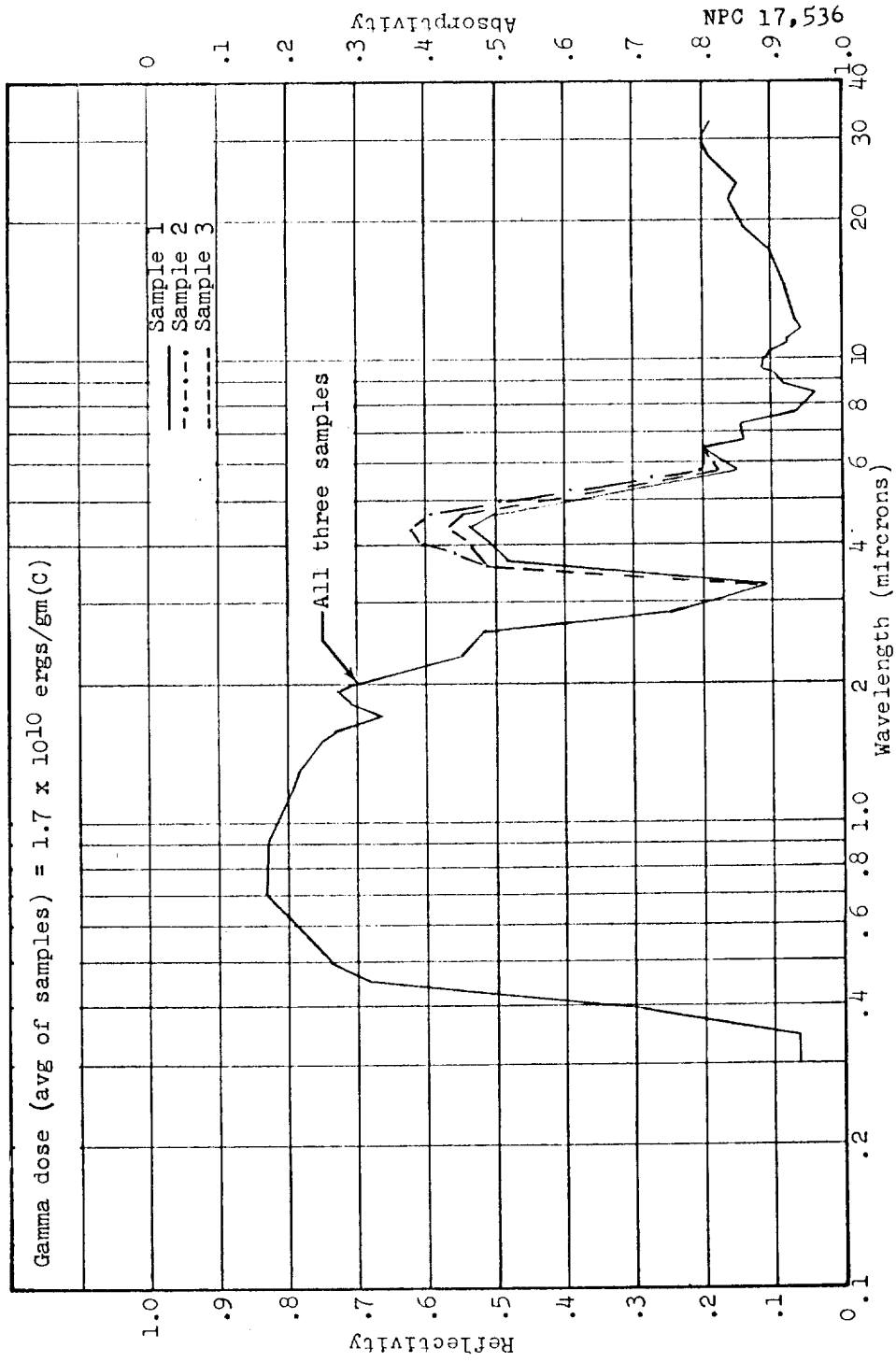

Figure E-7 Monochromatic Reflectivity and Absorptivity: Silicone White; Vacuum-Irradiated Samples

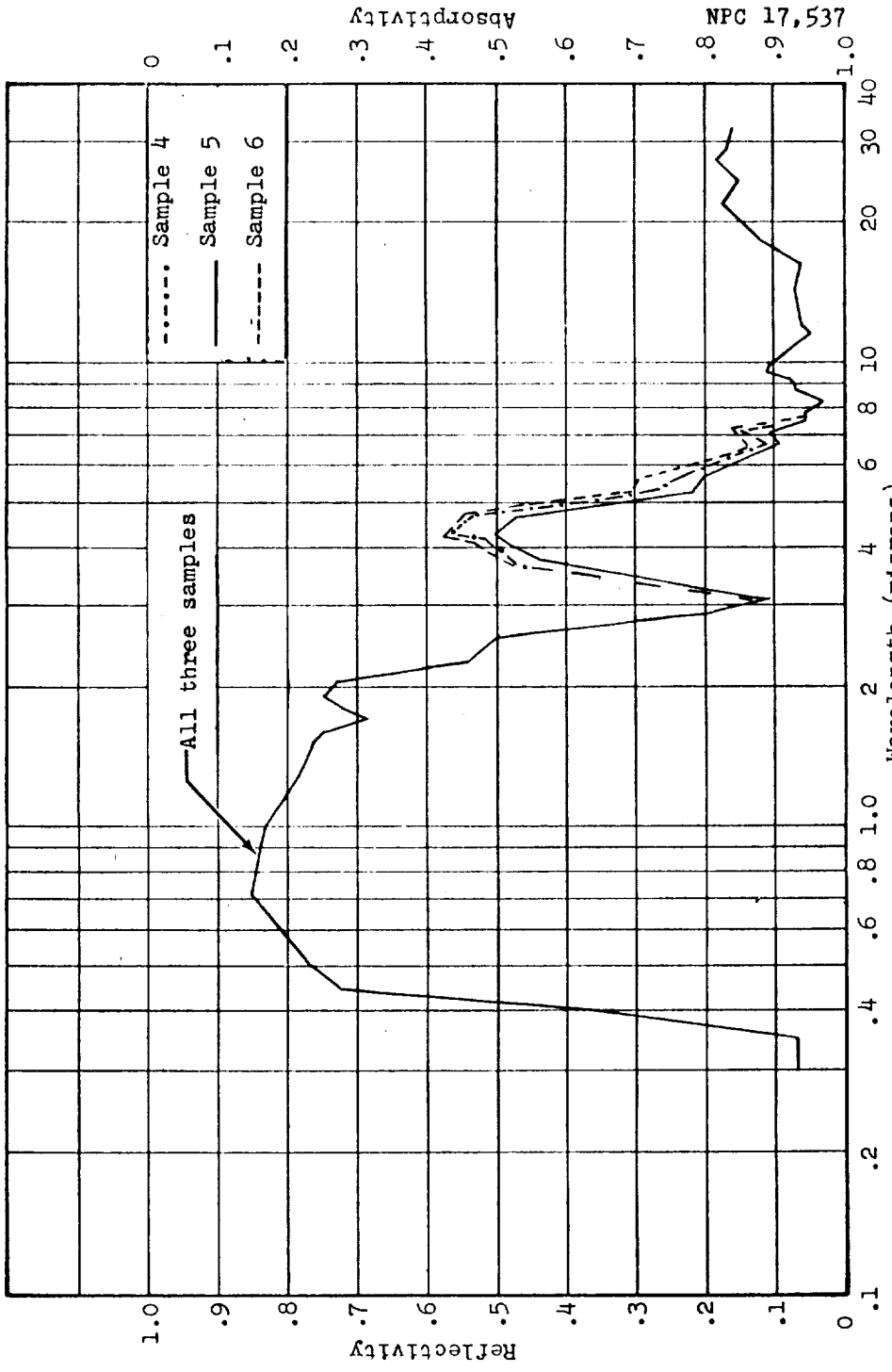

Figure E-8 Monochromatic Reflectivity and Absorptivity: Silicone White; Test Control Samples

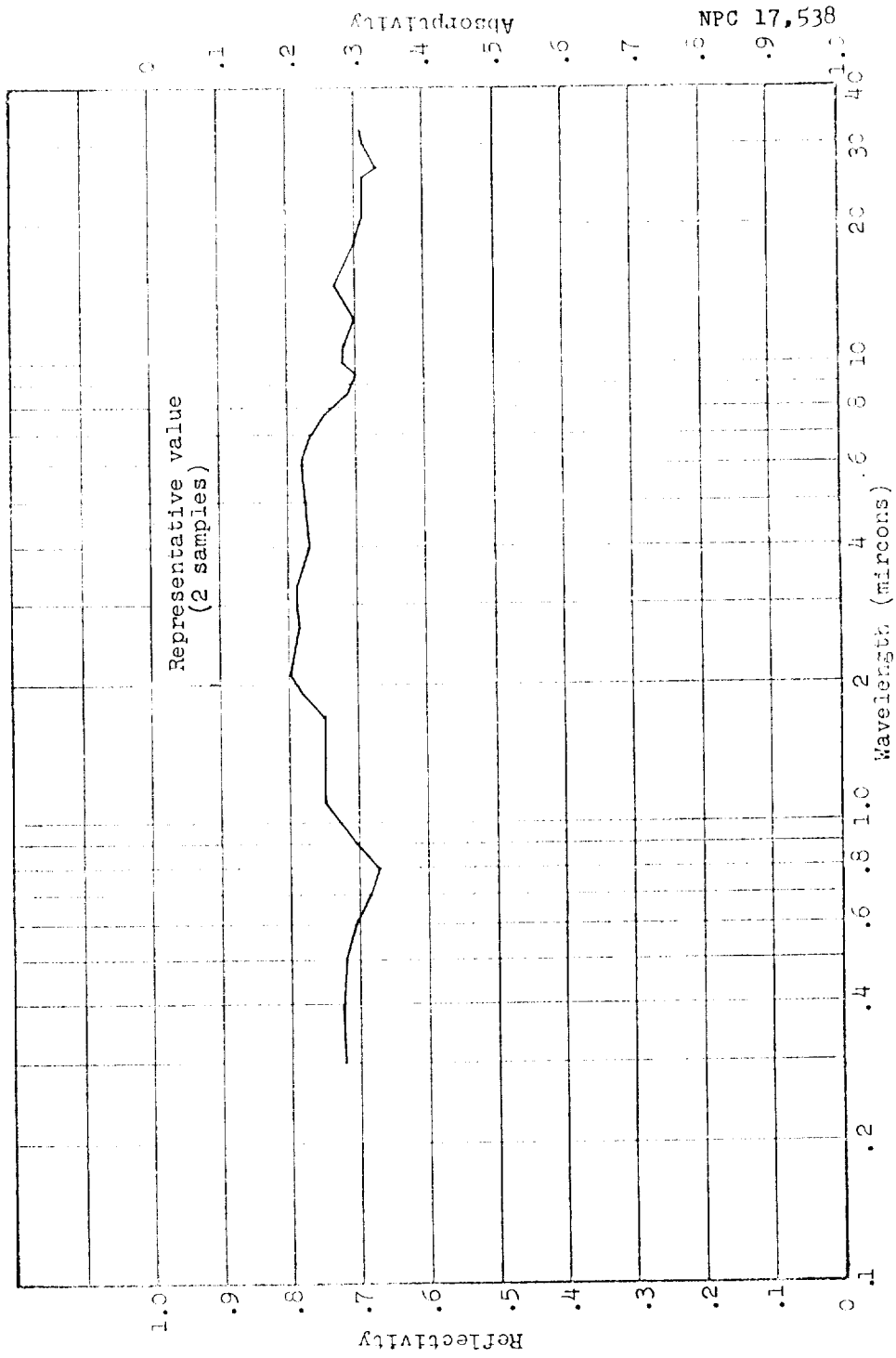

Figure E-9 Monochromatic Reflectivity and Absorptivity: Silicone Aluminum; Preshipment Control Samples

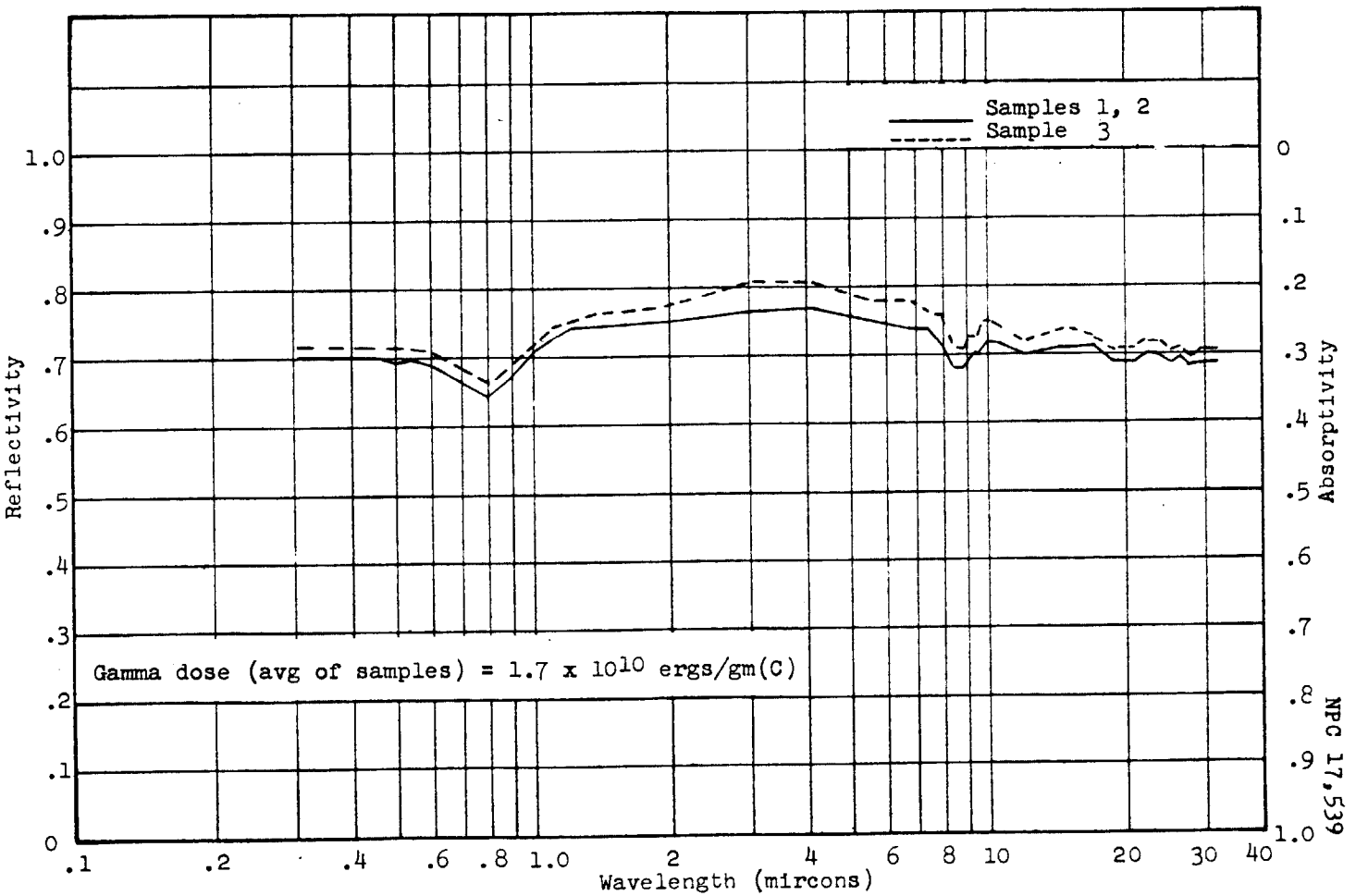

Figure E-10 Monochromatic Reflectivity and Absorptivity: Silicone Aluminum; Vacuum-Irradiated Samples

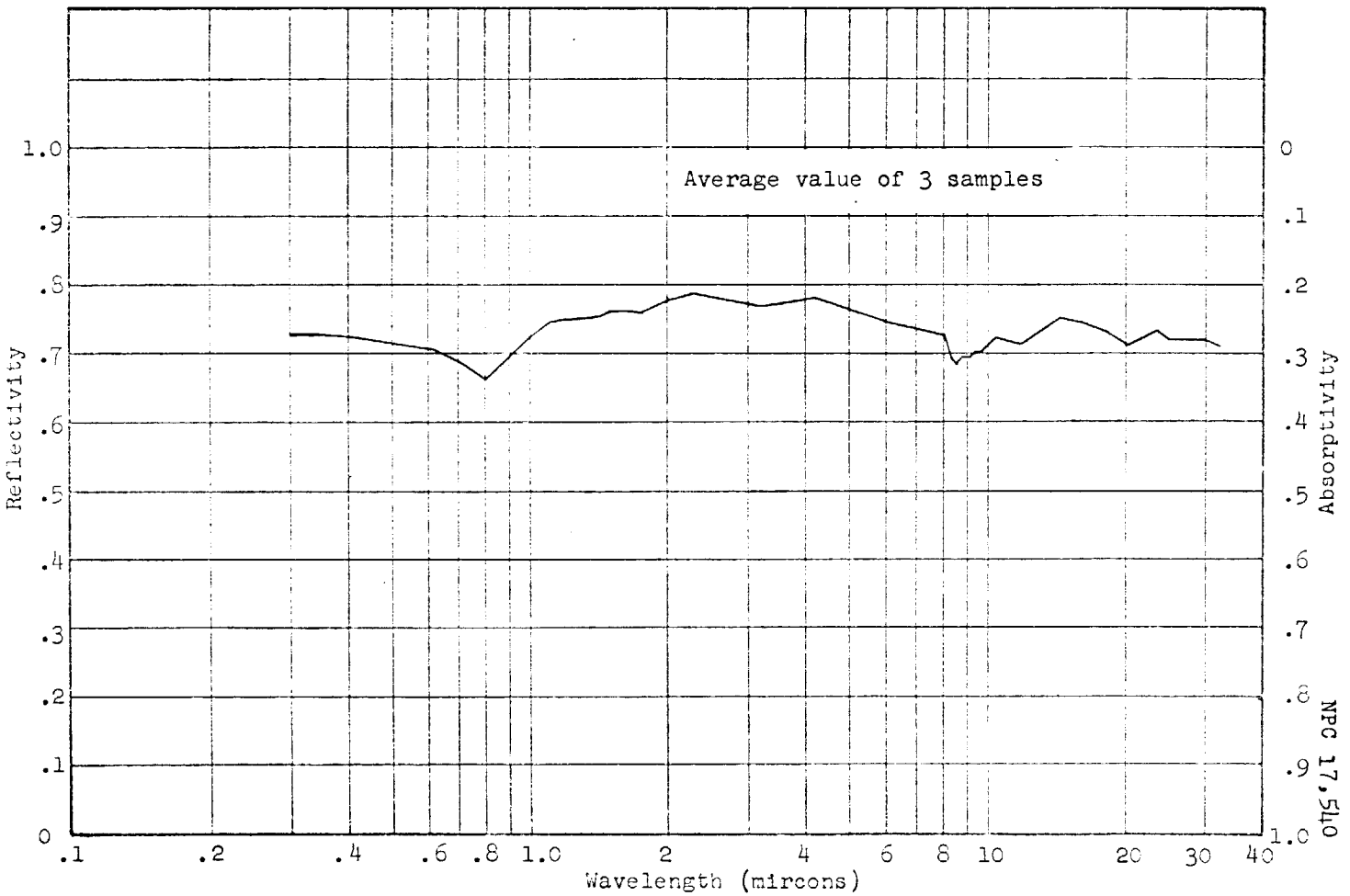

Figure E-11 Monochromatic Reflectivity and Absorptivity: Silicone Aluminum; Test Control Samples

REFERENCES*

1. Smith, E. T., Investigation of Combined Effects of Radiation and Cryotemperatures on Engineering Materials. Vol. II: Radiation/Cryotemperature Tests. General Dynamics/Fort Worth Report FZK-161-2 (28 December 1962). U

2. Park, W., Test Analysis of the 3 MW Ground Test Reactor. Convair-Fort Worth Report MR-N-254 (NARF-61-151, May 1961). U

3. Dushman, S., Scientific Foundations of Vacuum Techniques. New York: John Wiley & Sons, Inc. (1949(, pp. 90-111.

4. Kerlin, E. E., and Smith, E. T., Investigation of Combined Effects of Radiation and Vacuum on Engineering Materials (Second Quarterly Progress Report. General Dynamics/Fort Worth Report FZK-147 (4 June 1962). U

5. Dungan, W. E., and Lewis, J. H., Nuclear Measurement Techniques for Radiation Effects Environmental Testing. General Dynamics/Fort Worth Report FZK-9-175 (NARF-62-4T, 31 March 1962). U

6. Dungan, W. E., Specification of Neutron Flux in the Convair Radiation Effects Testing Facility. Convair-Fort Worth Report MR-N-270 (NARF-60-23T, 30 June 1960). U

7. Radiation Effects Facility Capability. General Dynamics/Fort Worth Document FZK-9-163-A (NARF-61-7T, 1 June 1962).

8. Bell, J. R., and Miles, J. K., Calibration of Foils for Neutron Flux Measurements. General Dynamics/Fort Worth Report MR-N-279 (NARF-61-18T, 6 June 1961). U

9. Sandia-Convair Irradiation Test No. 1, Addendum 1. Convair-Fort Worth Report MR-N-243-1 (NARF-59-22R, 15 September 1959). SRD

10. Kerlin, E. E., and Smith, E. T., Investigation of Combined Effects of Radiation and Vacuum and of Radiation and Cryogenic Temperatures on Engineering Materials (Third Quarterly Progress Report). General Dynamics/Fort Worth Report FZK-152 (15 August 1962). U

* All GD/FW reports published prior to June 1961 are referenced as Convair-Fort Worth reports.

Preceding page blank

REFERENCES (cont'd)

11. Kerlin, E. E., General Dynamics/Fort Worth unpublished experimental results, 1961. U

12. Harrington, R., and Giberson, R., "Chemical and Physical Changes in Gamma-Irradiated Plastics." Modern Plastics, 36 (3), (November 1958), pp 199-221.

13. Newell, D.M., "Radiation Effects on 23 Silicone Rubbers at Ambient Temperatures." Paper No. 65 (Vol. 5 of Proceedings) presented at the Third Semi-Annual Radiation Effects Symposium at Marietta, Ga., 28-30 October 1958.

14. Shinkle, F. J., Emissivity of the Atlas Stainless Steel Skin. Convair-Astronautics Report ERR-AN-037 (23 February 1961). U

15. Shinkle, F. J., The Total Normal Absorptivities and Total Normal Emissivities of Sherwin William's Flat Black Acrylic Paint at -32°F, 0°F, and 100°F. Convair-Astronautics Report ERR-AN-056 (29 May 1961). U

16. Clauss, F. J., Editor, Surface Effects on Spacecraft Materials. New York: John Wiley & Sons, Inc. (1960) First Symposium sponsored by Air Research and Development Command, USAF, and by Missile and Space Division, Lockheed Aircraft Corporation, held at Palo Alto, California, 12-13 May 1959.

17. Hill, O. H., and Kerlin, E. E., Experimental Investigations of Radiation Heating in Materials. Convair-Fort Worth Report MR-N-290 (NARF-61-38T, 29 December 1961). U

18. Collins, C. G., and Calkins, V. P., Radiation Damage to Elastomers, Plastics, and Organic Liquids, 11th ed. General Electric Report TID 4500 (APEX 261, September 1956). U

19. Schoffner, J. P., "The Effects of Radiation on Teflon Resins in Space." Journal of Teflon, 2 (1), (January 1961).

20. Eggen, J. B., "Scattered Radiation in Dry Side of Pool." General Dynamics/Fort Worth Internal Memo N-S/1-321 (13 December 1961).

21. "Dow Corning 704 Fluid." Dow Corning Electronics Notebook, Sec. G, p. 7. U

DISTRIBUTION LIST

ADDRESSEE	NO. OF COPIES
National Aeronautics and Space Administration George C. Marshall Space Flight Center Huntsville, Alabama Attn: M-P&C-CA	12
National Aeronautics and Space Administration Langley Research Center Langley Field, Virginia	1
National Aeronautics and Space Administration Manned Spacecraft Center Houston, Texas	1
National Aeronautics and Space Administration Ames Research Center Moffett Field, California	1
Bernard Ackhammer National Aeronautics and Space Administration Washington 25, D. C.	1
Robert Brock National Aeronautics and Space Administration Rich Building - Rm. 271 6040 Telephone Road Houston, Texas	1
SNPO-Cleveland Lewis Research Center 21000 Brookpark Road Cleveland 35, Ohio	1
Mort Krasner Reactor Division Lewis Research Center 21000 Brookpark Road Cleveland 35, Ohio	1
Dr. Henry Frankel Goddard Space Flight Center Greenbelt, Maryland	1

DISTRIBUTION LIST (cont'd)

ADDRESSEE	NO. OF COPIES
Dan Reigert National Aeronautics and Space Administration Instrumentation and Electronic Systems Division Rich Building 6040 Telephone Road Houston, Texas	1
J. H. Kimzey Mechanical Systems Branch SEDD National Aeronautics and Space Administration 6040 Telephone Road Houston, Texas	1
Capt. Harold E. Pilcher Headquarters SSD (SSZMS) AF Unit Post Office Los Angeles 45, California	1
Scientific and Technical Information Facility P. O. Box 5700 Bethesda, Maryland Attn: NASA Representative (S-AK/RKT)	2
John Morrissey Space Nuclear Propulsion Office Division of Reactor Development U. S. Atomic Energy Commission Germantown, Maryland	1
Oscar Sisman Solid State Division Oak Ridge National Laboratory Oak Ridge, Tennessee	1
Plastics Technical Evaluation Center Picatinny Arsenal Dover, New Jersey Attn: H. E. Pebly	2
R. E. Bowman Radiation Effects Information Center Battelle Memorial Institute 505 King Avenue Columbus 1, Ohio	1

DISTRIBUTION LIST (cont'd)

ADDRESSEE	NO. OF COPIES
John B. Rittenhouse Lockheed Missiles and Space Company Research Laboratories, 52-30 3251 Hanover Street Palo Alto, California	1
Dr. F. J. Clauss Lockheed Missiles and Space Company Palo Alto, California	1
D. M. Newell Dept. 52-10, Bldg. 204 Lockheed Missiles and Space Company Palo Alto, California	1
Oliver Burford Lockheed Georgia Company Marietta, Georgia	1
Dr. Hand Plank Lockheed Missiles and Space Company Sunnyvale, California	1
Dr. George Yasui Dept. 3202, Bldg. 537 Lockheed Missiles and Space Company Sunnyvale, California	1
L. D. Jaffe Jet Propulsion Laboratory 4800 Oak Grove Drive Pasadena 3, California	1
Robert Harrington Jet Propulsion Laboratory 4800 Oak Grove Drive Pasadena 3, California	1
William F. Emmons Dept. 746, Bldg. 160 Aerojet General Corporation Azusa, California	1

DISTRIBUTION LIST (cont'd)

ADDRESSEE	NO. OF COPIES
P. H. Sager GD/Astronautics San Diego, California	1
S. A. Yalof GD/Astronautics San Diego, California	1
AVCO Corporation Spaceflight Program Office 6501 E. Admiral Place Tulsa 15, Oklahoma Attn: M. I. Gamble	1

best sellers

NTIS

from NATIONAL TECHNICAL INFORMATION SERVICE

Product Liability: Industry Study. Volumes I and II
PB-265 542/PSK 886 p PC$21.25/MF$3.00

An Atlas of Radiation Histopathology
TID-26676/PSK 234 p PC$7.60/MF$3.00

The Medical School Admissions Process. A Review of the Literature, 1955-76
PB-263 962/PSK 193 p PC$7.50/MF$3.00

Integrated Energy Vocabulary
PB-259 000/PSK 459 p PC$22.50/MF$3.00

Nuclear Air Cleaning Handbook. Design, Construction, and Testing of High-Efficiency Air Cleaning Systems for Nuclear Application
ERDA-76/21/PSK 300 p PC$9.75/MF$3.00

Evaluation of the Air-To-Air Heat Pump for Residential Space Conditioning
PB-255 652/PSK 293 p PC$9.25/MF$3.00

Federal Information Processing Standards Register: Guidelines for Documentation of Computer Programs and Automated Data Systems. Category: Software. Subcategory: Documentation
FIPS-PUB38/PSK 55 p PC$4.50/MF$3.00

Life Cycle Costing Emphasizing Energy Conservation: Guidelines for Investment Analysis
ERDA-76/130/PSK 117 p PC$5.50/MF$3.00

Analysis of Projected Vs. Actual Costs for Nuclear and Coal-Fired Power Plants
FE-2453-2/PSK 38 p PC$4.00/MF$3.00

Quality Criteria for Water
PB-263 943/PSK 537 p PC$13.00/MF$3.00

Passive Solar Heating and Cooling Conference and Workshop Proceedings May 18-19, 1976, University of New Mexico, Albuquerque, New Mexico
LA-6637-C/PSK 352 p PC$10.50/MF$3.00

Predicting the Performance of Solar Energy Systems
AD-A035 608/PSK 45 p PC$4.00/MF$3.00

NIOSH Analysis Methods for Set J
PB-263 959/PSK 128 p PC$6.00/MF$3.00

Flat-Plate Solar Collector Handbook: A Survey of Principles, Technical Data and Evaluation Results
UCID-17086/PSK 96 p PC$5.00/MF$3.00

How to Order

When you indicate this method of payment, please note if a purchase order is not accompanied by payment, you will be billed an additional $5.00 *ship and bill* charge. And please include the card expiration date when using American Express.

Normal delivery time takes three to five weeks. It is vital that you order by number or your order will be manually filled, insuring a delay. You can opt for *priority mail* for $3.00 outside North American continent charge per item. Just check the *priority mail* box. If you're really pressed for time, call the NTIS Rush Handling Service (703) 557-4700. For a $10.00 charge per item, your order will be sent *priority mail* within 48 hours. Or, you can pick up your order in the Washington Information Center & Bookstore or at our Springfield Operations Center within 24 hours for a $6.00 per item charge.

You may also place your order by telephone or if you have an NTIS Deposit Account or an American Express card order through TELEX. The order desk number is (703) 557-4650 and the TELEX number is 89-9405.

Thank you for your interest in NTIS. We appreciate your order.

METHOD OF PAYMENT

- ☐ Charge my NTIS deposit account no. _____
- ☐ Purchase order no. _____
- ☐ Check enclosed for $ _____
- ☐ Bill me. Add $5.00 per order and sign below. (Not available outside North American continent.)
- ☐ Charge to my American Express Card account number

Card expiration date _____.

Signature _____

☐ Priority mail requested

NAME _____

ADDRESS _____

CITY, STATE, ZIP _____

Item Number	Quantity		Unit price*	Total Price*
	Paper Copy (PC)	Microfiche (MF)		
			Sub Total	
			Additional Charge	
			Enter Grand Total	

All prices subject to change. The prices above are accurate as of 12/77
Foreign Prices on Request.

Clip and mail to:

NTIS

National Technical Information Service
U.S. DEPARTMENT OF COMMERCE
Springfield, Va. 22161
(703) 557-4650 TELEX 89-9405